การพัฒนาพิร์โรลิดินิลเพปไทด์นิวคลีอิกแอซิดเรืองแสงเป็นโพรบสำหรับตรวจลำดับเบสของดีเอ็นเอ

นางสาวชโลธร บุญเหลือ

วิทยานิพนธ์นี้เป็นส่วนหนึ่งของการศึกษาตามหลักสูตรปริญญาวิทยาศาสตรดุษฎีบัณฑิต
สาขาวิชาเคมี ภาควิชาเคมี
คณะวิทยาศาสตร์ จุฬาลงกรณ์มหาวิทยาลัย
ปีการศึกษา 2555

DEVELOPMENT OF FLUORESCENCE PYRROLIDINYL PEPTIDE NUCLEIC ACID AS PROBES FOR DETERMINATION OF DNA SEQUENCES

Miss Chalothorn Boonlua

A Dissertation Submitted in Partial Fulfillment of the Requirements

for the Degree of Doctor of Philosophy Program in Chemistry

Department of Chemistry

Faculty of Science

Chulalongkorn University

Academic Year 2012

Thesis Title	DEVELOPMENT OF FLUORESCENCE PYRROLIDINYL PEPTIDE NUCLEIC ACID AS PROBES FOR DETERMINATION OF DNA SEQUENCES
By	Miss Chalothorn Boonlua
Field of study	Chemistry
Thesis Advisor	Associate Professor Tirayut Vilaivan, D.Phil.

Accepted by the Faculty of Science, Chulalongkorn University in Partial Fulfillment of the Requirements for the Doctoral Degree

……...…....Dean of the Faculty of Science
(Professor Supot Hannongbua, Dr.rer.nat.)

THESIS COMMITTEE

…….……...Chairman
(Assistant Professor Warinthorn Chavasiri, Ph.D.)

…….…….....Thesis Advisor
(Associate Professor Tirayut Vilaivan, D.Phil.)

……Examiner
(Associate Professor Mongkol Sukwattanasinitt, Ph.D.)

……Examiner
(Professor Thawatchai Tuntulani, Ph.D.)

……External Examiner
(Chaturong Suparpprom, Ph.D.)

ชโลธร บุญเหลือ: การพัฒนาพิร์โรลิดินิลเพปไทด์นิวคลีอิกแอซิดเรืองแสงเป็นโพรบสำหรับตรวจลำดับเบสของดีเอ็นเอ (DEVELOPMENT OF FLUORESCENCE PYRROLIDINYL PEPTIDE NUCLEIC ACID AS PROBES FOR DETERMINATION OF DNA SEQUENCES) อ.ที่ปรึกษาวิทยานิพนธ์หลัก: รศ. ดร. ธีรยุทธ วิไลวัลย์, 170 หน้า.

ในงานวิจัยนี้ได้มีการออกแบบและประเมินสมบัติของเพปไทด์นิวคลีอิกแอซิดเรืองแสงที่สามารถเปลี่ยนแปลงการเรืองแสงเมื่อมีดีเอ็นเอเป้าหมายที่ถูกต้อง เพปไทด์นิวคลีอิกแอซิดที่ใช้ในงานวิจัยนี้คือ พิร์โรลิดินิลเพปไทด์นิวคลีอิกแอซิดที่ประกอบด้วยโพรลีน / 2-อะมิโนไซโคลเพนเทนคาร์บอกซิลิกแอซิด เป็นโครงสร้างหลัก (acpcPNA) ที่มีความสามารถจับยึดกับดีเอ็นเอได้อย่างเสถียรและจำเพาะเจาะจงกว่าดีเอ็นเอและพีเอ็นเอที่มีจำหน่าย งานในส่วนแรก ได้สังเคราะห์ 5-(pyren-1-yl)uracil (U^{Py}) โมโนเมอร์และได้สังเคราะห์พีเอ็นเอที่มีโมโนเมอร์ดังกล่าว โดยเบส U^{Py} ใน acpcPNA มีความสามารถในการจดจำเบสอะดีนีนในดีเอ็นเอเป้าหมายได้อย่างจำเพาะเจาะจง นอกจากนี้การเรืองแสงแสงงของเบส U^{Py} ก็เพิ่มขึ้นอย่างมาก เมื่อพีเอ็นเอจับยึดกับดีเอ็นเอเป้าหมายที่มีลำดับเบสคู่สมโดยไม่ขึ้นกับเบสข้างเคียง การเพิ่มขึ้นของการเรืองแสงนี้จำเพาะเจาะจงต่อการเข้าคู่กันระหว่างเบส U^{Py} กับ dA งานในส่วนที่สองได้ทำการต่อไพรีนผ่านพันธะโควาเลนซ์ด้วยตัวเชื่อม butyryl และปฏิริยาเอซิลเลชั่นที่ปลาย N ของ acpcPNA หรือไนโตรเจนของวงพิร์โรลิดีนที่ตำแหน่งกลางสาย การเรืองแสงของพีเอ็นเอที่มีไพรีนที่ตำแหน่งปลายเมื่อจับยึดกับดีเอ็นเอให้ผลหลากหลายขึ้นกับการเรืองแสงเริ่มต้นของพีเอ็นเอสายเดี่ยวและชนิดของเบสที่อยู่ใกล้กับไพรีน การเรืองแสงของพีเอ็นเอที่มีไพรีนที่กลางสายเมื่อจับยึดกับดีเอ็นเอจะเพิ่มขึ้นอย่างมากเมื่อเทียบกับพีเอ็นเอสายเดียว งานในส่วนที่สามได้ทำการประเมินพีเอ็นเอที่ติดฉลากเรืองแสงร่วมกับดีเอ็นเอสายสั้นที่ติดฉลากด้วยตัวดับแสงเป็นโพรบแทนที่สำหรับตรวจวัดดีเอ็นเอ เมื่อมีดีเอ็นเอเป้าหมายการเรืองแสงจะเพิ่มขึ้นแต่ไม่กลับไปเท่ากับตอนเริ่มต้นเนื่องจากเกิดการแทนที่อย่างไม่สมบูรณ์และยังถูกเควันช์ด้วยเบสในสายดีเอ็นเอ ในทุกกรณีพิร์โรลิดินิลพีเอ็นเอสามารถแยกความแตกต่างของดีเอ็นเอคู่สมกับดีเอ็นเอที่มีลำดับเบสผิดไปหนึ่งตำแหน่งได้อย่างจำเพาะเจาะจงสูง

ภาควิชา เคมี ลายมือชื่อนิสิต.....

สาขาวิชา เคมี ลายมือชื่อ อ.ที่ปรึกษาวิทยานิพนธ์หลัก.....

ปีการศึกษา 2555

##5073917023: MAJOR CHEMISTRY
KEYWORDS: PEPTIDE NUCLEIC ACID / PYRENE / FLUORESCENCE / MOLECULAR BEACONS / QUENCHER-FREE

CHALOTHORN BOONLUA: DEVELOPMENT OF FLUORESCENCE PYRROLIDINYL PEPTIDE NUCLEIC ACID AS PROBES FOR DETERMINATION OF DNA SEQUENCES. ADVISOR: ASSOC. PROF. TIRAYUT VILAIVAN, D.Phil., 170 pp.

In this research, fluorescence peptide nucleic acid (PNA) probes that can change the fluorescence in response to the presence of correct DNA target were designed and evaluated. The PNA employed in this work is the pyrrolidinyl peptide nucleic acid with an alternating proline/2-aminocyclopentanecarboxylic acid backbone (acpcPNA) which shows superior binding to DNA in terms of stability and specificity compared to DNA and commercial PNA. In the first part, 5-(pyren-1-yl)uracil (U^{Py}) PNA monomer was synthesized and incorporated into the acpcPNA. The U^{Py} base in acpcPNA retained the ability to specifically recognize the base A in its complementary DNA strand. Furthermore, the fluorescence of the U^{Py} base is significantly enhanced when the acpcPNA is hybridized to its complementary DNA target, irrespective of the nature of the flanking bases. The fluorescence enhancement is specific to the pairing between U^{Py} and dA. In the second part, pyrene was covalently attached to N-terminal positions of acpcPNA or to internal positions of APC-modified acpcPNA through a flexible butyryl linker *via* acylation of the N-termini of acpcPNA or the pyrrolidine nitrogen atom of 3-aminopyrrolidine-4-carboxylic acid (APC)-modified acpcPNA. Hybridization of the terminally pyrene-modified PNA to its complementary DNA gave variable fluorescence change, depending on the original fluorescence of the single stranded PNA and the identity of the DNA base in vicinity of the pyrene label. Hybridization of the internally pyrene-labeled acpcPNA to its complementary DNA target resulted in a consistent large increase in fluorescence signal relative to the single stranded DNA. In the third part, the combination of terminally fluorophore-modified acpcPNAs (Flu- or TMR-acpcPNA) with a short quencher DNA were evaluated as strand-displacement probes for DNA sequence determination. In the presence of complementary DNA, the fluorescence was increased, but never returned to the original level due to incomplete strand displacement and also quenching by the DNA target. In all cases, the high specificity of the acpcPNA system allows unambiguous discrimination between the complementary and single mismatched DNA target.

Department: Chemistry Student's Signature.....

Field of Study: Chemistry Advisor's Signature.....

Academic Year: 2012

ACKNOWLEDGEMENTS

I would like to express my sincere appreciation to Associate Professor Dr. Tirayut Vilaivan, my thesis advisor, for guidance, suggestions and assistance throughout this research. I'm also grateful to thesis examiners: Assistant Professor Dr. Warinthorn Chavasiri, Associate Professor Dr. Mongkol Sukwattanasinitt, Professor Dr. Thawatchai Tuntulani and Dr. Chaturong Suparpprom for all valuable comments and suggestions regarding this thesis. And I would like to thank the following: The Development and Promotion of Science and Technology Talent Project (DPST) for the financial support; Organic Synthesis Research Unit (OSRU) and Department of Chemistry, Chulalongkorn University for the use of facilities, equipment, glassware and chemicals; Supramolecular Chemistry Research Unit (SCRU) for the use of fluorescence spectrophotometer; Dr. Mongkol Sukwattanasinitt for the nuclease S1 sample; the Thai government stimulus package 2 (TKK2555, SP2) under the Project for Establishment of Comprehensive Center for Innovative Food and Health Products and Agriculture, the National Research University Grant from the Commission of Higher Education, and the Ratchadaphiseksomphot Endowment (AM1006A) for CD spectrometer; members of TV group for their friendship, advice and their helpful; my friends for their advice, understanding and social experience through my study period; Finally, I am deeply grateful to my family for their love and encouragement throughout my Ph.D. study.

CONTENTS

Page

Page

Page

LIST OF TABLES

Table Page

LIST OF FIGURES

Figure Page

Figure Page

Figure Page

Figure Page

Figure Page

Figure Page

Figure Page

Figure Page

Figure Page

Figure Page

Figure Page

LIST OF ABBREVIATIONS

δ	:	chemical shift
µL	:	microliter
µmol	:	micromole
$[\alpha]_D$	:	specific rotation
A	:	adenine
A^{Bz}	:	*N*^{6}-benzoyladenine
Ac	:	acetyl
Ac_2O	:	acetic anhydride
Boc	:	*tert*-butoxycarbonyl
BHQ	:	black hole quencher
Bz	:	benzoyl
c	:	concentration
C	:	cytosine
calcd	:	calculated
C^{Bz}	:	*N*^{4}-benzoylcytosine
CCA	:	α-cyano-4-hydroxy cinnamic acid
$CDCl_3$	:	deuterated chloroform
CD_3OH	:	deuterated methanol
d	:	doublet
DABCYL		4-(4-dimethylaminophenylazo)benzoic acid
DBU	:	1,8-diazabicyclo[5.4.0]undec-7-ene
DCM	:	dichloromethane
DIAD	:	diisopropylazodicarboxylate
DIEA	:	diisopropylethylamine
DMF	:	*N*,*N*'-dimethylformamide
DNA	:	deoxyribonucleic acid
Dpm	:	diphenylmethyl
ds	:	double strand
equiv	:	equivalent (s)

Flu	:	fluorescein
Fmoc	:	9-fluorenylmethoxycarbonyl
FmocCl	:	9-fluorenylmethyl chloroformate
FmocOSu	:	9-fluorenylmethyl succinimidyl carbonate
FRET	:	fluorescence resonance energy transfer
g	:	gram
G	:	guanine
G^{Ibu}	:	N^2-isobutyrylguanine
h	:	hour
HATU	:	*O*-(7-azabenzotriazol-1-yl)-*N*,*N*,*N'*,*N'*-tetramethyluronium hexafluorophosphate
HOAt	:	1-hydroxy-7-azabenzotriazol
HPLC	:	high performance liquid chromatography
Hz	:	hertz
Ibu	:	isobutyryl
J	:	coupling constant
Lys	:	lysine
m	:	multiplet
M	:	molar
MALDI-TOF	:	matrix-assisted laser desorption/ionization-time of flight
MeCN	:	acetonitrile
MeOH	:	methanol
mg	:	milligram
MHz	:	megahertz
min	:	minute
mL	:	milliliter
mM	:	millimolar
mmol	:	millimol
mRNA	:	messenger ribonucleic acid
MS	:	mass spectrometry
m/z	:	mass to charge ratio

nm	:	nanometer
NMR	:	nuclear magnetic resonance
^{o}C	:	degree celsius
Pfp	:	pentafluorophenyl
Ph	:	phenyl
PNA	:	peptide nucleic acid or polyamide nucleic acid
R_f	:	retention factor
RNA	:	ribonucleic acid
s	:	singlet
ss	:	single strand
t	:	triplet
T	:	thymine
TEA	:	triethylamine
TFA	:	trifluoroacetic acid
THF	:	tetrahydrofuran
TLC	:	thin layer chromatography
T_m	:	melting temperature
TMR	:	tetramethylrhodamine
t_R	:	retention time
U	:	uracil or uridine
UV	:	ultraviolet
δ	:	chemical shift

CHAPTER I

INTRODUCTION

1.1 Hybridization probes

A biosensor is a device that combines a sensitive biological component, which can interact specifically with a certain analyte, and a signal transducer or physicochemical detector component for the detection of that specific analyte. The transducer transforms the signal obtained from the specific interaction between the biological sensing element and the target analyte into measurable and quantifiable signals. The output signal can be amplified, stored, or displayed.

Deoxyribonucleic acid (DNA) is a molecule that contains all of the information required to build and maintain an organism. The order, or sequence, of these bases determines what biological instructions are contained in a strand of DNA. DNA/RNA sequence analysis is important in molecular biology, genetics, and molecular medicine. One of the fastest growing areas in DNA/RNA technology is the development of DNA-based biosensors for determination of DNA/RNA sequences such as genetic mutation analysis. A DNA biosensor normally employs one or more DNA probes as the recognition element and measures specific binding processes such as the formation of DNA·DNA and DNA·RNA hybrids at the biosensor surface or in homogeneous solution. Hybridization probes are widely used in many fields for example molecular biology, genetics, and medical diagnostics [1–4]. Many techniques have been employed for DNA hybridization detection, including fluorescence label-based optical methods [5], mass spectrometry [6–7], electrochemical [8–9], surface plasmon resonance-based optical methods [10–11] and DNA microarray [12]. Natural nucleic acids (DNA, RNA) or oligonucleotides are traditionally used as hybridization probes. More recently, other synthetic oligonucleotide analogues, for example peptide nucleic acids (PNA) [13–14] and locked nucleic acids (LNA) [15], which offered some advantages over conventional oligonucleotide probes, have been used.

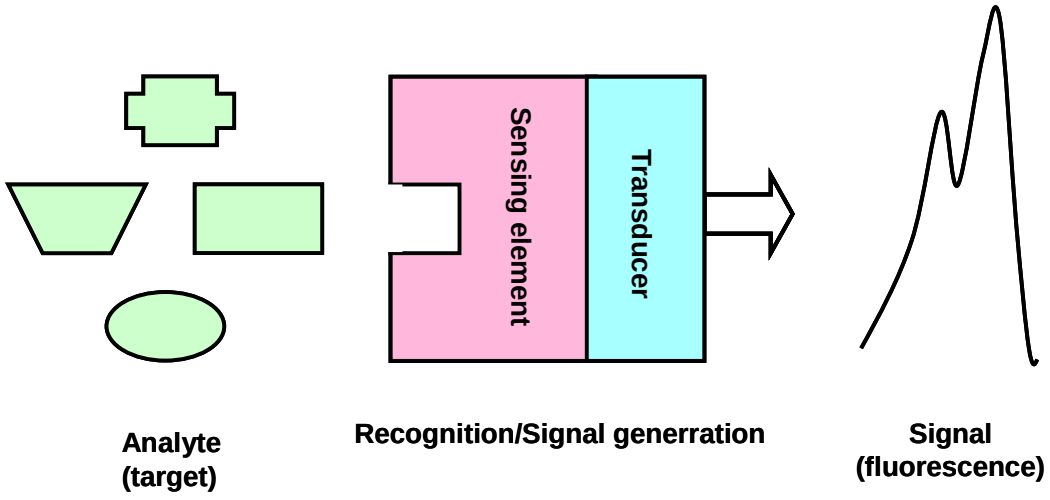

Figure 1.1 Schematic of a fluorescent biosensor

Fluorescent oligonucleotide probes can be regarded as a typical example of DNA-biosensor (**Figure 1.1**). The probe must first hybridize with the complementary DNA target (analyte). Transduction of the analyte binding into an analytical signal is achieved through one or more environment-sensitive fluorophore, which are often covalently attached to the probe. Ideal fluorescent probes should give fluorescence change that is specific to the binding of the probe to the target DNA. In recent years, a number of fluorescence DNA probes have been developed. These probes have become inexpensive, sensitive and easy to use tools for DNA sequence analyses.

1.2 Molecular beacon probes

One of the most important developments in the area of fluorescence DNA probes was the introduction of molecular beacons (MBs). The first MBs, described by Tyagi *et al*. in1996 [16], relied on fluorescence quenching and complementary pairing principles. **Figure 1.2** shows the general design of typical MBs and their working principle. MBs are single-stranded oligonucleotide that can form a stem-and-loop (hairpin) structure. The loop contains a region that is complementary to the target sequence and thus functions as the probe. The stem is a separate domain formed by the complementary pairing of several terminal bases. A donor fluorophore is

covalently linked to the end of one arm and an acceptor quencher is covalently linked to the end of the other arm of the stem.

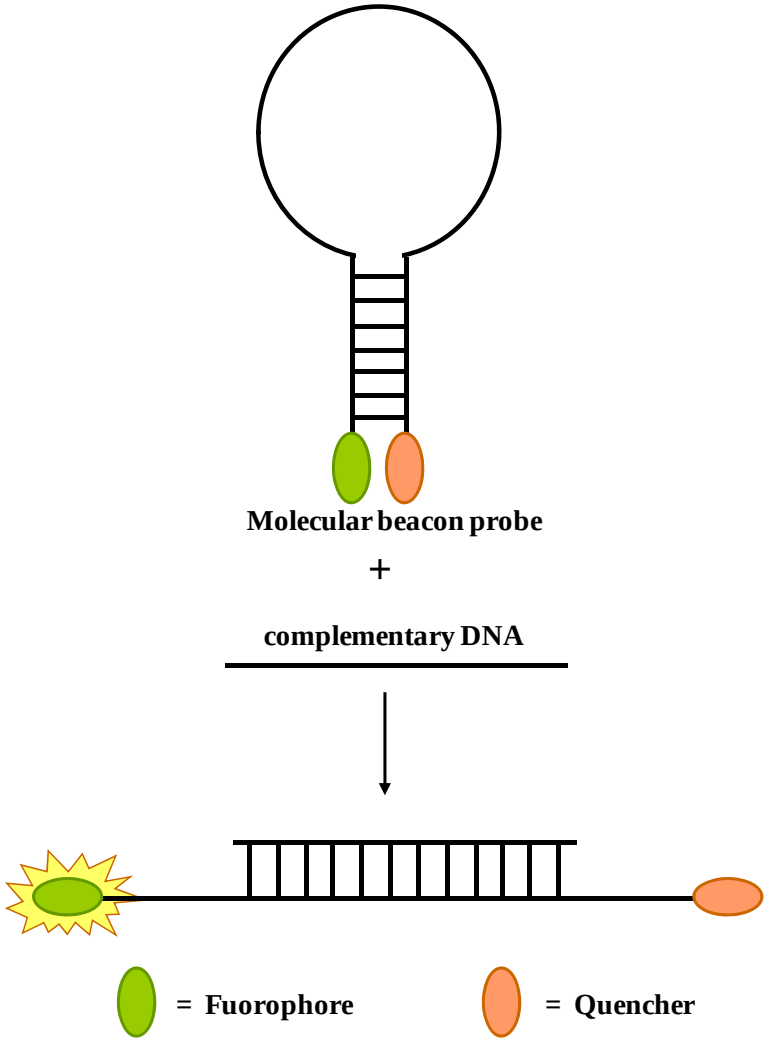

Figure 1.2 Schematic representations of molecular beacon probes [16]

MBs do not fluoresce when they are free in solution. When a donor fluorophore is in its excited state, the energy is transferred to an acceptor quencher in close proximity by the stem formation, called fluorescence resonance energy transfer (FRET). FRET occurs due to the interaction between the electronic excited states of two dye molecules. The excitation is transferred from one (the donor) dye molecule to the other (the acceptor) dye molecule without emission of a photon. However, when MBs hybridize to a nucleic acid strand containing a target sequence they undergo a conformational change that enables them to fluoresce brightly. When the probe

encounters a target molecule, the loop region of the MBs forms more stable hybrids with the target than the stem hybrid. The stem part will therefore open up and cause the fluorophore and the quencher to move away from each other. This event is accompanied by an increase in fluorescence emission which implied that the hybridization to the complementary target has occurred.

One of the advantages of the MB is that the light-up signaling mechanism allows MB to perform highly sensitive detection and monitoring of nucleic acids in real time. Because of its usually low background signal, MB can display a fluorescence enhancement of more than 200 times upon hybridization of its target, under optimal conditions [17]. This provides the MBs with a significant advantage in sensitive analysis. MBs can be used in detection without separation of the probe–target hybrids from an excess of the unhybridized probes. Only hybridized MBs, whose amount is proportional to that of the target can produce high fluorescence signal. The excess MBs are in quenched state and therefore there is no need to remove the hybridized and unhybridized MB. A variety of applications of MB to DNA or RNA detection have been developed. Detection of single point mutations can be achieved by MB through careful design of the sequence and selection of the detection temperature [18–20]

1.3 Quencher-free molecular beacon probes

Recently, it has been shown that certain oligonucleotide probes carrying just one fluorophore can function as MB even without the attachment of quencher moiety and can be called ‘‘quencher-free molecular beacons (quencher-free MBs)’’. Like normal MBs, the quencher-free MBs must be able recognize the complementary DNA in a sequence specific manner [21]. There must be some mechanism to quench the fluorophore, e.g. by stacking with a nucleobase such as G. Alternatively, the fluorophore may be in the dark state due to free rotation in the single stranded probe, and become fluorescence upon intercalation or binding to the groove of the hybridized probe. For example, Kim and co-workers designed and prepared a quencher-free MB containing fluorescent nucleoside analogue at the middle position of the hairpin as fluorescent DNA probe. The fluorescent base analogue, U^{FL}, having a fluorene

anchored to the nucleobase of deoxyuridine through an ethynyl linker via Sonogashira coupling, and was incorporated it into the central position of the hairpin loop (**Figure 1.3**). This quencher-free-MB can be successfully used for detection of SNP in oligonucleotides. The increased fluorescence on hybridization is due to disruption of quenching interactions in the single-stranded probe DNA between the fluorophore and nucleobases [22].

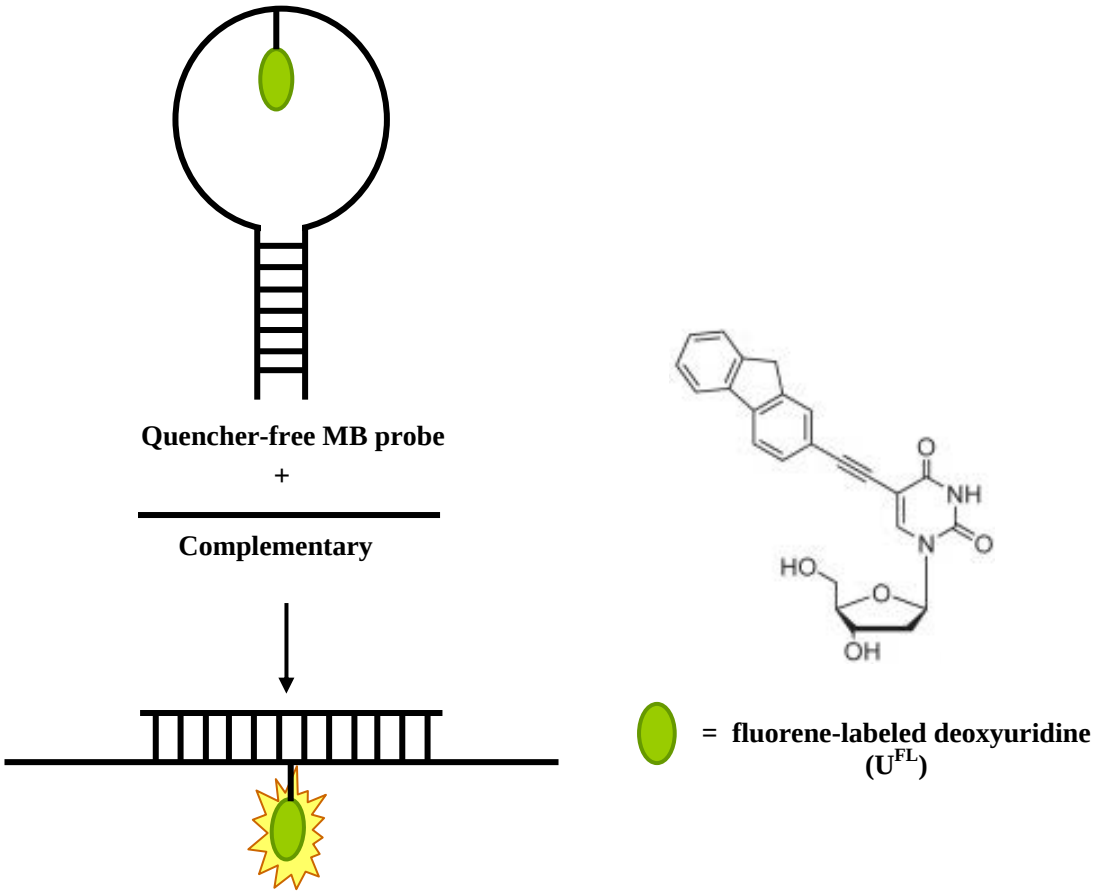

Figure 1.3 Schematic illustration of quencher-free MBs DNA sensor for SNPs typing and a fluorene unit $\mathbf{U^{FL}}$ [22]

1.4 Binary probes

Two short probes (7 to 10 nucleotide) designed to bind to adjacent positions on a target DNA sequence are known binary-probes [23]. Each probe was labeled with a fluorophore, one at the 3′ and the other at 5′ ends. The two fluorophores are

chosen in such a way that they can interact by FRET, for example one probe is labeled with a donor and the other probe is labeled with an acceptor fluorophore. After hybridization of both probes to the complementary oligonucleotide target at the designed adjacent locations, the donor and acceptor fluorophores are in close proximity and result in generation of a FRET signal (**Figure 1.4**).

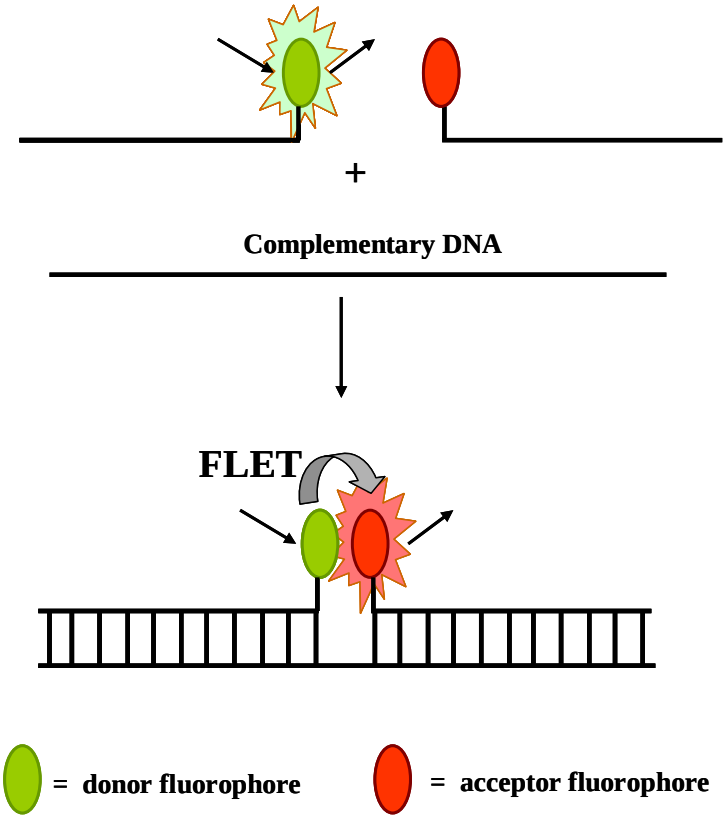

Figure 1.4 Schematic representation of binary probe [23]

In a related an example, Marti *et al.* described the binary probe system in which the both strands were labeled with pyrene [24]. When the two probes are free in solution, the pyrene groups are separated from each other and pyrene monomer fluorescence is observed. When the two probes are hybridized to the target, the pyrene groups are close to one another, and the pyrene excimer emission is observed. This probe was showed strong excimer emission peak in the presence of the DNA target and no excimer emission in the absence of the target. This system was also used for unambiguous detection of mRNA by time-resolved fluorescence spectroscopy.

1.5 Fluorescent modified nucleosides

Replacement of the natural nucleobase with aromatic hydrocarbons or heterocycles has resulted in modified nucleosides with fluorescent properties. These can be accommodated within oligonucleotides although they do not form conventional base pairs. Occasionally even molecules that lack the ability to form hydrogen bonds to the natural. Balakin *et al.* reported the incorporation of dual pyrene chromophores into oligonucleotides at the middle of sequence (**Figure 1.5**) [25]. The significant changes to the pyrene fluorescence were observed upon hybridization of the complementary sequences, which were excimer formation between the two pyrene groups. The pyrene as fluorophore was selected to label on DNA probes because of the sensitivity of pyrene fluorescence to its microenvironment.

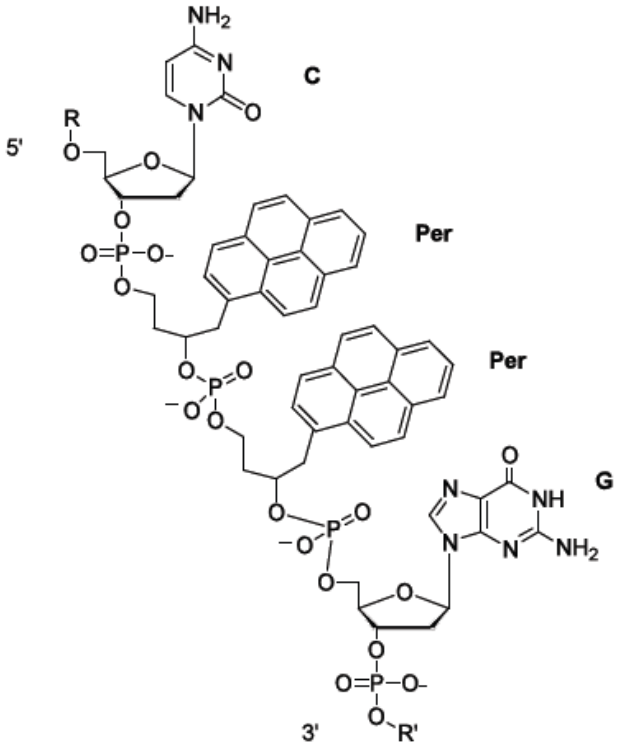

Figure 1.5 Pyrene groups incorporated into an oligonucleotide strand [25]

1.6 Base discriminating fluorescent nucleotides

All nutural nucleobases involved in replication have very low fluorescence quantum yields. Fluorescent nucleoside probes and oligonucleotides were designed and implemented, by attached the fluorophore moiety to the nucleobase, to elucidate fundamental biochemical transformations. Fluorescent nucleoside analogs those are sensitive to the environment, demonstrating changes in the fluorescent properties when induced by changes in polarity, pH, or even structure. Fluorescent nucleosides become powerful tools for the investigation of nucleic acid structure and recognition. To be a useful probe for the study of biological function, the fluorescent nucleotide analogs must have an easily observable emission at physiological conditions and also be sensitive to changes in its environment. Thus, the ideal fluorophore would display differences in emission intensity, or a shift in wavelength of absorbance and emission, or excitation upon changes in its physical environment. Fluorescent modified nucleosides were widely studied as fluorescent probes for single nucleotide polymorphisms (SNPs) detection. Among the fluorescent probes that are most interesting are “base discriminating fluorescent nucleotides” or BDFs as named by Saito and coworkers [26, 27]. The concept of the BDF probes is based on the fluorescence change of the BDF nucleobase itself in response to the bases on a complementary strand. Saito and co-workers performed a chemical modification of 7-de-azaadenosine (**Figure 1.6**) by Sonagashira coupling to incorporate a pyrene moiety directly attached to the adenosine nucleobase [28]. It was found that, upon hybridization of the ^{Py}A strand to the latter four sequences, striking changes occurred in the fluorescence of the pyrene. When DNA containing mismatched base, it was found that the pyrene emission at 390 nm was not perturbed. However, upon hybridization with the strand with correct base pair (T) opposite to the ^{Py}A residue, fully complementary sequence, that the emission was effectively switched off, less than the fluorescence of the single stranded ^{Py}A. The mechanism of the quenching was believed to arise from intercalation of the pyrene unit into the double stranded DNA. Under mismatch conditions i.e. when X = A, C and G the pyrene did not intercalate, due to steric blocking of the mismatched base pair. As the signal is switched on under the condition of base mismatch the potential of BDF nucleotides.

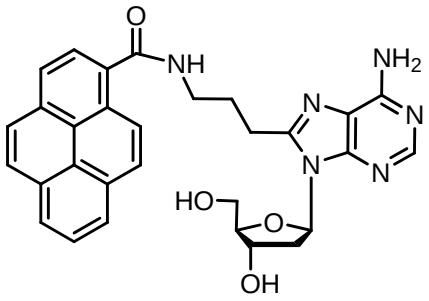

^{Py}A

Figure 1.6 Chemical structure of nucleosides ^{Py}A

In another related work, pyrenecaboxamide-labeled uracil (^{Py}U) and cytosine (^{Py}C) nucleobases were synthesized as a BDF base for use in a simple fluoroassay for detection of SNPs by Okamoto *et al*. [29]. The labels were attached at the C5-position of the uridine *via* a propargyl linker (**Figure 1.7**). The results showed that the ^{Py}U and ^{Py}C-containing oligonucleotides behave as base-discriminating fluorescent (BDF) probes that can be used for homogeneous SNPs typing of DNA samples containing BRCA2 SNPs sites (human breast cancer gene). As the signal is switched on, when probes hybridized to target DNA. The results using the probe showed the same as traditional sequencing techniques. It can identify the point mutation in much less time and effort, and presumably at a much reduced cost and with better sensitivity. These BDF bases typically maintain the hybridization properties to complementary oligonucleotide targets.

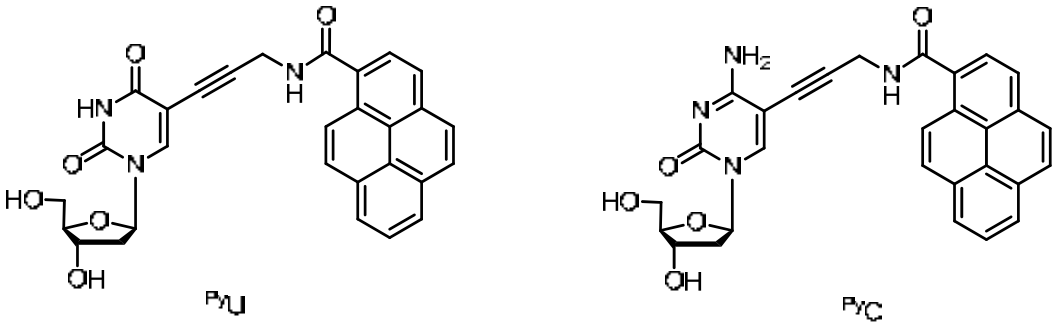

^{Py}U ^{Py}C

Figure 1.7 Chemical structures of nucleosides ^{Py}U and ^{Py}C

Kim and co-workers modified oligodeoxyribonucleotide containing a 5-(1-ethynylpyrenyl)-2'-deoxyuridine (U*) unit at the central position as a probe for SNP detection [30]. The pyrenes were also attached at the C5-position of the uridine using Sonogashira coupling. The single-stranded probe exhibits typical pyrene monomer emission. However, the emission intensities of single-base mismatched duplexes are reduced the fluorescence relative to that of single-stranded probe (**Figure 1.8**). The pyrene-labeled oligonucleotides are therefor sensitive probes that can discriminate between perfect and single-base mismatched by changes in their fluorescence intensities.

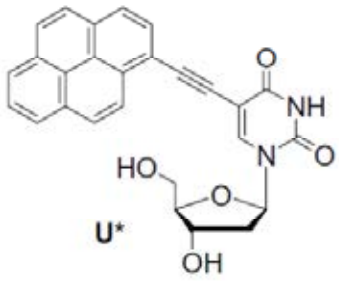

Figure 1.8 Chemical structures of nucleosides U*

Modification of bases with pyrene chromophores has since been a popular synthetic approach to BDF nucleotides. Wagenknecht and co-workers have also used pyrene as a fluorescent sensor for SNPs detection [31]. The pyrene was attached without linker to the guanine base, giving a new fluorobase ^{Py}G (**Figure 1.9**). The DNA duplex hybridization can be observed by fluorescence and absorption spectroscopy since the ^{Py}G group exhibits altered properties in single strands versus double stranded versus double stranded DNA.

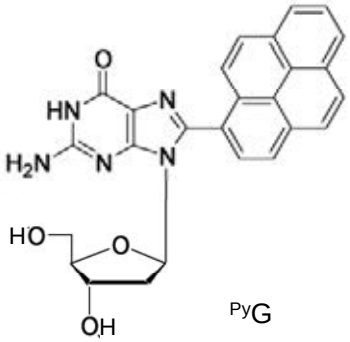

Figure 1.9 Chemical structures of nucleosides ^{Py}G

Next, Saito and co-workers have synthesized oligonucleotide with perylene (^{Per}U) and anthracene (^{2Ant}U, ^{9Ant}U) bases as SNP sensors (**Figure1.10**) [32–33]. As before, the fluorescent chromophore was directly attached to the uracil base under Sonagashira conditions. The perylene labeled-probe was useful for detection of mismatches in short oligonucleotides, displaying an increase in fluorescence at 496 nm for mismatch duplex compared to the complementary duplex. This behaviour was proposed to arise from the expulsion of the intercalating perylene into the bulk polar solvent when a complementary base pair was formed. In the mismatched cases, the perylene could intercalate into the non-polar double-helix and fluorescence were switched off. When anthracene were used as fluorophore, it found that ^{2Ant}U probe be useful as SNPs sensors. The anthracene fluorescence was observed to increase under match conditions. ^{2Ant}U was able to effectively discriminate between A and C in DNA strand.

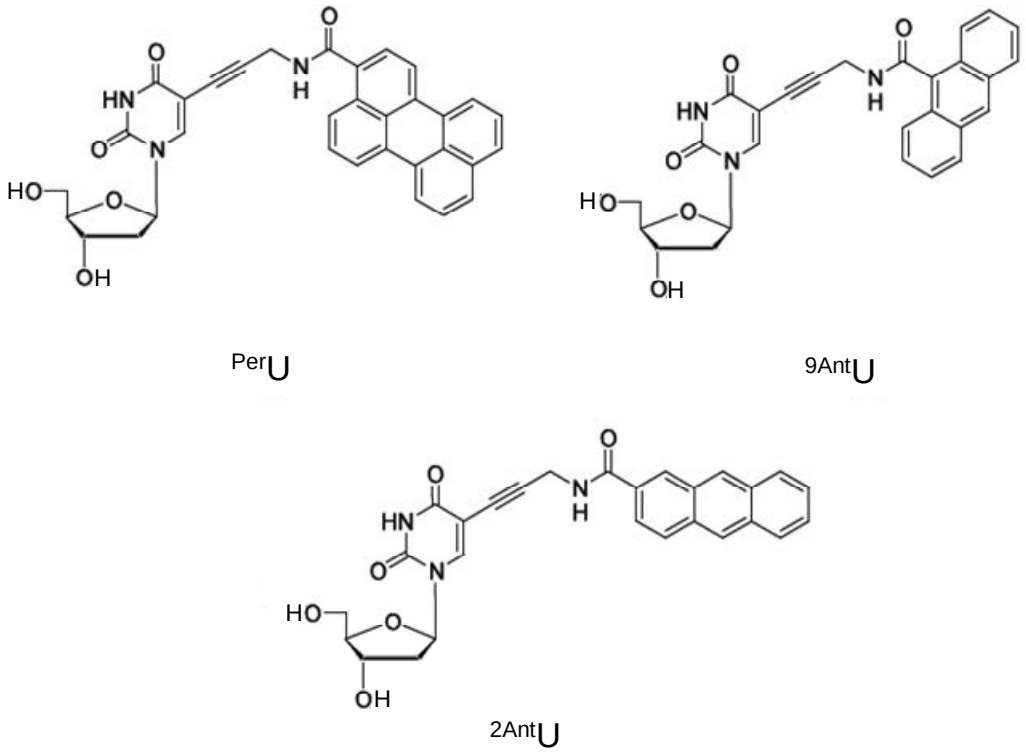

Figure 1.10 Chemical structures of nucleosides ^{Per}U, ^{8Ant}U and ^{2Ant}U

In 2008, Wagenknecht was reported 5-(1-pyrenyl)-2′-deoxyuridine (^{1Py}dU) and 5-(2-Pyrenyl)-2′-deoxyuridine (^{2Py}dU) as fluorescence thymidine analogues (**Figure 1.11**), pyrene chromophore is connected covalently to the 5-position of uridine through a single C–C bond [34]. A pyrene-labeled deoxyuridines were successfully synthesized by Suzuki–Miyaura cross-coupling between 2-(4,4,5,5-tetramethyl-1,3,2-dioxaborolan-2-yl)pyrene and a 5-iodo-2′-deoxyuridine. The ^{1Py}dU and ^{2Py}dU were converted into the corresponding phosphoramidites as DNA building blocks. The ^{2Py}dU shows the ability for Watson–Crick base-pairing inside the DNA, as showed by the absorption and fluorescence spectra. ^{2Py}dU changes its absorption properties upon DNA hybridization and undergoes fluorescence quenching by charge transfer.

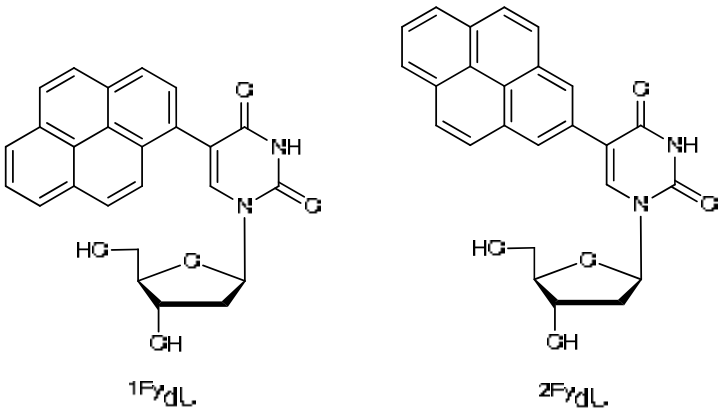

Figure 1.11 Chemical structures of nucleosides ^{1Py}dU and ^{2Py}dU

Brown and co-workers reported the use of the thymine analogues ^{Ne}T, ^{Ae}T, and ^{Aee}T which utilized anthracene and naphthalene fluorophores as SNP sensors (**Figure 1.12**) [35]. Each thymine analogue was found the same behavior, undergoing fluorescence enhancement for a complementary target sequences and quenching for T-G mismatch.

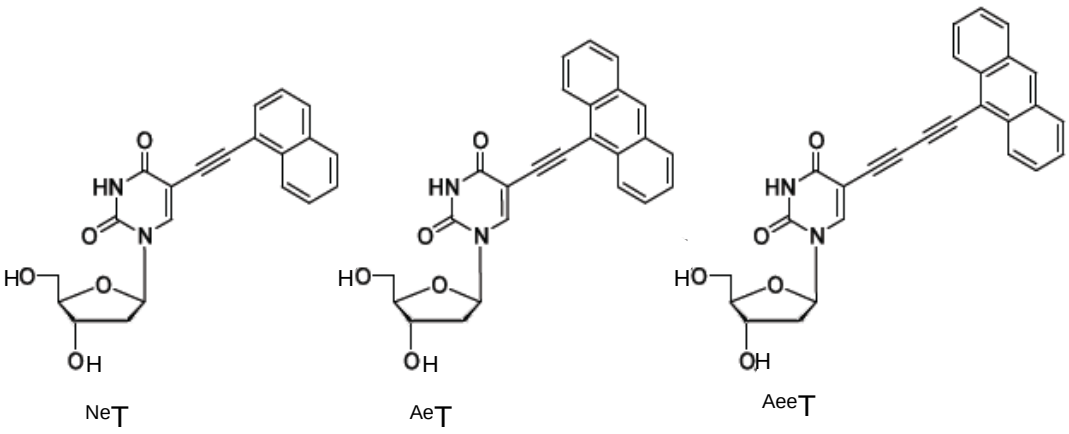

Figure 1.12 Chemical structures of nucleosides ^{Ne}T, ^{Ae}T and ^{Aee}T

1.7 Peptide Nucleic Acid (PNA)

1.7.1 Aminoethylglycyl PNA or aegPNA

Peptide nucleic acid (PNA) are synthetic DNA mimics with an achiral backbone containing repeating units of *N*-(2-aminoethyl)-glycine (aeg) linked together by peptide bonds introduced by Nielsen *et al*. in 1991 [13]. The four nucleobases adenine, cytosine, guanine or thymine (A, C, G or T) are attached to the backbone by methylenecarbonyl linkages. (**Figure 1.13**)

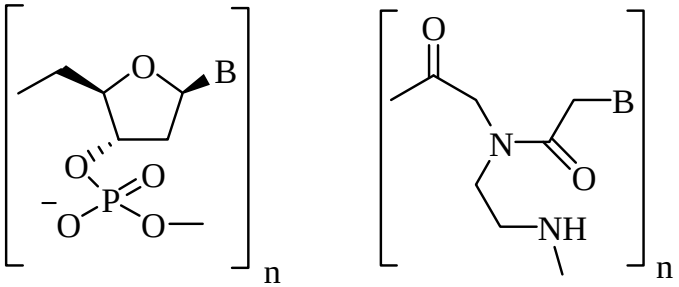

DNA aegPNA

Figure 1.13 Structures of DNA and aegPNA; B = nucleobase (A, C, G or T).

By convention, PNA has an amine-terminus (N-terminus) and a carboxy-terminus (C-terminus), corresponding to the 5'- and 3'-ends of a DNA, respectively (**Figure 1.14**). PNA hybridization to complementary nucleic acids is follows Watson-Crick hydrogen bonding base-pairing rules with the anti-parallel formation prefer [14, 36, 37]. Unlike DNA, aegPNAs do not contain the sugar moieties and phosphate groups. The ribose-phosphodiester backbone of the DNA oligonucleotide was replaced with an achiral uncharged polyamide backbone. The lack of a negative charge on the aegPNA backbone eliminates Coulombic repulsion from target DNA strands, which resulted in a greater binding between complementary aegPNA·DNA than between complementary DNA·DNA at low to medium ionic strength, and they display a stronger resistance to both nuclease and protease digestion [38]. PNAs hybridize specifically to complementary oligonucleotides with also higher affinity

than DNA·DNA or RNA·DNA duplexes. Furthermore, a single base mismatch aegPNA·DNA duplex is generally more destabilizing than a single base mismatch DNA·DNA duplex.

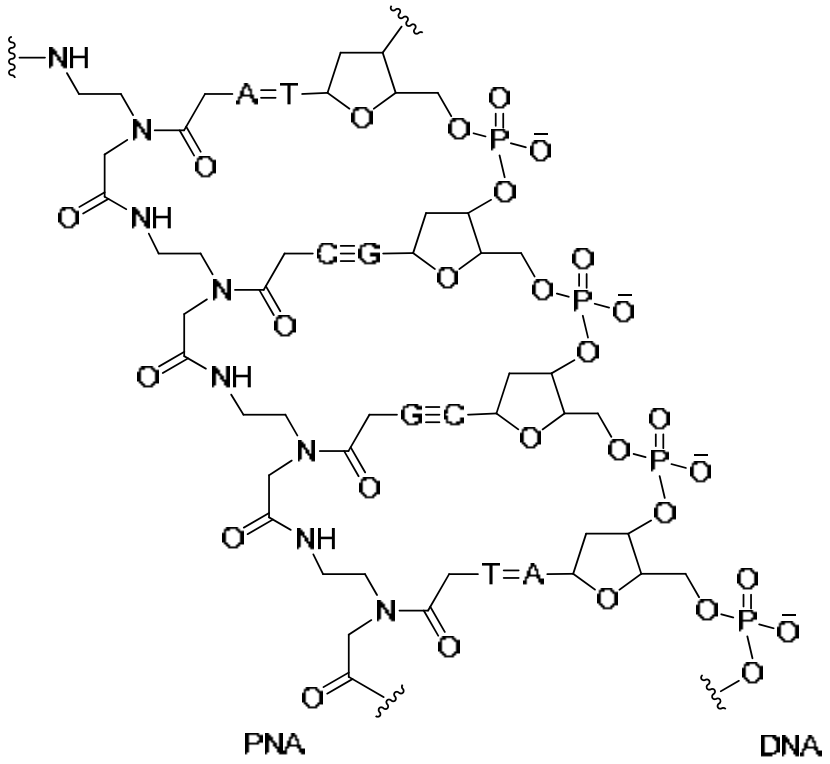

Figure 1.14 Chemical structures of aegPNA molecule and DNA molecule. The amide (peptide) bond characteristic of PNA is boxed in.

1.7.2 Pyrrolidinyl PNA or acpcPNA

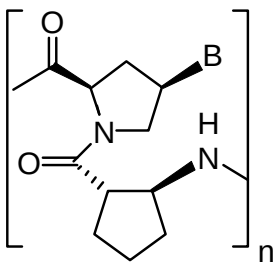

Figure 1.15 Structure of acpcPNA ; B = nucleobase (A, C, G or T).

Pyrrolidinyl PNA bearing a D-prolyl-2-aminocyclopentanecarboxylic acid (ACPC) backbone (denotes as "**acpcPNA**") (**Figure 1.15**) has been developed by Vilaivan *et a*l. in 2005 [39, 40]. Analysis of the DNA hybridization ability of this acpcPNA, suggested this acpcPNA can form PNA·DNA duplex with higher affinity and specificity than the original aegPNA. On the other hand, the acpcPNA showed a much stronger preference for the antiparallel binding fashion (**Figure 1.16**).

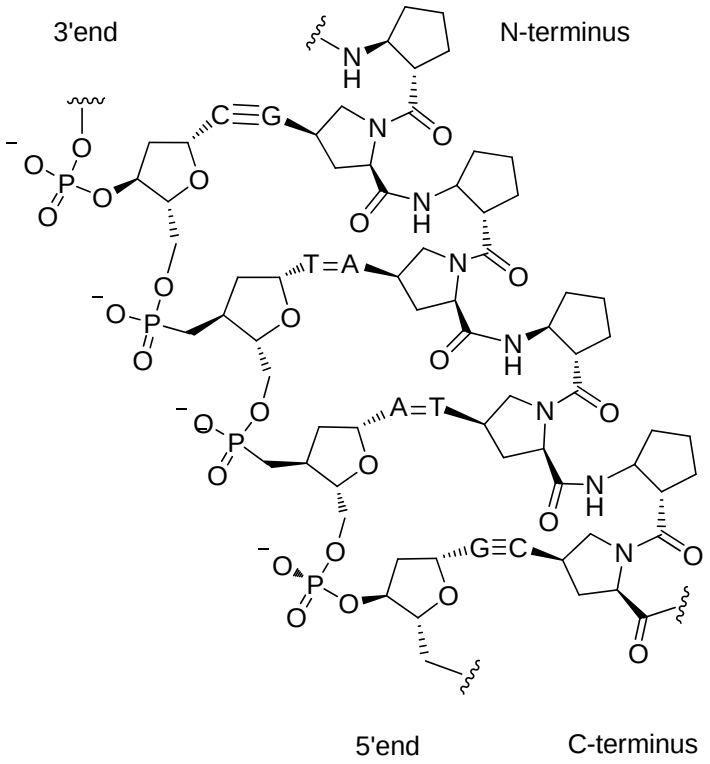

Figure 1.16 Chemical structures of acpcPNA·DNA duplex following Watson-Crick base paring rule.

The high binding affinity to complementary DNA and the powerful discrimination for single mismatched DNA, together with the high directional specificity, render the new acpcPNA system a potential candidate for the development of a highly effective DNA sequence determination. In addition, acpcPNA has been applied as a probe to detect DNA base sequence with various techniques. The high mismatch discrimination ability of the acpcPNA combination with ion-exchange technique led to successful applications in detection of single nucleotide

polymorphisms (SNP) genotyping [41]. The presence of the hybridized PNA in the form of negatively charged PNA·DNA duplex on the positively charged ion-exchanger (Q-sepharose) was analyzed directly by MALDITOF mass spectrometry. Then, Ananthanawat *et al.* used surface plasmon resonance (SPR) technique to demonstrate the performance and hybridization properties of acpcPNA in comparison with DNA, and aegPNA in term of base-pairing specificity or ability to discriminate single base mutation, direction of binding (parallel or antiparallel) [42-43].

Next, Reenabthue and co-worker developed a new ACPC spacer analogue, aza (3*R*,4*S*)-3-aminopyrrolidine-4-carboxylic acid (APC) spacer (**Figure 1.17**), to site-specifically label acpcPNA [44]. The APC-modified acpcPNA contains a secondary amine which can be further labeled with a label (e.g. fluorophore) by acylation *via* an amide bond. To investigate the viability of using APC spacer as a handle for internal modification of acpcPNA with a fluorophore, the pyrene-labeled acpc/apcPNAs were synthesized by acylation chemistry. Pyrene-1-carboxylic acid and 4-(pyrene-1-yl)-butyric acid were chosen as the fluorophore labels. In the single stranded state, the pyrenebutyryl-labeled acpc/apcPNA showed a fluorescence quenching due to strongly interact with the nucleobases of the PNA. Upon hybridization with the complementary DNA, the pyrene-labeled acpc/apcPNA duplex exhibited high fluorescence intensity. Form the result suggests that fluorescence properties of the pyrenebutyryl -labeled acpc/apcPNAs are sensitive to their hybridization state.

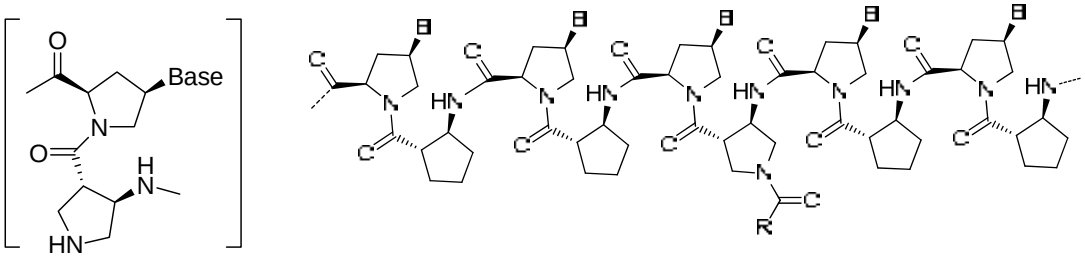

(A) APC-modified acpcPNA (B) Fluorophore-labeled acpc/apcPNAs (R=fluorophore)

Figure 1.17 Chemical structure of (A) : apcPNA, (B) : Fluorophore-labeled acpc/apcPNAs *via* an amide bond

1.8 Self-reporting fluorescence probes derived from PNA

The development of PNA-based fluorescence probes as DNA biosensor had increased considerably over the past few years, most of which rely on the use of original Nielsen's *aeg*PNA. In an early example, Svanvik and co-workers developed a light-up PNA probes for detection of nucleic acid by attaching thiazole orange at *N*-termini of aegPNA (**Figure 1.18**). The single-stranded thiazole orange-labeled PNA probes showed low fluorescence intensities but when they were hybridized with their complementary DNA targets, the fluorescence emissions were markedly increased as a result of interaction between thiazole orange and the hanging part of the DNA strand [45].

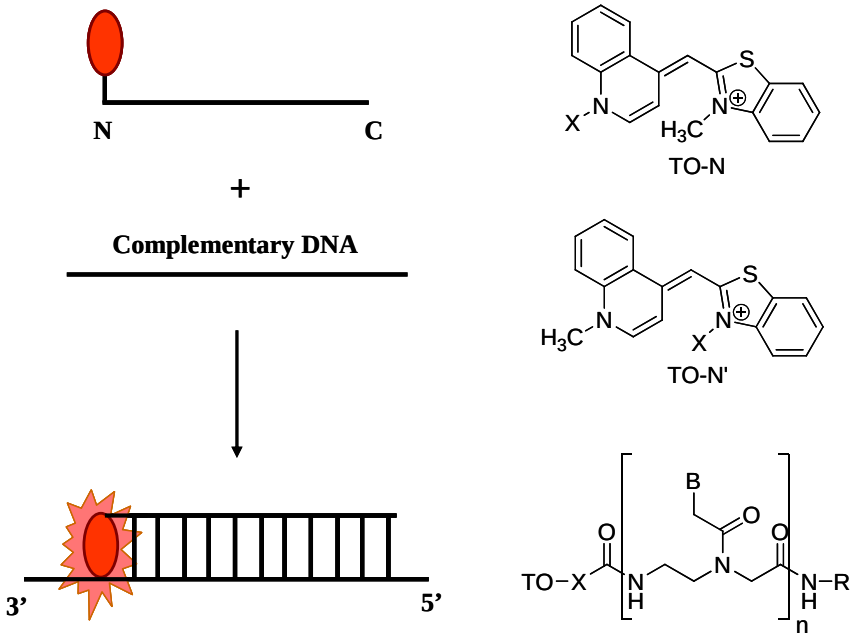

Figure 1.18 Chemical structure and working principle of TO-labeled PNA (light-up probes) [45]

PNA can also be used as molecular beacon probes for DNA sequence determination. In 2002, Kuhn and co-workers reported the use of PNA opener in combination with stemless PNA molecular beacons (PNA-MBs) for direct detection of DNA targets sequence in double stranded DNA [46]. Due to the hydrophobicity of PNA, the fluorophore is in close contact with the quencher in the single stranded state in the aqueous environment without requiring the conventional stem-loop structure as in DNA. Moreover, the use of stemless PNA beacons improved the specificity of the detection against single mismatched targets (**Figure 1.19**).

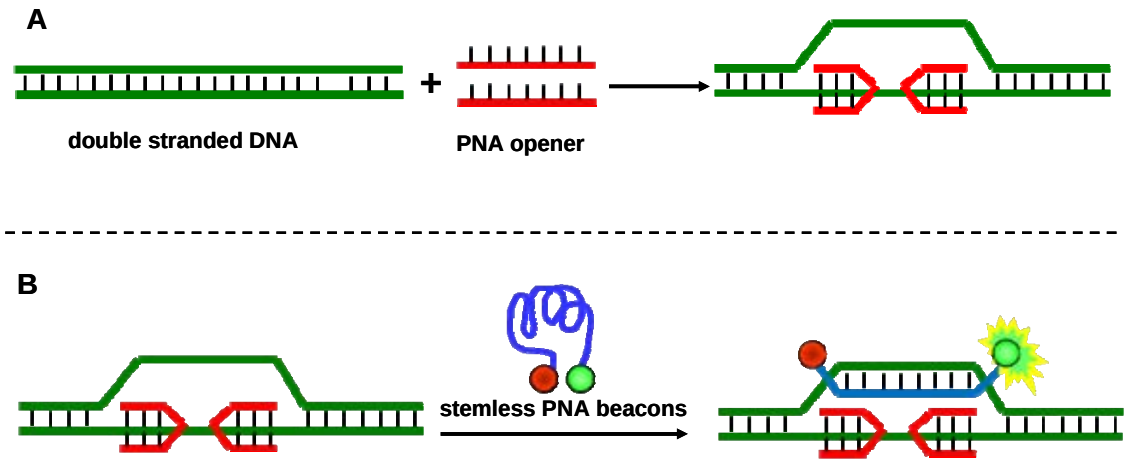

Figure 1.19 Schematic representations of the procedure for hybridization of stemless PNA beacons to double stranded DNA [46]

Recently, Komiyama *et al.* had employed PNA molecular beacons (PNA-MBs) in combination with nuclease S1, an enzyme that specifically hydrolyzes single stranded DNA, as a fluorescent sensor for genotyping of SNPs [47]. The PNA-MBs contained the fluorescein and dabcyl at the *C*- and *N*-terminus respectively. The nuclease S1 rapidly digested the DNA component in the mismatched PNA·DNA hybrids while only slowly digested the complementary hybrid (**Figure 1.20**). As a result, the nuclease S1 digestion in combination with PNA-MBs was a powerful technique to improve the differentiation between complementary and mismatched DNA targets.

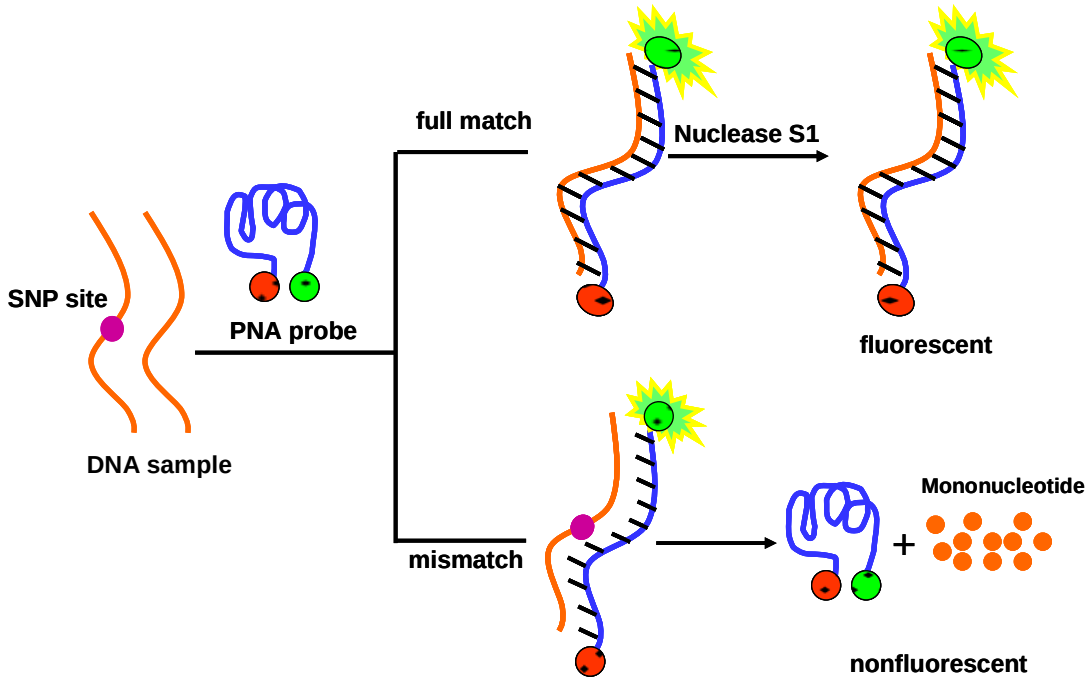

Figure 1.20 Schematic representations for SNPs detection using the combination of PNA-MBs and enzymatic digestion [47]

In 2005, Appella and co-worker reported a prototype of quencher-free molecular beacon PNA probes for DNA sequence detection. The fluorene fluorophore was attached to the side-chain of lysine inserted at an internal position of the PNA strand *via* amide bond formation (**Figure 1.21**) [48]. The fluorene-labeled PNA probes showed an increase in fluorescence emission upon binding to complementary DNA targets, which was explained by the separation of the fluorene chromopore from the nucleobases which act as the quencher.

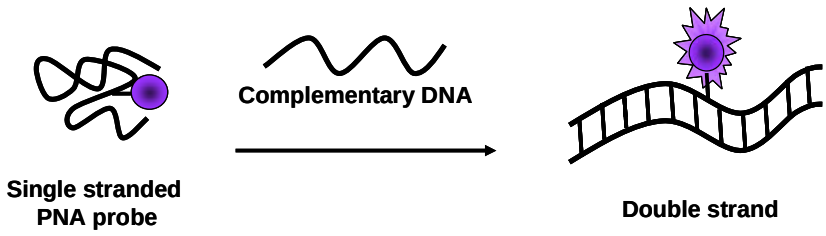

Figure 1.21 Schematic representations and Chemical structure of Fluorene-labeled aegPNA probes **[48]**

In another example of hybridization responsive fluorescent-labeled PNA probe, Socher and co-worker recently described the thaizole orange modified forced intercalation (FIT) PNA probes in 2008 [49]. In this design, one nucleobase of the PNA probe was replaced by a thiazole orange (TO) dye, which behaved as a fluorescent universal base. The duplex of FIT probes with complementary DNA showed a strong fluorescent signal due to the TO dye was stacked in the duplex, thereby enforcing a coplanar arrangement even in the excited state. In presence of single base mismatch DNA, the fluorescent signal of TO dye was significantly lower because of the TO dye could undergo torsional motions that led to rapid depletion of the excited state as illustrated in **Figure 1.22**.

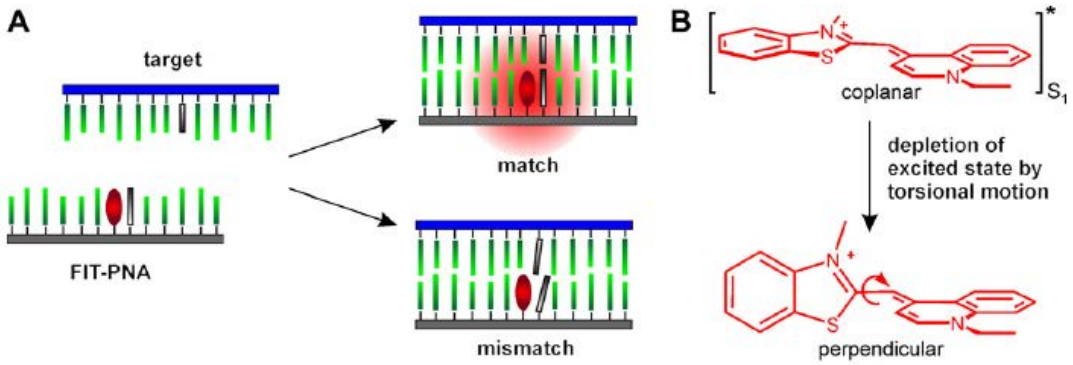

Figure 1.22 Schematic representations of thaizole orange modified forced intercalation (FIT) PNA probes [49]

1.9 Objectives of this research

The objective of this research is to develop a new fluorescence acpcPNA probe that can change the fluorescence properties in response to the presence of correct DNA target that should be sensitive, simple, rapid and cost-effective. We wish to develop quencher-free acpcPNA modified with a single fluorophore, by modification of the nucleobase or the acpcPNA backbone. This research was divided into three parts. In the first part is modification of fluorescence nucleobase (5-pyren-1-yluracil, U^{Py}) as hybridization-responsive fluorescence probe. The second part, the optical properties of acpcPNA modified with a pyrenebutyryl group is also studied. The last part involves development of a single-labeled acpcPNA as a displacement probe.

CHAPTER II

EXPERIMENTAL SECTION

2.1 General Procedures

2.1.1 Materials

All chemicals were purchased from standard suppliers and were used as received. Commercial grade solvents for column chromatography were distilled before use. Solvents for the reactions were AR grade and used without purification. Methanol and acetonitrile for HPLC experiment were HPLC grade, obtained from BDH and were filtered through a membrane filter (13 mmϕ, 0.45 μm Nylon Lida) before use. Unless otherwise stated, all reactions were performed in oven-dried glasswares under ambient conditions. Tetrahydrofuran (THF) for Mitsunobu reaction was dried by refluxing with fresh thin-cut sodium metal and benzophenone under nitrogen atmosphere. Nitrogen gas was obtained from TIG with 99.9 % purity. The progress of the reaction was followed by thin layer chromatography (TLC) performed on Merck D.C. silica gel 60 F_{254} 0.2 mm pre-coated aluminium plates cat. no. 1.05554 and visualized using UV light (254 nm). Column chromatography was performed on silica gel 70-230 mesh for column chromatography.

For solid phase peptide synthesis, anhydrous *N*,*N*′-dimethylformamide (DMF) for solid phase peptide synthesis was obtained from RCI Labscan (Thailand) and was dried over activated 3Å molecular sieves. The solid support for peptide synthesis (TentaGel S RAM Fmoc resin) was obtained from Fluka. The protected amino acids, Fmoc-L-Lys(Boc)-OPfp was obtained from Calbiochem Novabiochem Co., Ltd. (USA). Piperidine, trifluoroacetic acid (TFA), 1,8-diazabicyclo[5.4.0]undec-7-ene (DBU), O-(7-azabenzotriazol-1-yl)-*N*,*N*,*N*′,*N*′-tetramethyluronium hexafluoro-phosphate (HATU) and *N*,*N*-diisopropylethylamine (DIEA) were purchased from Fluka. Acetic anhydride was prepared by distillation of acetyl chloride and sodium acetate. 1-Hydroxy-7-azabenzotriazole (HOAt) was purchased from Avocado. Oligonucleotides were purchased from the Pacific Science Co.,Ltd. (Thailand) and

BioDesign Co., Ltd. (Thailand). All aqueous solutions were made with MilliQ water, obtained by purification with a Millipak® 40 filter unit (0.22 μm, Millipore, USA).

2.1.2 Equipment

Optical rotations ($[\alpha]_D$) were measured on a Jasco P-1010 Polarimeter using sodium light (D line, 589.3 nm). Evaporation of solvents was carried out on Büchi Rotavapor R-124 with a water aspirator model B-490 or a Refco Vacuubrand pump or a diaphragm pump. ^{1}H and ^{13}C NMR spectra were recorded in deuterated solvents on a Bruker Avance 400 or Varian Mercury 400+, operating at 400 MHz (^{1}H) and 100 MHz (^{13}C), respectively. High resolution mass spectra were recorded in positive ESI mode on a Bruker Daltonics micrOTOF mass spectrometer (Faculty of Science, Mahidol University). IR spectra were recorded on Nicolet iS10 FT-IR spectrometer. Reverse phase HPLC experiments were performed on Water Delta 600™ system equipped with gradient pump and Water 996™ photodiode array detector. An ACE® C18-AR HPLC column (4.6×150 mm, 5 μ particle size) was used for analytical purposes. MALDI-TOF mass spectra were obtained on a Bruker Daltonics Microflex Instrument in positive linear mode using doubly recrystallized α-cyano-4-hydroxy cinnamic acid (CCA) as matrix. Melting temperature (T_m) measurements of PNA·DNA duplex and UV/vis spectra were performed on a CARY 100 Bio UV-Visible spectrophotometer (Varian, Inc., USA) equipped with a thermal melt system. The fluorescence spectra were recorded on Varian Cary Eclipse Fluorescence Spectrophotometer. CD experiments were performed on JASCO Model J-815 spectrometer (JASCO).

2.2 Experimental Procedure

2.2.1 Synthesis of pyrrolidinyl PNA monomers, ACPC spacer, and APC spacer

Pyrrolidinyl PNA monomers namely (*N*-Fluoren-9-ylmethoxycarbonylamino)-*cis*-4-(N^6-benzoyladenin-9-yl)-D-proline pentafluorophenyl ester, (*N*-Fluoren-9-yl methoxycarbonylamino)-*cis*-4-(N^4-benzoylcytosine-9-yl)-D-proline pentafluorophenyl

ester, (*N*-Fluoren-9-ylmethoxy carbonylamino)-*cis*-4-(N^2-isobutyrylguanin-9-yl)-D-proline pentafluorophenyl ester, (*N*-Fluoren-9-ylmethoxycarbonylamino)-*cis*-4-(thymin-1-yl)-D-proline, and ACPC spacer namely (1*S*,2*S*)-2-(*N*-Fluoren-9-ylmethoxycarbonyl)-aminocyclopentane carboxylic acid pentafluoro phenyl ester were synthesized according to Vilaivan and co-workers [39, 40]. The APC spacer (3*R*,4*S*)-1-(2,2,2-trifluoroacetyl)-3-(9*H*-fluoren-9-yl-methoxycarbonyl amino)-pyrrolidine-4-carboxylic acid pentafluorophenyl ester was synthesized according to Suparpprom and co-workers [44].

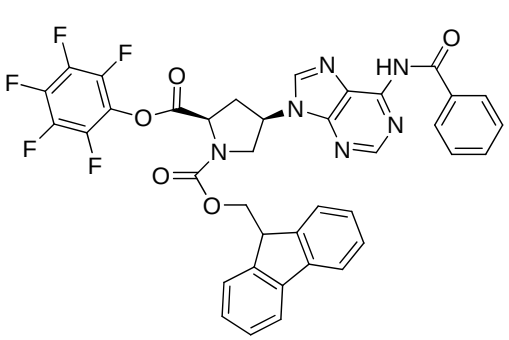

Fmoc-A^{Bz}-OPfp

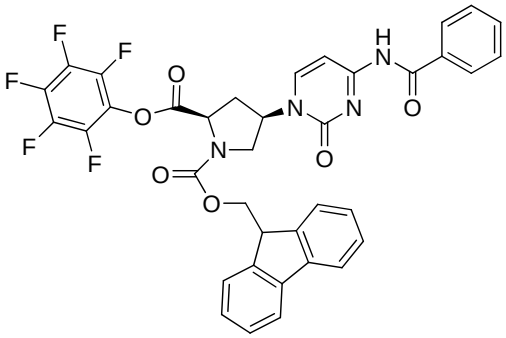

Fmoc-C^{Bz}-OPfp

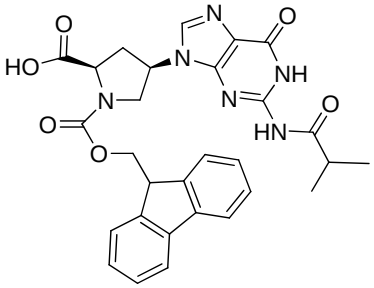

Fmoc-G^{Ibu}-OH

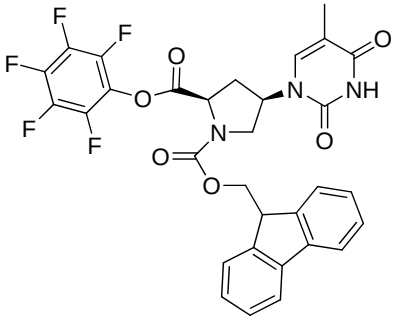

Fmoc-T-OPfp

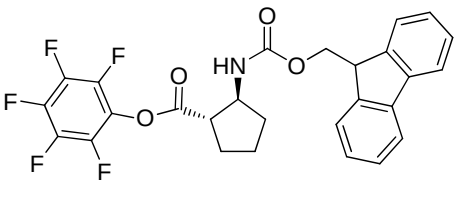

(1*S*,2*S*)-ACPC-OPfp

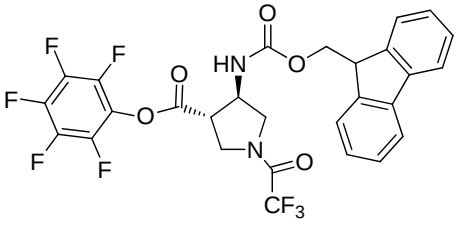

(3*R*,4*S*)-APC-OPfp

Figure 2.1 Structure of activated acpcPNA monomers, ACPC spacer and APC spacer for solid phase peptide synthesis

2.2.2 Synthesis of the U^{Py}-pyrrolidinyl PNA monomer

2.2.2.1 *N*-*tert*-Butoxycarbonyl-*cis*-4-(N^3-benzoyl-5-iodouracil-1-yl)-D-proline diphenylmethyl ester (3)

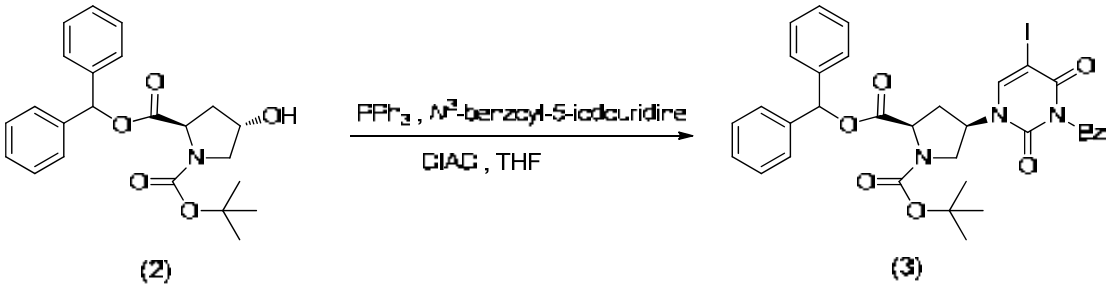

(2) (3)

N-*tert*-Butoxycarbonyl-*trans*-4-hydroxy-D-proline diphenylmethyl ester (0.9938 g, 2.5 mmol), triphenylphosphine (**2**) (0.7213 g, 2.75 mmol) and N^3-benzoyl-5-iodouridine (0.9407 g, 2.75 mmol) were dissolved in dry THF (10 mL) with stirring and cooled down to 0 °C in an ice-salt bath. The reaction mixture was slowly added DIAD (3.7 mL, 18.8 mmol) *via* syring with in 15 min and allowed to stir under nitrogen at rt for 24 h. The solvent was evaporated and the residue was directly recrystallized from ethanol to afford the product (**3**) as white solid (0.5424 g, 47% yield). $[\alpha]^{25}_{D}$ = +50.2 (*c*=1.0 g/100 mL $CHCl_3$); ^{1}H NMR (400 MHz, $CDCl_3$) (**Figure A1**): δ = 1.33 and 1.51 (2×s, 9H; CH_3Boc), 2.05 [m, 1H; 1×CH_2(3′)], 2.85 [m, 1H; 1×CH_2(3′)], 3.59, and 3.73 [m, 1H; 1×CH_2(5′)], 4.02 [m, 1H; 1×CH_2(5′)], 4.52 and 4.61 [m, 1H; CH(4′)] 5.19 [m, 1H; CH(2′)], 6.99 (s, 1H; CHPh_2), 7.29 (s, 1H; C6H Thymine), 7.37 (m, 10H; Phenyl Dpm), 7.51 [dd, *J* = 7.0, 7.4 Hz, 2H; CH(3,5) ArBz], 7.68 [t, *J* = 7.1 Hz, 1H; CH(4) ArBz], 7.88 [m, 2H; CH(2,6) ArBz]; ^{13}C NMR (100 MHz, $CDCl_3$) (**Figure A2**): δ = 28.1 and 28.3 (CH_3Boc rotamers), 34.2 and 35.9 [CH_2(3′) rotamers], 49.6, 49.9 [CH(5′) rotamers], 53.3 and 53.7 [CH(4′) rotamers], 57.4 and 57.5 [CH(2′) rotamers], 68.4 (C5 Thymine), 78.3 and 78.5 (C CH_3Boc rotamers), 81.6 (CH Dpm), 127.1-128.8 (CH ArDpm), 129.2 (C4′ Ar), 130.5 (C2′ and C6′ Ar), 130.9 (C3′ and C5′ Ar), 135.3 (C1′ Ar), 139.2 (C6H Thymine), 149.6 (C Dpm), 153.4 (C2 Thymine), 158.5 (C4 Thymine), 167.4 (CO Boc), 171.2 (CO

Proline); HRMS (FAB+): *m/z* calcd for $C_{34}H_{32}O_7N_3INa$: 744.1183 $[M+Na]^+$; found: 744.1105.

2.2.2.2 *N*-*tert*-Butoxycarbonyl-*cis*-4-(5-(1-pyrenyl)uracil-1-yl)-D-proline diphenylmethyl ester (4)

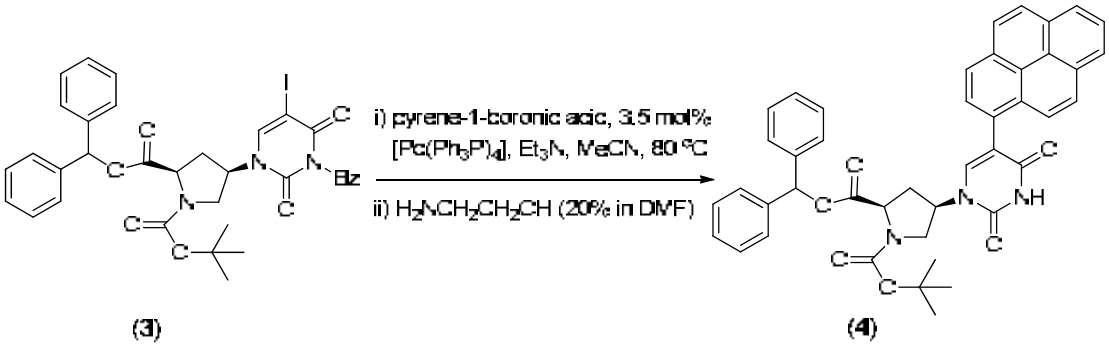

A round bottom flask was charged with *N*-*tert*-butoxycarbonyl-*cis*-4-(N^3-benzoyl-5-iodouracil-1-yl)-D-proline diphenylmethyl ester (**3**) (0.3430g, 0.475 mmol), 1-pyreneboronic acid (0.1862g, 0.755 mmol) and tetrakis(triphenylphosphine) palladium [$Pd(PPh_3)_4$] (0.0200g, 0.0165 mmol). The air in the flask was removed and replaced with dry nitrogen. Degassed CH_3CN (3 mL) was subsequently added and the reaction was stirred and heated to 80 °C under nitrogen. Triethylamine (0.3 mL, 0.500 mmol) was added to the reaction mixture *via* syringe and kept stirring for 40 h (the reaction was monitored by TLC). When the starting material was completely consumed, the solvent was removed under reduced pressure and the residue was separated by column chromatography eluting with CH_2Cl_2: acetone (30:1) on silica gel to obtain the yellowish oil which was further treated with ethanolamine (0.2 mL) in DMF (1 mL) for 20 min. After the reaction was finished as indicated by TLC, the residue was dissolved in CH_2Cl_2 (20 mL). The organic layer was washed with 10% HCl (2×15 mL), dried with Na_2SO_4 and the solvent was removed. The residue was purified by column chromatography eluting with hexanes:ethyl acetate (1:1) on silica gel to obtain the title compound (**4**) as an off-white solid (0.2010 g, 60% yield). $[\alpha]^{25}_D$ = +46.6 (*c*=1.0 g/100 mL $CHCl_3$); ^{1}H NMR (400 MHz, $CDCl_3$) (**Figure A3**): δ = 1.33 and 1.51 (2×s, 9H; C<u>H</u>$_3$Boc), 2.05 [m, 1H; 1×C<u>H</u>$_2$(3′)], 2.85 [m, 1H; 1×C<u>H</u>$_2$(3′)], 3.59 and 3.73 [m, 1H; 1×C<u>H</u>$_2$(5′)], 4.02 [m, 1H; 1×C<u>H</u>$_2$(5′)], 4.52 and 4.61 [m, 1H;

C<u>H</u>(4′)], 5.19 [m, 1H; C<u>H</u>(2′)], 6.87 (s, 1H; C<u>H</u>Ph_2), 7.25 (s, 1H; C6<u>H</u> Thymine), 7.28-7.51 (m, 10H; Phenyl Dpm), 7.86-8.24 (m, 9H; C<u>H</u> Pyr), 9.09 (s, 1H; NH Thymine); ^{13}C NMR (100 MHz, $CDCl_3$) (**Figure A4**): δ = 28.0 and 28.3 (<u>C</u>H_3 Boc rotamers), 34.2 and 35.5 [<u>C</u>H_2(3′) rotamers], 49.0 and 49.4 [<u>C</u>H(5′) rotamers], 52.8 and 53.6 [<u>C</u>H(4′) rotamers], 57.3 and 57.5 [<u>C</u>H(2′) rotamers], 77.9 and 78.2 (<u>C</u>CH_3 Boc rotamers), 81.3 (<u>C</u>H Dpm), 115.7 (<u>C</u>5 Thymine), 126.8-128.6 (<u>C</u>H ArDpm), 129.1 (<u>C</u>4′ Ar), 130.4 (<u>C</u>1′ and <u>C</u>6′ Ar), 135.0 (<u>C</u>3′ and <u>C</u>5′ Ar), 135.8 (<u>C</u>1′ Ar), 139.2 (<u>C</u>6H Thymine), 150.7 (<u>C</u>Dpm), 153.3 (<u>C</u>2 Thymine), 161.8 (<u>C</u>4 Thymine), 168.7 (<u>C</u>O Boc), 170.9 (<u>C</u>O Proline); HRMS (FAB+): *m/z* calcd for $C_{43}H_{37}O_7N_3Na$: 714.2580 $[M+Na]^+$; found: 714.2519.

2.2.2.3 *N*-Fluoren-9-ylmethoxycarbonyl-*cis*-4-(5-(1-pyrenyl)uracil-1-yl)-D-proline (1)

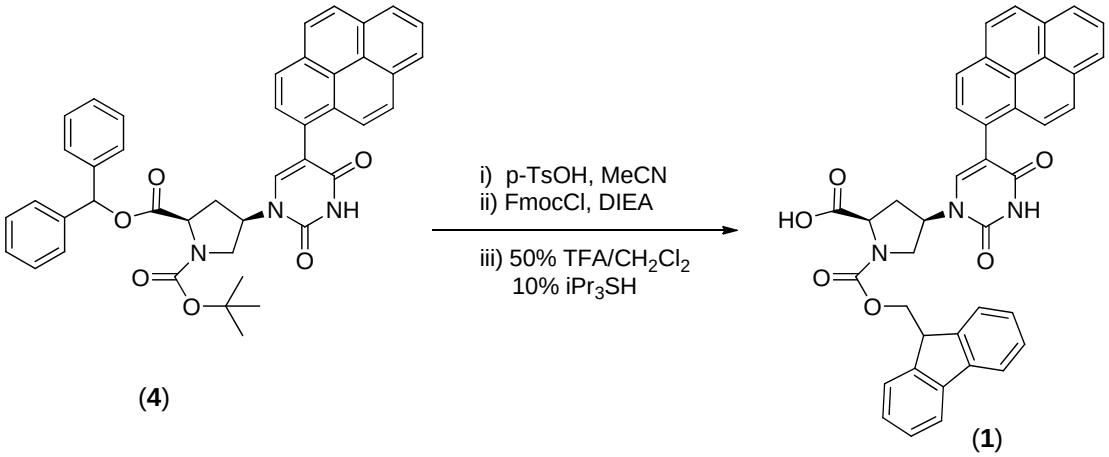

N-tert-Butoxycarbonyl-*cis*-4-(5-(1-pyrenyl)uracil-1-yl)-D-proline diphenyl methyl ester (**4**) (0.1200 g, 0.170 mmol) was stirred with *p*-toluenesulfonic acid monohydrate (0.0950 g, 0.5 mmol) in MeCN (2 mL) for 3 h at room temperature. After the Boc deprotection was complete (monitored by TLC), diisopropylethylamine (DIEA) (150 μL, 0.85 mmol) was added to the reaction mixture followed by addition of 9-fluorenylmethoxycarbonyl chloride (0.0660 g, 0.255 mmol). After the reaction was completed as indicated by TLC, the solvent was removed and the residue was purified by column chromatography on silica gel eluting with hexanes:ethyl acetate (1:1) to give the protected intermediate, *N*-fluoren-9-ylmethoxycarbonyl-*cis*-4-(5-(1-

pyrenyl)uracil-1-yl)-D-proline diphenylmethyl ester, as a white solid (0.0954g). This solid was treated with trifluoroacetic acid:CH_2Cl_2 (1:1) containing 10% triisopropylsilane (1 mL) and left at rt for 30 min. After that, the solvent was removed by a gentle stream of nitrogen. The residue was triturated and washed with diethyl ether to give a white solid which was collected by filtration (0.0600g, 55% yield). $[\alpha]^{25}_D$ = -4.7 (*c*=1.0 g/100 mL DMF); ^{1}H NMR (400 MHz, CD_3OD) (**Figure A5**): δ = 2.35 and 2.35 [2×m, 1H; 1×C$\underline{H}_2$(3′) rotamers], 2.60 and 2.78 [2×m, 1H; 1×C$\underline{H}_2$(3′) rotamers], 3.73 [m, 1H; 1×C$\underline{H}_2$(5′) rotamers], 3.90 [m, 1H; 1×C$\underline{H}_2$(5′) rotamers], 4.17 (m, 1H; C$\underline{H}$Fmoc), 4.34 (m, 2H; C$\underline{H}_2$Fmoc), 4.31 and 4.43 [2×m, 1H; C$\underline{H}$(2′) rotamers], 5.13, 5.27 [2×m, 1H; C$\underline{H}$(4′) rotamers], 7.02-7.21 (m, 2H; C$\underline{H}$ Fmoc), 7.31-7.37 (m, 2H; C$\underline{H}$ Fmoc), 7.50-7.61 (m, 2H; C$\underline{H}$ Fmoc), 7.66-7.75 (m, 2H; C$\underline{H}$ Fmoc), 7.92 (s, 1H; C6$\underline{H}$ Thymine)8.00-8.23 (m, 9H; C$\underline{H}$ Pyr); ^{13}C NMR (100 MHz, CD_3OD) (**Figure A6**): δ = 34.2 and 34.9 [$\underline{C}H_2$(3′) rotamers], 46.9 ($\underline{C}$H Fmoc), 48.8 and 49.3 [$\underline{C}$H(5′) rotamers], 53.2 and 54.2 [$\underline{C}$H(4′) rotamers], 58.6 and 58.9 [$\underline{C}$H(2′) rotamers], 67.4 and 68.0 ($\underline{C}H_2$ Fmoc rotamers), 119.4 ($\underline{C}$H ArFmoc), 124.4 ($\underline{C}$5 Thymine), 124.5 (CH Pyr),124.6 (CH Pyr), 124.8 ($\underline{C}$H Pyr), 124.9 ($\underline{C}$ Pyr), 125.0 ($\underline{C}$H Pyr), 125.1 ($\underline{C}$Pyr), 125.7 ($\underline{C}$H ArFmoc), 126.7 ($\underline{C}$H Pyr), 126.8 ($\underline{C}$ Pyr), 127.0 ($\underline{C}$H Pyr), 127.3 ($\underline{C}$H Pyr), 127.4 ($\underline{C}$H Pyr), 127.7 ($\underline{C}$H ArFmoc), 128.5 ($\underline{C}$H ArFmoc), 130.0 ($\underline{C}$ Pyr), 130.9 ($\underline{C}$Pyr), 131.3 ($\underline{C}$Pyr), 131.4 ($\underline{C}$H Pyr), 141.1 ($\underline{C}$H ArFmoc), 143.6 ($\underline{C}$6H Thymine), 144.1 ($\underline{C}$ArFmoc),151.5 ($\underline{C}$2 Thymine), 154.9 and 155.2 ($\underline{C}$O Fmoc), 163.7 ($\underline{C}$4 Thymine) 173.1 and 173.7 ($\underline{C}$O Proline rotamers); HRMS (FAB^+): *m/z* calcd for $C_{40}H_{29}N_3O_6Na$: 670.1954 $[M+Na]^+$; found: 670.1923.

2.2.3 The procedure for solid phase synthesis of PNA

2.2.3.1 Preparation of reaction column and apparatus for solid phase synthesis

All peptide oligomers were synthesized in a custom-made peptide synthesis column equipped with a fritted glass tip as described previously [50]. The Tentagel S-RAM resin (2.4–7.1 mg, equivalent to 0.5–1.5 μmol), was weighed accurately into the column, and the column was equipped with a rubber teat. The resin was swollen in

anhydrous DMF for at least 15 min before use. For each reaction, the reagent was directly sucked in, holds on or ejected out by manual control for the specified period of time. After the reaction was complete in each step, the resin was washed with DMF in order to eliminate the excess reagent.

Synthesis of each U^{Py}-acpcPNA, and pyrene-modified acpcPNA were carried out on 1.5 μmol scale. Three reagents for solid phase peptide synthesis were prepared as follows.

1. **Reagent #1** (Deprotection solution) consists of 20% piperidine and 2% DBU in anhydrous DMF
2. **Reagent #2** (DIEA stock for coupling and capping) that consists of 7% DIEA in anhydrous DMF
3. **Reagent #3** (HOAt stock solution) consists of HOAt (5.5 mg) in anhydrous DMF (100 μL)

2.2.3.2 Solid Phase Peptide Synthesis Protocol

Solid phase synthesis is a process by which chemical transformations are carried out on a solid support. Solid phase synthesis of acpcPNA oligomers consists of three major steps as follows:

i) Removal of the *N*-terminal Fmoc group from the growing PNA oligomer
ii) Coupling of the PNA monomers onto the N-terminus of the growing PNA chain
iii) Capping of the unreacted amino group

Each of the steps in the synthesis has been previously optimized for the preparation of acpcPNA oligomers [50]. After coupling of last monomer, the resin-bound PNA was end-capped, side-chain deprotected and cleaved from the resin using the appropriate reagents [50–51]. The general synthesis protocol was divided as follows:

i) Removal of the N-terminal Fmoc protection group of the resin

The reaction column was charged with TentaGel S-RAM Fmoc resin (7.1 mg, 1.5 μmol). The pre-swollen resin was treated 100 μL of deprotection solution (**reagent #1**) in a 1.5 mL eppendorf tube at room temperature for 5 min with occasional agitation. After the specified period of time, the **reagent #1** was squeezed off and the resin was exhaustively washed with DMF.

ii) Anchoring with the first amino acid (Lys) residue

Lysine was first attached to the free amino group on the resin. The prepared resin from step i) was immersed in a mixture solution of Fmoc-L-Lys (Boc)-OPfp (9.52 mg, 15 μmol), **reagent #2** (15 μL) and **reagent #3** (15 μL) for 30 min at room temperature with occasional agitation. After the specified period, the reagent was squeezed off and the resin was extensively washed with DMF.

iii) Deprotection of the Fmoc protection group at *N*-terminus

After the coupling and capping were completed, the resin was treated 100 μL of deprotection solution (**reagent #1**) in a 1.5 mL at room temperature for 5 min with occasional agitation. After the specified period of time, the reagent was squeezed off and the resin was extensively washed with DMF.

iv) Coupling with PNA monomer or spacer

- Coupling with pyrrolidine nucleobase monomer

After deprotect Fmoc protection group, the free amino groups were further coupled with the pyrrolidine nucleobase monomer. The coupling solution consisted of the activated nucleobase monomer (6 μmol), **reagent #2** (15 μL) and **reagent #3** (15 μL) in a 1.5 mL eppendorf tube at room temperature for 5 min with occasional agitation. After the specified period of time, the reagent was squeezed off and the resin was extensively washed with DMF.

- Coupling with U^{Py} acpcPNA monomer

After coupling of ACPC spacer, capping and removing of Fmoc group were completed. The resin treated with a mixture of Fmoc-U^{Py}-OH (2.68 mg, 6 μmol, 4 equiv.), HATU (2.2 mg, 6 μmol) and 30 μL of **reagent #2** in a 1.5 mL eppendorf tube. The reaction column was treated with this solution at room temperature for 30 min with occasional agitation. After the specified period of time, the reagent was squeezed off and the resin was extensively washed with DMF.

- Coupling with ACPC or APC spacer

After coupling of pyrrolidine nucleobase monomer, capping and removing of Fmoc group were completed. The resin was treated with the activated ACPC spacer (3.10 mg, 6 μmol) or APC spacer (3.71 mg, 6 μmol), **reagent #2** (15 μL) and **reagent #3** (15 μL) in a 1.5 mL eppendorf tube at room temperature for 5 min with occasional agitation. After the specified period of time, the reagent was squeezed off and the resin was extensively washed with DMF.

v) Capping

After each coupling step, the free amino residue was capped with 5 μL of acetic anhydride and 30 μL of **reagent #2** in a 1.5 mL eppendorf tube at room temperature for 5 min. After the specified period of time, the reagent was squeezed off and the resin was extensively washed with DMF. This process was routinely carried out to prevent the formation of deletion sequences and facilitate purification.

After this step, the next cycle (deprotection, coupling and capping) were carried out with the same method until the resin bound peptide had been extended up to nonamer.

vi) End-capping of PNA oligomers by acetylation or benzoylation

After final removal of the *N*-terminal Fmoc group, the PNA was treated with 5 μL of acetic anhydride and 30 μL of **reagent #2** (for acetylation) or 2 mg of benzoic anhydride and 30 μL of **reagent #2** (for benzoylation). The reaction column was occasionally agitated with this solution for 5 min. After that, the reagent was squeezed off and the resin was extensively washed with DMF.

vii) Modifying the *N*-terminus with pyrene butyryl

After final removal of the *N*-terminal Fmoc group, the PNA was treated with a mixture of 4-(1-pyrenyl)butyric acid (1.6 mg, 6 μmol, 12 equiv.), HATU (2.2 mg, 6 μmol) and 30 μL of **reagent #2** in a 1.5 mL eppendorf tube. The reaction column was treated with this solution at room temperature for 30 min with occasional agitation. After the specified period of time, the reagent was squeezed off and the resin was extensively washed with DMF.

viii) Deprotection of nucleobase and APC protecting group

For PNA oligomers bearing adenine, cytosine or guanine bases as well as APC spacer in the sequence, the protecting group (Bz for A and C, Ibu for G, Tfa for APC) must be removed before the cleavage of PNAs from the resin. To remove these protecting groups, the resin was treated with aqueous ammonia/dioxane (1/1, v/v) in a sealed test tube at 60 ºC for 12 hours. After the specified period of time, the reagent was squeezed off and the resin was extensively washed with methanol.

ix) Attachment of pyrene labels at APC spacer

Coupling of the pyrenebutyryl labeling group at the nitrogen atom in the pyrrolidine ring of the (3*R*,4*S*)-APC spacer was carried out after removal of the protecting groups by ammonia treatment (step vii). The washed resin was re-swollen in DMF. The resin (0.5 μmol) treated with a mixture of 4-(1-pyrenyl) butyric acid (1.6 mg, 6 μmol, 12 equiv.), HATU (2.2 mg, 6 μmol) and 30 μL of **reagent #2** in a 1.5 mL eppendorf tube. The reaction column was treated with this solution at room temperature for 30 min with occasional agitation. After the specified period of time, the reagent was squeezed off and the resin was extensively washed with DMF.

x) Modification of the *N*-terminus of acpcPNA with fluorescein (Flu) or tetramethylrhodamine (TMR)

After final removal of the final *N*-terminal Fmoc group and the nucleobase side chain protecting groups, the PNA oligomer was treated with a solution of the activated diethylene glycol (egl) linker (Fmoc-$NHCH_2CH_2OCH_2CH_2OCH_2CO$-OPfp) (3.3 mg, 6 μmol, 12 equiv) and 30 μL of anhydrous DMF. After the coupling of the

ethylene glycol (egl) linker was completed, the resin was extensively washed with DMF and treated with 100 μL of deprotection solution (reagent #1) at room temperature for 5 min. After washing with DMF, the PNA was treated with a solution of the 5(6)-carboxyfluorescein *N*-hydroxysuccinimide ester (2.0 mg, 4.2 μmol, 8.4 equiv) (Fluka) or 5(6)-carboxy-X-rhodamine *N*-succinimidyl ester (3.5 mg, 5.5 μmol, 11 equiv) (Fluka) in 30 μL of anhydrous DMF. The reaction column was left in the dark at room temperature for 12 hours with occasional agitation. After the specified period of time, the reagent was squeezed off and the resin was extensively washed with DMF.

xi) Cleavage of PNA oligomers from the resin

The resin-bound PNA was cleaved from the resin by treatment with 10% triisopropylsilane (TIPS) in trifluoroacetic acid (3 × 0.5 mL × 1 hour) in a 1.5 mL eppendorf tube at room temperature with occasional agitation. The removal of trifluoroacetic acid was achieved by gentle nitrogen stream in a fume hood. The resulting residue was treated with diethyl ether (1 mL), centrifuged and decanted to obtain the crude PNA as a white solid. Finally the crude PNA was air-dried at room temperature and stored at -20 °C until further use.

2.2.4 Purification and characterization of PNA oligomers

2.2.4.1 Purification of PNA oligomers

The crude acpcPNA sample was prepared for reverse phase HPLC purification by dissolving a mixture in 120 μL of MilliQ water. The HPLC purification and analysis were performed in reverse phase mode, monitoring by UV-absorbance at 300 nm and eluting with a gradient system of 0.1% trifluoroacetic acid in methanol/water. The HPLC gradient consists of two solvent systems which are solvent A (0.1% trifluoroacetic acid in MilliQ water) and solvent B (0.1% trifluoroacetic acid in methanol). The elution began with A:B (90:10) for 5 min followed by a linear gradient to A:B (10:90) over a period of 60 min, then hold for 10 min before reverted back to A:B (90:10).

2.2.4.2 Characterization of PNA oligomers

After lyophilization, the identity of the acpcPNA oligomer was verified by MALDI-TOF mass spectrometry. The samples were prepared by mixing 1 μL of the sample with 10 μL of matrix solution containing CCA in 0.1% trifluoroacetic acid in acetonitrile:water (1:2) and deposited on the MALDI target. The mass spectra of acpcPNA were recorded on a Microflex MALDI-TOF mass spectrometry in linear positive ion mode with accelerating voltage of 25 kV.

The sequences of U^{Py} acpcPNAs synthesized in this work are shown in **Table 2.1**.

Table 2.1 Sequences of U^{Py}-acpcPNAs used in this work

Code of PNA	Sequences (*N*-terminus to *C*-terminus)
$TU^{Py}T$	Ac-TTTTU^{Py}TTTT-Lys-NH_2
$AU^{Py}A$	Ac-TTTAU^{Py}ATTT-Lys-NH_2
$CU^{Py}C$	Ac-TTTCU^{Py}CTTT-Lys-NH_2
$GU^{Py}G$	Ac-TTTGU^{Py}GTTT-Lys-NH_2
$CU^{Py}C13$	Ac-TTTTTCU^{Py}CTTTTT-Lys-NH_2
MixU^{Py}	Ac-AGTTAU^{Py}CCCTGC-Lys-NH_2
MixAU^{Py}	Ac-CTAAAAU^{Py}TCAGA-Lys-NH_2
MixTU^{Py}	Ac-CTAAATU^{Py}TCAGA-Lys-NH_2
AU^{Py}	Ac-AAAAU^{Py}AAAA-Lys-NH_2
T^6AU^{Py}	Ac-AAATU^{Py}AAAA-Lys-NH_2
T^7AU^{Py}	Ac-AATAU^{Py}AAAA-Lys-NH_2
T^8AU^{Py}	Ac-ATAAU^{Py}AAAA-Lys-NH_2
T^9AU^{Py}	Ac-TAAAU^{Py}AAAA-Lys-NH_2

The sequences of pyrenebutyryl-modified acpcPNAs synthesized in this work are shown in **Table 2.2**.

Table 2.2 Sequences of pyrenebutyryl-acpcPNAs used in this work

Code of PNA	**Sequences (*N*-terminus to *C*-terminus)**
PyT9	Py-TTTTTTTTT-Lys-NH_2
PyM12	Py-AGTTATCCCTGC-Lys-NH_2
PyM11	Py-CTAAATTCAGA-Lys-NH_2
PyM10	Py-GTAGATCACT-Lys-NH_2
T9^{Py}	Ac-TTTT$^{(Py)}$TTTTT-LysNH_2
M12^{Py}T	Ac-Lys-AGTTA$^{(Py)}$TCCCTGC-LysNH_2
M12^{Py}C	Ac-Lys-AGTTAT$^{(Py)}$CCCTGC-LysNH_2
M11^{Py}A	Ac-Lys-CTAA$^{(Py)}$ATTCAGA-LysNH_2
M11^{Py}T	Ac-Lys-CTAAAT$^{(Py)}$TCAGA-LysNH_2
M11^{Py}C	Ac-Lys-CTAAATT$^{(Py)}$CAGA-LysNH_2

The sequences of Flu-acpcPNAs and TMR-acpcPNAs synthesized in this work are shown in **Table 2.3**.

Table 2.3 Sequences of fluorescein-acpcPNAs and TMR-acpcPNAs used in this work (O = aminoethoxyethoxyacetyl linker)

Code of PNA	**Sequences (*N*-terminus to *C*-terminus)**
Flu1	Flu-O-CTAAATTCAGA-Lys-NH_2
Flu2	Flu-O-AGTTATCCCTGC-Lys-NH_2
TMR1	TMR-O-TTATCACTATGA-Lys-NH_2

2.2.4.3 Determination of PNA concentration

The concentrations of modified-PNA were determined by UV absorption measurements at 260 nm using a CARY 100 Bio UV-visible spectrophotometer (Varian, Inc., USA). A portion of the PNA solution (5 µL) was diluted to 1000 µL with 10 mM sodium phosphate buffer pH 7.0, and UV absorbance at 260 nm was measured. This value was used for calculation of the PNA concentrations. Extinction coefficients of PNA was calculated as the sum of individual extinction coefficients (ε) of the corresponding nucleobases and fluorophores. The individual extinction coefficients at 260 nm used in the calculation were ε(A) = 10.8 $mM^{-1}\cdot cm^{-1}$, ε(C) = 7.4 $mM^{-1}\cdot cm^{-1}$, ε(G) = 11.5 $mM^{-1}\cdot cm^{-1}$, ε(T) = 8.8 $mM^{-1}\cdot cm^{-1}$, ε(U^{Py}) = 17.0 $mM^{-1}\cdot cm^{-1}$ [34], ε(Py) = 13.3 $mM^{-1}\cdot cm^{-1}$ [44], ε(Flu)= 20.9 $mM^{-1}\cdot cm^{-1}$ and ε(TMR) = 32.2 $mM^{-1}\cdot cm^{-1}$.

2.3 Studies of PNA-DNA hybridization

2.3.1 T_m experiments

T_m curves were measured at 260 nm with a CARY 100 Bio UV-Visible spectrophotometer (Varian, Inc., USA) equipped with a thermal melt system. The sample for T_m experiment was prepared by mixing calculated amount of stock oligonucleotide and PNA solution together to give final concentration of nucleotides, 10 mM sodium phosphate buffer (pH 7.0), and final volumes were adjusted to 1000 µL in a 10 mm quartz cell with a Teflon stopper and equilibrated at the starting temperature for 10 min. The A_{260} was recorded in heating from 20–90 ºC or 20–95 ºC (block temperature) with a temperature ramp of 1ºC/min. The temperature recorded was the block temperature and was corrected by a built-in temperature probe.

Correct temperature and normalized absorbance are defined as follows.

$$\text{Correct Temp.} = (0.9696 \times T_{block}) - 0.8396$$

$$\text{Normalized Abs.} = Abs_{obs}/Abs_{init}$$

The melting temperature was determined from the maximum of the first derivative after smoothing using KaliedaGraph 3.6 (Synergy Software). Data analysis was performed on a PC compatible computer using Microsoft Excel XP (Microsoft Corp.). T_m values obtained from independent experiments were accurate to within ±0.5 ºC

2.3.2 UV/Vis absorption spectroscopy

Absorption spectra were performed on a CARY 100 Bio UV-Visible spectrophotometer (Varian, Inc., USA). The sample for absorption measurements was prepared by mixing the calculated amount of stock oligonucleotide and PNA solutions together to give the specified concentration in 10 mM sodium phosphate buffer (pH 7.0). The final volumes were adjusted to 1000 μL in a 10 mm quartz cell with a Teflon stopper.

2.3.3 Fluorescence experiments

Fluorescence experiments were performed on a Cary Eclipse Fluorescence Spectrophotometer (Varian and Agilent Technologies). The sample for fluorescence experiment was prepared by mixing the calculated amount of stock oligonucleotide and PNA solutions together to give the specified concentration in 10 mM sodium phosphate buffer (pH 7.0). The final volumes were adjusted to 1000 μL in a 10 mm quartz cell with a Teflon stopper. The excitation slit and emission slit both were set to 5 nm and the photomultiplier (PMP) tube voltage value of either medium or high volts were used.

2.3.4 Fluorescence quantum yield (Φ)

The fluorescence quantum yield (Φ) of the single stranded-PNA and PNA·DNA duplex were calculated using quinine sulfate (Φ = 0.54) [52] as the standard. A stock solution of quinine sulfate (1.0 mM) was prepared by dissolving in 0.1 M H_2SO_4. For calculation of quantum yield, five concentrations of quinine sulfate

solutions were prepared, all of which had absorbance less than 0.1 at 350 nm. Absorption spectra of the quinine sulfate standards and samples were measured on a CARY 100 Bio UV/Visible spectrophotometer and fluorescence spectra were measured on a Cary Eclipse Fluorescence Spectrophotometer (Agilent Technologies). The integrated fluorescence intensities (excited at 345 and 350 nm) and the absorbance values (at 345 and 350 nm) of the quinine sulfate standards and the sample were plotted and the slopes were determined to give $m_{standard}$ and m_{sample}, respectively.

The quantum yield of sample was then calculated using the equation:

$$\Phi_{sample} = \Phi_{standard} (m_{sample} / m_{standard}) (\eta_{sample}^2 / \eta_{standard}^2)$$

Where m is the slope from the plot of integrated fluorescence intensity *vs* absorbance and η is the refractive index of the solvent

2.3.5 S1 nuclease digestion

Fluorescence experiments for enzymatic digestion were performed on a Cary Eclipse Fluorescence Spectrophotometer (Agilent Technologies). The sample for digestion by nuclease S1 was prepared by mixing the calculated amounts of stock oligonucleotide and PNA solution together in 30 mM sodium acetate buffer (pH 4.6) containing 1.0 mM zinc acetate, 5% (v/v) glycerol at the final volume of 500 μL in a 10 mm quartz cell. The enzyme stock (S1 from *Aspergillus oryzae*, 1000 unit/mL) was added to give the final concentration of 5 unit/mL. The progress of the enzymatic digestion was monitored by Fluorescence Spectrophotometry (kinetic mode, the fluorescence spectra were recorded every 5 min until no further change was observed).

2.3.6 Circular dichroism (CD) spectroscopy

CD experiments were performed on JASCO Model J-815 spectrometer (JASCO). The sample for CD experiment was prepared by mixing the calculated amount of stock oligonucleotide and PNA solutions together to give the specified final concentration in 10 mM sodium phosphate buffer (pH 7.0), and final volumes were adjusted to 1000 μL in a 10 mm quartz cell with a Teflon stopper. The spectra were recorded at 20 °C from 200 to 400 nm with scanning speed 200 nm/min and averaged 4 times then subtracted from a spectrum of the blank (10 mM sodium phosphate buffer pH 7.0) under the same conditions.

2.4.7 Photographing

The samples for photographing were prepared as described above. The photograph was taken under black light in the dark room by a digital camera (Canon PowerShot SX110 IS) in manual mode (ISO 80, F4.0, shutter speed 1 sec).

CHAPTER III

RESULTS AND DISCUSSION

The work described in this dissertation involves development of fluorescence PNA probe that can change the fluorescence signal in response to the presence of correct DNA target. More specifically, the probes from acpcPNA modified with a single fluorophore were developed, by modification of the nucleobase and the PNA backbone or its N terminus. This chapter is divided into three parts. The first part consists of the synthesis and optical properties of acpcPNA with 5-pyren-1-yluracil (U^{Py}) as a fluorescent nucleobase as well as its hybrids with DNA. The second part involves synthesis and fluorescence properties of acpcPNA modified with a pyrenebutyryl group and its hybrids with DNA. The third part involves our attempts to develop a modular approach to utilize single-labeled acpcPNA as a molecular beacon that does not require the stem-loop structures. In all cases, it is expected that these singly-labeled PNA would change its fluorescence properties in response to the presence of correct DNA target, preferably in an off-on fashion (i.e. low fluorescence in the absence and high fluorescence in the presence of DNA). These singly labeled PNA probe would be useful as a tool for determination of DNA sequence that can be easily synthesized and is more soluble than the multiply-labeled PNA probes that have been described in the literature [53].

3.1 acpcPNA carrying U^{Py} modification

In this work, a quencher-free PNA beacon was designed by applying the base-discriminating fluorescent (BDF) nucleobase concept [26] to pyrrolidinyl PNA with a proline/2-aminocyclopentanecarboxylic acid backbone (acpcPNA). The pyrene moiety was covalently linked to the 5-position of the nucleobase uracil through a single C-C bond to give a modified acpcPNA monomer called U^{Py} which was subsequently incorporated into the acpcPNA by solid phase peptide synthesis. It was proposed that the environment of the pyrene label in single stranded PNA should be quite different from the double stranded PNA·DNA hybrid. In the single stranded

form, the pyrene unit should associate with nucleobases by hydrophobic interactions, resulting in quenching. Upon pairing with the DNA, the pyrene linked to the uracil via a rigid linker must point away from the major groove side, exposing to the aqueous environment, thereby resulting in an increase fluorescence of the pyrene fluorophore. (**Figure 3.1**) Examples of similar concept have been described with DNA [34] but not yet with PNA.

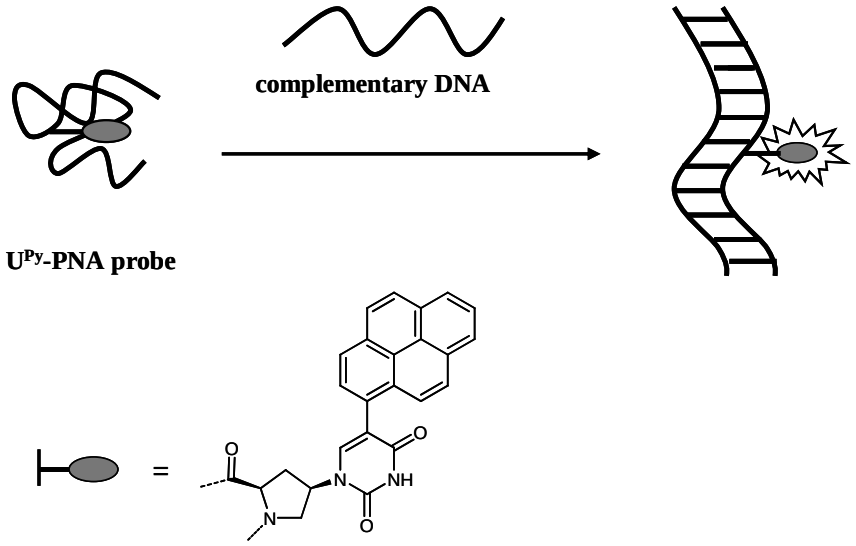

Figure 3.1 A schematic diagram showing the concept of a quencher-free PNA beacon using a U^{Py} as base-discriminating fluorescent (BDF) nucleobase in acpcPNA

3.1.1 Synthesis of the U^{Py}-pyrrolidinyl PNA monomer

In order to synthesize the U^{Py}-modified acpcPNA, the U^{Py} monomer was first required in the *N*-Fmoc-protected form. The monomer - *N*-Fluoren-9-ylmethoxycarbonyl-(4'*R*)-[5-(pyren-1-yl)uracil-1-yl]-(2'*R*)-proline (Fmoc-U^{Py}-OH, **1**) was successfully synthesized according to the synthetic scheme shown in **Figure 3.2** [54–56] The known Boc/diphenylmethyl-protected *trans*-hydroxy-D-proline intermediate (**2**) was synthesized according to previously reported [57]. The iodouracil was first installed on the pyrrolidine ring, with inversion of configuration, via Misunobu reaction between N^3-benzoyl-5-iodouracil and the protected *trans*-4-hydroxy-D-proline **2** to form the corresponding iodouracil monomer (**3**) in 58% yield.

In the next step, Suzuki-Miyaura cross coupling was performed between the pyren-1-boronic acid and the protected iodouracil compound (**3**) to give the Boc-protected pyrene intermediate (**4**) in 60% yield after removal of the thymine protecting group (Bz) by treatment with ethanolamine in DMF. Next, the protecting group must be exchanged from *N*-Boc to *N*-Fmoc and the carboxyl protecting group (Dpm) must be removed. Attempts to directly remove both the N and C-protecting groups followed by Fmoc-protection was not successful due to the low solubility of the completely deprotected monomer in acetonitrile/aqueous $NaHCO_3$ mixture required for the Fmoc protection. Accordingly, a three-step protocol was employed whereby the Boc/Dpm-protected intermediate **3** was first treated with *p*-toluenesulfonic acid (*p*TsOH) in acetonitrile to selectively remove the Boc group, leaving the Dpm ester intact [57]. The N-deprotected intermediate was then treated with 9-fluorenylmethoxycarbonyl chloride (FmocCl) in the presence of diisopropylethylamine (DIEA). Next, the Dpm group was removed by treatment with a mixture of trifluoroacetic acid/dichloromethane (1:1) containing 10% triisopropylsilane to give the U^{Py} acpcPNA monomer **1** (Fmoc-U^{Py}-OH) in 55% yield. The purpose of the silane was to scavenge the electrophilic carbocations released during the deprotection that might react with the electron-rich pyrene resulting in undesired side reactions. All newly synthesized compounds were characterized by ^{1}H and ^{13}C NMR, as well as high resolution mass spectrometry. Once the Fmoc-protected U^{Py} monomer **1** was available, it was incorporated into acpcPNA by substituting a PNA monomer as will be described next.

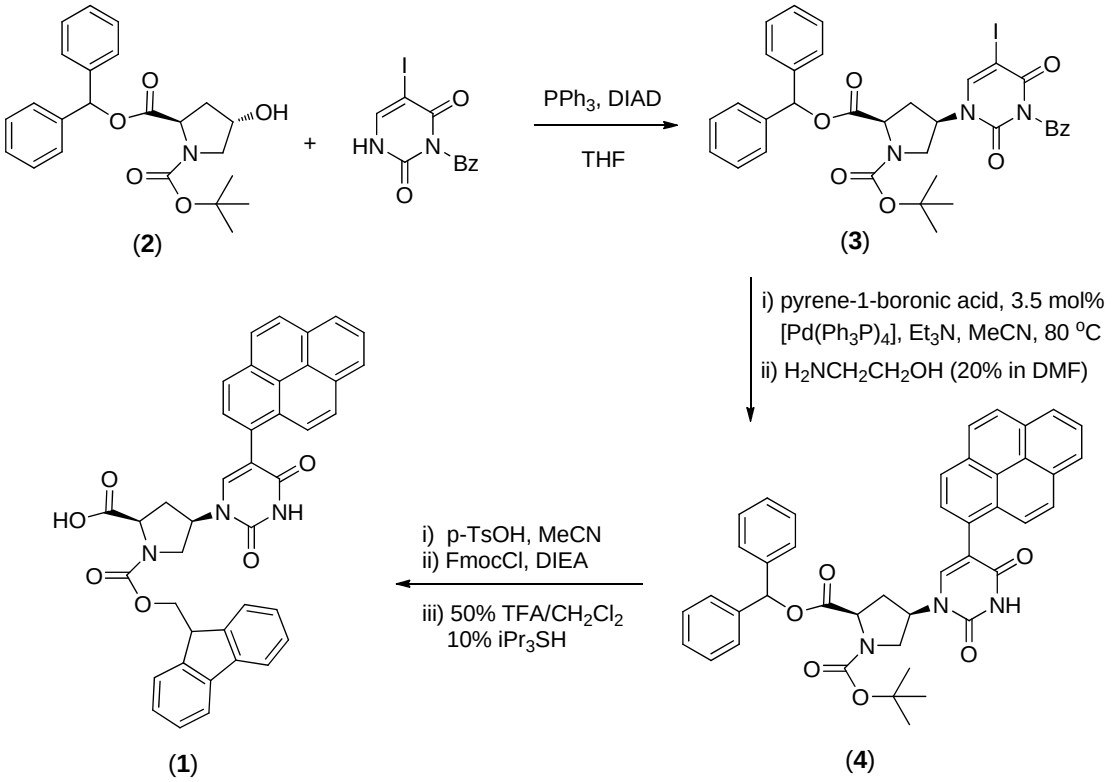

Figure 3.2 Synthesis of intermediate and U^{Py}-pyrrolidinyl PNA monomer (Fmoc-U^{Py}-OH)

3.1.2 Synthesis of U^{Py}-modified acpcPNA oligomers

The PNA oligomers were synthesized by Solid Phase Peptide Synthesis (SPPS) based on the Fmoc strategy according to the standard protocol previously developed in Vilaivan's laboratory [50, 51]. The technique involves stepwise growing of the peptide chains from amino acid building blocks by attachment onto a solid support. The peptide bond formation reactions are usually performed starting from *C* (carboxyl) terminus to *N* (amino) terminus in a series of coupling cycles.

The TentaGel S RAM [58] resin containing a moderately acid labile Rink amide (RAM) linker immobilized via a grafted polyethylene glycol (PEG) linker on polystyrene resin was used as the solid support for all PNA syntheses. For all PNA sequences, lysine was first coupled to the resin (i.e., included at the *C*-termini of the PNA) in order to prevent the self aggregation of the peptide chain and to increase the

solubility of the peptide in aqueous medium due to the presence of the positively charged side chain [13]. The next step of the synthetic cycle consisted of i) deprotection of the Fmoc group by using 20% piperidine, ii) alternated coupling with acpcPNA monomer and spacer, and iii) capping with acetic anhydride. Extensive washing with DMF was performed after each step. The synthesis cycle was repeated until the growing peptide chain was extended up to the desired oligomers.

The Fmoc-protected U^{Py} momomer (Fmoc-U^{Py} -OH, **1**) was incorporated into internal positions of the PNA strand through standard HATU coupling similar to other PNA monomers. After completion of the PNA synthesis, the last Fmoc group was removed and the end-capping was performed by acetylation or benzoylation. Next, the nucleobase side chain protecting groups (Bz for A, C and Ibu for G) were removed by treatment with 1:1 aqueous ammonia/dioxane at 60 ºC overnight. Finally, the U^{Py}-modified acpcPNA oligomer was cleaved from the resin by treatment with 10% triisopropylsilane in TFA. The crude PNA was obtained as a sticky residue after TFA removal under a stream of nitrogen gas. The crude PNA was then washed with ether and air-dried to give the crude PNA as a white solid.

3.1.3 Purification and identification of U^{Py}-modofied acpcPNA oligomers

The crude PNA oligomers were purified by C-18 reverse phase HPLC, monitoring by UV-absorbance at 300 nm and eluting with a gradient system of 0.1% TFA in methanol/water. Fractions containing the pure PNA as determined by MALDI-TOF MS were combined and lyophilized. The residues were re-dissolved in 120 μL of water and the concentration of the PNA was determined by UV/Vis spectrophotometry. The identities of the PNA oligomers were verified by MALDI-TOF mass spectrometry. The *m/z* data obtained from MALDI-TOF analysis for each PNA are illustrated in **Table 3.1**. The purities of all modified PNA were determined to be >90% by reverse phase HPLC analyses.

Table 3.1 Characteristics of U^{Py}-acpcPNA oligomers synthesized in this study.

Code of PNA	Sequences (*N*-terminus to *C*-terminus)	Mass	
		$m/z_{(calcd)}$	$m/z_{(found)}$
$TU^{Py}T$	Ac-TTTTU^{Py}TTTT-Lys-NH_2	3365.65	3366.28
$AU^{Py}A$	Ac-TTTAU^{Py}ATTT-Lys-NH_2	3383.67	3384.02
$GU^{Py}G$	Ac-TTTGU^{Py}GTTT-Lys-NH_2	3415.67	3415.90
$CU^{Py}C$	Ac-TTTCU^{Py}CTTT-Lys-NH_2	3335.62	3335.69
$CU^{Py}C13$	Ac-TTTTTCU^{Py}CTTTTT-Lys-NH_2	4665.04	4665.79
$MixU^{Py}$	Ac-AGTTAU^{Py}CCCTGC-Lys-NH_2	4370.72	4370.59
$MixAU^{Py}$	Bz-CTAAAAU^{Py}TCAGA-Lys-NH_2	4132.48	4132.83
$MixTU^{Py}$	Bz-CTAAATU^{Py}TCAGA-Lys-NH_2	4123.47	4124.35
AU^{Py}	Ac-AAAAU^{Py}AAAA-Lys-NH_2	3437.75	3439.33
T^6AU^{Py}	Ac-AAATU^{Py}AAAA-Lys-NH_2	3428.74	3430.27
T^7AU^{Py}	Ac-AATAU^{Py}AAAA-Lys-NH_2	3428.74	3430.54
T^8AU^{Py}	Ac-ATAAU^{Py}AAAA-Lys-NH_2	3428.74	3430.28
T^9AU^{Py}	Ac-TAAAU^{Py}AAAA-Lys-NH_2	3428.74	3430.50

3.2 Synthesis of pyrenebutyryl-modified acpcPNA (Py-PNA)

In this work, a hybridization-responsive pyrrolidinyl peptide nucleic acid (acpcPNA) probe was synthesized by modification of the PNA backbone or its *N*-terminus. The acpcPNA probe was covalently modified at the end of sequence (*N*-terminus) and the internal backbone with a pyrenebutyryl through a flexible linker *via* acylation. Pyrene was used as a fluorophore because the fluorescence of pyrene is largely affected by environmental factors, such as nearby nucleotide bases and polarity of the solvent [59]. Pyrene was covalently to the backbone at the end of an acpcPNA sequence, which can be referred to as the terminally pyrenebutyryl-modified acpcPNA (Py-PNA). In an alternative mode of attachment, the pyrene moiety was covalently at an internal position of the acpcPNA backbone *via* acylation

of 3-aminopyrrolidine-4-carboxylic acid (APC)-modified acpcPNA [44]. This can be referred to as an internally pyrenebutyryl-modified acpcPNA (PNA^{Py}). It was hypothesized that in the single-stranded state, the fluorescence of the pyrene-labeled acpcPNA should be quenched by the nucleobases in the strand because the hydrophobic pyrene chromophore should interact with nucleobases to avoid contact with water. Hybridization of the pyrene-labeled acpcPNA to its complementary DNA target resulted in exposure of the pyrene to the aqueous environment and caused a change in the fluorescence signal (**Figure 3.3**).

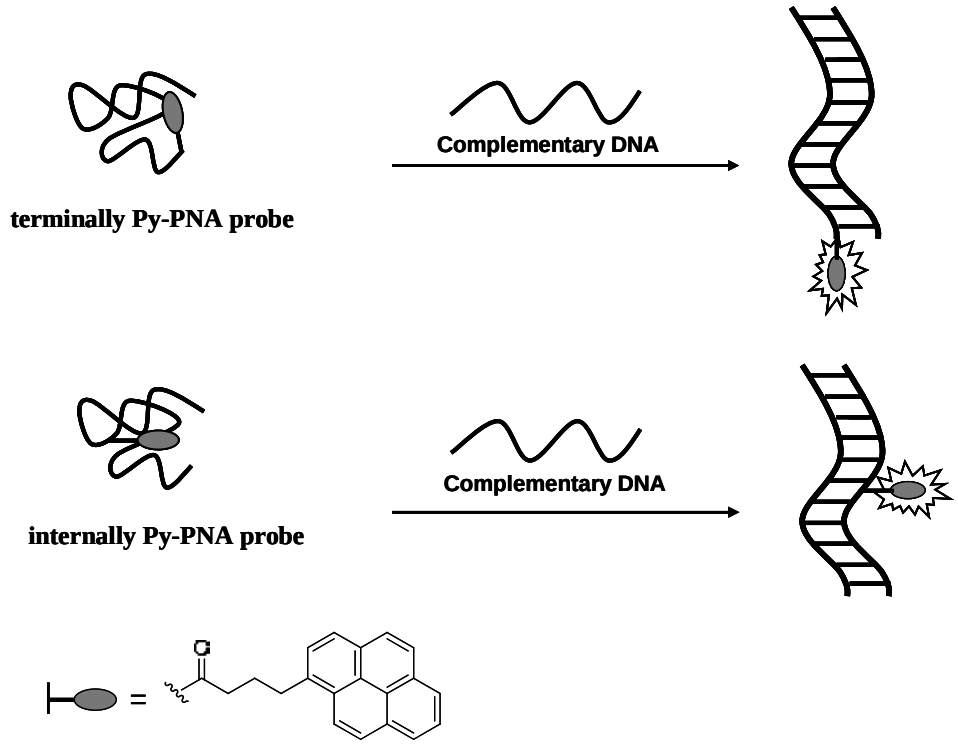

Figure 3.3 A schematic diagram showing a quencher-free, hybridization-responsive pyrenebutyryl-modified acpcPNA (Py-PNA) probe

3.2.1 Synthesis of terminally pyrenebutyryl-modified acpcPNA (Py-PNA)

After Fmoc cleavage of the last PNA residue (normally an ACPC spacer), the *N*-terminus was coupled with the 4-(1-pyrenyl)butyric acid (Py) by using HATU/DIEA as activators. The nucleobase side chain deprotection was accomplished by treatment of the resin with 1:1 aqueous ammonia/dioxane at 60 ºC overnight as described earlier for U^{Py}-modified acpcPNA. Finally, the Py-PNA oligomer was cleaved from the resin by treatment with 10% triisopropylsilane in TFA and washed with ether as described in section 3.1.2.

3.2.2 Synthesis of internally pyrenebutyryl-modified acpcPNA (PNA^{Py})

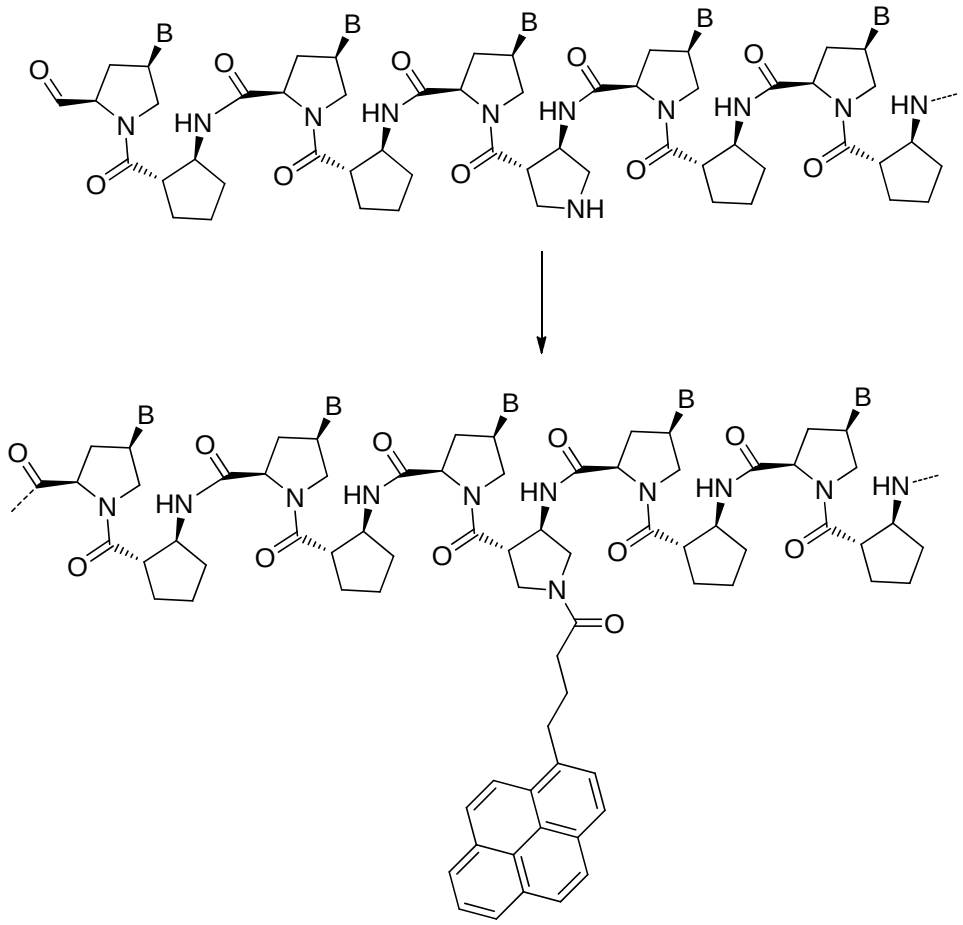

Figure 3.4 A synthetic strategy for internal labeling of acpcPNA via acylation of APC-modified acpcPNA by pyrenebutyric acid

To synthesize internally modified acpcPNA, the approach developed by Reenabthue *et al* [44] was employed. According to this strategy, an ACPC spacer at the position to attach the label was replaced with a 3-aminopyrrolidine-4-carboxylic acid (APC) residue that carried a trifluoroacetyl protecting group at the pyrrolidine nitrogen atom. This pyrrolidine nitrogen provides a convenient handle for attachment of the pyrenebutyryl label by acylation chemistry. In general, the pyrene-labeled PNA prepared by this method requires inclusion of an additional lysine residue to improve aqueous solubility. After removal of the final Fmoc group, the *N*-terminus of the PNA oligomer was coupled with the Fmoc-L-Lys(Boc)-OPfp. The Fmoc group on the lysine was next removed and the free amino residue was capped with acetic anhydride. Subsequently, the nucleobase side chain protecting groups were removed by treatment with 1:1 aqueous ammonia/dioxane at 60 ºC overnight. This condition also at the same time removed the *N*-Tfa protecting group on the Tfa-protected APC unit to give a free secondary amino group ready for further functionalization. The 4-(1-pyrenyl)butyric acid (Py) label was then coupled directly to the nitrogen atom of APC spacer of the PNA using HATU/DIEA as activators for 30 min. The progress of the reaction was monitored by MALDI-TOF mass spectrometry. It is important not to leave the coupling reaction for too long because modification of the amino groups of the fully deprotected nucleobase, especially on the rather nucleophilic NH_2 group of C, may take place. This resulted in contamination by multiply-labeled PNA which is difficult to remove from the desired singly-labeled PNA.

3.2.3 Cleavage, purification and identification of the synthesized acpcPNA oligomers

After completing the synthesis, the cleavage and purification was performed as described in section 3.1.3. The identities of the PNA oligomers were verified by MALDI-TOF mass spectrometry (**Table 3.2**) and the purities determined to be >90% by reverse phase HPLC analyses.

Table 3.2 Characteristics of pyrenebutyryl-modified acpcPNA oligomers synthesized in this study

Code of PNA	Base Sequences (*N*-terminus to *C*-terminus)	Mass	
		$m/z_{(calcd)}$	$m/z_{(found)}$
PyT9	Py-TTTTTTTTT-Lys-NH_2	3407.73	3409.08
PyM12	Py-AGTTATCCCTGC-Lys-NH_2	4412.80	4414.27
PyM11	Py-CTAAATTCAGA-Lys-NH_2	4112.49	4111.89
PyM10	Py-GTAGATCACT-Lys-NH_2	3787.13	3788.23
T9^{Py}	Ac-TTTT$^{(Py)}$TTTTT-LysNH_2	3450.75	3452.03
M12T^{Py}	Ac-Lys-AGTTA$^{(Py)}$TCCCTGC-LysNH_2	4583.99	4583.53
M12C^{Py}	Ac-Lys-AGTTAT$^{(Py)}$CCCTGC-LysNH_2	4583.99	4583.26
M11A^{Py}	Ac-Lys-CTAA$^{(Py)}$ATTCAGA-LysNH_2	4283.69	4284.71
M11T^{Py}	Ac-Lys-CTAAAT$^{(Py)}$TCAGA-LysNH_2	4283.69	4283.53
M11C^{Py}	Ac-Lys-CTAAATT$^{(Py)}$CAGA-LysNH_2	4283.69	4283.88

3.3 Fluorescein-modified acpcPNA (Flu-PNA) and tetramethylrhodamine-modified acpcPNA (TMR-PNA)

The strand displacement probe is a bimolecular version of a molecular beacon that does not require the stem-loop structures. The PNA·DNA strand-displacement probes consist of a fluorescent PNA probe and a short or mismatched DNA containing a quencher. When the two strands are combined, the fluorophore and quencher are brought in close proximity by the duplex formation, resulting in the quenching of the fluorophore. However, in the presence of the complementary DNA target sequence, the PNA probe can form a stronger hybrid with the target DNA than with the quencher DNA. This will result in releasing of the quencher DNA and increasing in fluorescence intensity (**Figure 3.5**). Fluorescein/DABCYL and TMR/BHQ were chosen as the fluorophore/quencher pairs in PNA probe and

quencher DNA as these two are common fluorophore/quencher combination.

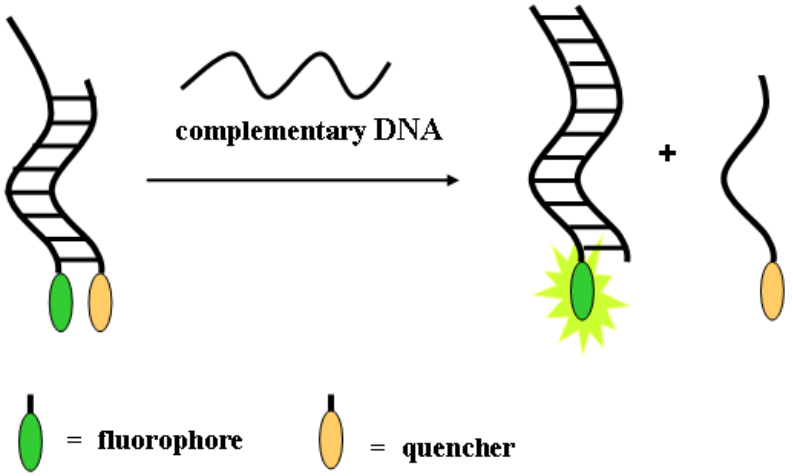

Figure 3.5 A schematic diagram showing the concept of strand displacement probe derived on fluorophore-modified acpcPNA and a quencher DNA.

Synthesis and purification of the terminally fluorescein-modified acpcPNA (Flu-PNA) and tetramethylrhodamine-modified acpcPNA (TMR-PNA) were performed as described in Chapter 2. After completing the synthesis, the cleavage and purification was performed as described in section 3.1.3. The identities of the PNA oligomers were verified by MALDI-TOF mass spectrometry (**Table 3.3**) and the purities determined to be >90% by reverse phase HPLC analyses.

Table 3.3 Characteristics of fluorescein-modified acpcPNA (Flu-PNA) and tetramethylrhodamine-modified acpcPNA (TMR-PNA) synthesized in this study

Code of PNA	Base Sequences (N-terminus to C-terminus)	Mass	
		$m/z_{(calcd)}$	$m/z_{(found)}$
Flu1	Flu-O-CTAAATTCAGA-Lys-NH_2	4345.63	4346.09
Flu2	Flu-O-AGTTATCCCTGC-Lys-NH_2	4645.93	4647.90
TMR1	TMR-O-TTATCACTATGA-Lys-NH_2	4724.11	4720.87

3.4 Thermal stability of U^{Py}-modified acpcPNA

3.4.1 Melting temperature (T_m) experiments

The melting temperature (T_m) is the temperature at which half of the DNA strands are in the double-helical state and half are in the random coil state. Random coil single-stranded DNA absorbs more light than double helical DNA. The separation of the double helix involves the breaking of hydrogen bonds between the bases in the duplex that are additionally stabilized by additional hydrophobic, π-π and dipole-dipole interactions between the stacked base pairs. This strand dissociation process is accompanied by a significant increase (10-20%) of absorbance at the wavelength where the nucleobases maximally absorb (260 nm), which can be monitored by spectrophotometry. The relationship between absorbance at 260 nm and temperature changes abruptly over a small range of temperature, giving an S-curve. The temperature at the middle of the S-curve is called melting temperature (T_m), which indicates the stability of the DNA duplex. Stable duplexes melt at higher temperatures than less stable duplexes. From the melting curve, the T_m value could be determined from the maxima of the first derivative plot against temperature. This T_m experiment can be used to estimate the binding affinity and sequence specificity of PNA towards DNA targets. The T_m values of U^{Py} acpcPNAs after hybridized with various complementary DNA and mismatched DNAs are summarized in **Table 3.4**.

Table 3.4 T_m values of hybrids between U^{Py} modified acpcPNA oligomers with different target DNAs.

PNA	DNA	DNA sequences(5′→3′)	T_m (°C)	ΔT_m (°C)	Note
TU^{Py}T	**dA9**	AAAAAAAAA	65.8	–	complementary
TU^{Py}T	**dA8T**	AAAATAAAA	25.7	40.1	single mismatch T
TU^{Py}T	**dA8C**	AAAACAAAA	27.3	38.5	single mismatch C
TU^{Py}T	**dA8G**	AAAAGAAAA	<20.0	>45.8	single mismatch G
AU^{Py}A	**dTAT**	AAATATAAA	60.2	–	complementary
GU^{Py}G	**dCAC**	AAACACAAA	54.1	–	complementary
CU^{Py}C	**dGAG**	AAAGAGAAA	<20.0	–	complementary
CU^{Py}C13	**dGAG13**	AAAAAGAGAAAAA	72.7	–	complementary
MixU^{Py}	**dcomMix**	GCAGGGATAACT	66.3	–	complementary
MixU^{Py}	**dmCMix**	GCAGGGCTAACT	54.3	12.0	single mismatch C
MixU^{Py}	**dmGMix**	GCAGGGGTAACT	54.2	12.1	single mismatch G
MixU^{Py}	**dmTMix**	GCAGGGTTAACT	54.5	11.8	single mismatch T
MixU^{Py}	**din5Mix**	GCAGGAATAACT	46.1	20.2	indirect mismatch
MixU^{Py}	**ddsMix**	GCAGGAGTAACT	40.0	26.3	double mismatch
AU^{Py}	**dA^{5}T8**	TTTTATTTT	68.8	–	complementary
T^{6}AU^{Py}	**dA^{6}T8**	TTTTTATTT	64.8	–	complementary
T^{7}AU^{Py}	**dA^{7}T8**	TTTTTTATT	66.3	–	complementary
T^{8}AU^{Py}	**dA^{8}T8**	TTTTTTTAT	64.0	–	complementary
T^{9}AU^{Py}	**dA^{9}T8**	TTTTTTTTA	64.4	–	complementary

Conditions: [PNA] = 2.5 mM; [DNA] = 3.0 mM, 10 mM sodium phosphate buffer, pH 7.0.

3.4.2 Thermal stabilities of homothymine acpcPNA carrying U^{Py} modification

Hybridization of the U^{Py}-modified acpcPNA was studied by thermal denaturation experiments. The T_m data in **Table 3.4** clearly indicated that homothymine acpcPNA carrying U^{Py} base can hybridize with its complementary DNA target (dA_9) with high stability as indicated by the high T_m value of **$TU^{Py}T$·dA9** hybrid = 65.8 ºC. This suggests that the U^{Py} base in acpcPNA can recognize the base A in the complementary DNA strand. Repeating the T_m experiments between **$TU^{Py}T$** and different target DNAs containing single mismatch bases resulted in much-lowered T_m values (25.7 and 27.3 ºC for **$TU^{Py}T$·dA8T** and **$TU^{Py}T$·dA8C** respectively) or no sigmoidal transition at all (**$TU^{Py}T$·dA8G**). The significant difference in the thermal stabilities between the complementary and single mismatched hybrids of more than 38.5 ºC (ΔT_m>38.5 ºC) clearly indicated that the U^{Py} base in modified acpcPNA could specifically recognize the adenine base in DNA strand.

To investigate the effect of neighboring nucleobases on the fluorescence properties of acpcPNA carrying U^{Py} modification, **$AU^{Py}A$, $GU^{Py}G$**, **$CU^{Py}C$** and **$CU^{Py}C15$** which had different bases adjacent to U^{Py} were synthesized as models. The results of T_m data demonstrated that PNA **$AU^{Py}A$** and **$GU^{Py}G$**, (which had A/A and G/G as neighboring bases, respectively) can formed stable hybrid with their complementary DNA. The T_m of the **$AU^{Py}A$·dTAT** and **$GU^{Py}G$·dCAC** hybrids were 60.2 and 54.1 ºC, respectively. On the other hand, the T_m experiments between **$CU^{Py}C$** (C/C as neighboring base) and its complementary DNA showed no sigmoidal transition at all (estimated T_m < 20 ^oC). The result is consistent with the known fact from previous experiments with unmodified acpcPNA that acpcPNA-DNA hybrids containing multiple TC/CT steps exhibited low stability [60]. To overcome this problem, the T_m experiment was repeated with a 13mer hybrid **$CU^{Py}C13$·dGAG13** having two pT·dA pairs extended from both termini of the original **$CU^{Py}C$** to increase the stability. The T_m value of **$CU^{Py}C13$·dGAG13** hybrid was found to be 72.7 ºC.

3.4.3 Thermal stabilities of mix sequence acpcPNA carrying U^{Py} modification

The thermal stabilities of mixed-sequence acpcPNA carrying U^{Py} base were also investigated. The 12mer PNA **MixU^{Py}** was used as a model. The results of T_m experiments indicated that **MixU^{Py}** can hybridize with its complementary DNA target with a strong affinity. Unsurprisingly, the hybrid between **MixU^{Py}** and complementary DNA was more thermally stable than the mismatch hybrids. The T_m value of the perfectly complementary hybrid between **MixU^{Py}** and **dcomMix** (complementary DNA) was 66.3 ºC. The T_m values of the hybrids between **MixU^{Py}** and single and double mismatched DNAs resulted in lowered T_m values (54.3, 54.2, 54.5, 46.1 and 40.0 ºC for **dmCMix**, **dmGMix**, **dmTMix**, **dinMix** and **ddsMix**, respectively). It is interesting to note that the "indirect" mismatch hybrid, whereby the position of the mismatch base is not directly opposite to the U^{Py}, gave a much-less thermally stable (T_m = 46.1 ºC) hybrid than the "direct" mismatched hybrids (T_m = 54.3–54.5 ºC) having the mismatch base exactly opposite to the U^{Py}. The decrease in the T_m values of the mismatch hybrid from the complementary hybrid suggested that the U^{Py} base in mixed sequence acpcPNA can still specifically recognize adenine base (A) in the complementary DNA strand. From the T_m results, it can be concluded that the U^{Py}-modified acpcPNAs can discriminate between complementary and mismatched DNA and it is possible to use the U^{Py}-modified acpcPNAs as a probe to detect DNA base sequences.

3.5 Optical properties of U^{Py}-modified acpcPNAs

3.5.1 Optical properties of homothymine acpcPNA carrying U^{Py} modification

The optical properties of homothymine acpcPNA carrying U^{Py} modification (**TU^{Py}T**) were studied first. The UV/Vis absorption spectrum of single-stranded **TU^{Py}T** showed a broad pyrene absorption band with a λ_{max} of 345 nm and a small shoulder at λ 331 nm in addition to the normal nucleobase absorption in the region of 260 nm (**Figure 3.6**). The shape of the pyrene absorption spectrum in **TU^{Py}T** is consistent with previous spectroscopic studies of DNA carrying the same U^{Py} base

[34, 61–62]. The broad featureless pyrene absorption indicates a strong electronic coupling between the pyrene chromophore and the U base. In the presence of complementary DNA target (**dA9**), the shape and magnitude of the pyrene absorption band changed noticeably. The absorption maxima of the **TU^{Py}T·dA9** hybrid was broadened and shifted slightly to a longer wavelength (353 nm) compared to the single stranded PNA. This red shift of the absorption maxima of the U^{Py} chromophore by 8 nm was also accompanied by a small hyperchromism. No significant change in the shape and magnitude of spectra in the pyrene absorption region could be observed in the three remaining mismatched hybrids (**TU^{Py}T·dA8T**, **TU^{Py}T·dA8C** and **TU^{Py}T·dA8G)**. The results suggest that the U^{Py} bases in the complementary hybrid and single-stranded acpcPNA are in different environment.

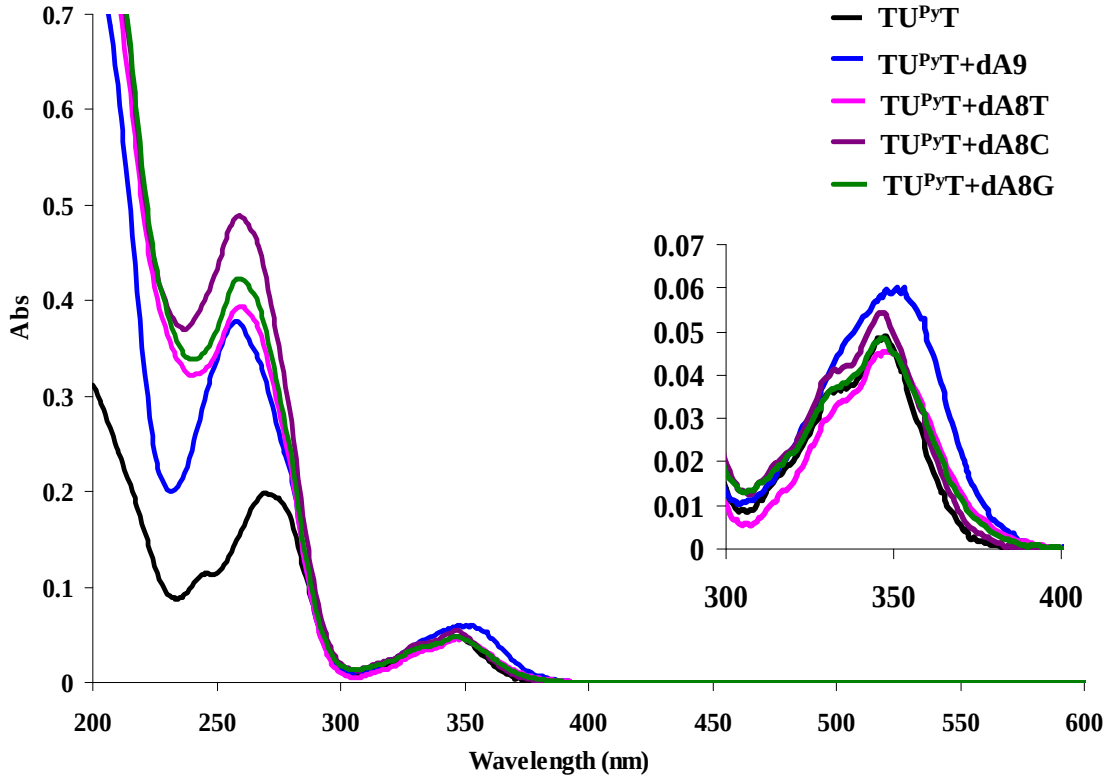

Figure 3.6 UV/Vis spectra of **TU^{Py}T** and **TU^{Py}T+dA9–dA8G** in 10 mm sodium phosphate buffer pH 7.0, [PNA] = 2.5 μM and [DNA] = 3.0 μM.

The change in the absorption spectra of **TU^{Py}T** upon hybridization with DNA was studied at different temperatures (**Figure 3.7**). The absorption of the **TU^{Py}T·dA9** hybrid was measured at different temperatures between 25 and 95 ºC. At low temperatures (below T_m) the pyrene absorption maxima can be found at ca. 353 nm. At high temperatures the absorption maximum was shifted by approximately 8 nm to ca. 345 nm and the absorption spectra of the U^{Py} base became similar to that of the single-stranded **TU^{Py}T** at room temperatures (25 ºC). After cooling, the absorption spectra changed back to that of the duplex again indicating that the change in the absorption spectra is associated with the duplex formation and is fully reversible. According to the absorption spectra as a function of temperature, a distinct change was observed between 65 and 75 ºC, which is coincident to the T_m of the **TU^{Py}T·dA9** hybrid (T_m= 65.8 ºC).

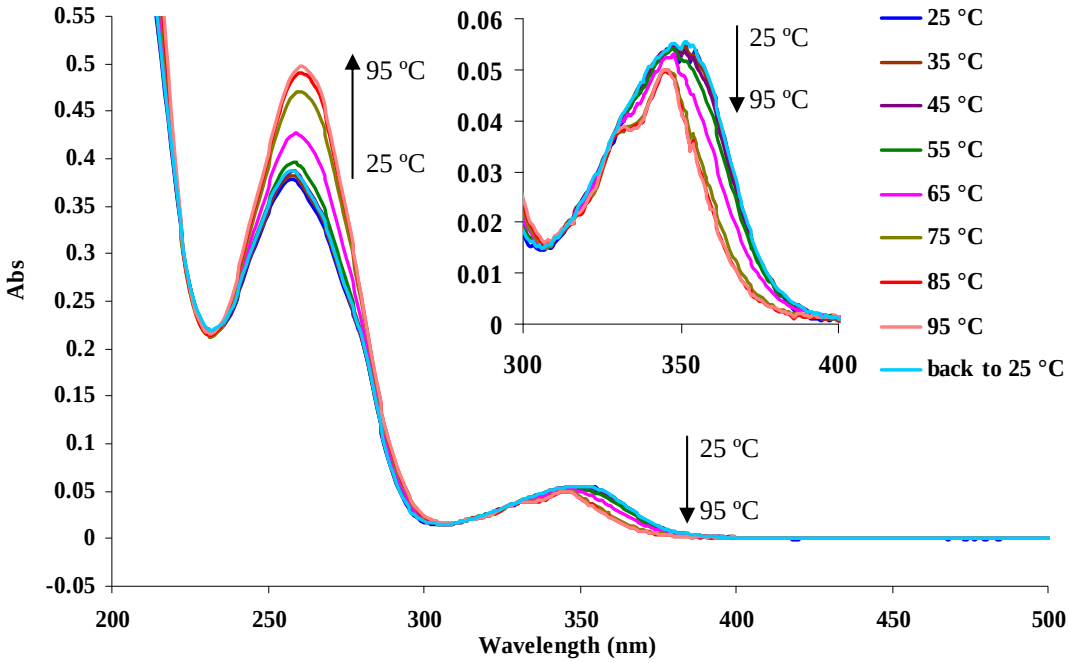

Figure 3.7 UV/Vis spectra of **TU^{Py}T+dA9** in 10 mm sodium phosphate buffer pH 7.0, [PNA] = 2.5 μM and [DNA] = 3.0 μM, from 25 to 95 ºC and back to 25 ºC, temperature step=10 ºC.

The fluorescence of **TU^{Py}T** in the absence and presence of target DNA in 10 mM sodium phosphate buffer pH 7.0 were next investigated. The quantum yields and fluorescence intensity ratios of **TU^{Py}T** and its DNA hybrids are summarized in **Table 3.5**. When excited at 350 nm, the single-stranded **TU^{Py}T** exhibited a broad and unstructured fluorescence peak owing to the U^{Py} base (**Figure 3.8**). The maximum emission wavelength appeared at 465 nm with a rather low efficiency as revealed by the very low fluorescence quantum yield (Φ_F = 0.006). In the presence of complementary DNA (**dA9**), the fluorescence intensity of the duplex at 465 nm was enhanced by a factor of 41.9 relative to the single-stranded **TU^{Py}T** and the quantum yield was also increased to 0.131 without change in the maximum emission wavelength.

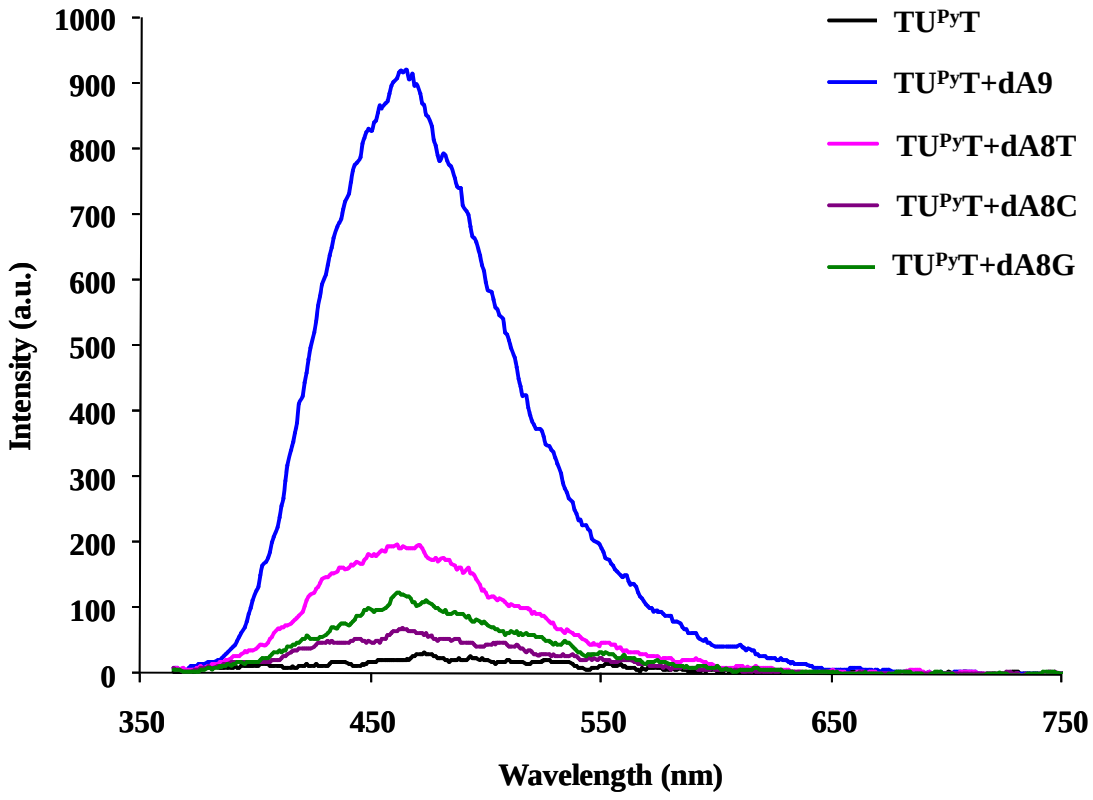

Figure 3.8 Fluorescence spectra of **TU^{Py}T** and **TU^{Py}T+dA9–dA8G** in 10 mm sodium phosphate buffer pH 7.0, [PNA] = 2.5 μM and [DNA] = 3.0 μM, excitation wavelength = 350 nm.

The discrimination between complementary and single base mismatched DNA targets by U^{Py}-containing PNA **TU^{Py}T** was next investigated by fluorescence spectroscopy. When the DNA strands contained a mismatched base directly opposite to the U^{Py}, the fluorescence intensities were also increased relative to the single stranded **TU^{Py}T,** but to a much smaller extent when compared to the complementary hybrid. When **TU^{Py}T** was hybridized with **dA8T**, **dA8C** and **dA8G**, the fluorescence intensities of the duplex were increased by 5.3, 8.7 and 3.0 folds, respectively, as opposed to the increase of 42 folds with **dA9**. This translates to a discrimination factor between complementary and single-mismatched hybrids of between 4.8 to 14 folds. From the results, it can be concluded that the fluorescence of the U^{Py}-containing acpcPNA was highly sensitive to its hybridization state. The fluorescence of the U^{Py}-modified PNA increased significantly when the U^{Py}-modified PNA was hybridized to its complementary DNA target.

The difference between the fluorescence of the complementary and mismatched hybrids of **TU^{Py}T**, as well as the single-stranded **TU^{Py}T**, could be visualized by the naked eye under UV light irradiation at 365 nm (**Figure 3.9**).

TU^{Py}T **TU^{Py}T+dA9** **TU^{Py}T+dA8T** **TU^{Py}T+dA8C** **TU^{Py}T+dA8G**

Figure 3.9 Photographs of **TU^{Py}T** and its hybrids with DNA **dA9**–**dA8G** in 10 mM sodium phosphate buffer pH 7.0, [PNA] = 2.5 μM and [DNA] = 3.0 μM under black light (365 nm).

3.5.2 Effect of neighboring bases on the fluorescence of homothymine acpcPNA carrying U^{Py} modification

To investigate the effect of neighboring nucleobases on the fluorescence properties of acpcPNA carrying U^{Py} modification, **AU^{Py}A, GU^{Py}G**, **CU^{Py}C** and **CU^{Py}C13** which had different bases adjacent to U^{Py} were used as models.

Table 3.5 Quantum yields, and fluorescence intensity ratios of **TU^{Py}T–CU^{Py}C13** and their hybrids with DNA.

Entry	PNA	DNA	Φ_F[a]	I_{465}/ I_{465}(ss)	I_{465}(comp)/ I_{465}	Note
1	**TU^{Py}T**	–	0.006	1.0	41.9	single strand
2	**TU^{Py}T**	**dA9**	0.131	41.9	1.0	complementary
3	**TU^{Py}T**	**dA8T**	0.022	5.3	7.9	single mismatch T
4	**TU^{Py}T**	**dA8C**	0.039	8.7	4.8	single mismatch C
5	**TU^{Py}T**	**dA8G**	0.013	3.0	14.0	single mismatch G
6	**AU^{Py}A**	–	0.011	1.0	6.2	single strand
7	**AU^{Py}A**	**dTAT**	0.051	6.2	1.0	complementary
8	**GU^{Py}G**	–	0.006	1.0	8.3	single strand
9	**GU^{Py}G**	**dCAC**	0.032	8.3	1.0	complementary
10	**CU^{Py}C**	–	0.006	1.0	2.0	single strand
11	**CU^{Py}C**	**dGAG**	0.010	2.0	1.0	complementary
12	**CU^{Py}C13**	–	0.009	1.0	6.8	single strand
13	**CU^{Py}C13**	**dGAG13**	0.048	6.8	1.0	complementary

Conditions: [PNA] = 2.5 mM; [DNA] = 3.0 mM, 10 mM sodium phosphate buffer, pH 7.0, excitation wavelength = 350 nm.

[a]Measured using quinine sulfate as a standard.

The quantum yields and fluorescence intensity ratios of **AU^{Py}A–CU^{Py}C13** and their DNA hybrids are summarized in **Table 3.3**. Similar to **TU^{Py}T**, in all cases the fluorescence intensities of the single-stranded PNAs were very low (Φ_F =0.006–0.011) (**Figure 3.10**). **AU^{Py}A**, which had a A/A neighboring base, was the brightest, with a quantum yield 0.0011. The fluorescence of **AU^{Py}A** was stronger than **TU^{Py}T**, **GU^{Py}G** and **CU^{Py}C** by approximately 2 folds. When hybridized with complementary DNA, the fluorescence intensities of the **AU^{Py}A·dTAT** and **GU^{Py}G·dCAC** duplexes at 465 nm were enhanced by a factor of 6.2 and 8.3, respectively relative to the single-stranded PNA. The increase in fluorescence of the U^{Py} upon hybrid formation could therefore be observed with A/A and G/G as neighboring bases. In contrast, the fluorescence intensity of the **CU^{Py}C·dGAG** duplex was increased from the single-stranded PNA by only 2.0-fold. The apparent absence of fluorescence increase with C/C neighboring bases in the PNA **CU^{Py}C** was attributed to the low stability of acpcPNA hybrids containing multiple TC/CT steps, which was supported by T_m experiment (see section 3.3.2). The fluorescence of the 13mer hybrid **CU^{Py}C13·dGAG13** was increased by a factor of 6.8 relative to the single-stranded **CU^{Py}C13**. It can be seen from this experiment that the fluorescence increase of the U^{Py} base in acpcPNA upon hybridization with complementary DNA is not dependent on the types of neighboring base. This is an important point, because many labels that reported to be environment sensitive can perform well only in limited sequence context. For example, most fluorescence labels are quenched by neighboring G bases [63].

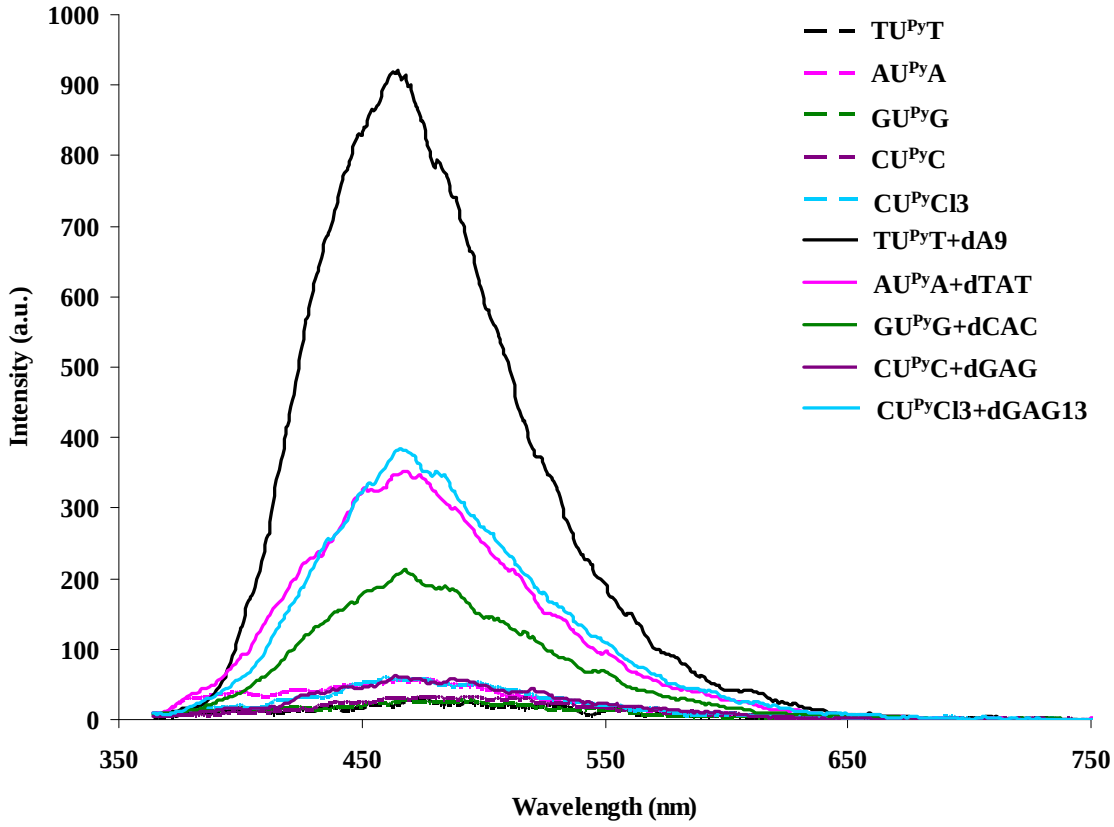

Figure 3.10 Fluorescence spectra of single stranded **XU^{Py}X–CU^{Py}C13** and their hybrids with complementary DNA in 10 mm sodium phosphate buffer pH 7.0, [PNA] = 2.5 μM and [DNA] = 3.0 μM, excitation wavelength = 350 nm.

In all cases, the fluorescence change of **XU^{Py}X·dYU^{Py}Y** could be easily visualized by naked eyes under UV light irradiation at 365 nm (**Figure 3.11**).

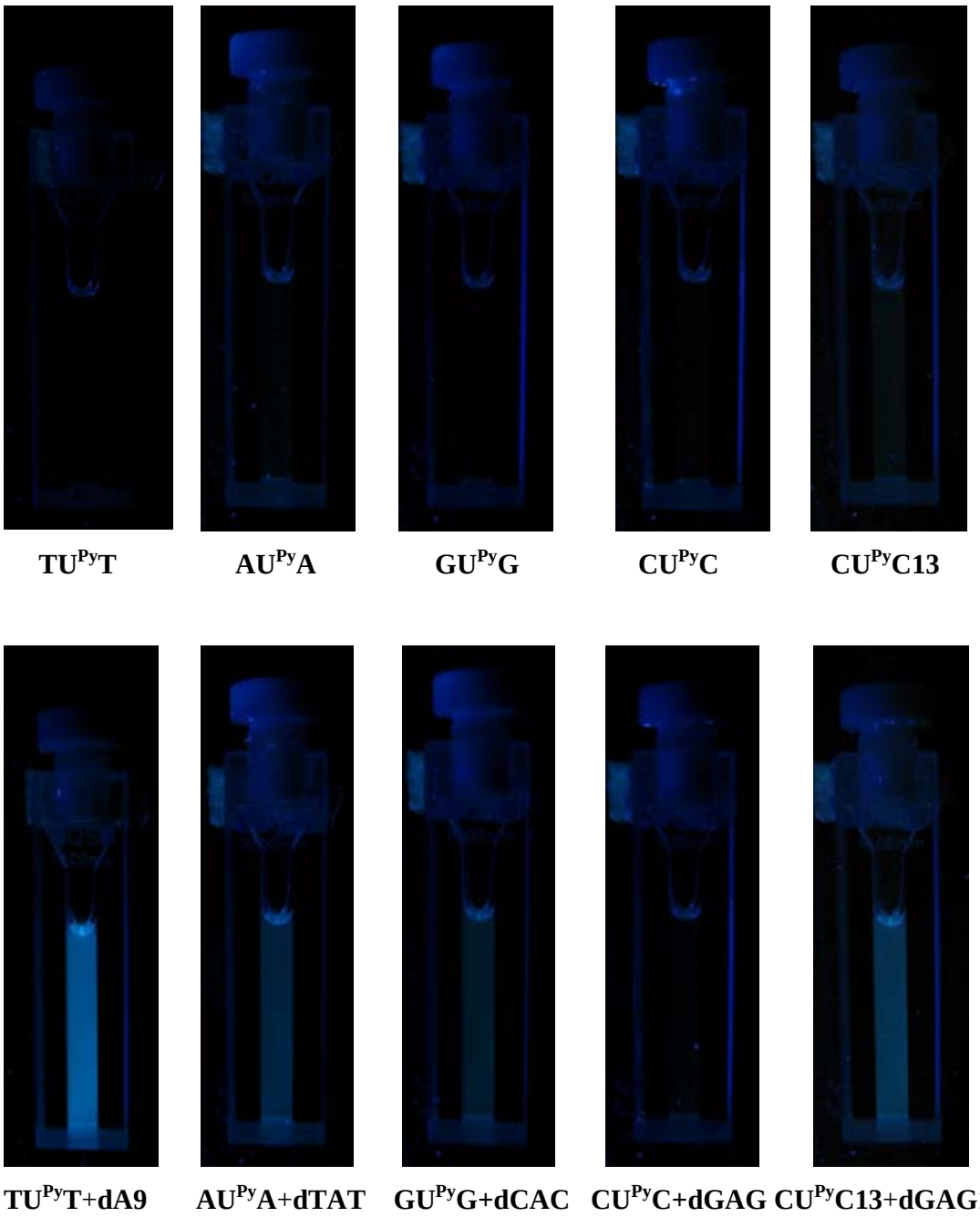

Figure 3.11 Photographs of single stranded **XU^{Py}X–CU^{Py}C13** and their hybrids with complementary DNA in 10 mm sodium phosphate buffer pH 7.0, [PNA] = 2.5 μM and [DNA] = 3.0 μM.

3.5.3 Optical properties of mixed sequence acpcPNA carrying U^{Py} modification

The UV/Vis absorption spectrum of single-stranded **MixU^{Py}** showed a broad pyrene absorption band with a λ_{max} of 347 nm and a small shoulder at λ 336 nm similar to the homothymine sequence **TU^{Py}T**. (**Figure 3.12**) In contrast to the homothymine sequence, the shape and magnitude of the pyrene absorption band changed only slightly upon addition of the complementary DNA (**dcomMix**). The absorption maxima was broadened and shifted slightly to a longer wavelength to 350 nm. The absorption spectra of mismatched hybrids carrying a mismatch base directly opposite to the U^{Py} base showed significant red-shifted absorption maxima to ca. 354 and 360 nm with a pronounced broadening (354 nm for **MixU^{Py}·dmGMix** and **MixU^{Py}·ddsMix**, and 360 nm for **MixU^{Py}·dmCMix** and **MixU^{Py}·dmTMix)**. These red shifts by 7 nm and 13 nm were also accompanied by small hypochromism of the pyrene absorption compared to the single-stranded **MixU^{Py}**. The spectra are very similar to those of DNA hybrids carrying U^{Py} base, irrespective of the matched-mismatched pairs, previously reported in the literature [34]. The difference in the pyrene absorption indicates that the pyrene chromophore is differently organized in the single stranded PNA and in the complementary and mismatched duplexes. The significant red shift and large hypochromism suggest that mismatched hybrids carrying a mismatch base directly opposite to the U^{Py} base probably have the U^{Py} twist out of the duplex so that the pyrene unit is intercalated between the base stack to compensate the absence of hydrogen bonding. In the case of the **MixU^{Py}·dinMix** pair carrying a mismatch base not directly opposite to the U^{Py} base, the absorption spectrum was remarkably similar to the complementary hybrid. In this particular case, the base pairing between the U^{Py} and dA prevented the intercalation of the pyrene moiety between the base stack, because this will result in breaking of the base pairing. The remarkable differences in pyrene absorbtion spectra in various U^{Py}-containing acpcPNA hybrids may thus be explained in this way.

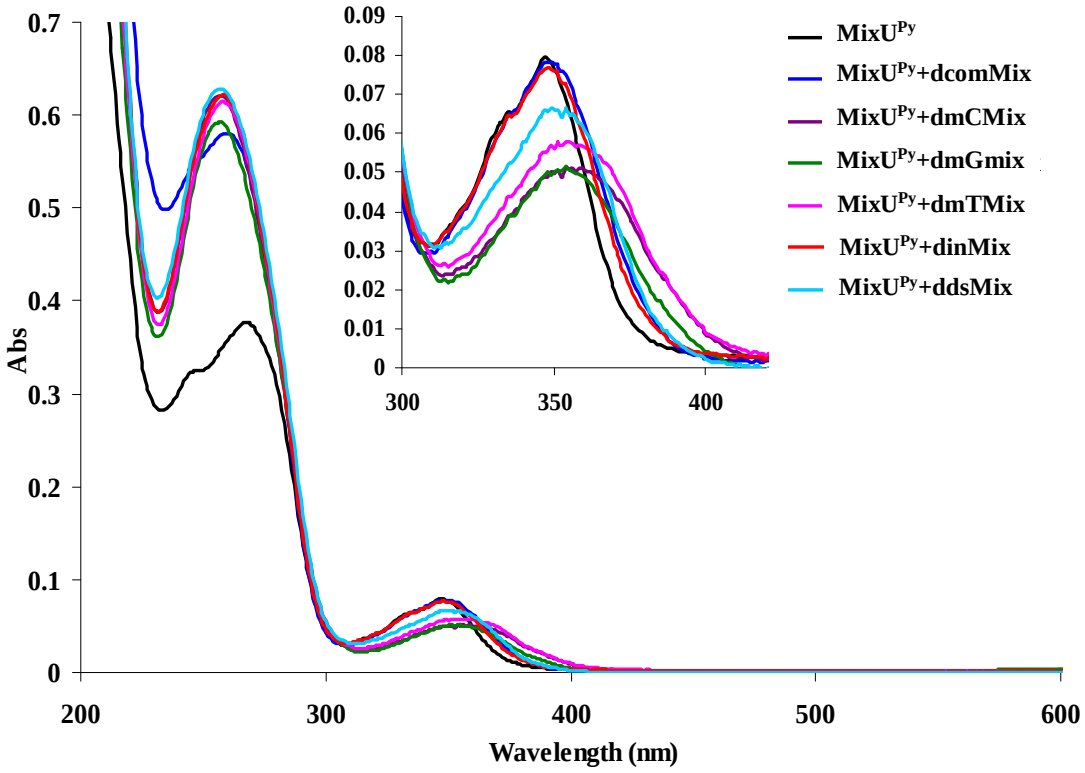

Figure 3.12 UV/Vis spectra of **MixU^{Py}** and and its hybrids with DNA **dcomMix–dsMix** in 10 mM sodium phosphate buffer pH 7.0, [PNA] = 2.5 μM and [DNA] = 3.0 μM.

The change in the absorption spectra of **MixU^{Py}** upon hybridization with complementary DNA is also reversible similar to **TU^{Py}T** (**Figure 3.13**). The absorption spectra of the **MixU^{Py}·dcomMix** hybrid was measured at different temperatures between 25 and 95 ºC. At room temperatures the broad pyrene absorption was observed with a maximum at ca. 350 nm. At high temperatures (above 65 ºC) the absorption spectra of the pyrene chromophore region became similar to that of the corresponding single-stranded **MixU^{Py}** at room temperatures (25 ºC) and, after cooling, the absorption spectrum changed back to that of the duplex again.

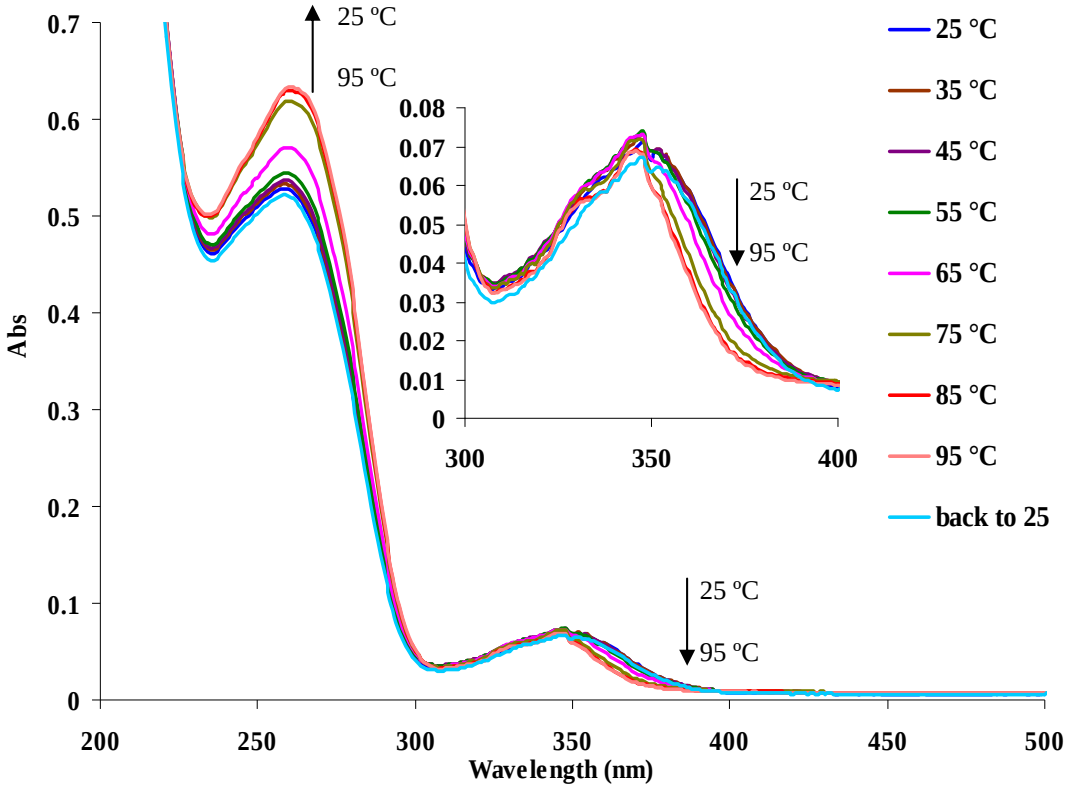

Figure 3.13 UV/Vis spectra of **MixU^{Py}+dcomMix** in 10 mm sodium phosphate buffer pH 7.0, [PNA] = 2.5 μM and [DNA] = 3.0 μM, from 25 to 95 ºC and back to 25 ºC, temperature step=10 ºC.

It is interesting to note that the absorption spectra of the DNA hybrids of **MixU^{Py}** were quite different from those of **TU^{Py}T**. The change in the UV absorption spectra of the pyrene chromophore of **MixU^{Py}·dcomMix** was much-smaller than that of **TU^{Py}T·dA9**. This result suggests that the **MixU^{Py}·dcomMix** and **TU^{Py}T·dA9** hybrids might adopt different structures. The unusual structure of homothymine/homopyrimidine sequence is well recognized in the DNA field, which is also supported here by the unusually high thermal stability and the very large increase in fluorescence change of the **TU^{Py}T·dA9** hybrid compared to the **MixU^{Py}·dcomMix** hybrid. Significant bathochromic shifts were also observed in the absorption spectra of mismatched duplexes of **MixU^{Py}**. However, these shifts are very different from what already observed in the mismatched duplexes of **TU^{Py}T** because the magnitudes of the shifts were much-larger and the shape of the absorption spectra were different (no shoulder was observed). The spectral change in mismatched

duplexes of **MixU^{Py}** supported the proposed intercalation of the pyrene into the base stack of the mismatched duplexes. No similar change was observed in the mismatched hybrids of **TU^{Py}T**, presumably because the poor ability of AT pairs to accommodate intercalation.

Circular Dichroism spectroscopy (CD) is a powerful technique widely used for the evaluation of the conformation and interaction of nucleic acids. In this work, CD was also used to investigate the interaction of U^{Py}-modified acpcPNA and DNA. If hybridization with DNA occurs, an induced CD signal should be observed especially in the wavelength region where the nucleobase chromophores absorb due to the bases becoming re-oriented as they from the stack [64]. In the case of complementary hybrids, CD spectra of **MixU^{Py}** with **dcomMix** showed a significantly different CD spectrum from the calculated sum of the CD spectra of individual components (**Figure 3.14A**). In addition, the pyrene chromophore in the **MixU^{Py}·dcomMix** duplex showed a slightly positive band with a maximum at 360 nm. This observation clearly indicates the conformation change upon hybridization between the PNA and DNA. On the other hand, when the DNA strands containing a mismatched base directly opposite to the U^{Py} base such as in the **MixU^{Py}·dmCMix** duplex, a slightly negative band was observed in the pyrene absorption region (**Figure 3.14B**). CD spectra of **MixU^{Py}** with other mismatched DNAs are shown in **Figure A60** and **61** (see Appendices). The difference in the pyrene absorption region (ca. 360 nm) suggests that the pyrene chromophore is differently organized in the complementary and mismatched duplexes. Taken together with the unusually high T_m and the UV absorption spectral change of the direct mismatched hybrids, the negative CD band at 360 nm may be attributed to the intercalated pyrene [65].

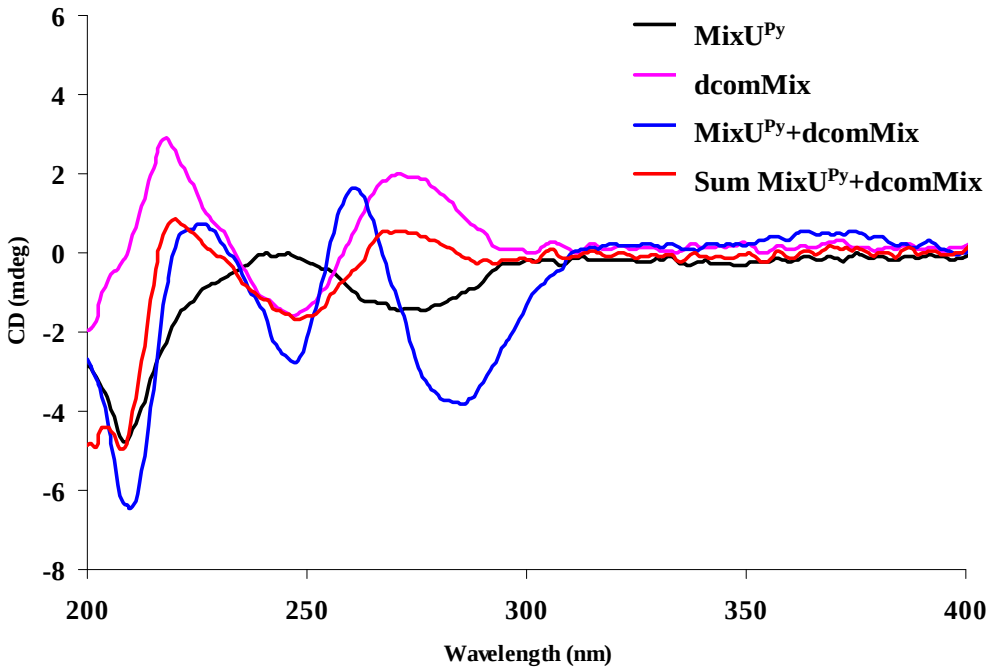

A

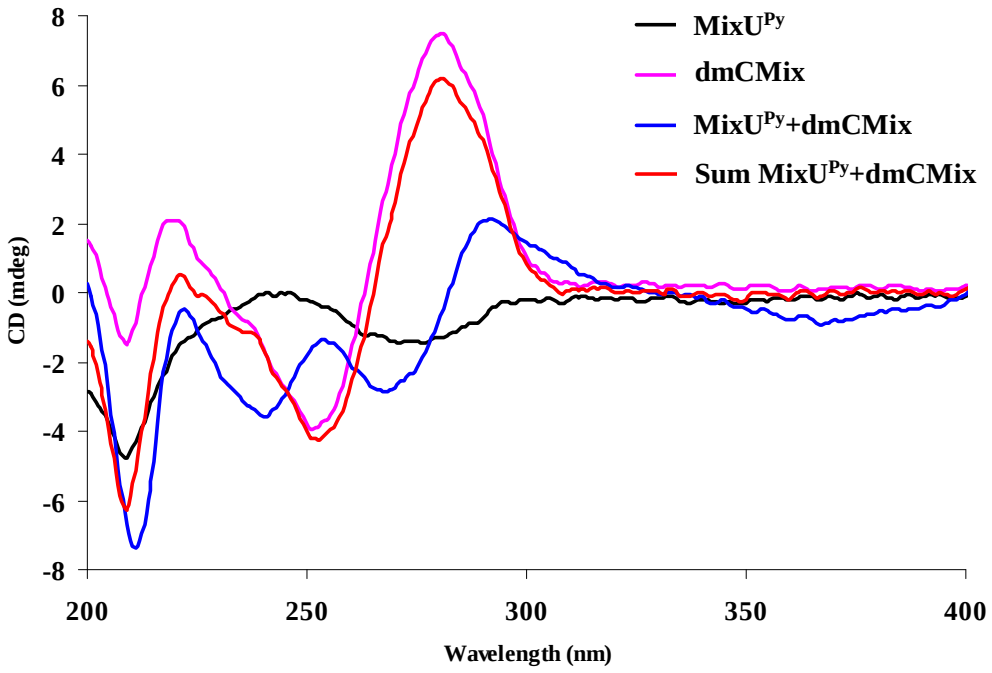

B

Figure 3.14 CD spectra of **MixU^{Py}** with **dcomMix** (complementary, **A**) and **dmCMix** (mismatched, **B**) in 10 mm sodium phosphate buffer pH 7.0, [PNA] = 2.5 μM and [DNA] = 3.0 μM.

The fluorescence properties of the PNA **MixU^{Py}** were next investigated. The **MixU^{Py}** in single stranded from exhibited a very weak fluorescence with a maximum emission at 465 nm. The fluorescence quantum yield was low (Φ_F =0.009) but was somewhat higher than **TU^{Py}T** (Φ_F =0.006). The fluorescence enhancement obtained upon hybridization of **MixU^{Py}** with complementary DNA (**dcomMix**). The fluorescence intensity of the duplex at 465 nm was enhanced by a factor of 6.5 relative to the single-stranded **MixU^{Py}** and the quantum yield was increased to 0.052 (**Figure 3.15**). **Table 3.6** summarized the fluorescence enhancement of complementary and various mismatched DNA hybrids of **MixU^{Py}** as calculated from the ratio of the fluorescence intensities of the duplex and single stranded PNA [I_{465}(ds)/I_{465}(ss)]. It can be seen that mismatched DNA targets carrying the mismatch base directly opposite to the U^{Py} base resulted in little or almost no change in the fluorescence intensities. The slight increase of fluorescence quantum yields (Φ_F =0.014-0.025) was due to the hypochromism of the pyrene chromophore absorption. The **MixU^{Py}·dmGMix** mismatch hybrid showed the highest fluorescence enhancement among all mismatched hybrids (1.6 folds enhancement relative to the single-stranded **MixU^{Py}**) but the signal was still much lower than that of the complementary hybrid (6.5 fold). Fluorescence discrimination between complementary and single base mismatched DNA targets [I_{465}(comp)/I_{465}] ranges between 4.1 to 6.5 folds.

On the other hand, when the mismatched base in the DNA strand was located in a position that is not directly opposite to the U^{Py} as in **dinMix**, a significant fluorescence enhancement relative to the single-stranded **MixU^{Py}** (3.1 folds) was observed despite a much lower T_m of this indirect single mismatched hybrid compared to other mismatched hybrids (see **Table 3.1**). When a second base mismatch was introduced to the DNA strand at the position opposite to the U^{Py} base as in **ddsMix**, the fluorescence became indistinguishable from the single-stranded **MixU^{Py}**. From the fluorescence experiments, it was concluded that the fluorescence property of the mixed sequence U^{Py}-containing acpcPNA is highly sensitive to its hybridization state. The U^{Py} in acpcPNA therefore acts as a base discriminating fluorescent (BDF) nucleobase in the acpcPNA system. The fluorescence enhancement of the U^{Py} is directly associated to the pairing between the U^{Py} in acpcPNA and the dA in DNA.

Importantly, the fluorescence of the U^{Py} base is always enhanced when the acpcPNA is hybridized to its complementary DNA target, irrespective of the neighboring bases or sequences (homothymine or mixed sequence).

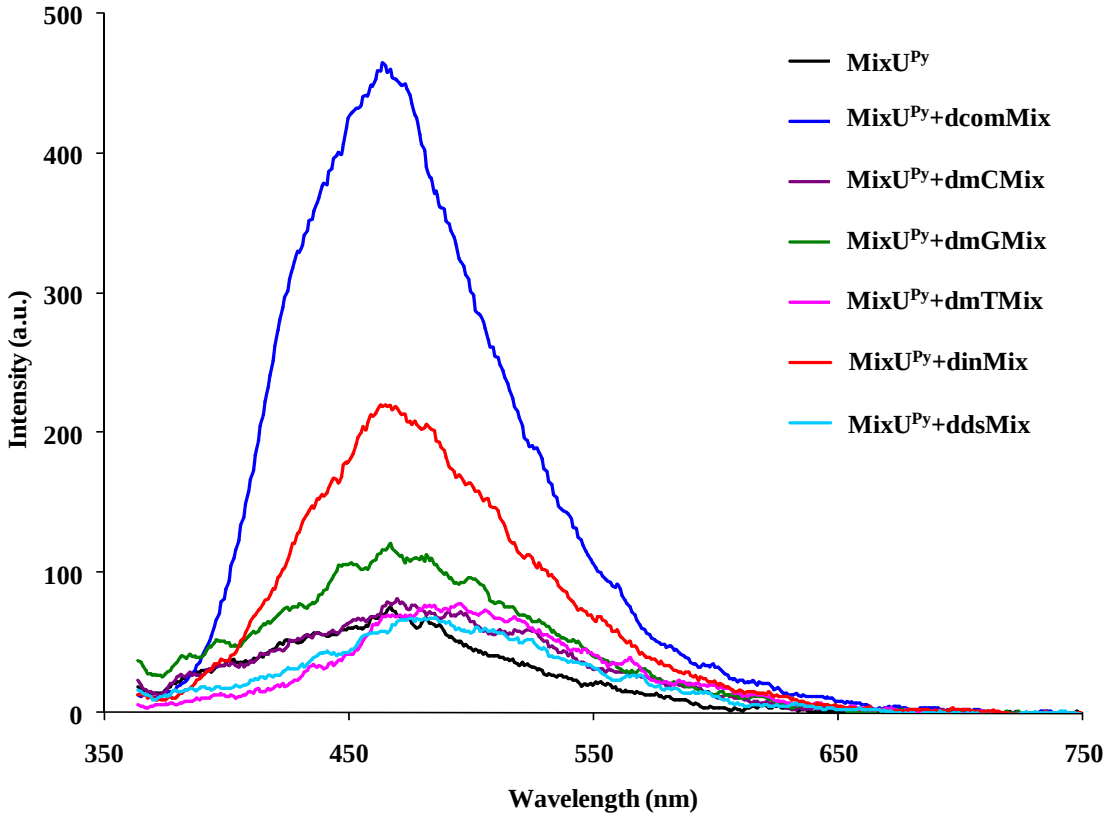

Figure 3.15 Fluorescence spectra of **MixU^{Py}** and and its hybrids with DNA **dcomMix-ddsMix** in 10 mM sodium phosphate buffer pH 7.0, [PNA] = 2.5 μM and [DNA] = 3.0 μM, excitation wavelength = 350 nm.

Table 3.6 Quantum yields and fluorescence intensity ratios of **MixU^{Py}**, **MixAU^{Py}** and **MixTU^{Py}** and their hybrids with DNA.

Entry	PNA	DNA	Φ_F[a]	I_{465}/ I_{465}(ss)	I_{465}(comp)/ I_{465}	Note
1	**MixU^{Py}**	–	0.009	1.0	6.5	single strand
2	**MixU^{Py}**	**dcomMix**	0.052	6.5	1.0	complementary
3	**MixU^{Py}**	**dmCMix**	0.018	1.1	5.9	single mismatch C
4	**MixU^{Py}**	**dmGMix**	0.025	1.6	4.1	single mismatch G
5	**MixU^{Py}**	**dmTMix**	0.014	1.0	6.5	single mismatch T
6	**MixU^{Py}**	**dinMix**	0.029	3.1	2.1	indirect mismatch
7	**MixU^{Py}**	**ddsMix**	0.011	0.8	8.1	double mismatch
8	**MixAU^{Py}**	–	0.030	1.0	2.7	single strand
9	**MixAU^{Py}**	**dcMixA**	0.066	2.7	1.0	complementary
10	**MixTU^{Py}**	–	0.027	1.0	4.0	single strand
11	**MixTU^{Py}**	**dcMixT**	0.084	4.0	1.0	complementary

Conditions: [PNA] = 2.5 mM; [DNA] = 3.0 mM, 10 mM sodium phosphate buffer, pH 7.0, excitation wavelength = 350 nm.

[a]Measured using quinine sulfate as a standard.

The fluorescence discrimination of the complementary and mismatched hybrids of **MixU^{Py}** could be visualized by the naked eye under UV light irradiation at 365 nm (**Figure 3.16**).

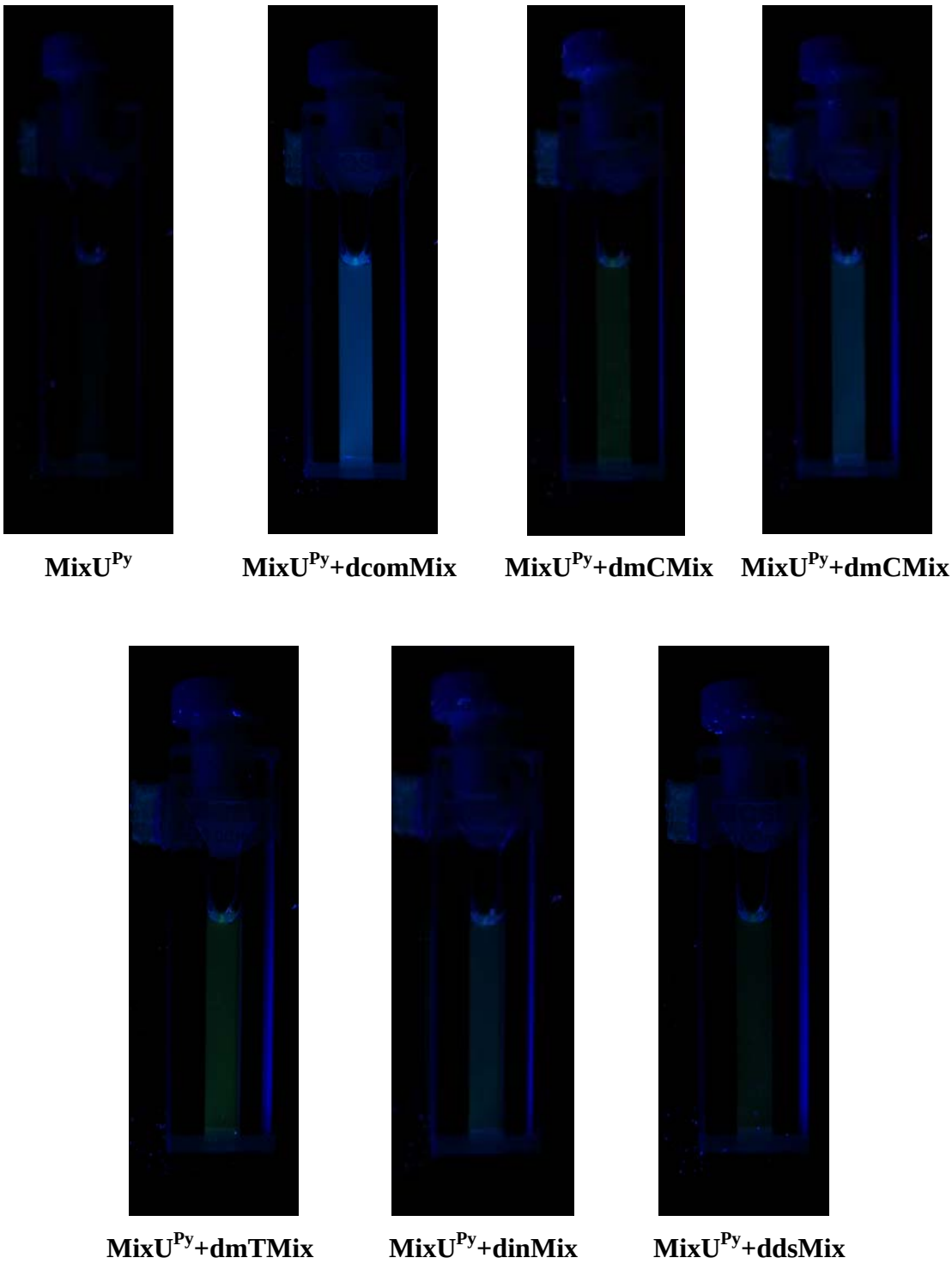

Figure 3.16 Photographs of **MixU^{Py}** and its hybrids with DNA **dcomMix**–**ddsMix** in 10 mM sodium phosphate buffer pH 7.0, [PNA] = 2.5 μM and [DNA] = 3.0 μM under black light (365 nm).

The same fluorescence enhancement upon hybridization with complementary DNA was also observed in another two acpcPNA sequences, **MixAU^{Py}** and **MixTU^{Py}** (**Figure 3.17**), which carry different flanking bases (AU^{Py}T and TU^{Py}T). **Table 3.6** shows relative fluorescence increase upon formation of matched duplex of **MixAU^{Py}** and **MixTU^{Py}**. The fluorescence enhancements in these cases are smaller than in the case of **MixU^{Py}** owing to a relatively high fluorescence background of the single stranded **MixAU^{Py}** and **MixTU^{Py}**. (Φ_F = 0.030 and 0.027, respectively) The fluorescence quantum yield of the single stranded **MixAU^{Py}** and **MixTU^{Py}** were both higher than **MixU^{Py}**. Nevertheless, significant fluorescence enhancements were still observed (4.0 and 2.7 folds with **MixTU^{Py}·dcMixT** and **MixAU^{Py}·dcMixA**, respectively), which could still be readily distinguished by naked eyes (**Figure 3.18**).

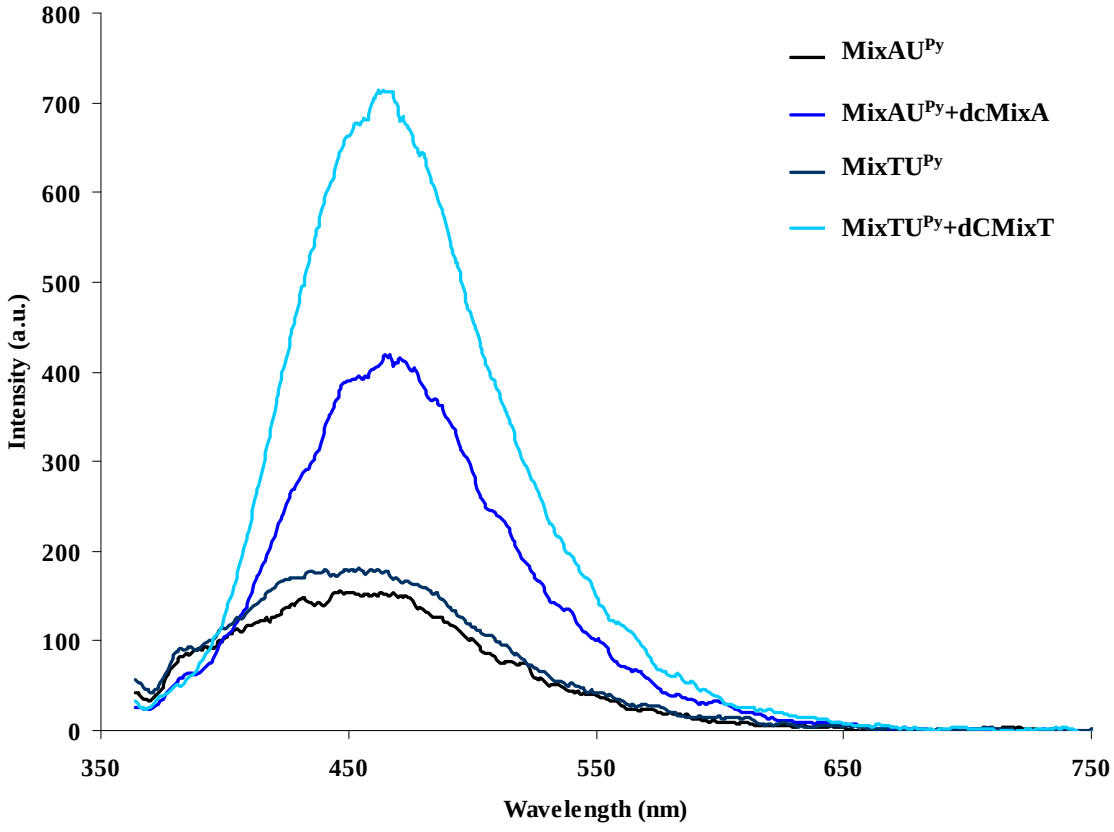

Figure 3.17 Fluorescence spectra of **MixAU^{Py}**, **MixTU^{Py}** and theirs hybrids with complementary DNA in 10 mM sodium phosphate buffer pH 7.0, [PNA] = 2.5 μM and [DNA] = 3.0 μM, excitation wavelength = 350 nm.

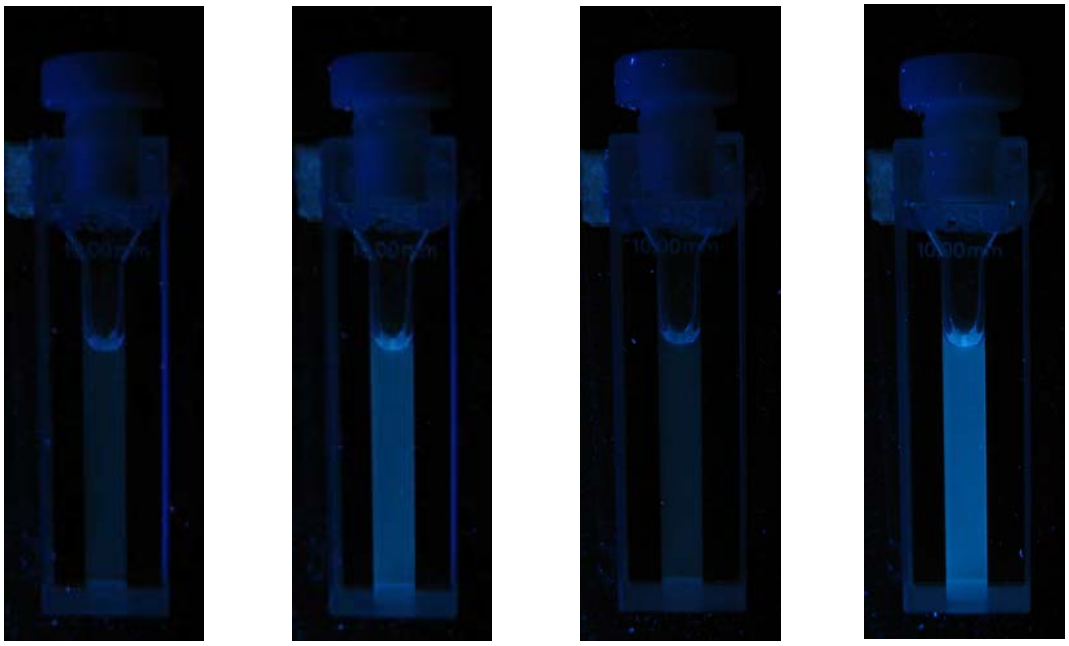

MixAU^{Py} **MixAU^{Py}+dcMixA** **MixTU^{Py}** **MixTU^{Py}+dcMixT**

Figure 3.18 Photographs of **MixAU^{Py}**, **MixTU^{Py}** and theirs hybrids with complementary DNA in 10 mM sodium phosphate buffer pH 7.0, [PNA] = 2.5 μM and [DNA] = 3.0 μM under black light (365 nm).

3.5.4 Effects of thymine base on the fluorescence of the single stranded U^{Py}-modified acpcPNA

In the single-stranded acpcPNA, the U^{Py} base should be quenched by photoinduced electron transfer because of interactions with neighboring nucleobases.[34] In the same buffer, the homothymine PNA (**TU^{Py}T**) exhibited the weakest fluorescence emission compared to the mixed base sequence PNA (**MixU^{Py}**, **MixU^{Py}** and **MixU^{Py}**). These results suggest that fluorescence of the U^{Py} in single stranded acpcPNA was quenched by neighboring thymine base in the strand. To investigate the fluorescent quenching of pyrene by neighboring base in the PNA strand, the homoadenine U^{Py}-acpcPNA carrying a different position of a thymine base (**AU^{Py}–T^{9}AU^{Py}**) were used as models because it is known from other's work that A is the poorest quencher and T is the best quencher of pyrene [59]. The fluorescence spectra of single stranded **AU^{Py}–T^{9}AU^{Py}** are as shown in **Figure 3.19**. It was found

that all single stranded **AU^{Py}–T^{9}AU^{Py}** exhibited very weakly fluorescent similar to **TU^{Py}T** and the fluorescence increase were observed upon hybridization with complementary DNA in all cases (**Figure A62**, see Appendices). From the results, it was not yet possible to conclude about the factor that affect the brightness of the single stranded U^{Py}-modified acpcPNA, but it is clear that the quenching is not a simple relationship to type and position of neighboring nucleobases.

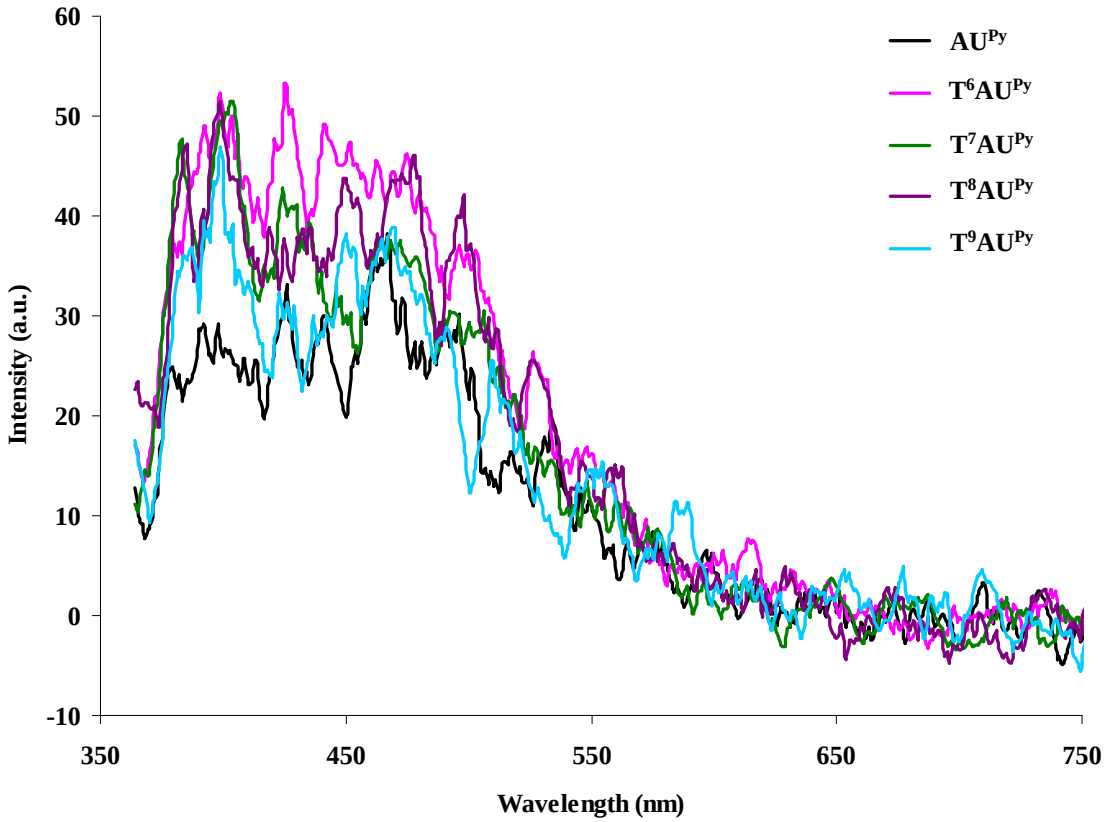

Figure 3.19 Fluorescence spectra of single strand acpcPNA **AU^{Py}–T^{9}AU^{Py}** in 10 mM sodium phosphate buffer pH 7.0, [PNA] = 2.5 μM, excitation wavelength = 350 nm.

3.6 Applications of U^{Py} labeled acpcPNA as a tool for monitoring DNA duplex invasion by acpcPNA

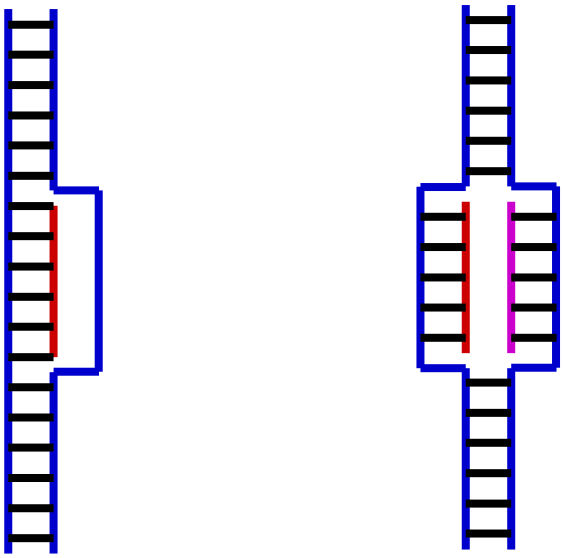

Duplex invasion **Double-duplex invasion**

A **B**

Figure 3.20 DNA duplex invasion by PNA

PNA has an ability to recognize the sequences within duplex DNA by forming a strand invasion complex. A PNA·DNA_2 duplex invasion (**Figure 3.20A**) occurs when the Watson-Crick pairs of the original double stranded DNA breaks apart, and one of the unpaired DNA strand forms a new hybrid with the PNA. The other single strand DNA region form a structure called “D-loop”. Another mode of invasion is called double-duplex invasion (**Figure 3.20B**), this complex occurs in the same way as described above, but the single stranded region of the other DNA strand forms a hybrid with another PNA strand [66]. Generally, to enable DNA double duplex invasion, the PNA strands need to be modified with special bases (diaminopurine in place of A and 2-thiouracil inplace of T) to avoid self-pairing between the two PNAs [67]. In this respect, acpcPNA is unique because it cannot form self-hybrid even when the two PNA strands are complementary. It is therefore expected that acpcPNA will

be a potentially important alternative to conventional PNA for DNA double duplex invasion that does not require base modification.

In this work, the U^{Py}-modified acpcPNA was used as a self-reporting probe for monitoring the DNA duplex invasion by acpcPNA. The sequence of acpcPNA and DNA targets in this study are as follow:

PNA **TU^{Py}T** : Ac-TTTTU^{Py}TTTT-Lys-NH_2
PNA **pA9** : Ac-AAAAAAAAA-Lys-NH_2
DNA **DNA1** : 5'-CGTACA AAAAAAAAGCATGC-3' (20 mer)
DNA **DNA2** : 5'-GCATGT TTTTTTTTCGTACG -3' (20 mer)
DNA **DNA3** : 5'- CGCGGCGTACAAAAAAAAAGCATGCCCTGG-3' (30 mer)
DNA **DNA4** : 5'- CCAGGGCATGCTTTTTTTTTGTACGCCGCG -3' (30 mer)

Firstly, the 20mer DNA duplex **DNA1·DNA2** was prepared in 10 mM phosphate buffer solutions (pH 7.0) without NaCl. **DNA1** can formed stable duplex with it complementary **DNA2** in 10 mM phosphate buffer solutions (pH 7.0) (T_m = 42.9 ºC). This duplex does not give fluorescence signals because of the absence of any fluorophores. After adding the PNA **TU^{Py}T**, the fluorescence spectra was recorded every 3 min for 30 min (excited at 350 nm). It was observed that the fluorescence at 465 nm was increased to ca. 300 a.u. in 30 min (**Figure 3.21**). Since the fluorescence of the single stranded PNA **TU^{Py}T** is very low, the large fluorescence observed suggests that the **TU^{Py}T** had invaded into the DNA duplex by forming a hybrid with the **dA9** region of **DNA1** (complementary sequence). This preliminary results indicate that **TU^{Py}T** can bind to the A9 region of the **DNA1** in the **DNA1·DNA2** duplex. Since the fluorescence intensity of **TU^{Py}T·DNA1** duplex under the same condition is ca. 750 a.u. (**Figure A63**, see Appendices), it can be estimated that the extent **of DNA1·DNA2** duplex invasion by **TU^{Py}T** was about 40%.

Similar to other experiments with U^{Py} PNA probes, the DNA duplex invasion by **TU^{Py}T** could be visualized by naked eyes under UV light irradiation at 365 nm (**Figure A65**, see Appendices).

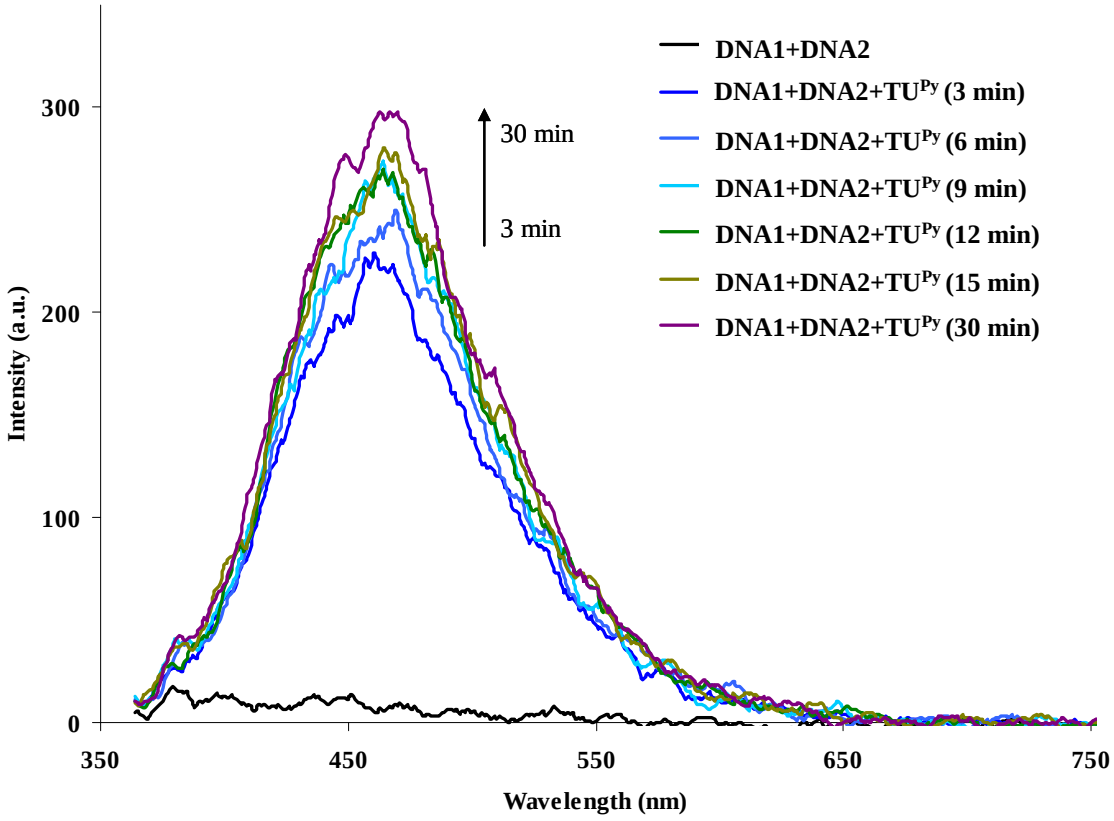

Figure 3.21 Fluorescence study of the DNA duplex invasion of **DNA1**·**DNA2** by **TU^{Py}T** in 10 mM sodium phosphate buffer pH 7.0, [PNA] = 2.5 μM and [DNA] = 3.0 μM, excitation wavelength = 350 nm.

The fluorescence experiment was repeated for 20mer of duplex of **DNA1**·**DNA2** (T_m = 58.6 ºC). After adding the **TU^{Py}T**, the fluorescence intensity was recorded every 5 min for 30 min. The fluorescence intensity was enhanced significantly to ca. 300 a.u. after 5 min as earlier observed. After that the fluorescence intensity was almost constant or very slightly increased. Subsequently, the unmodified acpcPNA **pA9** was added into the solution and the fluorescence was monitored every 5 min for 30 min. After adding the **pA9**, which has a sequence complementary to **DNA2** (and **TU^{Py}T**), the fluorescence intensity was further enhanced to 500 a.u. after 5 min and reached 750 a.u. after 30 min (**Figure 3.22**). The results suggest that in the presence of only **TU^{Py}T**, the Watson−Crick pairs between the double-strand DNA

was partially broken, allowing the pairing between **DNA1** and **TU^{Py}T**, leaving part of the **DNA2** looped out. Adding the **pA9** increased the efficiency of the strand invasion by pairing of the PNA with this looped out region of **DNA2**. The invasion efficiency of ca. 100% was estimated based on the fluorescence intensity of **TU^{Py}T·dA9** duplex under the same condition.

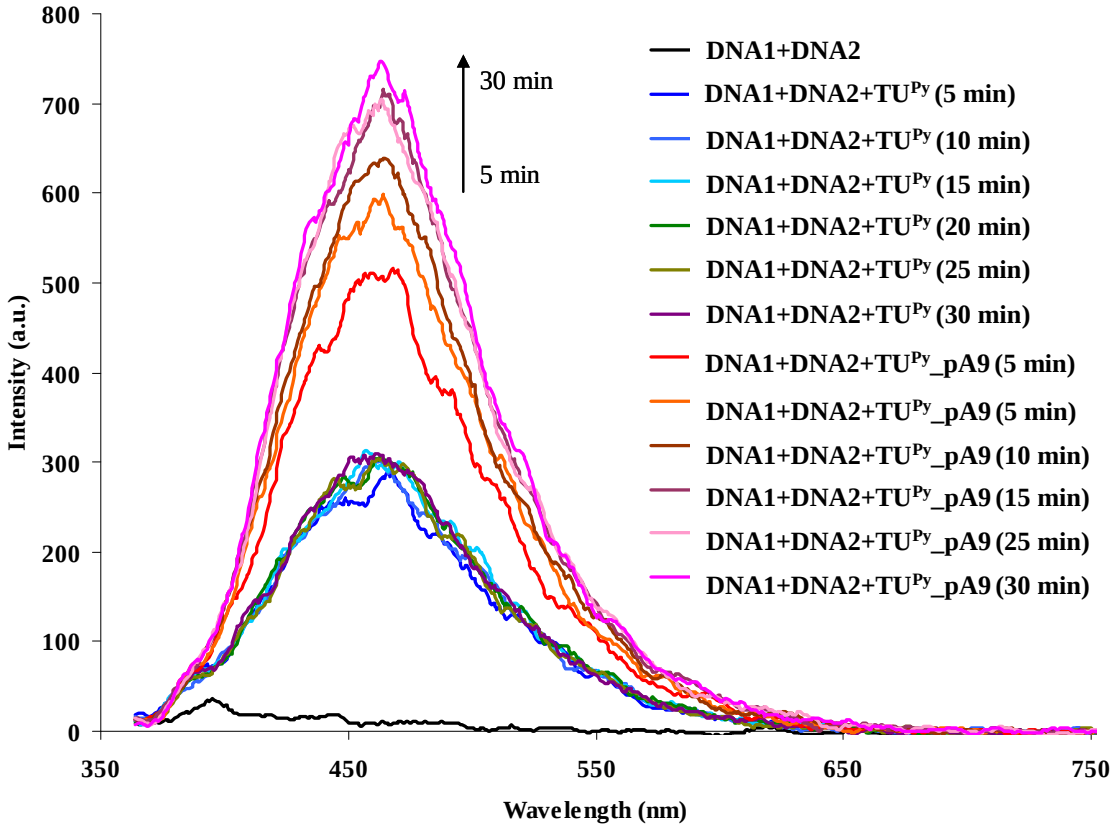

Figure 3.22 Fluorescence study of the DNA duplex invasion of **DNA1·DNA2** by **TU^{Py}T** and **pA9** and in 10 mM sodium phosphate buffer pH 7.0, [PNA] = 2.5 μM and [DNA] = 3.0 μM, excitation wavelength = 350 nm.

One might argue that the increase in fluorescence of **TU^{Py}T** after the addition of **pA9** could be due to the self pairing of the two acpcPNAs rather than the double duplex invasion as proposed. This self-pairing is, however, unlikely based on the knowledge that acpcPNA cannot form self-pairing hybrids. The 1:1 mixture of **TU^{Py}T** after the addition of **pA9** failed to show any fluorescence increase relative to the

single stranded U^{Py}-modified PNA, hence it can be concluded that the fluorescence enhancement was not due to the PNA·PNA self-hybrid formation.

So far, the experiments were performed under low salt conditions, whereby the DNA·DNA duplex was expected to be less stable in order to proof the concept. To study the double duplex invasion at high salt concentration, 10 mM phosphate buffer solutions (pH 7.0) containing 100 mM NaCl. The experiment was performed in the same way as described for another 30 mer of **DNA3·DNA4** duplex (T_m = 76.9 ºC). After adding the **TU^{Py}T**, the fluorescence intensity was increased to ca. 80 a.u. after 30 min (**Figure 3.23**). This indicated that the invasion efficiency by the ssPNA was low (<15%) probably because of the high stability of the DNA·DNA duplex under high salt consitions. Gratifyingly, after adding the **pA9**, the fluorescence intensity was also enhanced again to 320 a.u. for 5 min and to 460 a.u. after 30 min. The results suggest that that **TU^{Py}T** and **pA9** can cooperatively invade into the **DNA3·DNA4** duplex with the efficiency of about 60% at 100 mM NaCl concentration.

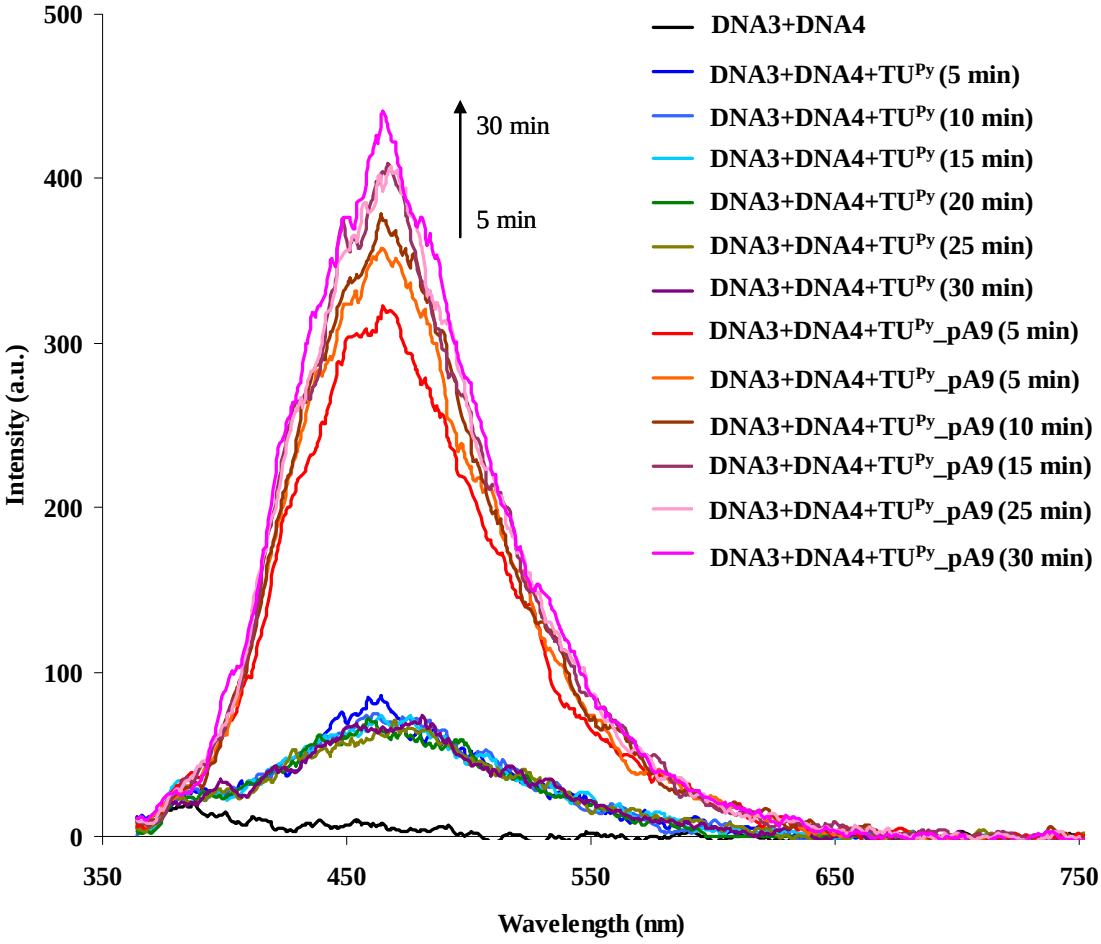

Figure 3.23 Fluorescence study of the DNA duplex invasion of **DNA3·DNA4** by **TU^{Py}T** and **pA9** and in 10 mM sodium phosphate buffer pH 7.0, 100 mM NaCl, [PNA] = 2.5 μM and [DNA] = 3.0 μM, excitation wavelength = 350 nm.

From the above results, it can be concluded that the invasion of acpcPNA (**TU^{Py}T)** into double-stranded DNA is more efficient at low ionic strength conditions when DNA duplex has a weaker binding affinity. The invasion both under low and high salt conditions were facilitated the presence of an additional unlabeled PNA strand (**pA9**) with a sequence complementary to the looped out region of the other DNA strand.

3.7 Pyrenebutyryl-modified acpcPNA (Py-PNA and PNA^{Py})

In addition to attachment of pyrene to nucleobase as described in earlier sections, another new hybridization-responsive acpcPNA probe was designed by attachment of pyrene directly to the N-terminal or internal positions of the acpcPNA backbone. The acpcPNA probe was covalently modified with a pyrene unit through a flexible butyryl linker *via* acylation reaction (section 2.2.3.1). Pyrene was chosen as a fluorophore because its fluorescence is sensitive to the environment such as polarity of the solvent and base stacking. It was proposed that in the single-stranded pyrene-labeled acpcPNA, the fluorescence of pyrene chromophore should be quenched by interaction with the nucleobases in the PNA strand. Upon hybridized with its correct DNA target, the pyrene should be unstacked, resulting in a change in the fluorescence.

3.7.1 Fluorescence properties of terminally pyrenebutyryl-modified acpcPNA (Py-PNA)

In this part of the study, the fluorescence properties of terminally pyrenebutyryl-modified acpcPNA (**PyT9**, **PyM12**, **PyM11** and **PyM10**) were investigated in the absence and presence of target DNA. The fluorescence intensities and quantum yields of terminally modified Py-PNAs and their DNA hybrids are summarized in **Table 3.7** and **3.8**, respectively. When excited at 345 nm, the single-stranded terminally Py-PNA showed highly variable results in their fluorescence intensities (F_{379}(ss) = 3.46 to >200 and Φ_F = 0.0050 to >0.1). The single-stranded **PyT9** with thymine (T) base adjacent to the pyrene moiety gave the lowest fluorescence in the single stranded form (Φ_F = 0.0050) due to the effective quenching of pyrene by the thymine base (**Figure 3.24**) [59]. In the presence of complementary DNA, the fluorescence intensity of the duplex was enhanced by a factor of 46 relative to the single-stranded **PyT9** (**Table 3.7**, entry 1) and the quantum yield was increased to 0.1028. When the DNA strand contained an internally mismatched T base (entry 2), the fluorescence intensity were also increased but to a smaller extent (14.2 folds) relative to the single stranded **PyT9**. When a terminal mismatch base (T) was

introduced to the 3'-terminus of the DNA strand (entry 3), the fluorescence was increased only slightly (3.6 folds relative to the single stranded **PyT9**).

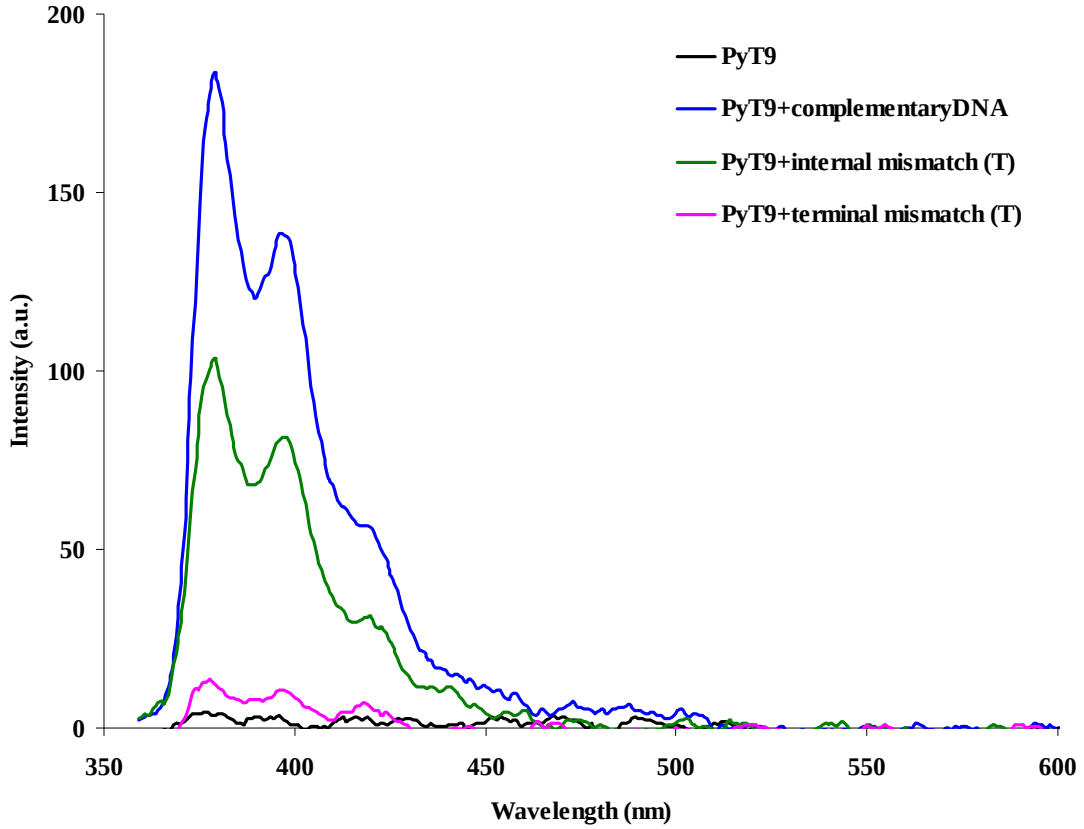

Figure 3.24 Fluorescence spectra of single strand acpcPNA **PyT9** and its hybrids with DNA in 10 mM sodium phosphate buffer pH 7.0, [PNA] = 2.5 μM, excitation wavelength = 345 nm.

The fluorescence properties of mixed-sequence terminally pyrenebutyryl-modified acpcPNA (**PyM12**) were next investigated. Unlike **PyT9**, the PNA **PyM12**, which carry adenine (A) base at the terminal position of the sequence adjacent to the pyrene label, exhibited very high fluorescence intensities (entries 4–14, see F_{379}(ss)) and high fluorescence quantum yields (Φ_F = 0.0820–0.1033) in its single stranded form. Upon hybridization of the complementary DNA (entry 4) and internally mismatched DNA (entry 8), the fluorescence was decreased relative to the single-stranded **PyM12** (F/F_0 = 0.33 and 0.24, respectively). These behaviors are in strikingly contrast to the thymine rich PNA **PyT9**. When an extra hanging nucleotide

was present at the 3'-end of the DNA strands (entries 9–12), the fluorescence intensities were also significantly decreased relative to the single stranded PNA (F/F_0 = 0.13–0.46). On the other hand, when the DNA strands contained a terminal mismatched base (entries 5–8) or 3'-base deletion (entries 13–14), the fluorescence intensities were increased by 1.98–2.48 folds relative to the single stranded **PyM12**.

The fluorescence properties of the mixed-sequence terminally pyrenebutyryl-modified 11mer (**PyM11**) and 10mer (**PyM10**) acpcPNA were next investigated. The single-stranded **PyM11** and **PyM10**, which cytosine (C) and guanine (G) at the N-termini of the sequences adjacent to the pyrene label, respectively, also exhibited low fluorescence intensities (entries 15–18, see F_{379}(ss)) and low fluorescence quantum yields (Φ_F = 0.0217– 0.0492). These values were, however, considerably higher than that of single-stranded **PyT9**. In the presence of complementary DNA, the fluorescence intensities of the duplexes were decreased by a factor of 0.46 and 0.23 (for **PyM11** and **PyM10**, respectively) when compared to the single-stranded PNA (entries 15 and 19). Similar to **PyM12**, when **PyM11** and **PyM10** were hybridized with their internal mismatched DNAs, the fluorescence intensities and quantum yields were also decreased (Φ_F = 0.0030 and 0.0116 for **PyM11** and **PyM10**, respectively) (entries 16 and 20). When a four base hanging multiple Gs sequence was introduced to the DNA strand, the fluorescence was also decreased (0.62 folds**)** (entry 18**).** However, hybridization of **PyM11** to terminal mismatched DNA (entry 17) resulted in fluorescence intensity increase to 2.49 folds of the single stranded **PyM11**. The same effect was also observed with **PyM12**.

The data suggest that fluorescence intensity of single-stranded terminally pyrenebutyryl-PNA is dependent on the nucleobase at the terminal of the strand, adjacent to the pyrene label. When base T, C and G were present at N-terminal to the pyrenebutyryl-PNA strands, the fluorescence of the single-stranded pyrenebutyryl-modified acpcPNAs were very low due to the effective quenching of pyrene by terminally nucleobase. When the pyrene-labeled PNA strand contained base A as the N-terminal base, high fluorescence of the single-stranded PNA was observed. This can be explained by the poor ability of the base A to act as a quencher of pyrene – the fact that is consistent with the literature [59]. Hybridization of the terminally pyrene-modified PNA with DNA resulted in variable results, depending on the original

fluorescence of the single stranded PNA and the identity of the DNA base in vicinity of the pyrene label. With perfectly complementary DNA, the PNA with pyrene label adjacent to base T in the same PNA strand gave an increase in fluorescence. On the other hand, the PNA with pyrene label adjacent to base A, C and G in the same PNA strand gave a decrease in fluorescence upon hybridization with perfectly complementary DNA. This can be explained by quenching of the pyrene with the base T, G and C at the terminal position of the DNA strand. This hypothesis was supported by the fact that deleting of these terminal bases in the DNA strand resulted in fluorescence increase (entries 13 and 14). The mismatched base at the DNA terminal gave opposite results to the complementary base, suggesting that the effective quenching requires the quenching base to be close enough to interact with the pyrene label. From the results obtained above, it can be seen that the hybridization of terminally pyrenebutyryl-modified acpcPNA to its DNA targets gave variable fluorescence change (decreased or increased relative to the single-stranded pyrenebutyryl-modified acpcPNA), depending on the identities of the nucleobases in the vicinity of the pyrenebutyryl label. Nevertheless, it can be concluded that the fluorescence of terminally pyrenebutyryl-modified acpcPNA probes was highly sensitive to its hybridization state.

Table 3.7 Fluorescence intensities of single stranded of terminally pyrenebutyryl-modified acpcPNAs (Py-PNAs) and their hybrids with DNA in this study.

Entry	System	F_{379} (ss)	F_{379} (ds)	F(ds)/ F(ss)	F(com)/ F	Note
1	Py-TTTTTTTTT(**PyT9**) 3'-AAAAAAAAA-5'	3.92	180.84	46.13	1.00	comple-mentary
2	Py-TTTTTTTTT(**PyT9**) 3'-AAAA<u>T</u>AAAA-5'	7.11	100.72	14.17	3.25	internal mismatch (T)
3	Py-TTTTTTTTT(**PyT9**) 3'-<u>T</u>AAAAAAAA-5'	3.46	12.31	3.56	12.96	terminal mismatch (T)
4	Py-AGTTATCCCTGC(**PyM12**) 3'-TCAATAGGGACG-5'	209.93	68.67	0.33	1.00	comple-mentary
5	Py-AGTTATCCCTGC(**PyM12**) 3'-<u>G</u>CAATAGGGACG-5'	219.03	501.62	2.29	0.14	terminal mismatch (G)
6	Py-AGTTATCCCTGC(**PyM12**) 3'-<u>C</u>CAATAGGGACG-5'	213.94	531.16	2.48	0.13	terminal mismatch (C)
7	Py-AGTTATCCCTGC(**PyM12**) 3'-<u>A</u>CAATAGGGACG-5'	200.15	395.62	1.98	0.17	terminal mismatch (A)
8	Py-AGTTATCCCTGC(**PyM12**) 3'-TCAAT<u>C</u>GGGACG-5'	124.88	29.59	0.24	1.38	internal mismatch (C)
9	Py-AGTTATCCCTGC(**PyM12**) 3'-<u>A</u>TCAATAGGGACG-5'	161.47	74.18	0.46	0.72	N-terminal extended (A)
10	Py- AGTTATCCCTGC(**PyM12**) 3'-<u>T</u>TCAATAGGGACG-5'	160.22	20.67	0.13	2.54	N-terminal extended (T)
11	Py-AGTTATCCCTGC(**PyM12**) 3'-<u>C</u>TCAATAGGGACG-5'	157.37	22.70	0.14	2.36	N-terminal extended (C)
12	Py-AGTTATCCCTGC(**PyM12**) 3'-<u>G</u>TCAATAGGGACG-5'	150.26	55.87	0.37	0.89	N-terminal extended (G)
13	Py-AGTTATCCCTGC(**PyM12**) 3'-_CAATAGGGACG-5'	157.67	331.21	2.10	0.16	N-terminal deleted (T)
14	Py-AGTTATCCCTGC(**PyM12**) 3'-__AATAGGGACG-5'	156.66	332.37	2.12	0.16	N-terminal deleted (TC)

Table 3.7 (continued)

Entry	System	F_{379} (ss)	F_{379} (ds)	F(ds)/ F(ss)	F(com)/ F	Note
15	Py-CTAAATTCAGA(**PyM11**) 3'-GATTTAAGTCT-5'	42.68	19.47	0.46	1.00	comple-mentary
16	Py-CTAAATTCAGA(**PyM11**) 3'-GATTTCAGTCT-5'	43.32	9.52	0.22	0.68	internal mismatch
17	Py-CTAAATTCAGA(**PyM11**) 3'-AATTTAAGTCT-5'	33.56	83.43	2.49	1.00	terminal mismatch (A)
18	Py-CTAAATTCAGA(**PyM11**) 3'-TGGGGATTTAAGTCT-5'	34.14	21.06	0.62	2.09	N-terminal extended
19	Py-GTAGATCACT(**PyM10**) 3'-CATCTAGTGA-5'	67.02	15.46	0.23	0.18	comple-mentary
20	Py-GTAGATCACT(**PyM10**) 3'-CATCCAGTGA-5'	49.70	16.90	0.34	0.74	internal mismatch (C)

Conditions: [PNA] = 2.5 mM; [DNA] = 3.0 mM, 10 mM sodium phosphate buffer, pH 7.0, excitation wavelength = 345 nm.

Table 3.8 Fluorescence quantum yields of single stranded of terminally pyrenebutyryl-modified acpcPNAs (Py-PNAs) and their hybrids with DNA in this study.

Entry	System	Φ_F (ss)	Φ_F (ds)	Φ_F(ds)/ Φ_F(ss)	Φ_F(com)/ Φ_F	Note
1	Py-TTTTTTTTT(**PyT9**) 3'-AAAAAAAAA-5'	0.0050	0.0925	18.5	1.00	comple-mentary
2	Py-TTTTTTTTT(**PyT9**) 3'-AAAA**T**AAAA-5'	0.0050	0.0468	9.36	1.98	internal mismatch (T)
3	Py-TTTTTTTTT(**PyT9**) 3'-**T**AAAAAAAA-5'	0.0050	0.0050	1.00	30.83	terminal mismatch (T)
4	Py-AGTTATCCCTGC(**PyM12**) 3'-TCAATAGGGACG-5'	0.1028	0.0221	0.21	1.00	comple-mentary
5	Py-AGTTATCCCTGC(**PyM12**) 3'-**G**CAATAGGGACG-5'	0.0938	0.1522	1.62	0.13	terminal mismatch (G)
6	Py-AGTTATCCCTGC(**PyM12**) 3'-**C**CAATAGGGACG-5'	0.0820	0.1297	1.58	0.13	terminal mismatch (C)
7	Py-AGTTATCCCTGC(**PyM12**) 3'-**A**CAATAGGGACG-5'	0.0924	0.1874	2.03	0.10	terminal mismatch (A)
8	Py-AGTTATCCCTGC(**PyM12**) 3'-TCAAT**C**GGGACG-5'	0.1033	0.0225	0.22	0.95	internal mismatch (C)
9	Py-AGTTATCCCTGC(**PyM12**) 3'-**A**TCAATAGGGACG-5'	0.1048	0.0524	0.50	0.42	N-terminal extended (A)
10	Py-AGTTATCCCTGC(**PyM12**) 3'-**T**TCAATAGGGACG-5'	0.1026	0.0104	0.10	2.10	N-terminal extended (T)
11	Py-AGTTATCCCTGC(**PyM12**) 3'-**C**TCAATAGGGACG-5'	0.1014	0.0359	0.35	0.60	N-terminal extended (C)
12	Py-AGTTATCCCTGC(**PyM12**) 3'-**G**TCAATAGGGACG-5'	0.0891	0.0148	0.17	1.24	N-terminal extended (G)
13	Py-AGTTATCCCTGC(**PyM12**) 3'-_CAATAGGGACG-5'	0.0938	0.1647	1.76	0.12	N-terminal deleted (T)
14	Py-AGTTATCCCTGC(**PyM12**) 3'-__AATAGGGACG-5'	0.0858	0.1634	1.90	0.11	N-terminal deleted (TC)

Table 3.8 (continued)

Entry	System	Φ_F (ss)	Φ_F (ds)	Φ_F(ds)/ Φ_F(ss)	Φ_F(com)/ Φ_F	Note
15	Py-CTAAATTCAGA(**PyM11**) 3'-GATTTAAGTCT-5'	0.0291	0.0104	0.36	1.00	comple-mentary
16	Py-CTAAATTCAGA(**PyM11**) 3'-GATTTCAGTCT-5'	0.0255	0.0030	0.12	3.00	internal mismatch
17	Py-CTAAATTCAGA(**PyM11**) 3'-AATTTAAGTCT-5'	0.0217	0.0453	2.09	0.17	terminal mismatch (A)
18	Py-CTAAATTCAGA(**PyM11**) 3'-TGGGGATTTAAGTCT-5'	0.0283	0.0167	0.59	0.61	N-terminal extended
19	Py-GTAGATCACT(**PyM10**) 3'-CATCTAGTGA-5'	0.0492	0.0105	0.21	1.00	comple-mentary
20	Py-GTAGATCACT(**PyM10**) 3'-CATCCAGTGA-5'	0.0447	0.0116	0.26	0.81	internal mismatch (C)

Conditions: [PNA] = 2.5 mM; [DNA] = 3.0 mM, 10 mM sodium phosphate buffer, pH 7.0, excitation wavelength = 345 nm.

3.7.2 Fluorescence properties of internally pyrenebutyryl-modified acpcPNA (PNA^{Py})

Reenabthue and co-workers has established a reliable strategy for internal modification of pyrene-labeled acpc/apcPNAs by acylation chemistry [44]. The preliminary experiments on internally pyrene-labeled acpcPNA had also been performed. Pyrene-1-carboxylic acid and 4-(pyrene-1-yl)-butyric acid were chosen as the fluorophores. The pyrenes were attached on the nitrogen atom in APC spacer of acpcPNA. The fluorescence emission of pyrene-1-carboxylic acid modified homothymine acpcPNA increased ~2.6-fold of the single-stranded PNA. The same PNA sequence with a pyrenebutyryl modification gave a much more dramatic fluorescence intensity increase to over 70 folds at 379 nm of the single-stranded PNA. These preliminary results suggest that the fluorescence of the pyrenebutyryl-labeled acpc/apcPNAs are more responsive to their hybridization state than that of

pyrenecarbonyl-labeled acpc/apcPNAs. In this work, we therefore focus on the fluorescence properties of internally pyrenebutyryl-labeled acpcPNAs in more details.

In this design, the acpcPNA was covalently modified at the backbone with a pyrene chromophore through a flexible C4 linker *via* acylation of 3-aminopyrrolidine-4-carboxylic acid (APC)-modified acpcPNA. To evaluate the effect of nucleobase in PNA strand on fluorescence property, internally-modified acpcPNAs with varying position of the pyrenebutyryl (**T9^{Py}**–**M11C^{Py}**) were synthesized. The results of T_m data (see APPENDICES**, Table A2**) demonstrated that all pyrene-modified acpcPNA oligomers can hybridize to their complementary DNA targets to give hybrids with high thermal stabilities. The hybrid between the singly internally pyrenebutyryl-modified homothymine acpcPNA (**T9^{Py}**) and the complementary DNA showed a high T_m (60.3 ºC). The T_m value was lower than homothymine unmodified *acpc*PNA by 21.5 ºC but still high when compared with normal DNA·DNA duplex (**Table A2**, entry 1). The results showed that the presence of the internal pyrenebutyryl label in the acpcPNA system moderately decrease the DNA binding stability. The T_m experiments between **T9^{Py}** and target DNA containing single mismatch base resulted in much-lowered T_m values (25.4 ºC) (**Table A2**, entry 2). The significant difference in the thermal stabilities between the complementary and single mismatched hybrids (ΔT_m = 34.9 ºC) clearly indicated that the internally pyrenebutyryl-modified homothymine acpcPNA could specifically recognize the complementary DNA strand. The high stabilities and specificities were also observed in other internally pyrenebutyryl-modified homothymine acpcPNA **(M12^{Py}T –M11^{Py}C**) (see **Table A2**).

The fluorescence properties of internally pyrenebutyryl-modified acpcPNA in the absence and presence of target DNA were next investigated. The fluorescence intensity ratios and quantum yields of PNA^{Py} and its DNA hybrids are summarized in **Table 3.9** and **3.10**, respectively. First, the fluorescence properties of internally pyrenebutyryl-modified homothymine acpcPNA (**T9^{Py}**), which had a T/T as neighboring base, were studied. Similar to the terminally modified **PyT9** PNA, the internally modified **T9^{Py}** PNA in single stranded from exhibited a very weak fluorescence with a maximum emission at 379 nm (entries 1–2, see F_{379}(ss)) (**Figure 3.25**). The florescence quantum yield was also very low (Φ_F =0.0029). The fluorescence was increased by 72.8 folds relative to the single-stranded **T9^{Py}** upon

hybridization to its complementary DNA (**dA9**). The quantum yield of complementary duplex was also increased to 0.3178. When hybridized with the DNA strand carrying an internally mismatched base directly opposite to the pyrene (entry 2), the fluorescence of **T9^{Py}** was also increased, but to a much smaller extent (10.8 folds relative to the single stranded **T9^{Py}**) compared to the complementary duplex. This translates to a fluorescence discrimination factor between complementary and single-mismatched hybrids of 6.7 folds. These results suggested that the fluorescence of the internally pyrene-labeled acpcPNA is quenched by the nucleobases (T in this case) in the single-stranded state and the fluorescence was increased upon hybridization of the **T9^{Py}** to the complementary DNA was due to exposure of the pyrene to the aqueous environment.

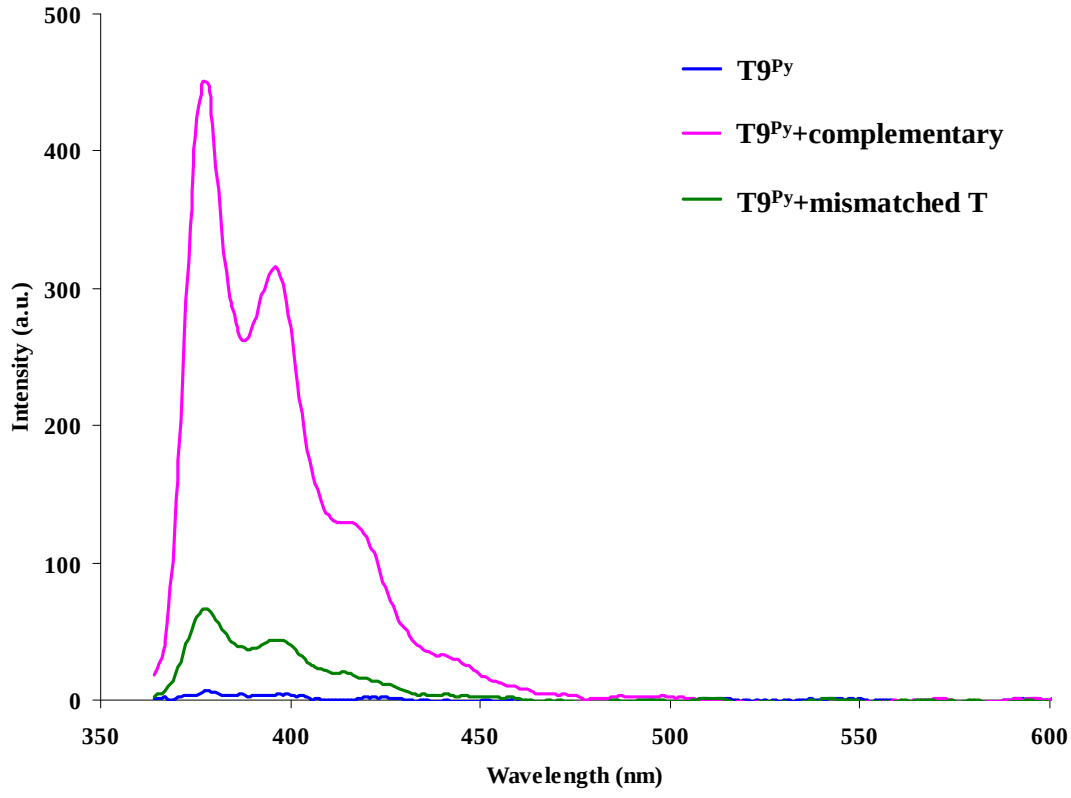

Figure 3.25 Fluorescence spectra of single strand acpcPNA **T9^{Py}** and its hybrids with DNA in 10 mM sodium phosphate buffer pH 7.0, [PNA] = 2.5 μM, excitation wavelength = 345 nm.

Next, the fluorescence properties of mixed-sequence internally pyrenebutyryl-modified acpcPNA were investigated. Internally pyrenebutyryl-modified acpcPNA 12 mer **M12^{Py}T**, which also had C/T as neighboring bases, showed low fluorescence emissions (entries 3–6, see F_{379}(ss)) and low fluorescence quantum yields (Φ_F = 0.0179–0.0419) in the single stranded form. Although the neighboring bases are also T, the fluorescence quantum yield in this case is considerably higher than that of single-stranded **T9^{Py}** (**Figure 3.26**). This suggests that the quenching may not be exclusively due to the effect of the immediate neighboring bases. It appears that more distant bases may also have some effects. Upon addition of complementary DNA, the fluorescence intensity of the complementary duplex was enhanced by a factor of 6.1 relative to the single-stranded **M12^{Py}T** (entry 3) and the quantum yield was increased to 0.2839. No fluorescence increase was observed in the presence of a single base mismatch C and G in the immediate vicinity of the the pyrene in the PNA strand in the DNA targets (entries 4–5). In the presence of mismatched DNA target (except mismatched T), the fluorescence was generally low similar to the single stranded PNA. Quite unexpectedly, the hybridization of **M12^{Py}T** with a DNA carrying a single mismatch T at the same position resulted in a significantly increased fluorescence (6.0 folds relative to the single stranded **M12^{Py}T**) (entry 6) that was almost similar to the complementary hybrid. The data suggest that the fluorescence of the **M12T^{Py}** increased significantly when the **M12T^{Py}** was hybridized to the complementary DNA.

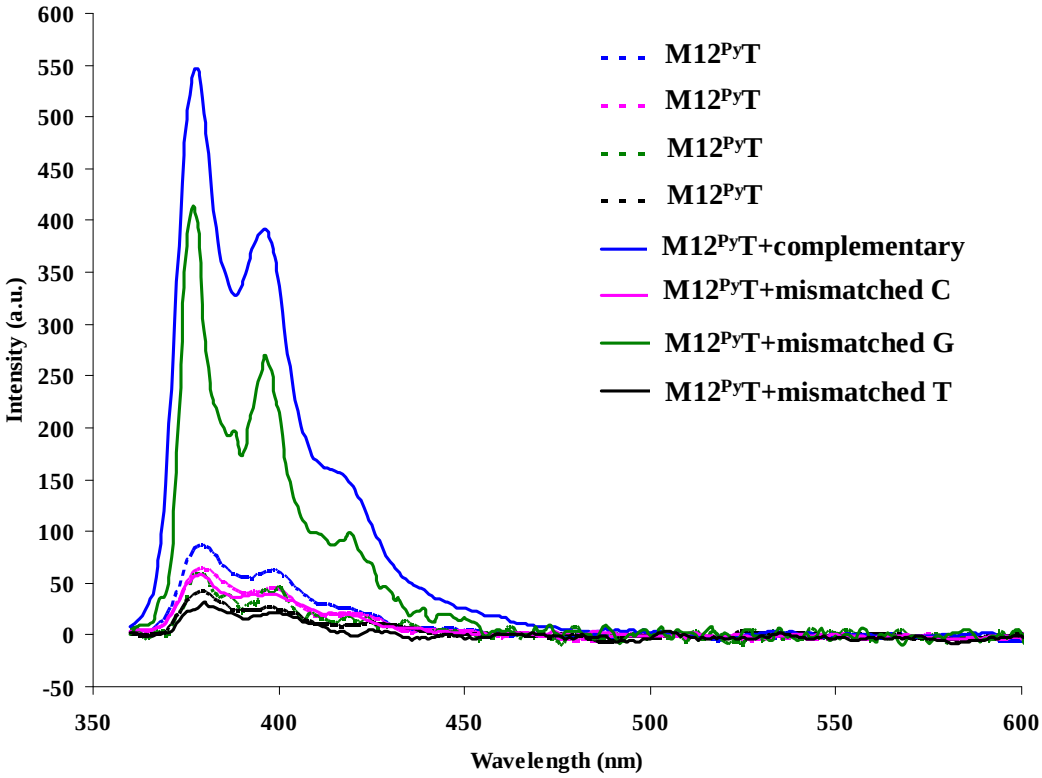

Figure 3.26 Fluorescence spectra of single strand acpcPNA **M12^{Py} T** and its hybrids with DNA in 10 mM sodium phosphate buffer pH 7.0, [PNA] = 2.5 μM, excitation wavelength = 345 nm.

The fluorescence properties of the PNA **M12^{Py}C**, which has the same sequence as **M12^{Py}T** but the pyrene label was shifted so that it had T/C as neighboring bases**,** was also studied (entries 7–8). The fluorescence of **M12^{Py}C** was (Φ_F = 0.0045–0.0061), which was brighter than **TU^{Py}T** but lower than **M12^{Py}T**. Similar fluorescence enhancement was observed upon hybridization of **M12^{Py}C** with its complementary DNA (entry 7). The fluorescence intensity of the complementary hybrid was increased by 20.5 folds relative to the single-stranded **M12^{Py}C** and the quantum yield was increased to 0.3211. In the presence of a mismatch base in the DNA target in close proximity to the pyrene label, the fluorescence increase was less pronounced (11.1 folds) (entry 8).

Three other sequences of internally pyrenebutyryl-modified acpcPNA 11 mer **M11^{Py}A**, **M11^{Py}T** and **M11^{Py}C**, which had a A/A, T/T and T/C as neighboring base, also exhibited low fluorescence intensities (entries 9–30, see F_{379}(ss)) and low

fluorescence quantum yields (Φ_F =0.0278–0.1832) in their single stranded forms. **M11^{Py}C**, which had a T/C neighboring base, was the brightest (entries 24–30), with the quantum yields 0.1239–0.1832. The fluorescence of **M11^{Py}C** was stronger than **M11^{Py}A** and **M11^{Py}T** by approximately 2–3 folds. When hybridized with complementary DNA, the fluorescence intensities of the complementary duplexes were enhanced by a factor of 6.8, 6.8 and 2.9 (for **M11^{Py}A**, **M11^{Py}T** and **M11^{Py}C** respectively) relative to the single-stranded PNA (entries 9, 12 and 24). On the other hand, hybridization of the pyrene-labeled acpcPNA to mismatched DNA showed variable results (unchanged, decreased or increased fluorescence relative to the single-stranded PNA).

Table 3.9 Fluorescence intensities of single stranded of internally pyrenebutyryl-modified acpcPNAs (Py-PNAs) and their hybrids with DNA in this study

Entry	System	F_{379} (ss)	F_{379} (ds)	F(ds)/ F(ss)	F(com)/ F	Note
1	TTTTTTTTT(**T9^{Py}**) 3'-AAAAAAAAA-5'	5.95	433.09	72.79	1.00	comple-mentary
2	TTTTTTTTT(**T9^{Py}**) 3'-AAAATAAAA-5'	5.95	64.33	10.81	6.73	internal mismatch(T)
3	AGTTATCCCTGC (**M12^{Py}T**) 3'-TCAATAGGGACG-5'	86.43	530.81	6.14	1.00	comple-mentary
4	AGTTATCCCTGC (**M12^{Py}T**) 3'-TCAATCGGGACG-5'	64.56	59.23	0.92	6.67	internal mismatch (C)
5	AGTTATCCCTGC (**M12^{Py}T**) 3'-TCAATGGGGACG-5'	41.61	28.96	0.70	8.77	internal mismatch (G)
6	AGTTATCCCTGC (**M12^{Py}T**) 3'-TCAATTGGGACG-5'	57.62	345.26	5.99	1.03	internal mismatch (T)
7	AGTTATCCCTGC (**M12^{Py}C**) 3'-TCAATAGGGACG-5'	22.81	468.28	20.53	1.00	comple-mentary
8	AGTTATCCCTGC (**M12^{Py}C**) 3'-TCAATCGGGACG-5'	19.07	211.20	11.07	1.85	internal mismatch (C)
9	CTAAATTCAGA (**M11^{Py}A**) 3'-GATTTAAGTCT-5'	71.33	483.39	6.78	1.00	comple-mentary
10	CTAAATTCAGA (**M11^{Py}A**) 3'-GATTCAAGTCT-5'	77.84	175.97	2.26	3.00	internal mismatch (C)
11	CTAAATTCAGA (**M11^{Py}A**) 3'-GATTTAACTCT-5'	74.66	351.38	4.71	1.44	internal mismatch (C)
12	CTAAATTCAGA (**M11^{Py}T**) 3'-GATTTAAGTCT-5'	84.19	573.91	6.82	1.00	comple-mentary
13	CTAAATTCAGA (**M11^{Py}T**) 3'-GATTTACGTCT-5'	85.03	54.05	0.64	10.66	internal mismatch (C)
14	CTAAATTCAGA (**M11^{Py}T**) 3'-GATTTAGGTCT-5'	107.00	72.10	0.67	10.18	internal mismatch (G)
15	CTAAATTCAGA (**M11^{Py}T**) 3'-GATTTATGTCT-5'	114.02	269.40	2.36	2.89	internal mismatch (T)

Table 3.9 (continue)

Entry	System	F_{379} (ss)	F_{379} (ds)	F(ds)/ F(ss)	F(com)/ F	Note
16	CTAAATTCAGA (**M11^{Py}T**) 3'-GATTTAAATCT-5'	127.46	346.89	2.72	2.51	internal mismatch (A)
17	CTAAATTCAGA (**M11^{Py}T**) 3'-GATTTAACTCT-5'	110.06	185.77	1.69	4.04	internal mismatch (C)
18	CTAAATTCAGA (**M11^{Py}T**) 3'-GATTTAATTCT-5'	129.62	378.70	2.92	2.34	internal mismatch (T)
19	CTAAATTCAGA (**M11^{Py}T**) 3'-GATTTGAGTCT-5'	115.24	115.94	1.01	1.01	internal mismatch (G)
20	CTAAATTCAGA (**M11^{Py}T**) 3'-GATTTTAGTCT-5'	133.65	548.22	4.10	1.66	internal mismatch (T)
21	CTAAATTCAGA (**M11^{Py}T**) 3'-GATTAAAGTCT-5'	102.94	615.96	5.98	1.14	internal mismatch (A)
22	CTAAATTCAGA (**M11^{Py}T**) 3'-GATTCAAGTCT-5'	102.66	447.34	4.36	1.56	internal mismatch (C)
23	CTAAATTCAGA (**M11^{Py}T**) 3'-GATTGAAGTCT-5'	99.27	497.93	5.02	1.36	internal mismatch (G)
24	CTAAATTCAGA (**M11^{Py}C**) 3'-GATTTAAGTCT-5'	214.27	622.98	2.91	1.00	comple-mentary
25	CTAAATTCAGA (**M11^{Py}C**) 3'-GATTTAAATCT-5'	267.38	88.49	0.33	8.82	internal mismatch (A)
26	CTAAATTCAGA (**M11^{Py}C**) 3'-GATTTAACTCT-5'	273.27	61.94	0.23	12.65	internal mismatch (C)
27	CTAAATTCAGA (**M11^{Py}C**) 3'-GATTTAATTCT-5'	269.93	59.38	0.22	13.23	internal mismatch (T)
28	CTAAATTCAGA (**M11^{Py}C**) 3'-GATTAAAGTCT-5'	249.13	387.33	1.55	1.88	internal mismatch (A)
29	CTAAATTCAGA (**M11^{Py}C**) 3'-GATTCAAGTCT-5'	260.34	390.05	1.50	1.94	internal mismatch (C)
30	CTAAATTCAGA (**M11^{Py}C**) 3'-GATTTAAGTCT-5'	272.34	283.39	1.04	2.80	internal mismatch (T)

Conditions: [PNA] = 2.5 mM; [DNA] = 3.0 mM, 10 mM sodium phosphate buffer, pH 7.0, excitation wavelength = 345 nm.

Table 3.10 Fluorescence quantum yields of single stranded of internally pyrenebutyryl-modified acpcPNAs (Py-PNAs) and their hybrids with DNA in this study.

Entry	System	Φ_F (ss)	Φ_F (ds)	Φ_F(ds)/ Φ_F(ss)	Φ_F(com)/ Φ_F	Note
1	TTTTTTTTT(**T9^{Py}**) 3'-AAAAAAAAA-5'	0.0029	0.3178	105.93	1.00	comple-mentary
2	TTTTTTTTT(**T9^{Py}**) 3'-AAAAAAAAA-5'	0.0029	0.0395	13.62	8.05	internal mismatch(T)
3	AGTTATCCCTGC (**M12^{Py}T**) 3'-TCAATAGGGACG-5'	0.0419	0.2839	6.47	1.00	comple-mentary
4	AGTTATCCCTGC (**M12^{Py}T**) 3'-TCAATCGGGACG-5'	0.0227	0.0347	0.92	4.45	internal mismatch (C)
5	AGTTATCCCTGC (**M12^{Py}T**) 3'-TCAATGGGGACG-5'	0.0179	0.1695	6.47	0.72	internal mismatch (G)
6	AGTTATCCCTGC (**M12^{Py}T**) 3'-TCAATTGGGACG-5'	0.0204	0.0132	0.92	10.41	internal mismatch (T)
7	AGTTATCCCTGC (**M12^{Py}C**) 3'-TCAATAGGGACG-5'	0.0045	0.3211	71.35	1.00	comple-mentary
8	AGTTATCCCTGC (**M12^{Py}C**) 3'-TCAATCGGGACG-5'	0.0061	0.2481	40.67	1.76	internal mismatch (C)
9	CTAAATTCAGA (**M11^{Py}A**) 3'-GATTTAAGTCT-5'	0.0333	0.3463	10.40	1.00	comple-mentary
10	CTAAATTCAGA (**M11^{Py}A**) 3'-GATTCAAGTCT-5'	0.0278	0.1296	4.66	2.23	internal mismatch (C)
11	CTAAATTCAGA (**M11^{Py}A**) 3'-GATTTAACTCT-5'	0.0307	0.2136	6.96	1.49	internal mismatch (C)
12	CTAAATTCAGA (**M11^{Py}T**) 3'-GATTTAAGTCT-5'	0.0563	0.3259	5.79	1.00	comple-mentary
13	CTAAATTCAGA (**M11^{Py}T**) 3'-GATTTACGTCT-5'	0.0515	0.0412	0.80	7.24	internal mismatch (C)
14	CTAAATTCAGA (**M11^{Py}T**) 3'-GATTTAGGTCT-5'	0.0482	0.0524	1.09	5.31	internal mismatch (G)
15	CTAAATTCAGA (**M11^{Py}T**) 3'-GATTTATGTCT-5'	0.0515	0.1571	3.05	1.90	internal mismatch (T)

Table 3.10 (continued)

Entry	System	Φ_F (ss)	Φ_F (ds)	Φ_F(ds)/ Φ_F(ss)	Φ_F(com)/ Φ_F	Note
16	CTAAATTCAGA (**M11^{Py}T**) 3'-GATTTAAATCT-5'	0.0499	0.1660	3.33	1.74	internal mismatch (A)
17	CTAAATTCAGA (**M11^{Py}T**) 3'-GATTTAACTCT-5'	0.0385	0.0849	2.21	2.62	internal mismatch (C)
18	CTAAATTCAGA (**M11^{Py}T**) 3'-GATTTAATTCT-5'	0.0486	0.1578	3.25	1.78	internal mismatch (T)
19	CTAAATTCAGA (**M11^{Py}T**) 3'-GATTTGAGTCT-5'	0.0568	0.0805	1.42	4.08	internal mismatch (G)
20	CTAAATTCAGA (**M11^{Py}T**) 3'-GATTTTAGTCT-5'	0.0535	0.3757	7.02	0.82	internal mismatch (T)
21	CTAAATTCAGA (**M11^{Py}T**) 3'-GATTAAAGTCT-5'	0.0575	0.3119	5.42	1.07	internal mismatch (A)
22	CTAAATTCAGA (**M11^{Py}T**) 3'-GATTCAAGTCT-5'	0.0538	0.2828	5.26	1.10	internal mismatch (C)
23	CTAAATTCAGA (**M11^{Py}T**) 3'-GATTGAAGTCT-5'	0.0485	0.2624	5.41	1.07	internal mismatch (G)
24	CTAAATTCAGA (**M11^{Py}C**) 3'-GATTTAAGTCT-5'	0.1239	0.3378	2.73	1.00	comple-mentary
25	CTAAATTCAGA (**M11^{Py}C**) 3'-GATTTAAATCT-5'	0.1514	0.0795	0.52	5.25	internal mismatch (A)
26	CTAAATTCAGA (**M11^{Py}C**) 3'-GATTTAACTCT-5'	0.1832	0.0493	0.27	10.11	internal mismatch (C)
27	CTAAATTCAGA (**M11^{Py}C**) 3'-GATTTAATTCT-5'	0.1506	0.0471	0.31	8.81	internal mismatch (T)
28	CTAAATTCAGA (**M11^{Py}C**) 3'-GATTAAAGTCT-5'	0.1392	0.277	1.99	1.37	internal mismatch (A)
29	CTAAATTCAGA (**M11^{Py}C**) 3'-GATTCAAGTCT-5'	0.1384	0.2692	1.94	1.41	internal mismatch (C)
30	CTAAATTCAGA (**M11^{Py}C**) 3'-GATTTAAGTCT-5'	0.1373	0.1952	1.42	1.92	internal mismatch (T)

Conditions: [PNA] = 2.5 mM; [DNA] = 3.0 mM, 10 mM sodium phosphate buffer, pH 7.0, excitation wavelength = 345 nm.

3.7.3 On the mechanism of fluorescence change of internally pyrenebutyryl-modified acpcPNA (PNA^{Py})

The mechanism of fluorescence change in these internally-pyrene labeled acpcPNA can be explained as follows. First in the single stranded form, the pyrene is quenched by the nucleobases of the PNA. It is known from the literature that the order of quenching of pyrene by nucleobase is T>C>G>>A [59]. The fact that the brightness of pyrene-labeled PNA with different immediate neighboring base pairs does not exactly follow this trend indicate that the quenching may involve longer range interactions with the more distant bases. In the duplex with complementary DNA (entries 1,3,7,9,12 and 24), or DNA carrying a mismatched base more distant from the pyrene label (entries 11, 16–23 and 28–30), the pyrene is forced to point away to the aqueous environment. It should be note that in normal DNA·DNA hybrids, it is commonly observed that pyrene linked to the DNA backbone via a flexible linker prefers to adopt an intercalated form therefore the fluorescence was quenched instead of enhanced [68]. Only when the linker was rigid that the fluorescence increase was observed in the case of DNA·DNA duplexes [69]. It is remarkable to observe consistent fluorescence increase in the case of PNA·DNA hybrid, which suggests the inability of the base pairs in acpcPNA·DNA duplex to accommodate the intercalated pyrene.

In the case of DNA carrying the mismatched base close to the pyrene label, the fluorescence was decreased (entries 13–14 and 25–27). The lower fluorescence in these cases indicates that the pyrene moiety was intercalated between the base stack of duplex. This is possible because the pyrene is hydrophobic and will try to hide away from water if this can be achieved without breaking the original base pairs in the PNA·DNA duplex, e.g. when a mismatched pair was present. This proposal is supported by the UV absorption spectra whereby a small red shift by c.a. 3 nm together with hypochromism of the pyrene absorption bands compared to the single stranded PNA were observed (**Figure 3.27**). These can be taken as the evidence for stacked pyrene. In the complementary duplex, the shift occurred to the opposite direction (blue side) and was accompanied by hyperchromism, indicating the free pyrene (**Figure 3.28**). Some exceptions to this generalization were observed, for

examples, when DNA containing directly mismatched C and T, the large fluorescence enhancements were observed (entries 10 and 15). This cannot be explained by this model, but from the UV absorption spectra, no stacking of the pyrene was observed in these cases similar to complementary duplex course by the pyrene unit is not intercalated between the base stack. Thus the mechanism of the fluorescence change by the pyrene label attached to the internal position of acpcPNA can be summarized as shown in **Figure 3.28**.

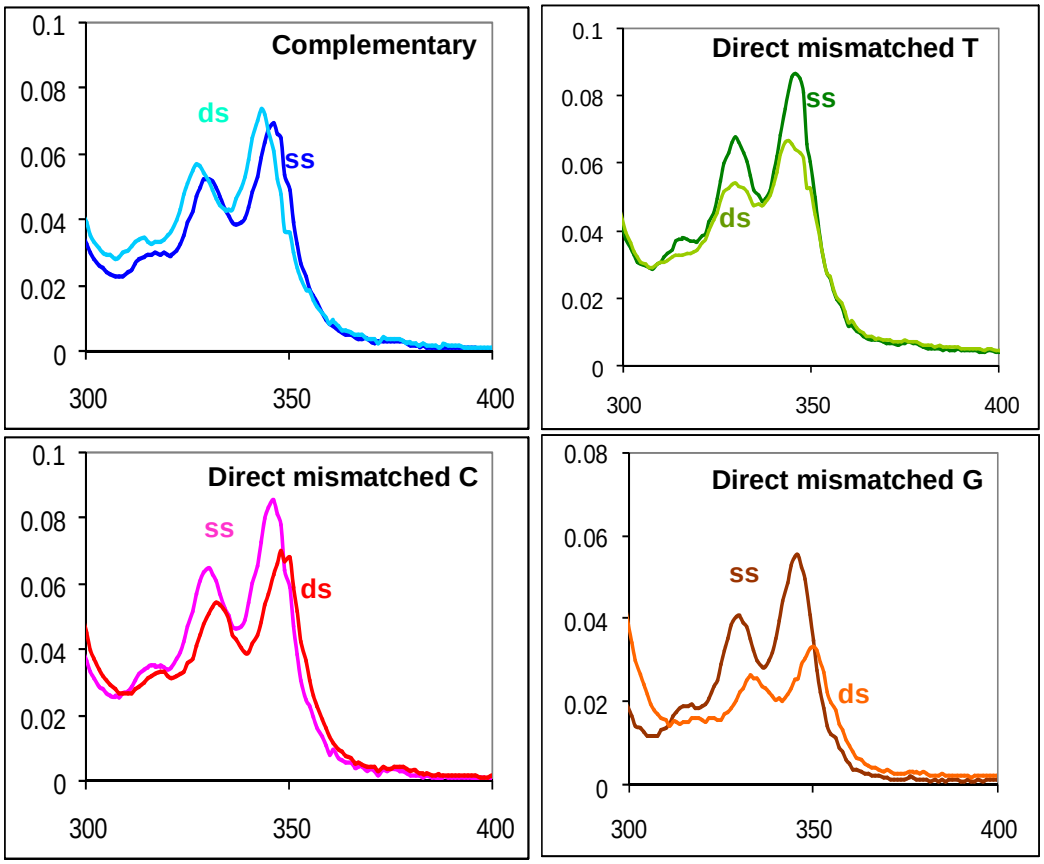

Figure 3.27 UV/Vis spectra of single strand acpcPNA **M12^{Py}T** and its hybrids with DNA in 10 mm sodium phosphate buffer pH 7.0, [PNA] = 2.5 μM and [DNA] = 3.0 μM,

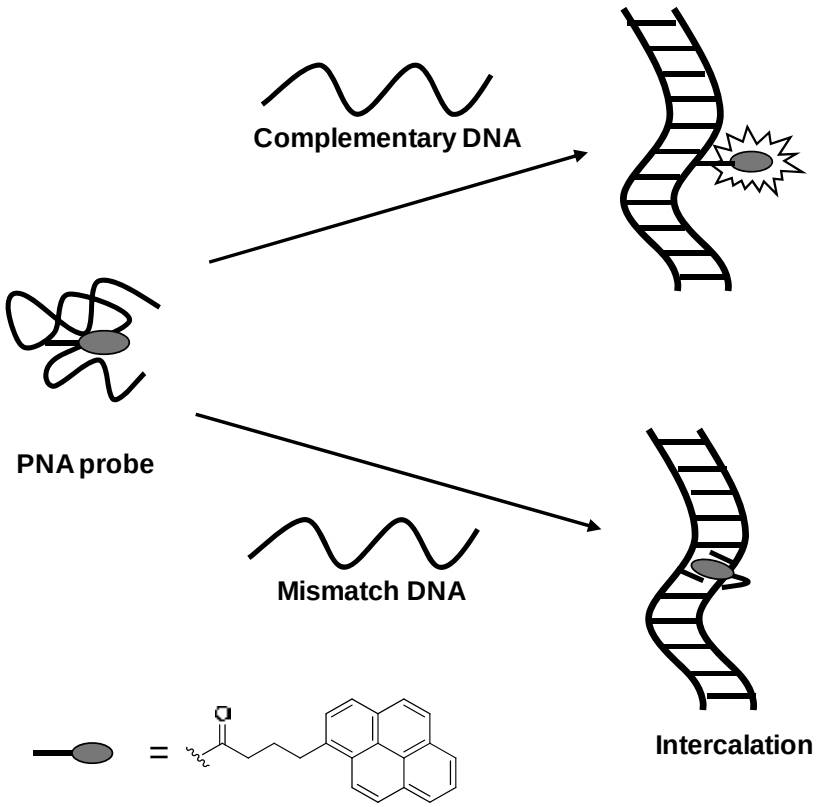

Figure 3.28 Schematic diagram of pyrene location in complementary and mismatched duplexes

In summary, the fluorescence of the internally pyrene-labeled acpcPNA (PNA^{Py}) generally increases upon hybridization with complementary DNA regardless of the identity of the neighboring base. Hybridization to mismatched DNA results in decreasing or increasing fluorescence relative to the single-stranded PNA, depending on the position and type of the mismatch pairs. In general, when the mismatched base is in the vicinity of the pyrene label, the fluorescence is quenched or not change from the single stranded PNA, although some exceptions are known. When the mismatched base is further away from the pyrene label, the fluorescence is high similar to that observed in perfectly complementary hybrid. As the results, internally pyrene-labeled acpcPNA is useful as a hybridization responsive fluorescence probe for DNA sequence determination.

3.7.4 Improving the specificity of internally pyrene-labeled acpcPNA by enzymatic digestion with nuclease S1

The fluorescence experiment results with internally pyrene-labeled acpcPNA above shows that some single base mismatch duplexes gave significant increased fluorescence intensity relative to the single stranded PNA, especially when the mismatched base in the DNA target is further away from the position of the pyrene label. It was proposed that, digestion by nuclease S1 – an enzyme that specifically hydrolyzes single stranded DNA - may be used to overcome this problem [47]. In the enzymatic digestion experiment, the internally pyrene-labeled acpcPNA **M11^{Py}T** was used as a probe together with various DNA targets as illustrated below.

PNA **M11^{Py}T** : Ac-Lys-CTAAAT$^{(Py)}$TCAGA-LysNH_2
DNA **DNA5** : 5'-TCTGAATTTAG-3' (complementary)
DNA **DNA6** : 5'-TCTG<u>T</u>ATTTAG-3' (direct mismatched T)
DNA **DNA7** : 5'-TCT<u>T</u>AATTTAG-3' (indirect mismatched T)
DNA **DNA8** : 5'-TCTGA<u>T</u>TTT AG-3' (indirect mismatched T)
DNA **DNA9** : 5'-TCTGAA<u>A</u>TTAG-3' (indirect mismatched A)
DNA **DNA10** : 5'-TCTGAA<u>C</u>TTAG-3' (indirect mismatched C)
DNA **DNA11** : 5'-TCTGAA<u>G</u>TTAG-3' (indirect mismatched G)

The enzymatic digestion of the **M11^{Py}T**·DNA hybrids was studied by fluorescence experiments. The sample for digestion by nuclease S1 was prepared by mixing the 1.0 μM **M11^{Py}T** and 1.0 μM DNA in 30 mM sodium acetate buffer (pH 4.6) containing 1.0 mM zinc acetate, 5% (v/v) glycerol. The nuclease S1 stock was added to give the final concentration of 5 unit/mL. The progress of the enzymatic digestion was monitored by recording the fluorescence spectra in kinetics mode for 30 min at every 5 min intervals).

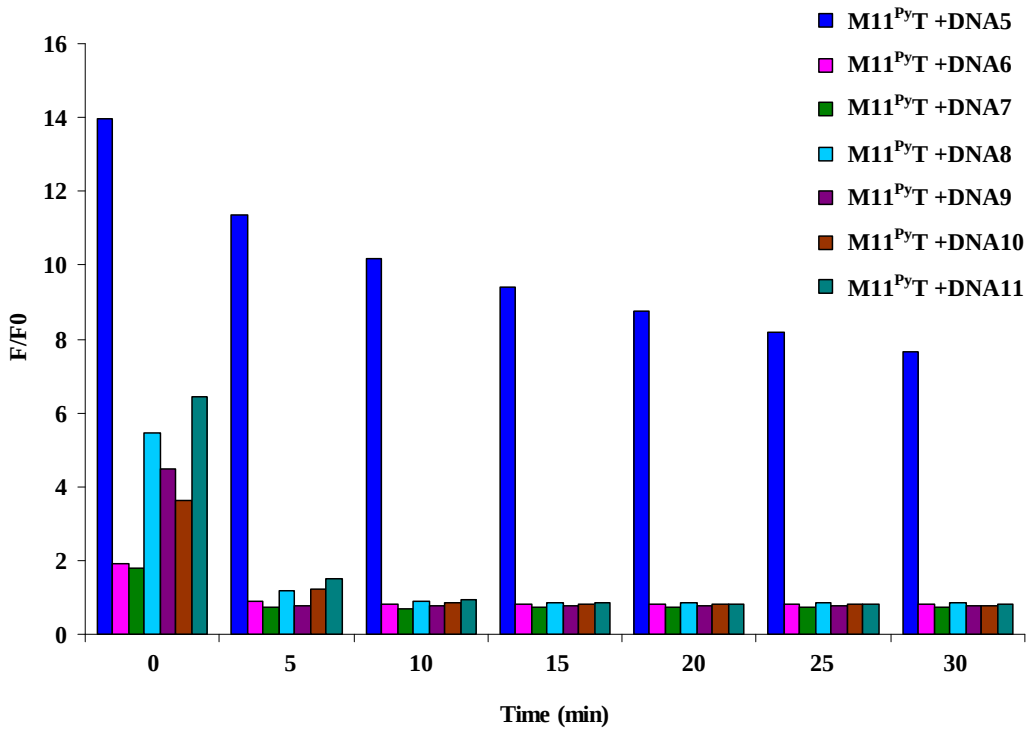

Figure 3.29 Studies kinetic for nuclease S1 digestion of **M11^{Py}T** with complementary and single base mismatch DNA; [PNA]=1.0 μM, [DNA]= 1.0μM in 30 mM sodium acetate buffer pH 4.6, 1mM zinc acetate, 5% Glycerol. Excitation wavelength was 345 nm.

The ratio of fluorescence intensity of **M11^{Py}T** as the duplex (*F*) with DNA to single standed (F_0) was plotted as a function of digestion time (min) as shown in **Figure 3.29**. The fluorescence spectra of **M11^{Py}T** with complementary DNA (**DNA5**) before and after digestion with nuclease S1 at 10 min intervals are also shown in **Figure 3.30.** The fluorescence experiments revealed that the duplex of PNA with perfect match DNA was much more slowly digested compared to the single mismatched DNA. The **M11^{Py}T·DNA5** duplex was digested about 40% after 30 min. On the other hand, the duplexes with single base mismatched DNA (**M11^{Py}T·DNA6–M11^{Py}T·DNA11)** were completely digested by nuclease S1 after 10 min. Accordingly, perfect discrimination between complementary and single mismatched DNA targets had been achieved after 10 min digestion by nuclease S1, whereby the

fluorescence of the mismatched hybrids returned to the same level as single-stranded PNA (F/F_0 ~1) but that of the complementary hybrid was only slightly decreased by 21 %. As a result, the nuclease S1 digestion is a powerful technique to improve the differentiation between complementary and various mismatched DNA targets employing internally pyrene-labeled acpcPNA as a quencher-free, singly-labeled PNA beacon probe.

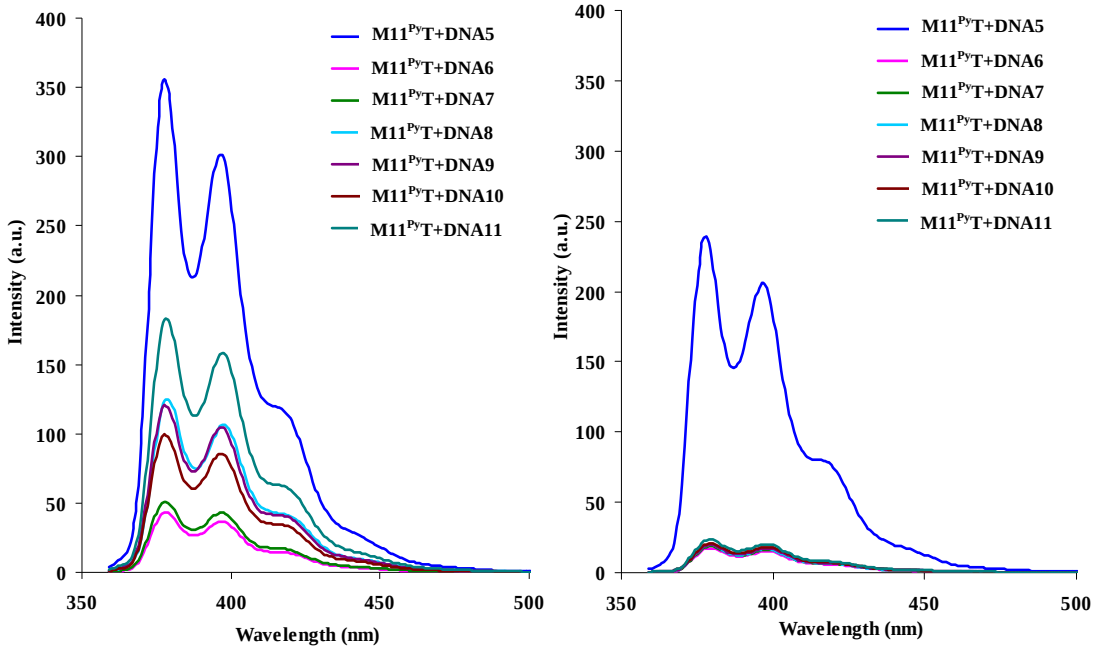

Figure 3.30 Fluorescence spectra from kinetic studies of nuclease S1 digestion of hybrids between **M11^{Py}T** with complementary and single base mismatch DNA; [PNA]=1.0 μM, [DNA]= 1.0μM in 30 mM sodium acetate buffer pH 4.6, 1mM zinc acetate, 5% Glycerol. Excitation wavelength was 345 nm. (Left: before digestion, Right: after digestion)

3.8 Fluorescent acpcDNA strand-displacement probes

In the third part, the acpcDNA strand-displacement probes were synthesized and its fluorescence properties investigated in the presence of complementary and mismatched DNA target by fluorescence experiments. The PNA·DNA strand-displacement probes consist of a fluorescein (Flu) or tetramethylrhodamine (TAMRA)-labeled acpcPNA probe (11-12 bases in length) and a shorter DNA containing a quencher (7-8 bases). The fluorescein/DABCYL and TMR/BHQ were chosen as the fluorophore/quencher pairs in the strand displacement probe and quencher DNA as these two are common fluorophore/quencher combination used in conventional MB probes. The sequences of Flu-acpcPNAs, TMR-acpcPNA and DNA targets used in this study are as follow:

PNA **Flu1** : Flu-O-CTAAATTCAGA-Lys-NH_2
PNA **Flu2** : Flu-O-AGTTATCCCTGC-Lys-NH_2
PNA **TMR1** : TMR-O-TTATCACTATGA-Lys-NH_2
DNA **dQ1** : 5'- GAATTTAG-Dabcyl-3' (short complementary to **Flu1**)
DNA **dQ2** : 5'- GTGATAA-BHQ-3' (short complementary to **TMR1**)
DNA **dcomF1** : 5'- TCTGAATTTAA -3' (complementary to **Flu1**)
DNA **dsmF1** : 5'- TCTG<u>C</u>ATTTAA -3' (internal mismatched to **Flu1**)
DNA **dcomF2** : 5'- GCA GGG ATA ACT -3' (complementary to **Flu2**)
DNA **dsmF2** : 5'- GCA GGG ATA AC<u>G</u> -3' (terminal mismatched to **Flu2**)
DNA **dcomT1** : 5'- TCATAGTGATAA-3' (complementary to **TMR1**)
(O = aminoethoxyethoxyacetyl linker)

The single stranded fluorescein-acpcPNA (**Flu1**) showed a high fluorescence signal. Upon hybridization with shorter DNA containing a DABCYL quencher (**dQ1**), the **Flu1** showed a decreased in fluorescence intensity due to the close proximity of the Flu and the DABCYL quencher (**Figure 3.31**). By comparison of the fluorescence intensity with single stranded probe, the efficiency of the fluorescein quenching by the short DABCYL quencher DNA probe was ca. 81 %. Next, an equivalent of DNA (**dcomF1)** with a sequence fully complementary to the PNA part in the **Flu1·dQ1**

probes was added and the fluorescence spectra were recorded every 3 min until no further change was observed. It was observed that the fluorescence was only slightly increased over the period of 30 min. It was earlier proposed in the presence of the complementary target sequence, the PNA probe should formed a more stable hybrid with the target DNA. This should result in releasing of the quencher DNA, and therefore the fluorescence of the PNA probe should increase. In contrast, only slight increase in the fluorescence intensity was observed. The fluorescence experiment was also repeated with an internal mismatched DNA target (**dsmF1**). After adding the **dsmF1** to **Flu1·dQ1** displacement probe, the fluorescence intensity did not change (**Figure 3.32**).

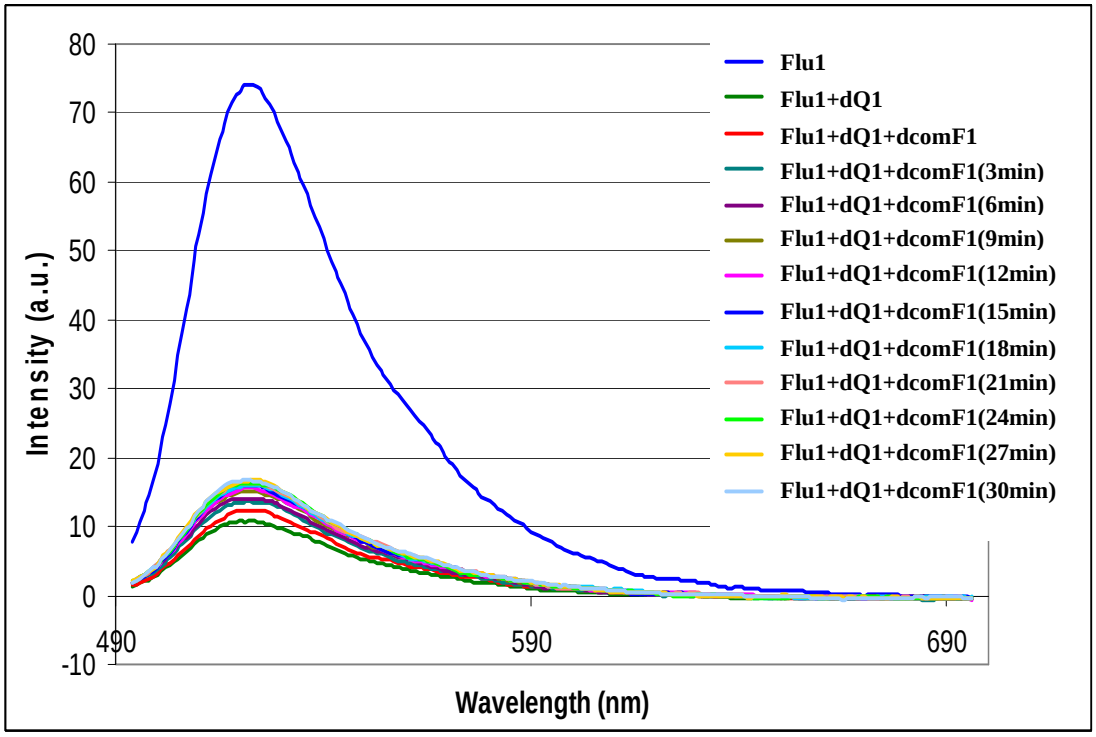

Figure 3.31 Fluorescence spectra of the **Flu1·dQ1** displacement probe after adding complementary DNA (**dcomF1)** in 10 mM sodium phosphate buffer pH 7.0, 100 mM NaCl, [PNA] = 0.1 μM and [DNA] = 0.1 μM, excitation wavelength = 480 nm.

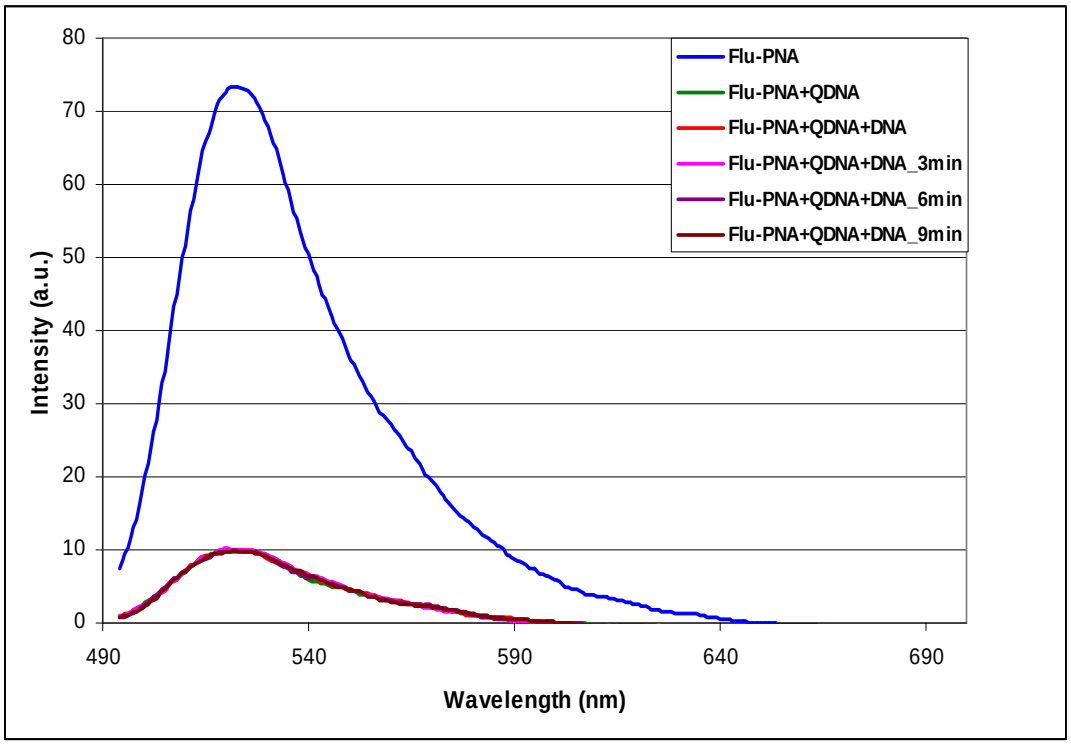

Figure 3.32 Fluorescence spectra of **Flu1·dQ1** displacement probes after adding mismatched DNA (**dsmF1)** in 10 mM sodium phosphate buffer pH 7.0, 100 mM NaCl, [PNA] = 0.1 μM and [DNA] = 0.1 μM, excitation wavelength = 480 nm.

For the sequence chosen, the *N*-terminal of the **Flu1** PNA strand carried the base C, the complementary DNA sequence must carry G at this position. It has been reported that a base G located close to a fluorescein can also quench up to 90% of its fluorescence [70]. To prove that the only slight increase in fluorescence after adding the complementary DNA was due to the formation of a fully complementary hybrid that is quenched by the opposite G in DNA strand, the fluorescence response of the single stranded probe **Flu1** (without the DNA quencher strand) was compared with the duplex formed with its complementary DNA (**dcomF1**). Thus, from the fluorescence spectra (**Figure 3.33**), it was clear that the emission intensity from the fluorescein-acpcPNA was substantially decreased. The results indicate that the fluorescein-acpcPNA strand could be quenched upon pairing with **dcomF1** up to ca. 64 %. Further addition of the quencher probe **dQ1** resulted in the same fluorescence spectra, suggesting the absence of displacement of the **dcomF1** by **dQ1**. The fluorescence experiment was also repeated for internal mismatched DNA **dsmF1**

(**Figure 3.34**). The fluorescence intensity of mismatched **Flu1·dsmF1** was also decreased but the quenching was much less pronounced (only about 30%) compared to the complementary duplex due to the low stability of mismatched hybrid. However, when the quencher DNA **dQ1** was further added, the fluorescence was further decreased, most likely due to the hybridization of the **Flu1** and **dQ1**.

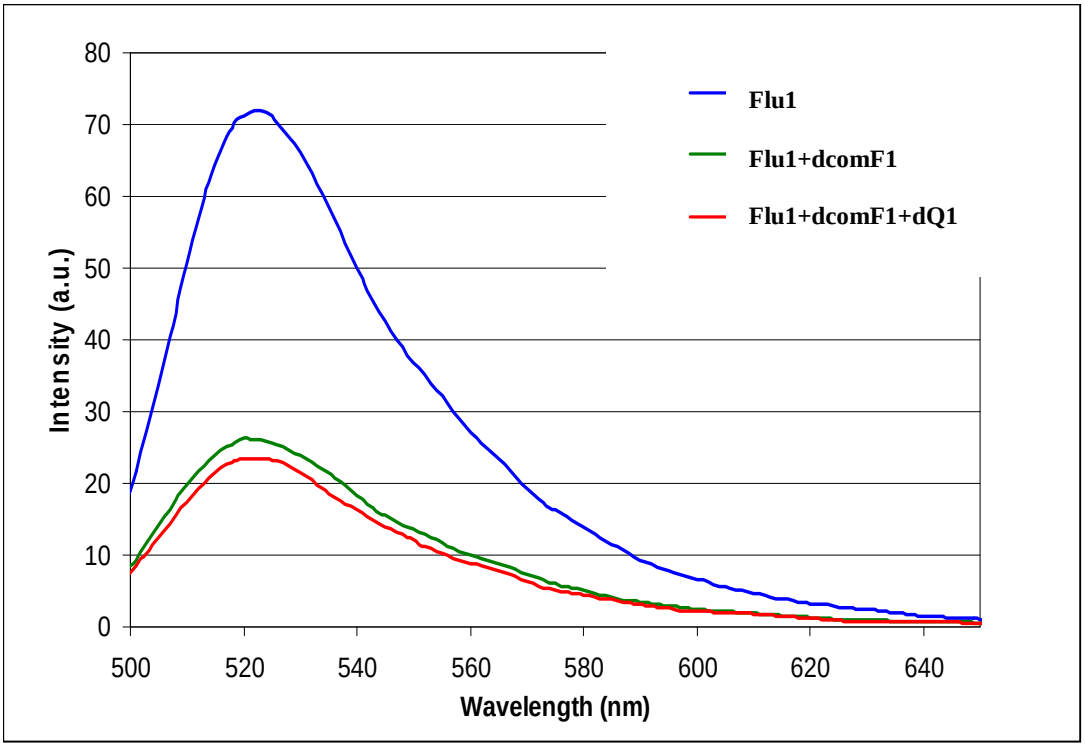

Figure 3.33 Fluorescence study of the **Flu1** with complementary DNA (**dsmF1)** and **dQ1** in 10 mM sodium phosphate buffer pH 7.0, 100 mM NaCl, [PNA] = 0.1 μM and [DNA] = 0.1 μM, excitation wavelength = 480 nm.

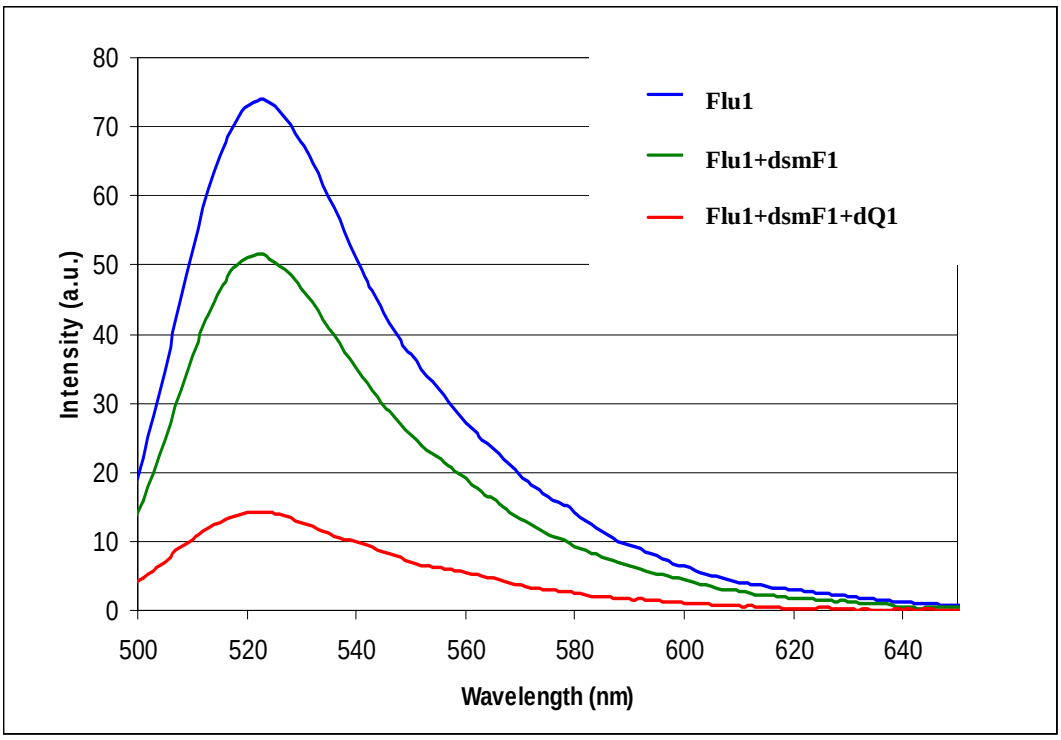

Figure 3.34 Fluorescence study of the **Flu1** with mismatched DNA (**dsmF1)** and **dQ1** in 10 mM sodium phosphate buffer pH 7.0, 100 mM NaCl, [PNA] = 0.1 μM and [DNA] = 0.1 μM, excitation wavelength = 480 nm.

With the hypothesis that the presence of a terminal C·G pair close to the fluorescein label is undesirable, the **Flu2** probe in which base A was present at the N-terminal position of the acpcPNA strand adjacent to the fluorescein label was also investigated. The fluorescence spectra of the probe **Flu2** before and after hybridization with complementary DNA (**dcomF2**) were first measured and showed only slightly decreased fluorescence intensity (**Figure 3.35**). When the base A at 3'-terminal of the DNA strand were replaced by base G as in **dsmF2**, the fluorescence was again decreased higher than complementary duplex of **Flu2** (containing base A at 3'-terminal) but not to the extent observed in the complementary duplex of **Flu1·dcomF1** (containing base G at 3'-terminal) (**Figure 3.36**). The lower fluorescence quenching may be explained by the mismatch base pairing between A and G at the end of the duplex, which preclude the base G from making a close contact to the fluorescein label. These results confirmed the hypotheses that the

fluorophore at N-terminal in the acpcPNA strands could be effective quenched by base G at 3' end of the complementary DNA.

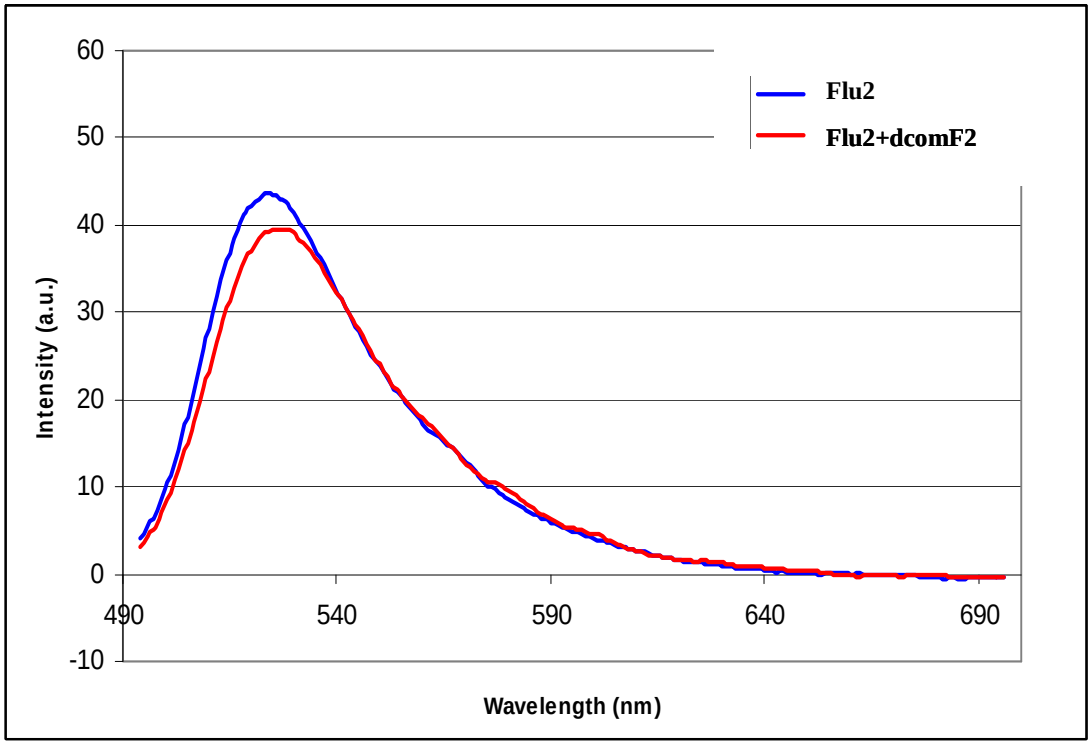

Figure 3.35 Fluorescence study of the **Flu2** with complementary DNA (**dcomF2)** in 10 mM sodium phosphate buffer pH 7.0, 100 mM NaCl, [PNA] = 0.1 μM and [DNA] = 0.1 μM, excitation wavelength = 480 nm.

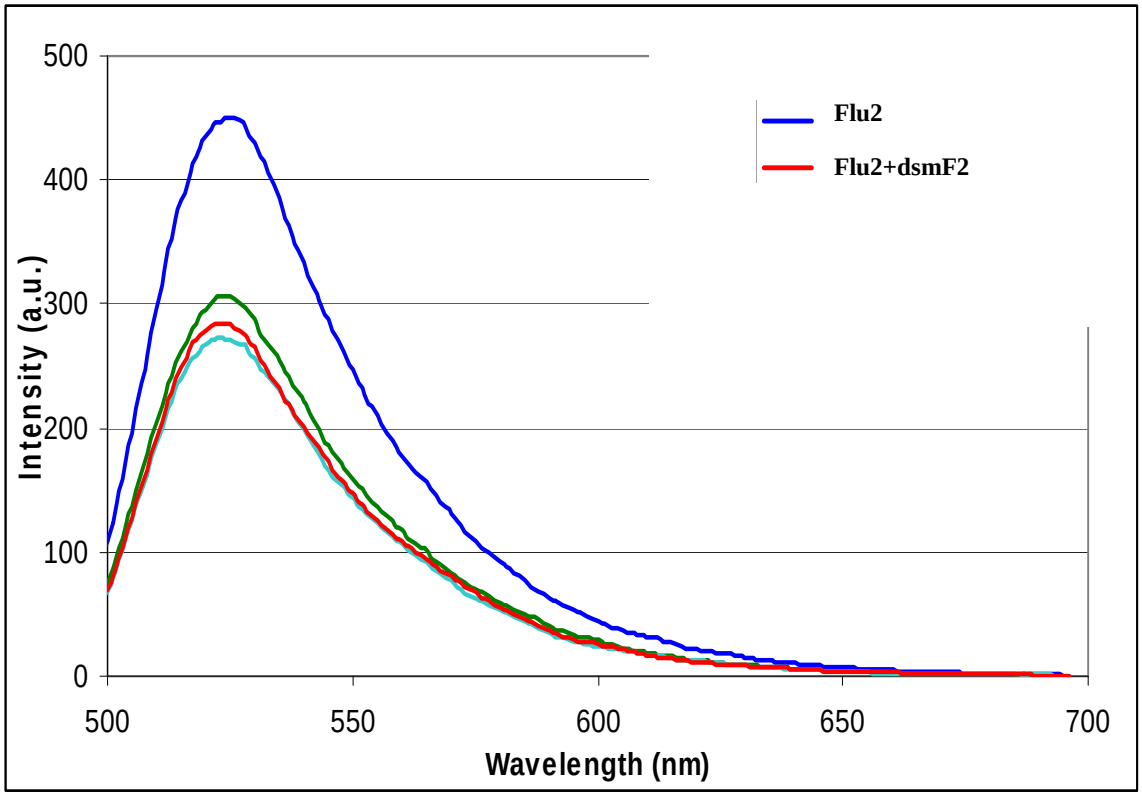

Figure 3.36 Fluorescence study of the **Flu2** with mismatched DNA (**dmsF2)** in 10 mM sodium phosphate buffer pH 7.0, 100 mM NaCl, [PNA] = 0.1 μM and [DNA] = 0.1 μM, excitation wavelength = 480 nm.

The concept was also tested with another fluorophore/quencher pair, namely TMR and BHQ. The TMR labeled-acpcPNA probe (**TMR1**) carrying base T at the N-terminal position next to the TMR label gave a high fluorescence signal. Upon hybridization with a short DNA carrying a BHQ quencher at the 3'end (**dQ2**), the **TMR1** probe exhibited a decreased in fluorescence intensity by ca.75 % (**Figure 3.37**). Next, one equivalent of complementary DNA (**dcomT1)** was added and the fluorescence spectra were recorded every 3 min until no further increase could be observed. The fluorescence was slowly increased and did not change further after 18 min, at which time the fluorescence intensity was increased from 25% (after adding **dQ2**, before adding **dcomT1**) to 77%, although this never reaches the fluorescence of the original TMR probe even when the **dcomT1** was added in excess. The results suggest an incomplete strand displacement, nevertheless they also demonstrated that the TMR labeled-acpcPNA (**TMR1**) when combined with a short DNA containing

BHQ can be used as a strand-displacement probe. However, more optimization is still required to make this probe useful for practical applications. Since this probe design still requires two different labels, which add to the cost of the analysis, the concept was not investigated further after obtaining the more successful results in the design of singly-labeled quencher-free PNA beacons.

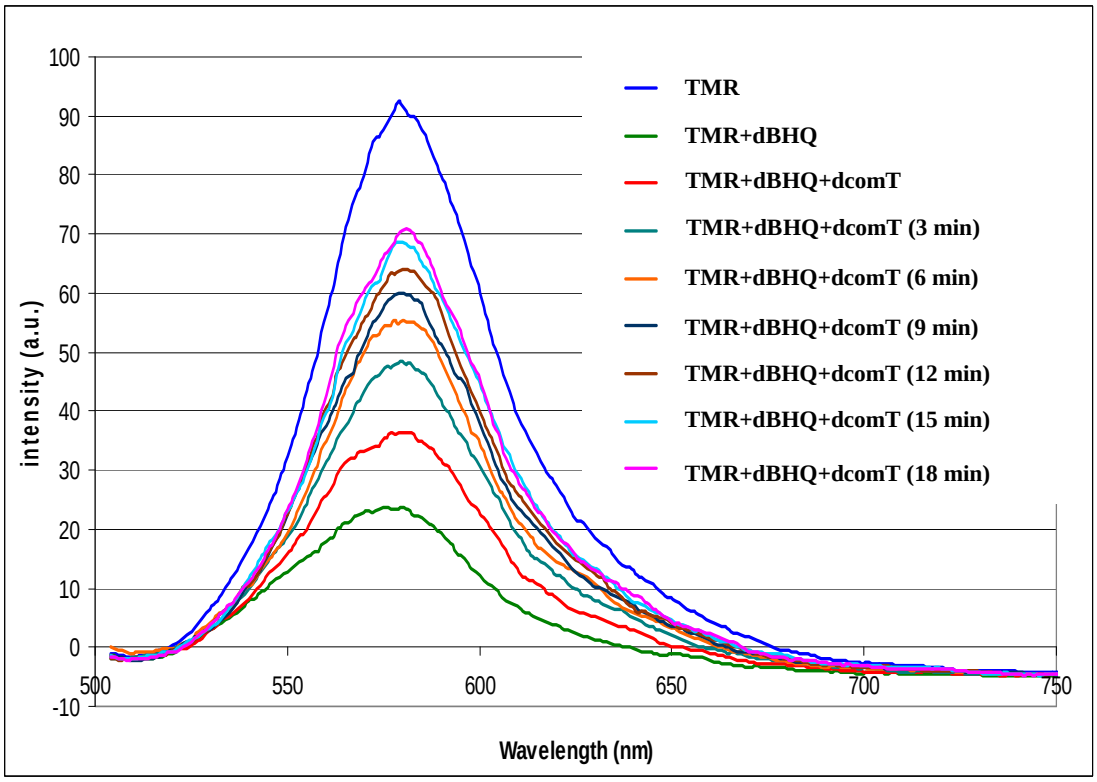

Figure 3.37 Fluorescence spectra of the **TMR1·dQ2** displacement probe after adding complementary DNA (**dcomT1)** in 10 mM sodium phosphate buffer pH 7.0, 100 mM NaCl, [PNA] = 0.1 μM and [DNA] = 0.1 μM, excitation wavelength = 480 nm.

CHAPTER IV

CONCLUSION

The objective of this work is to develop new fluorescence acpcPNA probes that can change their fluorescence in response to the presence of correct DNA target. The research was divided into three parts. The first part involves acpcPNA carrying a fluorescence nucleobase - 5-pyren-1-yluracil. The second part concerns with acpcPNA modified with a pyrenebutyryl group at terminal and internal positions. The last part summarizes our attempts to develop a strand-displacement probe from acpcPNA.

In the first part, a pyrene-labeled uridine (U^{Py}) monomer was successfully synthesized by Suzuki–Miyaura cross-coupling between pyrene-1-boronic acid and iodouracil acpcPNA monomer precursor. The U^{Py} monomer was incorporated into acpcPNA in the middle of the strand by standard Fmoc-solid phase peptide synthesis. The U^{Py} base in the modified acpcPNA could specifically recognize the base A in its complementary DNA target as determined by melting temperature (T_m) experiments. The T_m data showed that the pyrene-labeled acpcPNA could bind to complementary DNA to give a stable complementary hybrid. The fluorescence intensities of the single-stranded U^{Py} acpcPNAs were very weak in aqueous buffer (quantum yields Φ_F = 0.006-0.011). In the presence of complementary DNA, the fluorescence intensity was enhanced significantly (2.7–41.9 folds, depending on sequences). The fluorescence of the pyrene-modified acpcPNA is therefore sensitive to whether the PNA was hybridized to its complementary DNA target or not. On the other hand, when the DNA strand carried a mismatched base (C, G, and T) opposite to the U^{Py} label, the stabilities of the mismatched acpcPNA·DNA hybrids decreased. Very weak fluorescence was observed in case of mismatched acpcPNA·DNA hybrids. Experiments with DNA targets carrying mismatch base at other positions revealed that the fluorescence enhancement was specific to the pairing between U^{Py} and dA. The high specificity of the acpcPNA system allows discrimination between the complementary and single mismatched DNA targets. Form the results, it can be

concluded that 5-(pyren-1-yl)uracil (U^{Py}) behave as a bases discriminating fluorescent (BDF) nucleobase in the acpcPNA system and the U^{Py}-modified acpcPNA is potentially useful as a hybridization responsive fluorescence probe for DNA sequence determination.

In the second part of the study, the fluorescence properties of terminally and internally pyrenebutyryl-modified acpcPNA were investigated in the absence and presence of target DNA. The pyrene unit was covalently attached to N-terminal positions of acpcPNA or to internal positions of APC-modified acpcPNA through a flexible butyryl linker *via* acylation. The fluorescence of terminally modified pyrenebutyryl-PNA in single stranded form is dependent to the nucleobase at the terminal of the PNA strand. When N-terminal of the pyrenebutyryl-PNA strands carried the base T, C and G, the fluorescence of the single-stranded pyrenebutyryl-modified acpcPNAs were very low due to the quenching of pyrene chromophore by these nucleobases. On the other hand, when base A were present at N-terminal to the pyrenebutyryl-PNA strands, the high fluorescence of the single-stranded PNA was observed because of base A is a poor quencher for pyrene. Hybridization of the terminally pyrene-modified PNA to DNA yielded variable fluorescence change (decreased or increased fluorescence relative to the single-stranded PNA), depending on the original fluorescence of the single stranded PNA and the identity of the DNA base in vicinity of the pyrene label. Upon hybridization with perfectly complementary DNA, the PNA with pyrene label adjacent to base A, C and G in the PNA strand showed a decrease in fluorescence intensity, while base T showed an increase in fluorescence intensity. In contrast to the terminally pyrenebuyryl-modified acpcPNA, the fluorescence signal of the single stranded PNA was generally very weak due the effective quenching of pyrene unit by nucleobases in PNA strand. The fluorescence of the internally pyrene-labeled acpcPNA consistently increases upon hybridization with complementary DNA under a wide sequence context. In the duplex with DNA carrying a mismatched base more distant from the pyrene label, the fluorescence was also increased similar to the matched duplex. When the DNA carries a mismatched base opposite or close to the pyrene label, the fluorescence was generally decreased (although some exceptions exist), suggesting that the pyrene moiety was intercalated between the base stack of the PNA·DNA duplex. The internally pyrene-labeled

acpcPNA is therefore more suitable as a hybridization responsive fluorescence probe for DNA sequence determination than the terminally pyrenebutyryl-modified acpcPNA. The specificity of the pyrenebutyryl acpcPNA probe could be enhanced by employing enzymatic digestion by nuclease S1, an enzyme that specifically hydrolyzes single-stranded DNA. The complementary acpcPNA·DNA hybrid was much more resistant to S1 digestion than the mismatched hybrids. Accordingly, perfect discrimination between complementary and mismatched DNA targets had been achieved after 10-min digestion of the hybrids by the enzyme, whereby the fluorescence of the mismatched hybrids returned similar to single-stranded PNA and that of the complementary hybrid only slightly decreased. As a result, it can conclude the nuclease S1 digestion is a powerful technique to improve the differentiation between complementary and various mismatched DNA targets employing internally pyrene-labeled acpcPNA as a quencher-free, singly-labeled PNA beacon probe.

In the third part, the terminally fluorescein-modified acpcPNAs (Flu-acpcPNAs) and tetramethylrhodamine-modified acpcPNA (TMR-acpcPNA) in combination with a short complementary DNA strand were evaluated as strand-displacement probes. Fluorescence studies suggest that the fluorophore labeled PNA strand could be quenched by quencher (DABCYL or BHQ) in the shorter DNA upon hybrid formation. After addition of complementary DNA target, the fluorescence become increase, but never return to the original level. The results suggest incomplete (or very slow) strand displacement. There were also problems about quenching of the fluorophore by the base G in the complementary DNA target sequence. Although the concept has been proven, much works remain to be done to allow practical use of these PNA-based strand displacement probes.

REFERENCES

[1] Kerman, K., Saito, M., Tamiya, E. Electroactive chitosan nanoparticles for the detection of single-nucleotide polymorphisms using peptide nucleic acids. *Anal. Bioanal. Chem.* **2008**, *391*, 2759–2767.

[2] Tang, D., Lu, P., Liao, D., Yang, X., Zhang, Y., Yu, C. Label-free detection of polynucleotide single-base mismatch via pyrene probe excimer emission. *Spectrochim. Acta. A Mol. Biomol. Spectrosc.* **2011**, *78*, 747–752.

[3] French, D. J., Archard, C. L., Brown, T., McDowell, D. G. HyBeacon (TM) probes: a new tool for DNA sequence detection and allele discrimination, *Mol. Cell. Probe.* **2001**, *15*, 363–374.

[4] Whitcombe, D.; Theaker, J., Guy, S. P., Brown, T., Little, S. Detection of PCR products using self-probing amplicons and fluorescence. *Nat. Biotechnol.* **1999**, *17*, 804–807.

[5] Schotter, J., Kamp, P.B., Becker, A. Pühler, A., Reiss, G. Brückl, H. Comparison of a prototype magnetoresistive biosensor to standard fluorescent DNA detection. *Biosens. & Bioelect.* **2004**, *19*, 1149–1156.

[6] Hellweg, S., Jacob, A., Hoheisel, J. D., Grehl, T., Arlinghaus, H. F. Mass spectrometric characterization of DNA microarrays as a function of primary ion species, *Appl. Surf. Sci*. **2006**, *252*, 6742–6745.

[7] Isola, N. R., Allman, S. L., Golovlev, V. V., Chen, C. H. MALDI-TOF mass spectrometric method for detection of hybridized DNA oligomers. A*nal. Chem.* **2001**, *73*, 2126–2131.

[8] Drummond, T. G., Hill, M. G., Barton, J. K. Electrochemical DNA sensors. *Nat. Biotechnol*, **2003**, *21*, 1192–1199.

[9] Dharuman, V., Hahn, J. H. Label free electrochemical DNA hybridization discrimination effects at the binary and ternary mixed monolayers of single stranded DNA/diluent/s in presence of cationic intercalators. *Biosens. & Bioelect.* **2008**, *23*, 1250–1258.

[10] Su, X., Wu, Y-J., Robelek, R., Knoll, W. Surface plasmon resonance spectroscopy and quartz crystal microbalance study of MutS binding with single thymine-guanine mismatched DNA. *Front. Biosci.* **2005**, 10, 268–274.

[11] Malic, L., Cui, B., Veres, T., Tabrizian, M. Enhanced surface plasmon resonance imaging detection of DNA hybridization on periodic gold nanopost. *Opt. Lett.* **2007**, *32*, 3092–3094.

[12] Lee, D-Y., Seto, P., Korczak, R. DNA microarray-based detection and identification of waterborne protozoan pathogens. J. Microbiol. Med. **2010**, *80*, 129–133.

[13] Nielsen, P. E., Egholm, M., Berg, R. H., Buchardt, O. Sequence-selective recognition of DNA by strand displacement with a thymine-substituted polyamide. *Science* **1991**, *254*, 1497–1500.

[14] You, Y., Moreira, B. G., Behlke, M. A., Owczarzy, R. Design of LNA probes that improve mismatch discrimination. *Nucleic. Acids. Res.* **2006**, *34*, e60.

[15] Singh, S. K., Nielsen, P., Koshkin, A. Wengel, A. LNA (locked nucleic acids): synthesis and high-affinity nucleic acid recognition. *J. Chem. Commun.* **1998**, *3*, 455–456.

[16] Tyagi S, Kramer F.R. Molecular beacons: probes that fluoresce upon hybridization, *Nat. Biotechnol*. **1996**, *14*, 303–308.

[17] Tyagi S., Bratu D. P, Kramer F. R. Multicolor molecular beacons for allele discrimination. *Nat. Biotechnol*. **1998**, *16*, 49–53.

[18] Nitin, N., Santangelo, P. J., Kim, G., Nie S., Bao, G. Peptide-linked molecular beacons for efficient delivery and rapid mRNA detection in living cells. *Nucleic Acids Res.* **2004**, *32*, e58.

[19] Bonnet G., Tyagi S., Libchaber A., Kramer F.R. Thermodynamic basis of the enhanced specificity of structured. *Proc Natl. Acad. Sci .U.S.A.* **1999**, *96*, 6171–6176.

[20] Li, X., Huang, Y., Guan, Y., Zhao, M., Li, Y. A novel one cycle allele specific primer extension-molecular beacon displacement method for DNA point mutation detection with improved specificity. *Anal. Chim. Acta*, **2007**, *58*, 12–18.

[21] Hwang, G. T., Seo, Y. J., Kim, B. H. A highly discriminating quencher-free molecular beacon for probing DNA. J. *Am. Chem. Soc.* **2004**, *126*, 6528–6529

[22] Ryu, J. H., Seo, Y. J,. Hwang, G. T., Lee, J. Y. Kim, B. H. Triad base pairs containing fluorene unit for quencher-freeSNP typing. *Tetrahedron* **2007**, *63*, 3538–3547.

[23] Keller, G. H., Huang, D. P., Manak, M. M. Labeling of DNA probes with a photoactivatable hapten. *Anal. Biochem.* **1989**, *177*, 392–395

[24] Ebata, K., Masuko, M., Ohtani, H., Kashiwasake-Jibu, M. Nucleic acid hybridization accompanied with excimer formation from two pyrene-labeled probes. *Photochem. Photobiol*. **1995**, *62*, 836–839

[25] Masuko, M., Ohtani, H., Ebata, K., Shimadzu, A. Optimization of excimer-forming two-probe nucleic acid hybridization method with pyrene as a fluorophore. *Nucleic Acids Res*. **1998**, *26*, 5409–5416

[26] Okamoto, A., Saito, Y., Saito, I., Design of base-discriminating fluorescent nucleosides. *J. Photoch. Photobio. C*. **2005**, *6*, 108–122.

[27] Saito, Y., Kanatani, K., Ochi, Y., Okamoto, A., Saito, I. Design of base-discriminating fluorescent (BDF) nucleobase for SNP typing. *Nucleic Acids. Symp. Ser(Oxf)*. **2004**, *48*, 243–244.

[28] Saito, Y., Miyauchi, Y., Okamoto, A., Saito, I. Base-discriminating fluorescent (BDF) nucleoside: distinction of thymine by fluorescence quenching. *Chem. Commun.* **2004**, *15*, 1704–1705.

[29] Okamoto, A., Tainaka, K., Ochi, Y., Kanatani, K., Saito, I. Okamoto A, Tainaka K, Ochi Y, Kanatani K, Saito I. Simple SNP typing assay using a base-discriminating fluorescent probe. *Mol. Biosyst.* **2006**, *2*, 122–127.

[30] Hwang, G. T., Seo, Y. J., Kim, S. J., Kim, B. H. Fluorescent oligonucleotide incorporating 5-(1-ethynylpyrenyl)2'-deoxyuridine: sequence-specific fluorescence changes upon duplex formation. *Tetrahedron Lett.* **2004**, *45*, 3543–3546.

[31] Wanninger-Weiss, C., Valis, L., Wagenknecht, H.-A. Pyrene-modified guanosine as fluorescent probe for DNA modulated by charge transfer. *Bioorg. Med. Chem.* **2008**, *16*, 100–106.

[32] Bag, S. S., Saito, Y., Hanawa, K., Kodate, S., Suzuka, I., Saito, I. Intelligent fluorescent nucleoside in sensing cytosine base: importance of hydrophobic nature of perylene fluorophore. *Bioorg. Med. Chem. Lett.* **2006**, *16*, 6338–634.

[33] Saito, Y., Motegi, K., Bag, S. S., Saito, I. Anthracene based base-discriminating fluorescent oligonucleotide probes for SNPs typing: synthesis and photophysical properties. *Bioorg. Med. Chem.* **2008**, *16*, 107–113.

[34] Wanninger-Weiss, C., Wagenknecht, H.-A. Synthesis of 5-(2-Pyrenyl)-2'-deoxyuridine as a DNA modification for electron-transfer studies: The critical role of the position of the chromophore attachment *Eur. J. Org. Chem*. **2008**, *1*, 64–71.

[35] Xiao, Q., Ranasinghe, R. T., Tang, A. M. P., Brown, T. Naphthalenyl- and anthracenyl-ethynyl dT analogues as base discriminating fluorescent nucleosides and intramolecular energy transfer donors in oligonucleotide probes. *Tetrahedron* **2007**, *6*, 3483–3490.

[36] Hyrup, B., Nielsen, P.E. Peptide Nucleic Acids (PNA): Synthesis properties and potential appilcations. *Bioorgan. Med. Chem.* **1996**, *4*, 5–23.

[37] Egholm, M. PNA hybridizes to complementary oligonucleotides obeying the Watson–Crick hydrogen-bonding rules. *Nature* **1993**, *365*, 566–568.

[38] Uhlmann, E., Peyman, A., Breipohl, G., Will, D.W. PNA: Synthesis polyamide nucleic acids unsual binding properties. *Angrew. Chem. Int. Ed***. 1998,** *4*, 5–23.

[39] Suparpprom, C., Srisuwannaket, C., Sangvanich, P., Vilaivan, T. Synthesis and oligodeoxynucleotide binding properties of pyrrolidinyl peptide nucleic acids bearing prolyl-2-aminocyclopentanecarboxylic acid (ACPC) backbones. *Tetrahedron Lett.* **2005**, *46*, 2833–2837.

[40] Vilaivan, T., Srisuwannaket, C. Hybridization of pyrrolidinyl peptide nucleic acids and DNA: Selectivity, base-pairing specificity, and direction of binding. *Org. Lett.* **2006**, *8*, 1897–1900.

[41] Boontha, B., Nakkuntod, J., Hirankarn, N., Chaumpluk, P., Vilaivan, T. Multiplex mass spectrometric genotyping of single nucleotide polymorphisms employing pyrrolidinyl peptide nucleic acid in combination with ion-exchange capture, *Anal. Chem.* **2008**, *80*, 8178–8186.

[42] Ananthanawat, C., Vilaivan, T., Hoven, V. P. Synthesis and immobilization of thiolated pyrrolidinyl peptide nucleic acids on gold-coated piezoelectric quartz crystals for the detection of DNA hybridization. *Sensors and Actuat B-Chem*. **2009**, *137*, 215–221.

[43] Ananthanawat, C., Vilaivan, T., Mekboonsonglarp, W., Hoven, V. P. Thiolated pyrrolidinyl peptide nucleic acids for the detection of DNA hybridization using surface plasmon resonance. *Biosens. & Bioelect.* **2009**, *24*, 3544–3549.

[44] Reenabthue, N., Boonlua, C., Vilaivan, C., Vilaivan, T., Suparpprom, C. 3-Aminopyrrolidine-4-carboxylic acid as versatile handle for internal labeling of pyrrolidinyl PNA. *Bioorg Med Chem Lett.* **2011**, *21*, 6465–6469.

[45] Svanvik, N. Westman, G. Wang, D. Kubista. M. Light-up probes: Thiazole orange-conjugated peptide nucleic acid for detection of target nucleic acid in homogeneous solution. *Anal. Biochem*. **2000**, *281***,** 26–35.

[46] Kuhn H., Demidov, V. V. Coull, J. M. Fiandaca, M. J. Gildea, B. D. Frank-Kamenetskii. M. D. Hybridization of DNA and PNA Molecular Beacons to Single-Stranded and Double-Stranded DNA Targets *J. Am. Chem. Soc*. **2004**, *126*, 1097–1023.

[47] Ye, S., Miyajima, Y., Ohnishi, T., Yamamoto, Y., Komiyama, M. Combination of peptide nucleic acid beacon and nuclease S1 for clear-cut genotyping of single nucleotide polymorphisms. *Anal. Biochem.* **2007,** 363, 300–302

[48] Englund, E. A., Appella, D. H. Synthesis of *ç*-substituted peptide nucleic acids: A new place to attach fluorophores without affecting DNA binding. *Org. Lett*. **2005**, *7*, 3465–4367.

[49] Socher, E., Jarikote, D. V., Knoll, A., Röglin, L., Burmeister, J., Seitz, O. FIT-probes : Peptide nucleic acid probes with a fluorescent base surrogate enable real-time DNA quantification and SNP discovery. *Anal. Biochem.* **2008**, *375*, 318–330.

[50] Srisuwannaket, C. Synthesis and DNA-binding properties of novel peptide nucleic acids bearing (1S,2S)-2-aminocyclopentane carboxylic acid spacer. Doctoral Dissertation, Department of Chemistry, Chulalongkorn University. **2005**.

[51] Suprapprom, C. Synthesis and nucleic acids properties of novel peptide nucleic acids carrying beta amino acid spacer. Doctoral Dissertation, Department of Chemistry, Chulalongkorn University. **2006**.

[52] Melhuish W. H. Quantum efficiencies of fluorescence of organic substances - effect of solvent and concentration of fluorescent solute. *J. Phys. Chem*., **1961**, *65*, 229–235

[53] Kuhn, H., Demidov, V. V., Gildea, B. D., Fiandana, M. J., Coull, J. C., Frank-Kamenetskii, M. D., PNA beacons for duplex DNA. *Antisense nucleic A drug dev.* **2001**, *11*, 265–270.

[54] Mayer, E., Valis, L., Huber, R., Amann, N., Wagenknecht, H.-A. Preparation of pyrene-modified purine and pyrimidine nucleosides via Suzuki-Miyaura cross-couplings and characterization of their fluorescent properties. *Synthesis-Stuttgart* **2003**, *15*, 2335–2340.

[55] Pesnot, T., Wagner, G. K. Novel derivatives of UDP-glucose: concise synthesis and fluorescent properties. *Org. Biomol. Chem*. **2008**, *6*, 2884–2891.

[56] Amann, N.,Wagenknecht, H.-A. Preparation of pyrenyl-modified nucleosides via Suzuki-Miyaura cross-coupling reactions. *Synlett* **2002**, *30*, 687–691.

[57] Lowe, G., Vilaivan, T. Dipeptides bearing nucleobases for the synthesis of novel peptide nucleic acids. *J. Chem. Soc. Perkin Trans. 1* **1997**, *4*, 547–554.

[58] TentaGel is a trademark of Rapp Polymer GmbH, Tubingen, Germany.

[59] Wilson, J.N., Cho, Y., Tan, S., Cuppoletti, A., Kool, E.T. Quenching of fluorescent nucleobases by neighboring DNA: the "insulator" concep**t.** *Chem.biochem.* **2008**, *9*, 279–285.

[60] Ananthanawat, C. Development of DNA sensor based on peptide nucleic acid and surface plasmon resonance. Doctoral disertation, Macromolecular Science, Faculty of Science, Chulalongkorn university. **2009**.

[61] Netzel, T. The spectroscopy, dynamics, and electronic structure of pyrenyl-dU nucleosides: $P^{\circ +}/dU^{\circ -}$ charge transfer state photophysics. *Tetrahedron* **2007**, *63*, 3491–3514.

[62] Netzel, T. L., Zhao, M., Nafisi, K., Headrick, J., Sigman, M. S., Eaton, B. E. Photophysics of 2'-Deoxyuridine (dU) Nucleosides Covalently Substituted with Either 1-Pyrenyl or 1-Pyrenoyl: Observation of Pyrene-to-Nucleoside Charge-Transfer Emission in 5-(1-Pyrenyl)-dU. *J. Am. Chem. Soc*. **1995**, *117*, 9119–9128.

[63] Tomac, S., Sarrkar, M., Ratilainem, P., Nielsen, P. E., Norden, B., Gräslund, A. Ionic effect on the stability and conformation of peptide nucleic acid complexes. *J. Am. Chem. Soc.* **1996**, *118*, 5544–5552.

[65] Cosa, G., Focsaneanu, K. S., McLean, J. R. N., McNamee, J. P., Scaiano, J. C. Photophysical properties of fluorescent DNA-dyes bound to single- and double-stranded DNA in aqueous buffered solution. *Photochem. & Photobio*. **2001**, *73*, 585–599.

[66] Baker, E. S., Hong, J. W., Gaylord, B. S., Bazan, G. C. and Bowers, M. T. PNA/dsDNA complexes: site specific binding and dsDNA biosensor applications. *J Am Chem Soc*. **2006**, *128*, 8484–8492.

[67] Izvolsky K. I., Demidov V. V., Nielsen P. E., Frank-Kamenetskii M. D. Sequence-specific protection of duplex DNA against restriction and methylation enzymes by pseudocomplementary PNAs. *Biochemistry* **2000,** *39*, 10908–10913.

[68] Yamane, A. MagiProbe: a novel fluorescence quenching-based oligonucleotide probe carrying a fluorophore and an intercalator. *Nucleic Acids Res.* **2002**, *30*, e97.

[69] Okamoto, A., Kanatani, K., Saito, I. Pyrene-labeled base-discriminating fluorescent DNA probes for homogeneous SNP typing. *J. Am. Chem. Soc***. 2004**, *126*, 4820–4827.

[70] Seidel, C.A.M., Schulz A., Sauer M. H. M., Nucleobase-Specific Quenching of Fluorescent Dyes. 1. Nucleobase One-Electron Redox Potentials and Their Correlation with Static and Dynamic Quenching Efficiencies. *J. Phys. Chem.* **1996**, *100*, 5541−5553.

APPENDICES

Table A1 T_m values of hybrids between terminally pyrenebutyryl-modified acpcPNAs (Py-PNAs) with different target DNAs.

Entry	System	T_m (°C)	Note
1	Py-TTTTTTTTT(**PyT9**) 3'-AAAAAAAAA-5'	>80.0	complementary
2	Py-TTTTTTTTT(**PyT9**) 3'-AAAA<u>T</u>AAAA-5'	52.6	internal mismatch (T)
3	Py-TTTTTTTTT(**PyT9**) 3'-<u>T</u>AAAAAAAA-5'	>80.0	terminal mismatch (T)
4	Py-AGTTATCCCTGC(**PyM12**) 3'-TCAATAGGGACG-5'	73.5	complementary
5	Py-AGTTATCCCTGC(**PyM12**) 3'-<u>G</u>CAATAGGGACG-5'	72.1	terminal mismatch (G)
6	Py-AGTTATCCCTGC(**PyM12**) 3'-<u>C</u>CAATAGGGACG-5'	70.6	terminal mismatch (C)
7	Py-AGTTATCCCTGC(**PyM12**) 3'-<u>A</u>CAATAGGGACG-5'	71.6	terminal mismatch (A)
8	Py-AGTTATCCCTGC(**PyM12**) 3'-TCAAT<u>C</u>GGGACG-5'	50.2	internal mismatch (C)
9	Py-AGTTATCCCTGC(**PyM12**) 3'-<u>A</u>TCAATAGGGACG-5'	79.4	N-terminal extended (A)
10	Py-AGTTATCCCTGC(**PyM12**) 3'-<u>T</u>TCAATAGGGACG-5'	–	N-terminal extended (T)
11	Py-AGTTATCCCTGC(**PyM12**) 3'-<u>C</u>TCAATAGGGACG-5'	–	N-terminal extended (C)
12	Py-AGTTATCCCTGC(**PyM12**) 3'-<u>G</u>TCAATAGGGACG-5'	–	N-terminal extended (G)
13	Py-AGTTATCCCTGC(**PyM12**) 3'-<u>_</u>CAATAGGGACG-5'	67.3	N-terminal deleted (T)
14	Py-AGTTATCCCTGC(**PyM12**) 3'-<u>__</u>AATAGGGACG-5'	56.6	N-terminal deleted (TC)

Table A1 (continued)

Entry	System	T_m (°C)	Note
15	Py-CTAAATTCAGA(**PyM11**) 3'-GATTTAAGTCT-5'	>80.0	complementary
16	Py-CTAAATTCAGA(**PyM11**) 3'-GATTTCAGTCT-5'	78.5	internal mismatch (C)
17	Py-CTAAATTCAGA(**PyM11**) 3'-AATTTAAGTCT-5'	77.3	terminal mismatch (A)
18	Py-CTAAATTCAGA(**PyM11**) 3'-TGGGGATTTAAGTCT-5'	>80.0	N-terminal extended
19	Py-GTAGATCACT(**PyM10**) 3'-CATCTAGTGA-5'	–	complementary
20	Py-GTAGATCACT(**PyM10**) 3'-CATCCAGTGA-5'	42.2	internal mismatch (C)

Table A2 T_m values of hybrids between internally pyrenebutyryl-modified acpcPNAs (Py-PNAs) oligomers with different target DNAs.

Entry	System	T_m (°C)	Note
1	TTTTTTTTT(**T9^{Py}**) 3'-AAAAAAAAA-5'	60.3	complementary
2	TTTTTTTTT(**T9^{Py}**) 3'-AAAATAAAA-5'	25.4	internal mismatch(T)
3	AGTTATCCCTGC (**M12^{Py}T**) 3'-TCAATAGGGACG-5'	62.7	complementary
4	AGTTATCCCTGC (**M12^{Py}T**) 3'-TCAATCGGGACG-5'	45.6	internal mismatch (C)
5	AGTTATCCCTGC (**M12^{Py}T**) 3'-TCAATGGGGACG-5'	42.1	internal mismatch (G)
6	AGTTATCCCTGC (**M12^{Py}T**) 3'-TCAATTGGGACG-5'	35.3	internal mismatch (T)
7	AGTTATCCCTGC (**M12^{Py}C**) 3'-TCAATAGGGACG-5'	61.4	complementary
8	AGTTATCCCTGC (**M12^{Py}C**) 3'-TCAATCGGGACG-5'	–	internal mismatch (C)
9	CTAAATTCAGA (**M11^{Py}A**) 3'-GATTTAAGTCT-5'	69.9	complementary
10	CTAAATTCAGA (**M11^{Py}A**) 3'-GATTCAAGTCT-5'	27.3	internal mismatch (C)
11	CTAAATTCAGA (**M11^{Py}A**) 3'-GATTTAACTCT-5'	43.7	internal mismatch (C)
12	CTAAATTCAGA (**M11^{Py}T**) 3'-GATTTAAGTCT-5'	65.0	complementary
13	CTAAATTCAGA (**M11^{Py}T**) 3'-GATTTACGTCT-5'	42.6	internal mismatch (C)
14	CTAAATTCAGA (**M11^{Py}T**) 3'-GATTTAGGTCT-5'	37.6	internal mismatch (G)
15	CTAAATTCAGA (**M11^{Py}T**) 3'-GATTTATGTCT-5'	39.6	internal mismatch (T)

Table A2 (continued)

Entry	System	T_m (°C)	Note
16	CTAAATTCAGA (**M11^{Py}T**) 3'-GATTTAAATCT-5'	38.9	complementary
17	CTAAATTCAGA (**M11^{Py}T**) 3'-GATTTAACTCT-5'	38.2	internal mismatch(T)
18	CTAAATTCAGA (**M11^{Py}T**) 3'-GATTTAATTCT-5'	37.4	complementary
19	CTAAATTCAGA (**M11^{Py}T**) 3'-GATTTGAGTCT-5'	43.6	internal mismatch (C)
20	CTAAATTCAGA (**M11^{Py}T**) 3'-GATTTTAGTCT-5'	45.9	internal mismatch (G)
21	CTAAATTCAGA (**M11^{Py}T**) 3'-GATTAAAGTCT-5'	39.2	internal mismatch (T)
22	CTAAATTCAGA (**M11^{Py}T**) 3'-GATTCAAGTCT-5'	40.4	complementary
23	CTAAATTCAGA (**M11^{Py}T**) 3'-GATTGAAGTCT-5'	37.1	internal mismatch (C)
24	CTAAATTCAGA (**M11^{Py}C**) 3'-GATTTAAGTCT-5'	60.2	complementary
25	CTAAATTCAGA (**M11^{Py}C**) 3'-GATTTAAATCT-5'	43.7	internal mismatch (C)
26	CTAAATTCAGA (**M11^{Py}C**) 3'-GATTTAACTCT-5'	54.8	internal mismatch (C)
27	CTAAATTCAGA (**M11^{Py}C**) 3'-GATTTAATTCT-5'	56.7	complementary
28	CTAAATTCAGA (**M11^{Py}C**) 3'-GATTAAAGTCT-5'	34.2	internal mismatch (C)
29	CTAAATTCAGA (**M11^{Py}C**) 3'-GATTCAAGTCT-5'	33.0	internal mismatch (G)
30	CTAAATTCAGA (**M11^{Py}C**) 3'-GATTTAAGTCT-5'	29.8	internal mismatch (T)

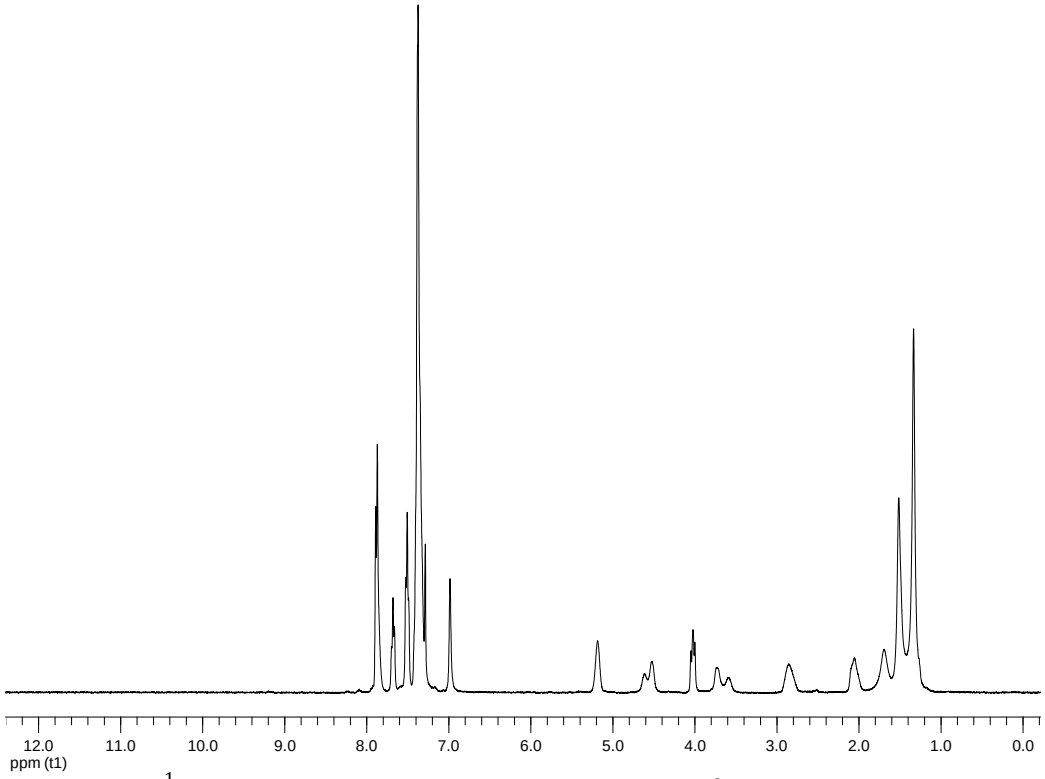

Figure A1. ^{1}H NMR spectrum (400 MHz, $CDCl_3$) of *N*-*tert*-Butoxycarbonyl-*cis*-4-(N^3-benzoyl-5-iodouracil-1-yl)-D-proline diphenylmethyl ester (**3**)

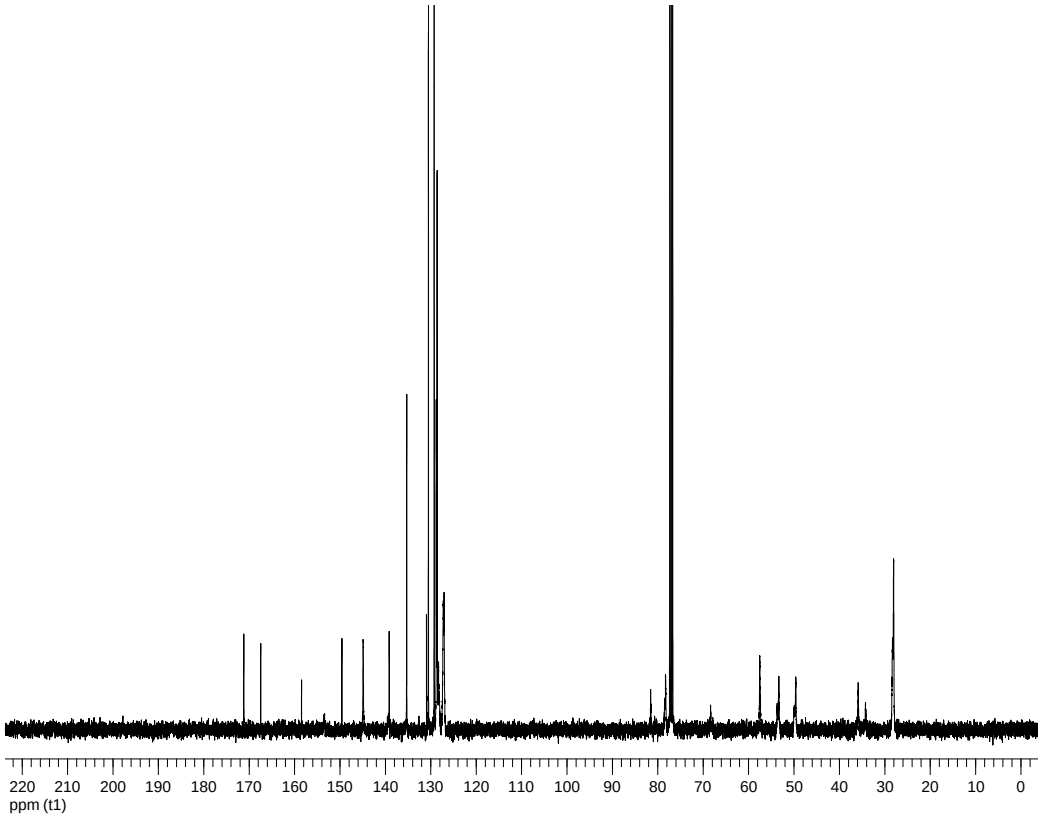

Figure A2. ^{13}C NMR spectrum (100 MHz, $CDCl_3$) of *N*-*tert*-Butoxycarbonyl-*cis*-4-(N^3-benzoyl-5-iodouracil-1-yl)-D-proline diphenylmethyl ester (**3**)

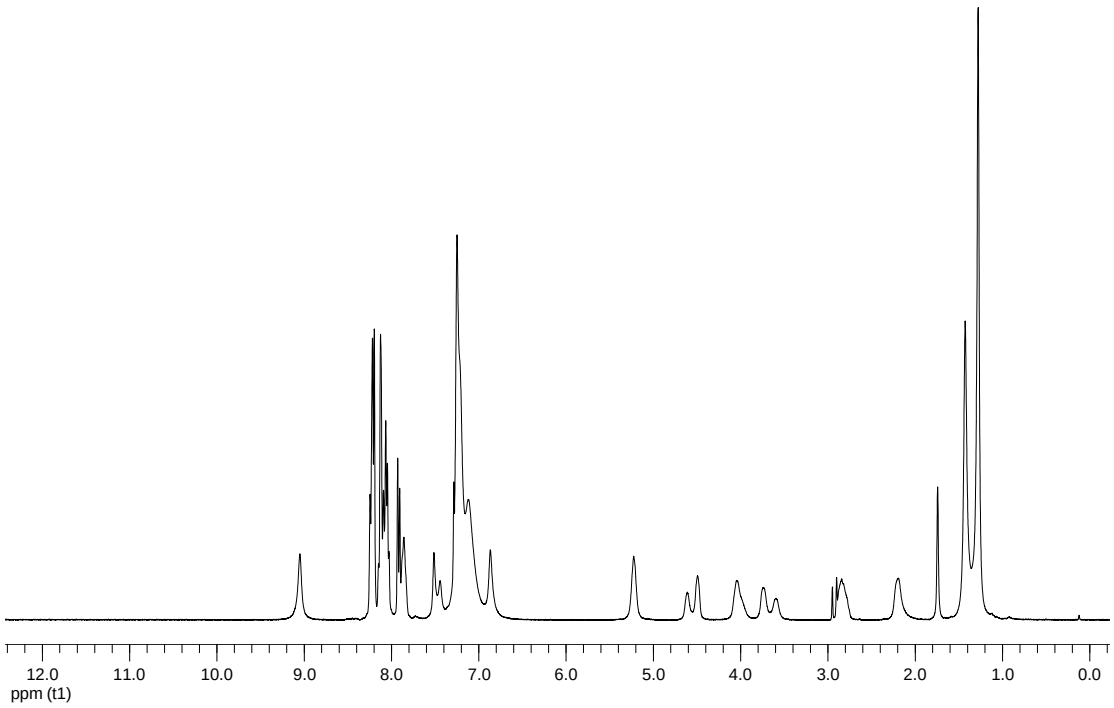

Figure A3. ^{1}H NMR spectrum (400 MHz, $CDCl_3$) of *N-tert*-Butoxycarbonyl-*cis*-4-(5-(1-pyrenyl)uracil-1-yl)-D-proline diphenylmethyl ester (**4**)

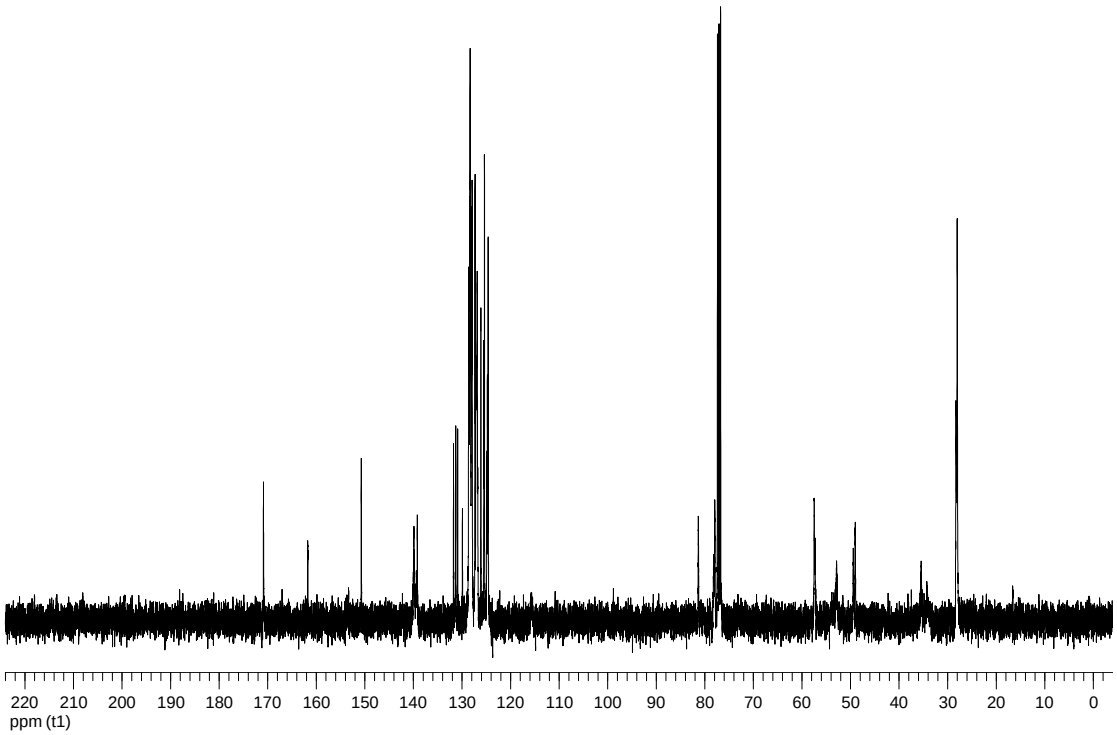

Figure A4. ^{13}C NMR spectrum (100 MHz, $CDCl_3$) of *N-tert*-Butoxycarbonyl-*cis*-4-(5-(1-pyrenyl)uracil-1-yl)-D-proline diphenylmethyl ester (**4**)

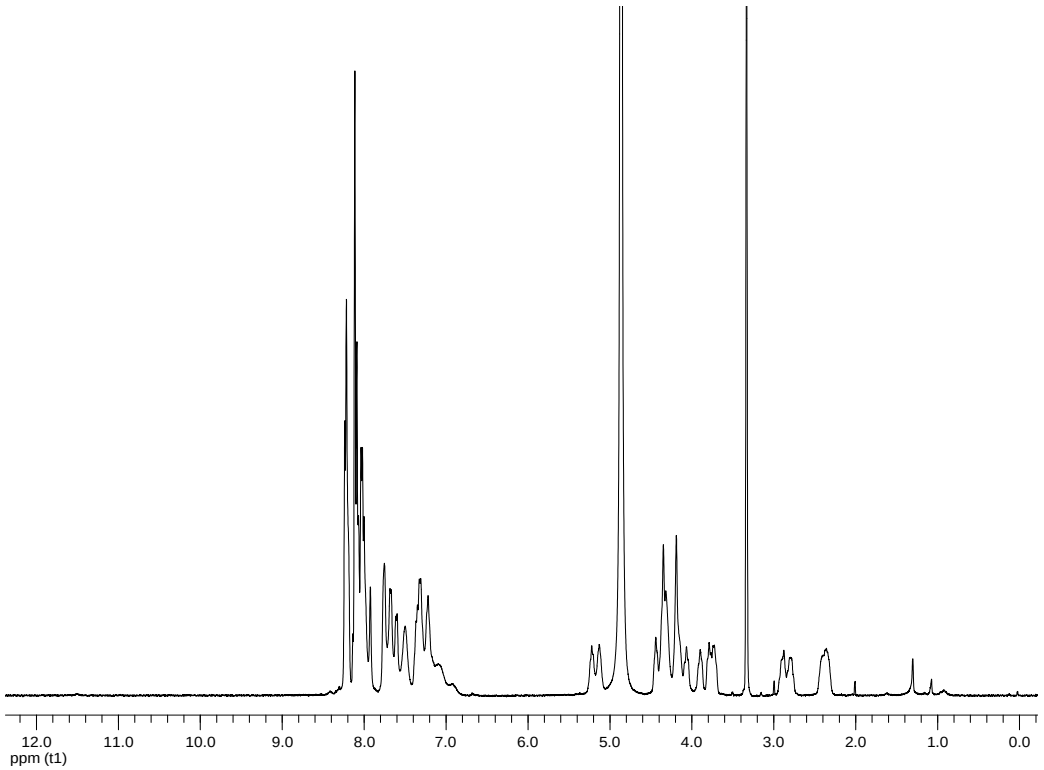

Figure A5. ^{1}H NMR spectrum (400 MHz, $CDCl_3$) of (*N*-Fluoren-9-ylmethoxy carbonyl)- *cis*-4-(5-(1-pyrenyl)uracil-1-yl)-D-proline (**1**)

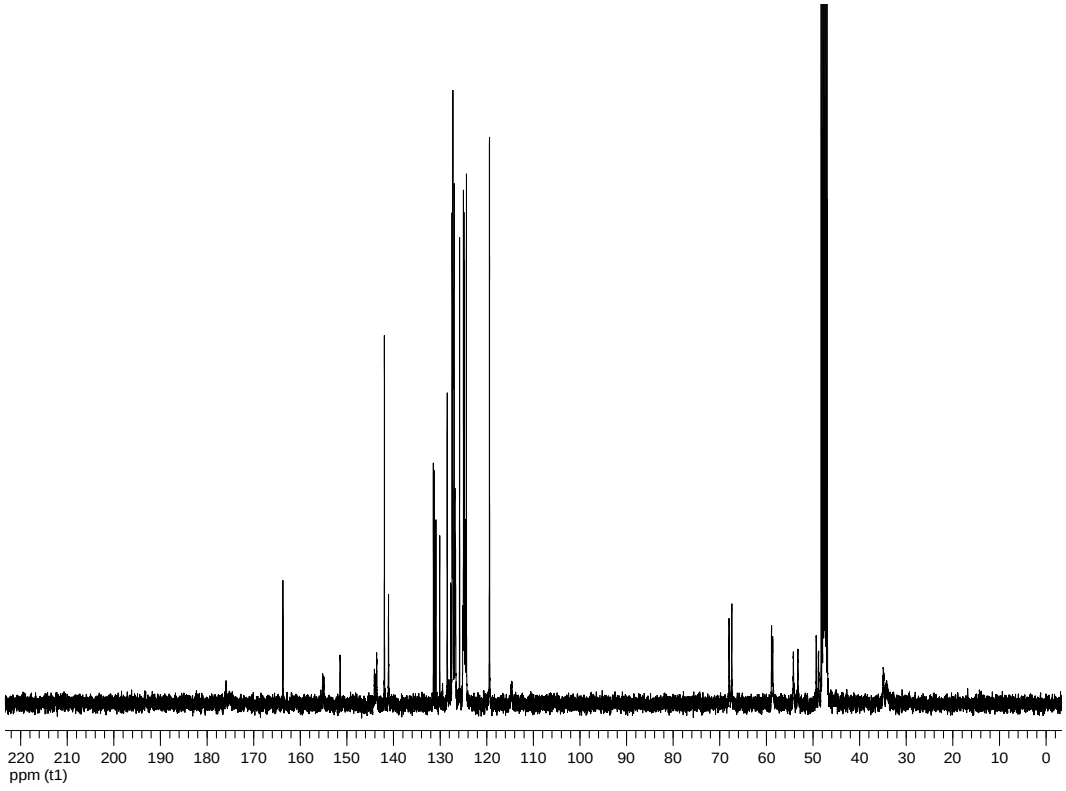

Figure A6. ^{13}C NMR spectrum (100 MHz, $CDCl_3$) of (*N*-Fluoren-9-ylmethoxy carbonyl)- *cis*-4-(5-(1-pyrenyl)uracil-1-yl)-D-proline (**1**)

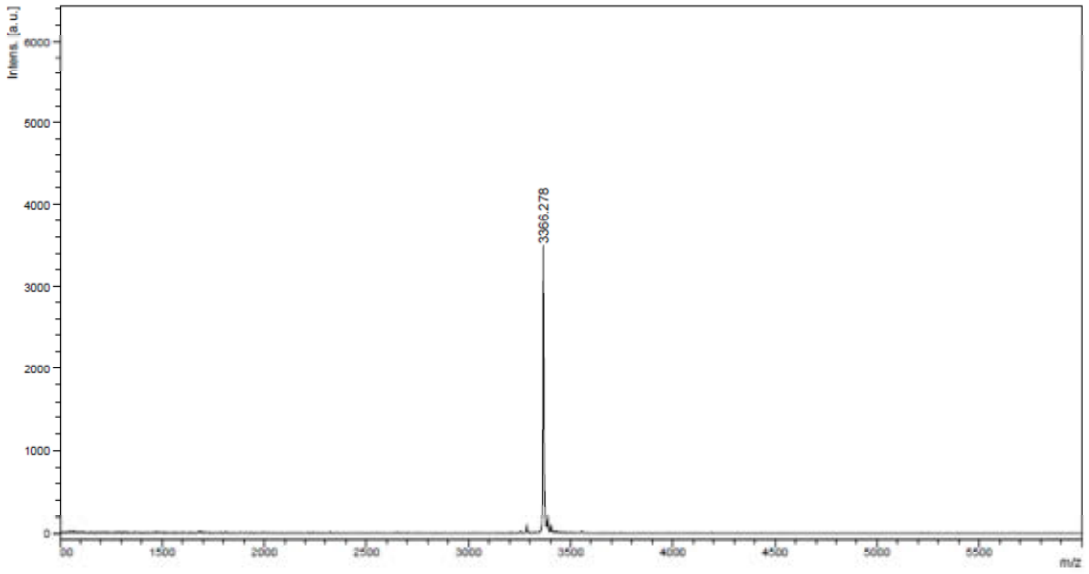

Figure A7. MALDI-TOF mass spectrum of Ac-TTTTU^{Py}TTTT-LysNH$_2$ (**TU^{Py}T**) (calcd for $[M+H]^+$: m/z=3365.65)

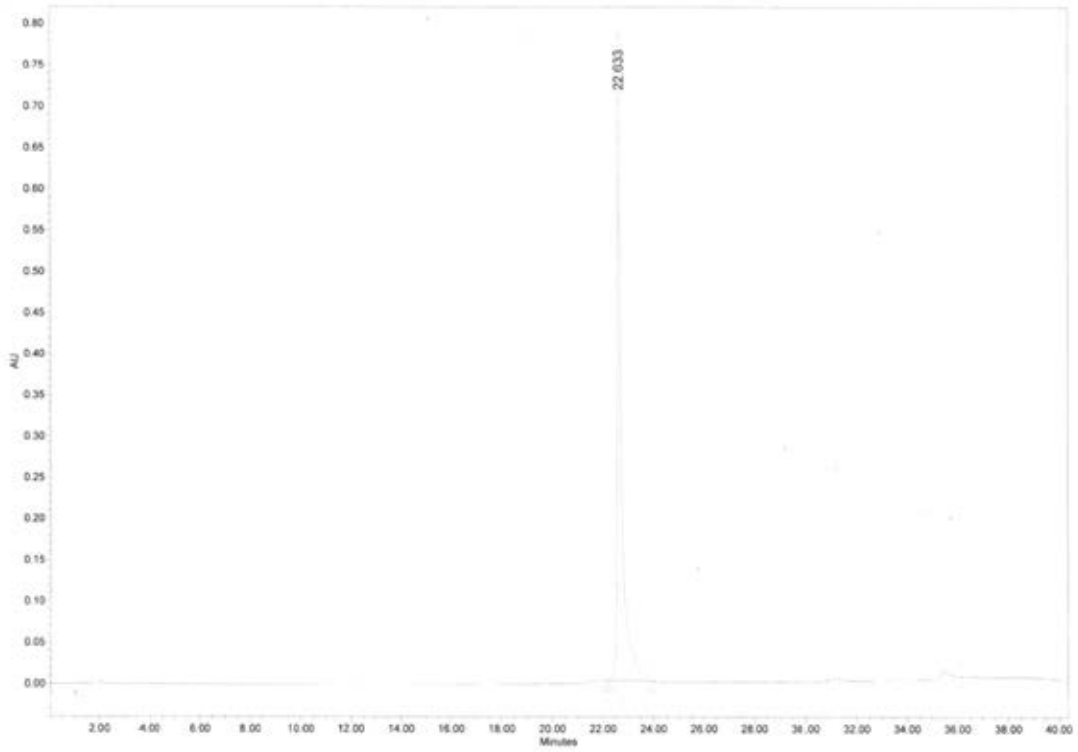

Figure A8. HPLC chromatogram of Ac-TTTTU^{Py}TTTT-LysNH$_2$ (**TU^{Py}T**)

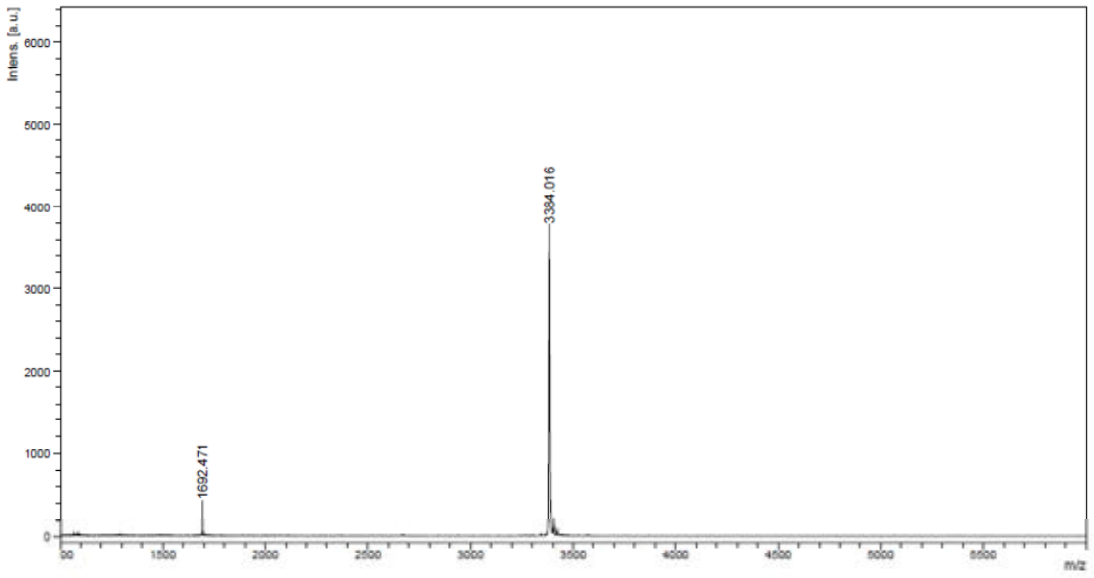

Figure A9. MALDI-TOF mass spectrum of Ac-TTTAU^{Py}ATTT-LysNH$_2$ (**AU^{Py}A**) (calcd for $[M+H]^+$: m/z=3383.67)

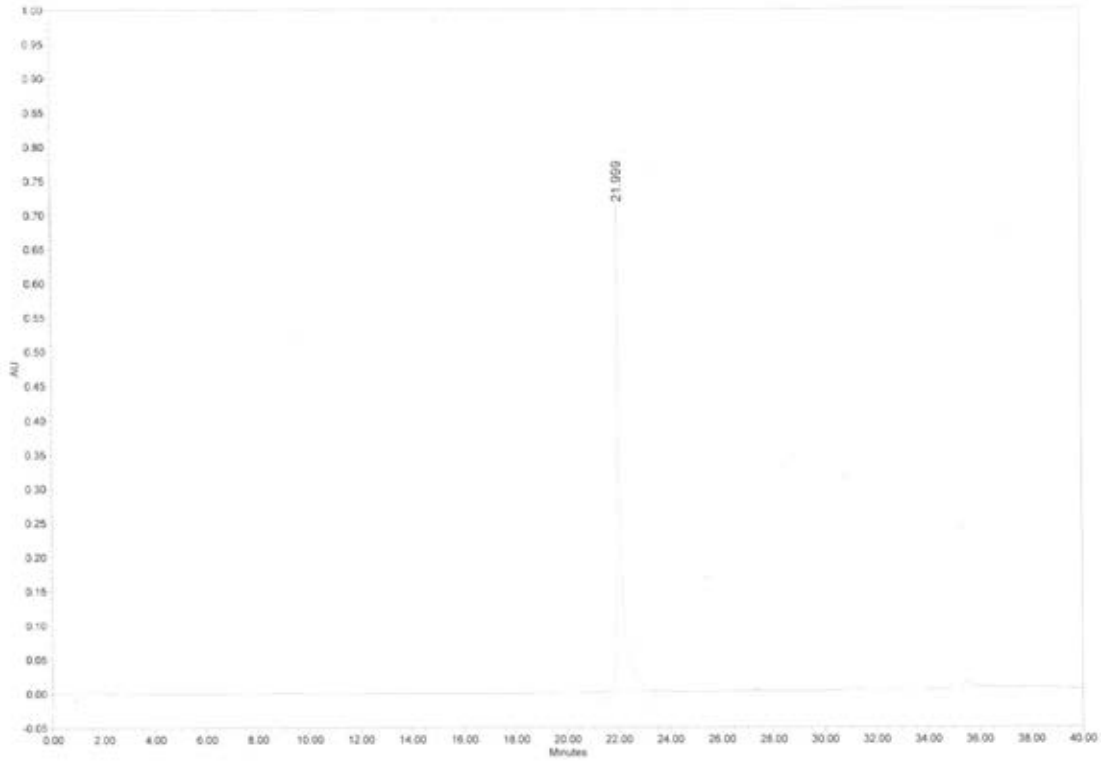

Figure A10. HPLC chromatogram of Ac-TTTAU^{Py}ATTT-LysNH$_2$ (**AU^{Py}A**)

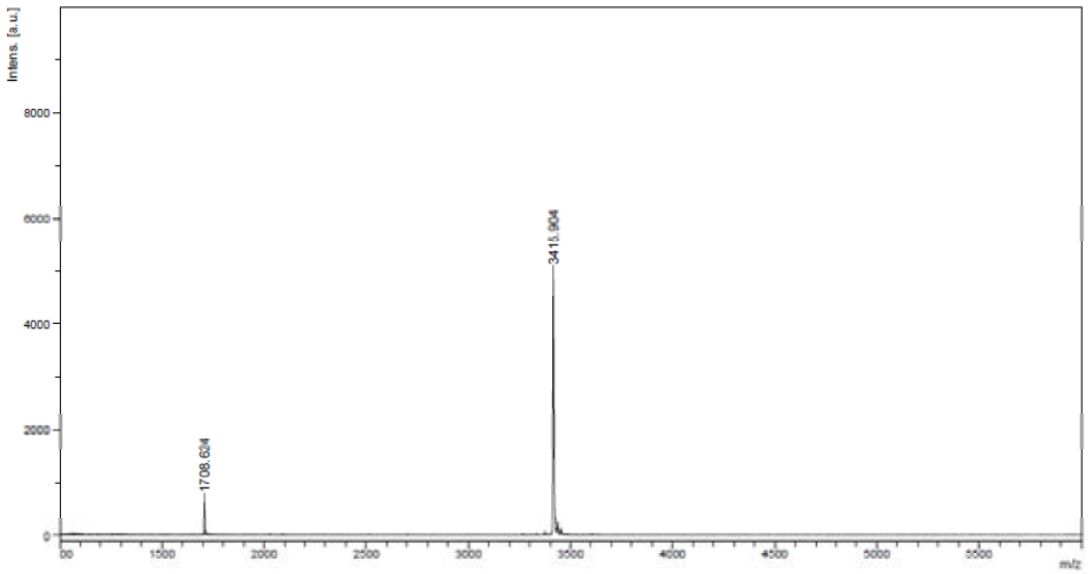

Figure A11. MALDI-TOF mass spectrum of Ac-TTTGU^{Py}GTTT-LysNH$_2$ (**GU^{Py}G**) (calcd for $[M+H]^+$: m/z=3415.67)

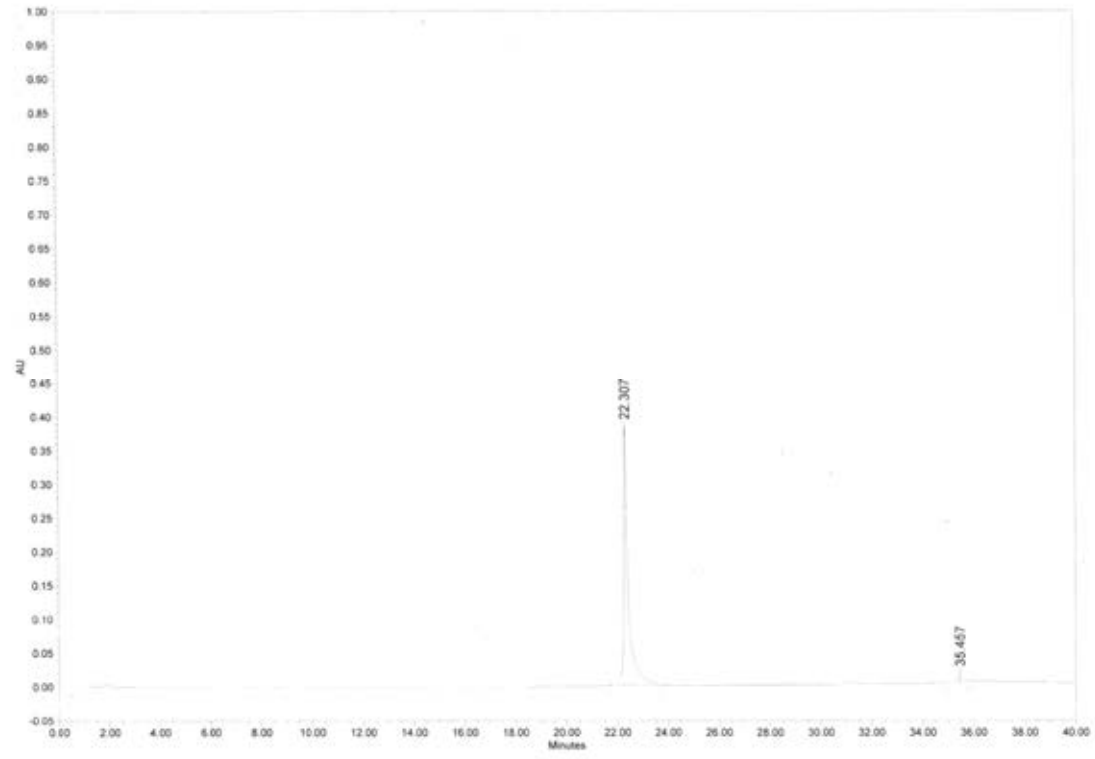

Figure A12. HPLC chromatogram of Ac-TTTGU^{Py}GTTT-LysNH$_2$ (**GU^{Py}G**)

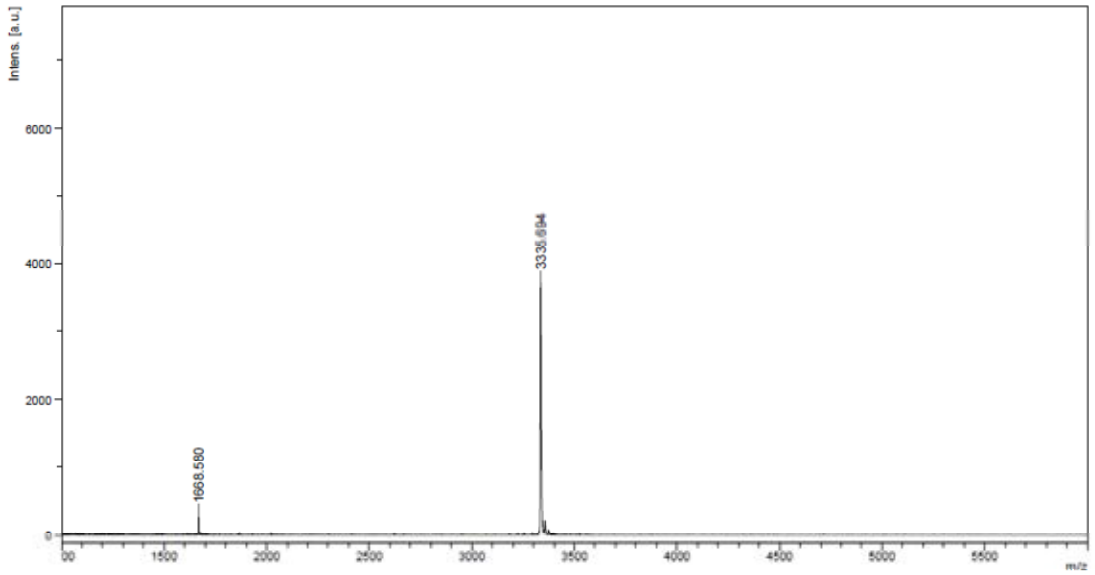

Figure A13. MALDI-TOF mass spectrum of Ac-TTTCU^{Py}CTTT-LysNH$_2$ (**CU^{Py}C**) (calcd for $[M+H]^+$: m/z=3335.62)

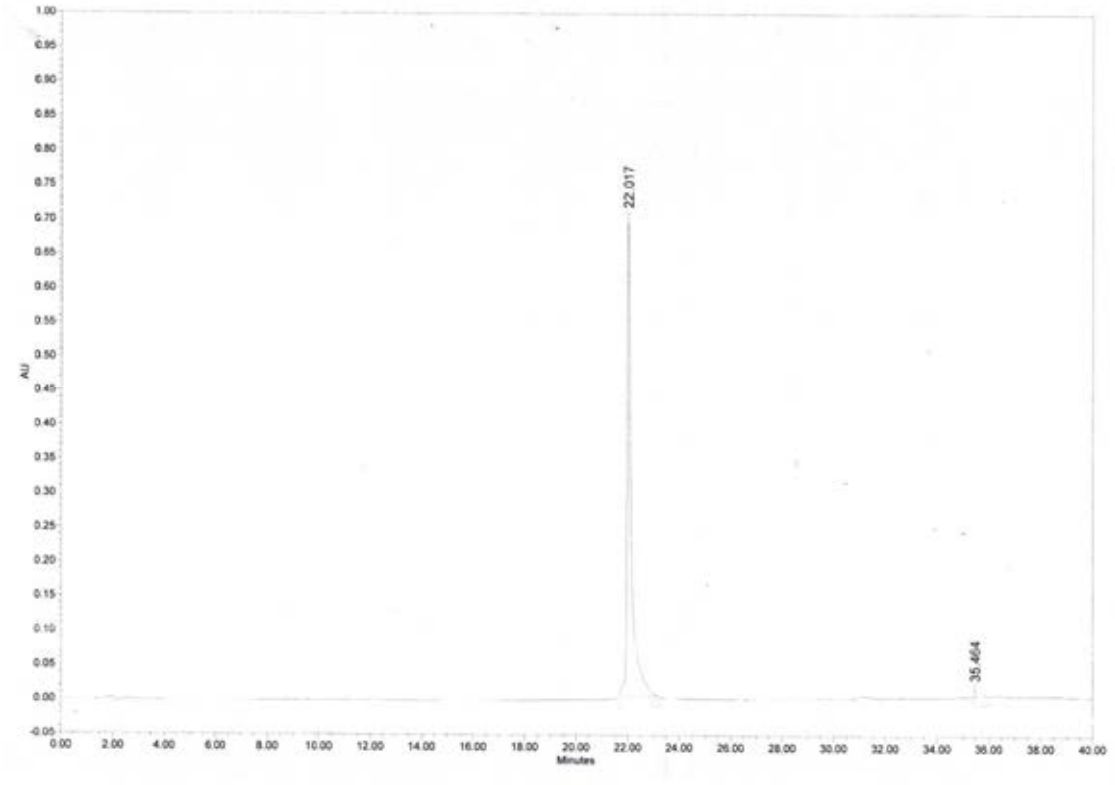

Figure A14. HPLC chromatogram of Ac-TTTCU^{Py}CTTT-LysNH$_2$ (**CU^{Py}C**)

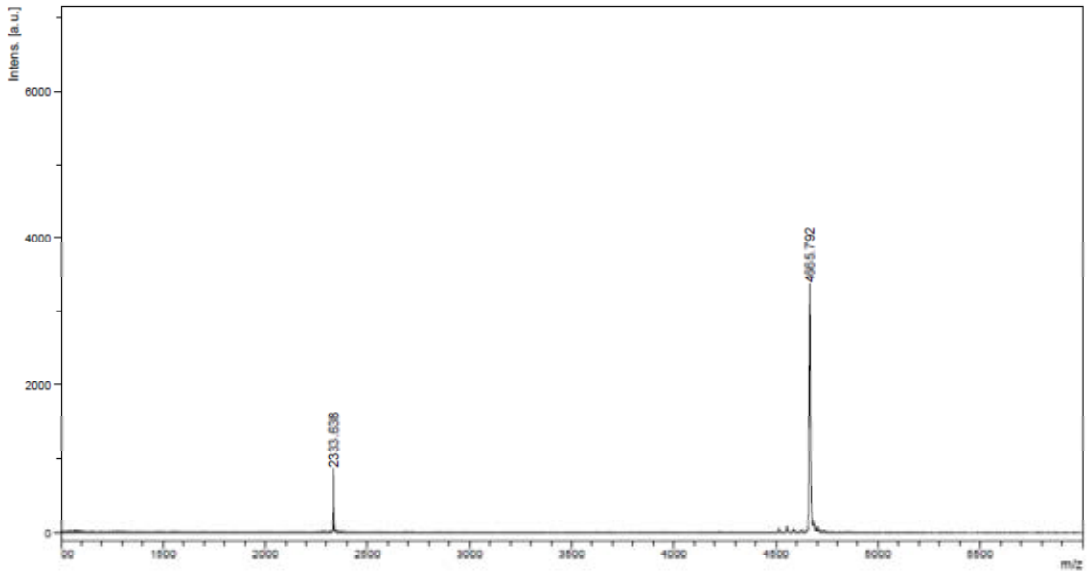

Figure A15. MALDI-TOF mass spectrum of Ac-TTTTTCU^{Py}CTTTTT-LysNH$_2$ (**CU^{Py}C13**) (calcd for [*M*+H]$^+$: m/z=4665.04)

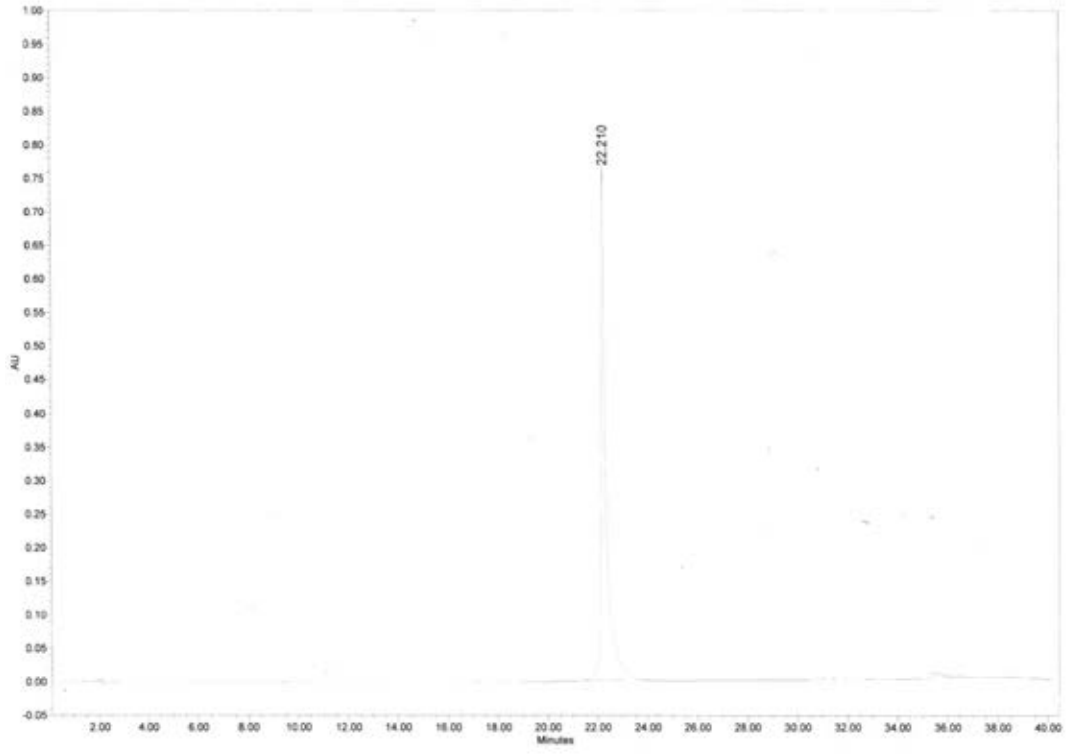

Figure A16. HPLC chromatogram of Ac-TTTTTCU^{Py}CTTTTT-LysNH$_2$ (**CU^{Py}C13**)

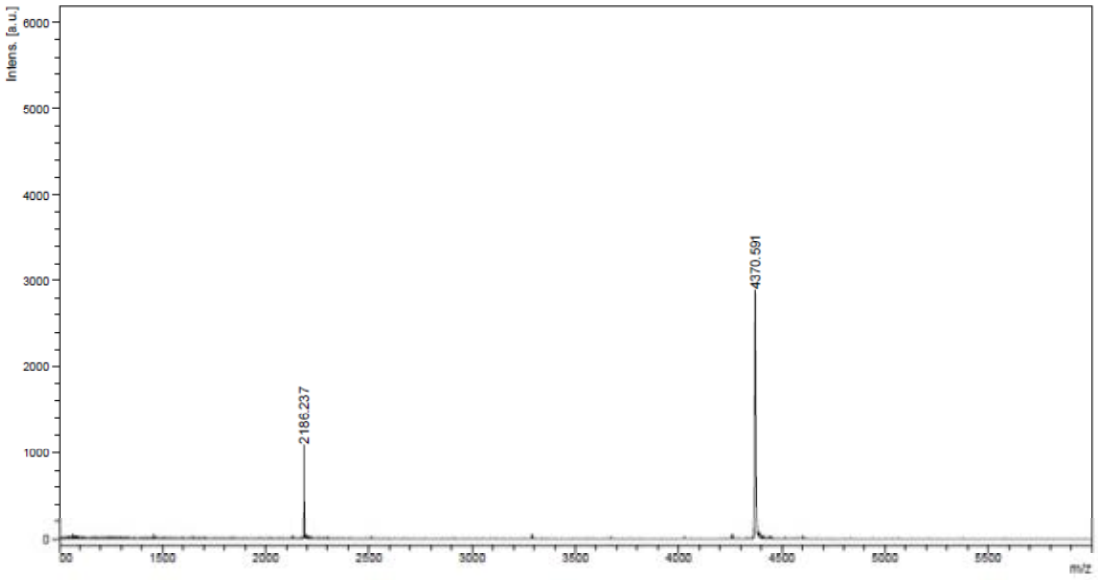

Figure A17. MALDI-TOF mass spectrum of Ac-AGTTAU^{Py}CCCTGC-LysNH$_2$ (**MixU^{Py}**) (calcd for $[M+H]^+$: m/z=4370.72)

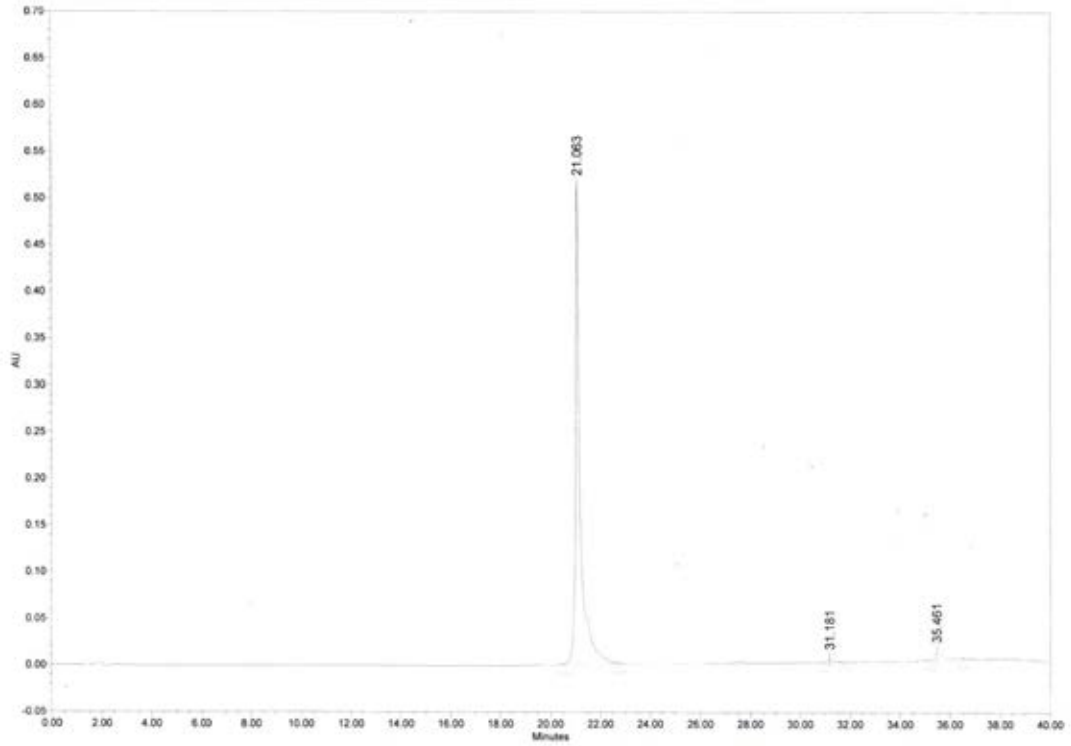

Figure A18. HPLC chromatogram of Ac-AGTTAU^{Py}CCCTGC-LysNH$_2$ (**MixU^{Py}**)

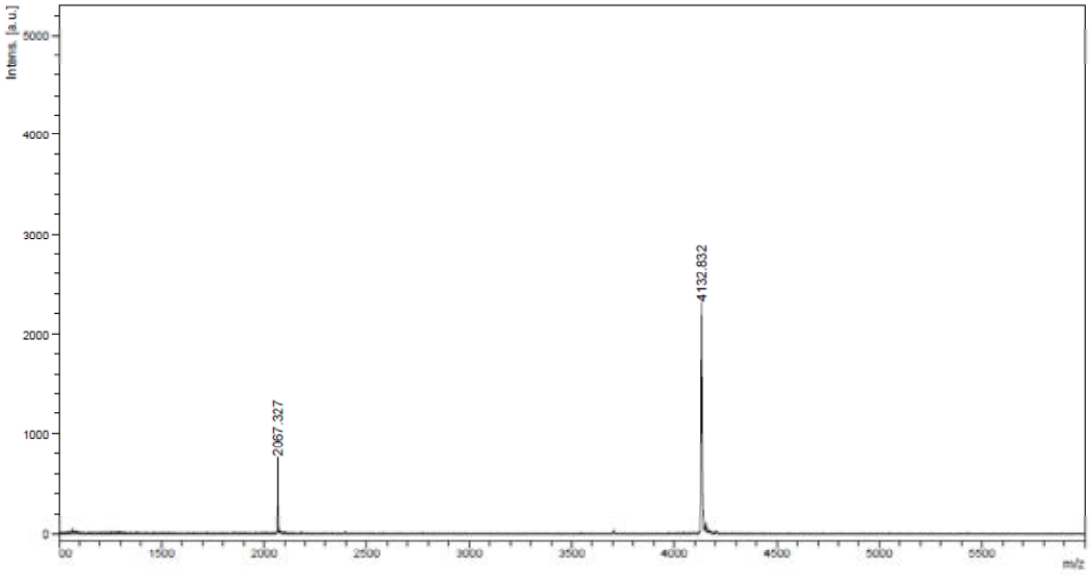

Figure A19. MALDI-TOF mass spectrum of Ac-CTAAAAU^{Py}TCAGA-LysNH$_2$ (**MixAU^{Py}**) (calcd for [*M*+H]$^+$: m/z=4132.48)

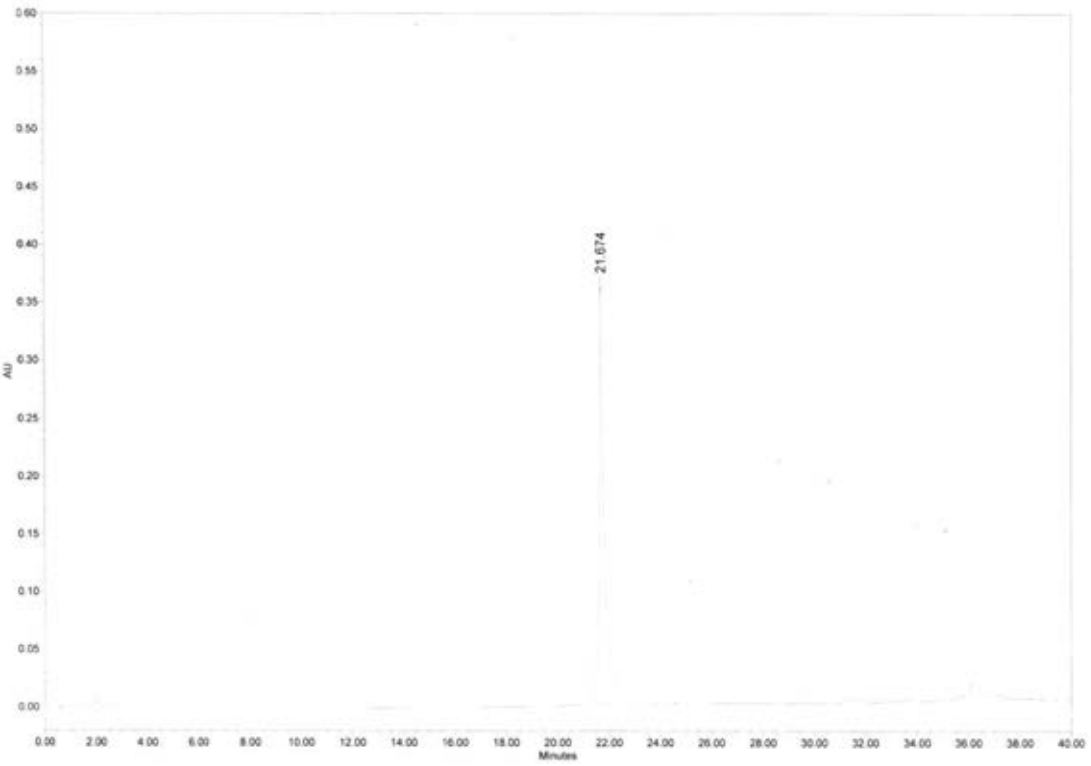

Figure A20. HPLC chromatogram of Ac-CTAAAAU^{Py}TCAGA-LysNH$_2$ (**MixAU^{Py}**)

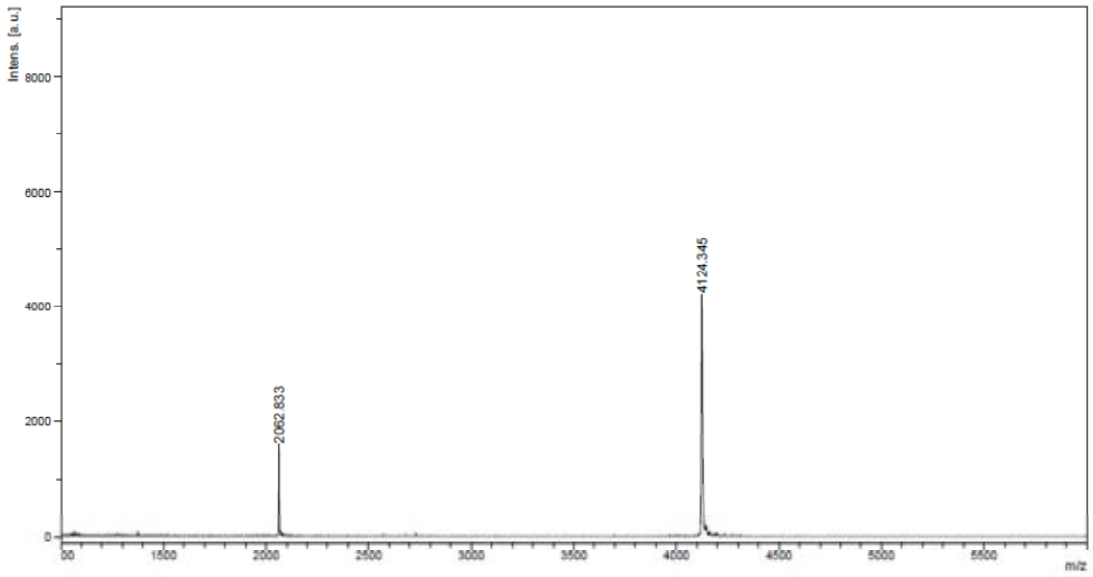

Figure A21. MALDI-TOF mass spectrum of Ac-CTAAATU^{Py}TCAGA-LysNH$_2$ (**MixTU^{Py}**) (calcd for $[M+H]^+$: m/z=4123.47)

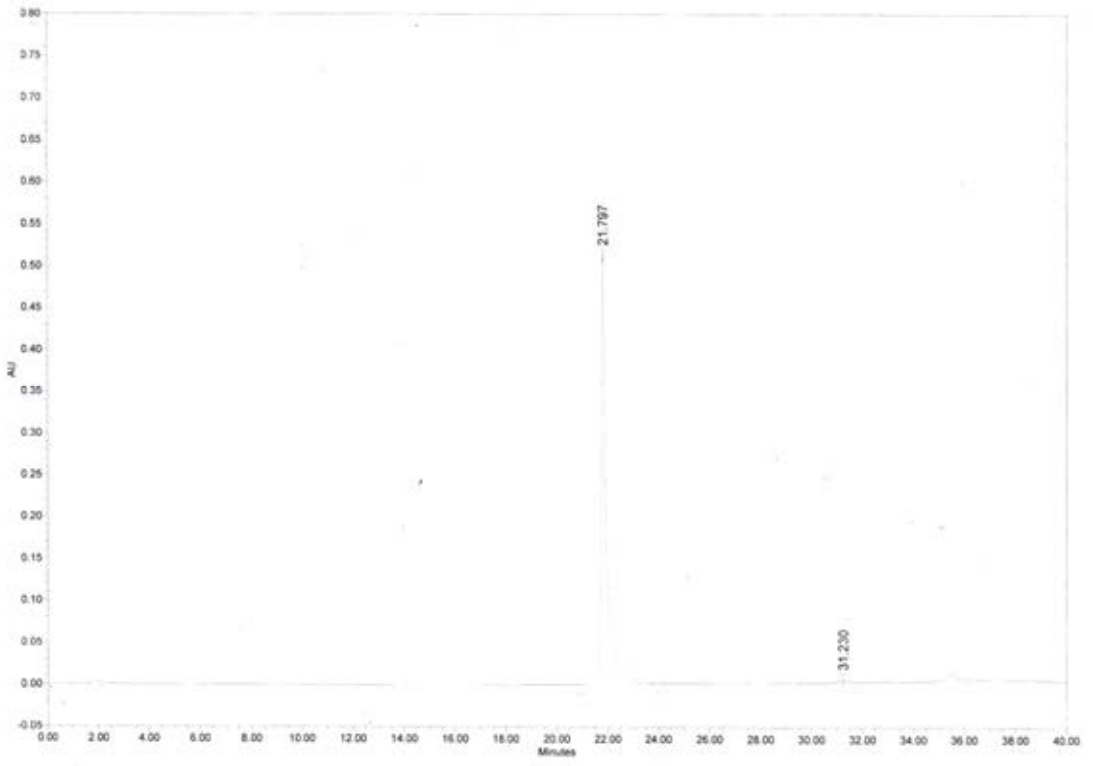

Figure A22. HPLC chromatogram of Ac-CTAAATU^{Py}TCAGA-LysNH$_2$ (**MixTU^{Py}**)

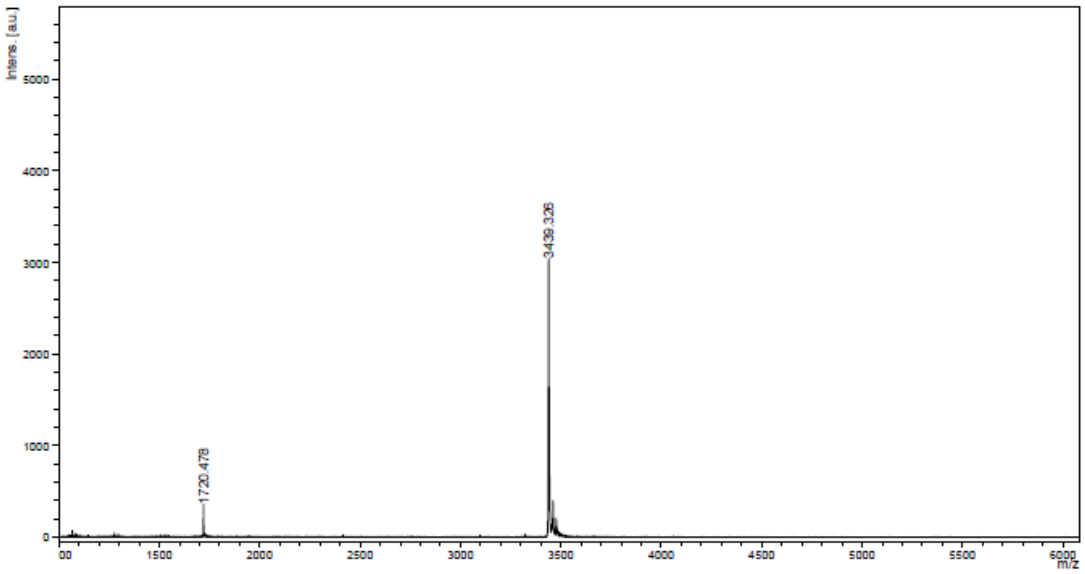

Figure A23. MALDI-TOF mass spectrum of Ac-AAAAU^{Py}AAAA-LysNH$_2$ (**MixTU^{Py}**) (calcd for $[M+H]^+$: m/z=3437.75)

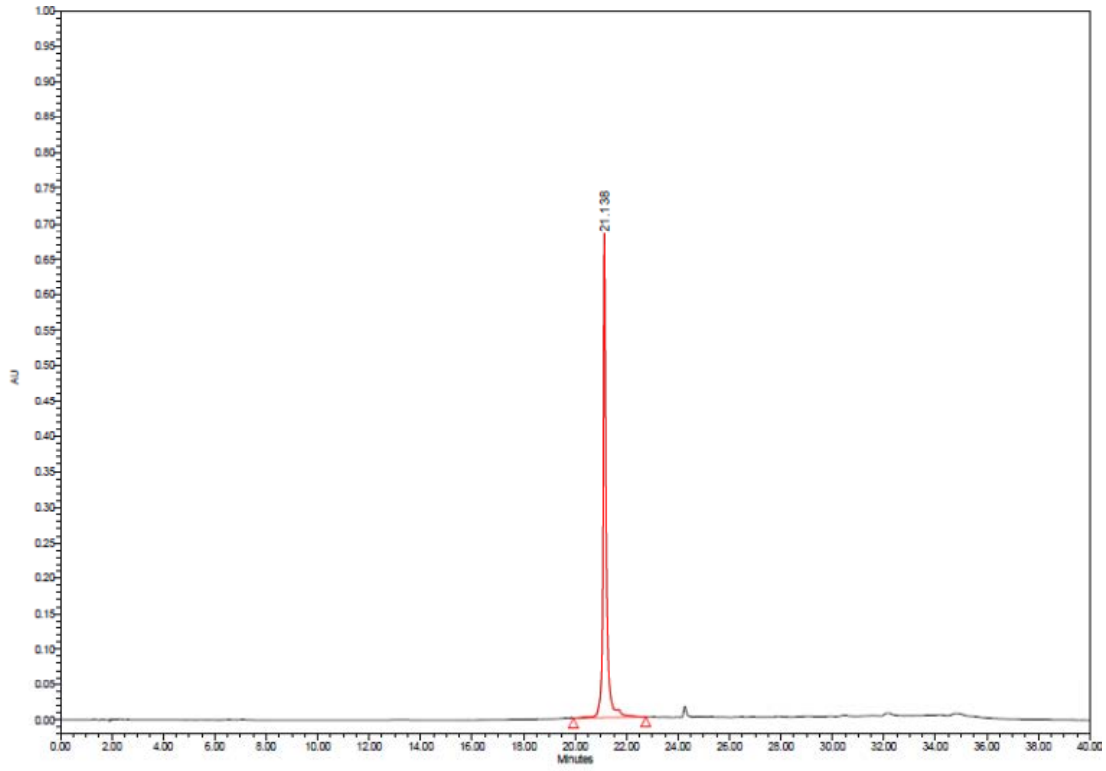

Figure A24. HPLC chromatogram of Ac-AAAAU^{Py}AAAA-LysNH$_2$ (**AU^{Py}**)

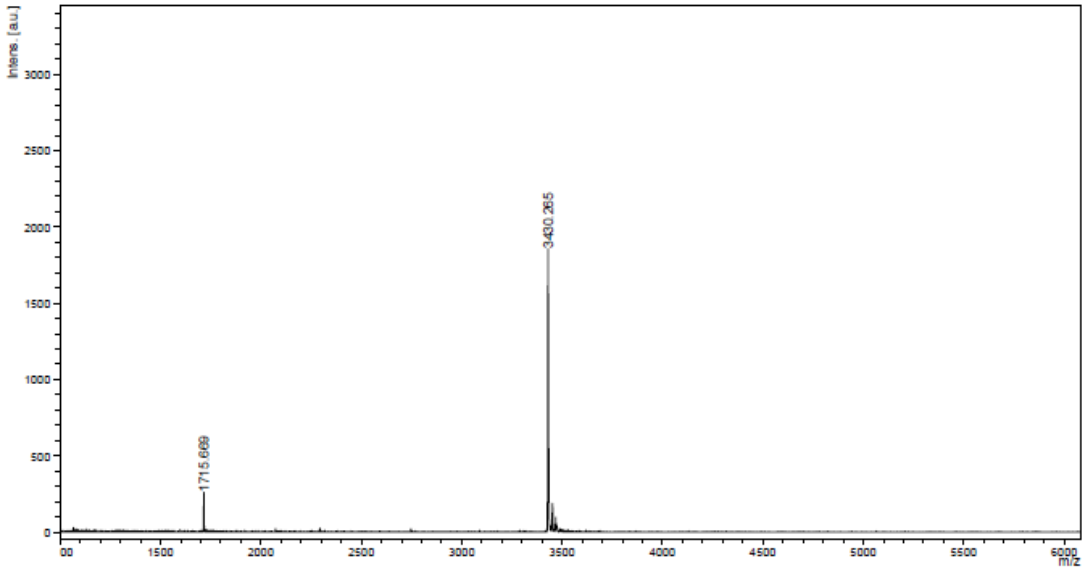

Figure A25. MALDI-TOF mass spectrum of Ac-AAATU^{Py}AAAA-LysNH$_2$ (**T^{6}AU^{Py}**) (calcd for $[M+H]^+$: m/z=3428.74)

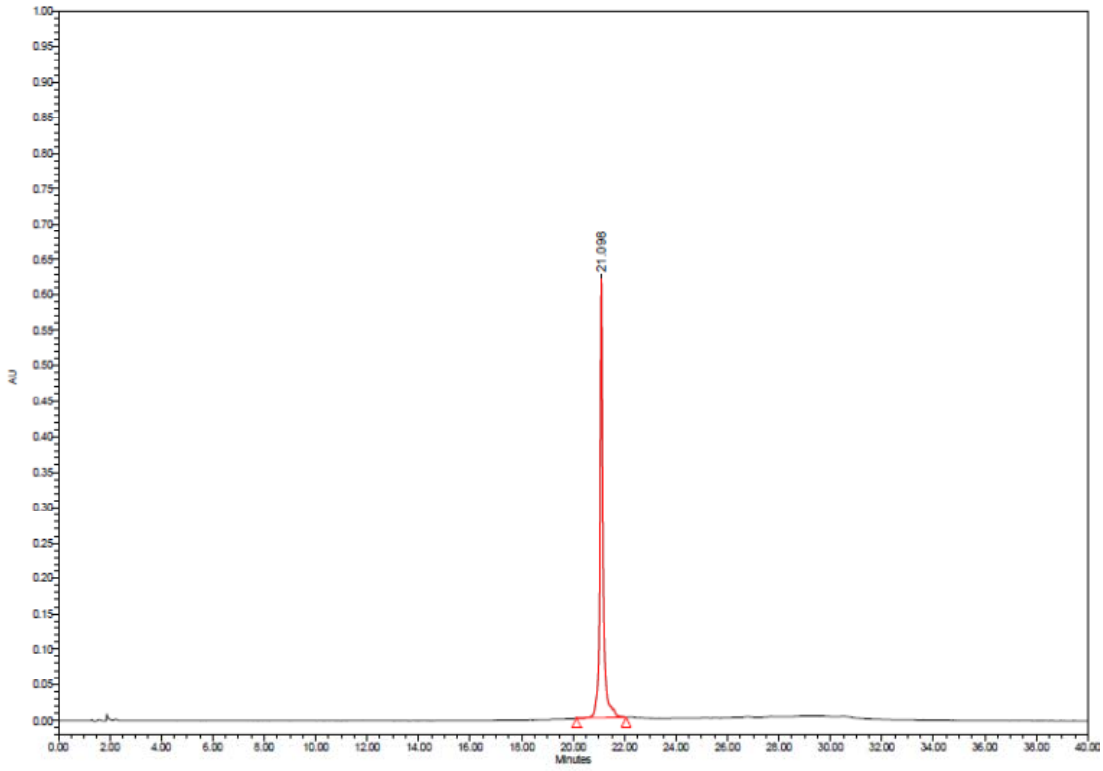

Figure A26. HPLC chromatogram of Ac-AAATU^{Py}AAAA-LysNH$_2$ (**T^{6}AU^{Py}**)

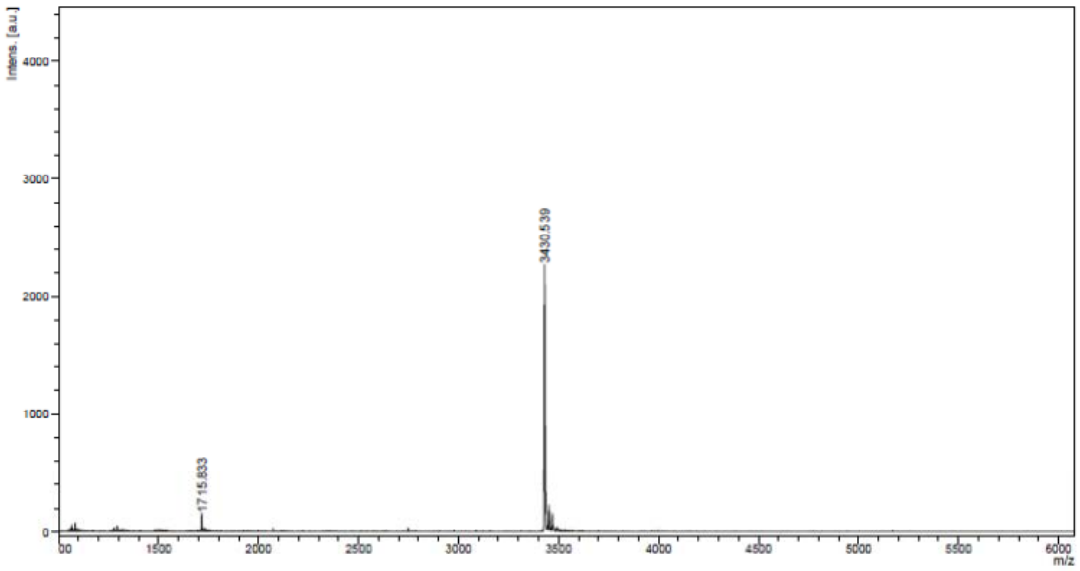

Figure A27. MALDI-TOF mass spectrum of Ac Ac-AATAU^{Py}AAAA-LysNH$_2$ (**T^{7}AU^{Py}**) (calcd for [*M*+H]$^+$: m/z=3428.74)

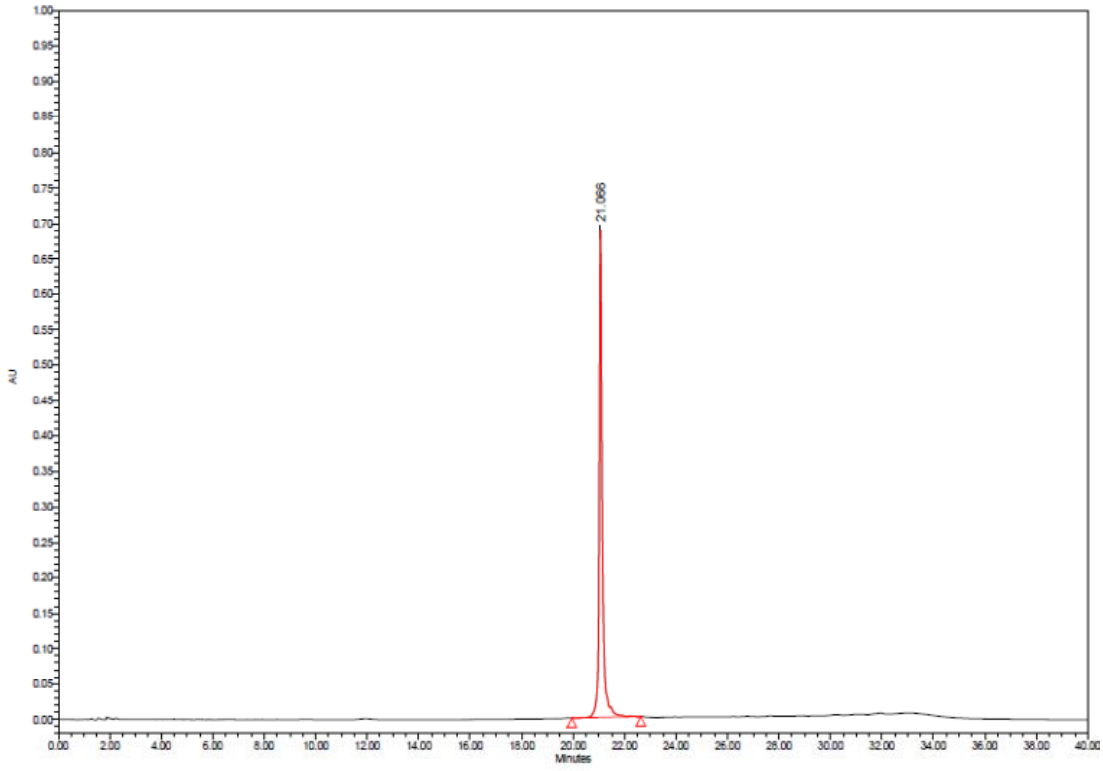

Figure A28. HPLC chromatogram of Ac-AATAU^{Py}AAAA-LysNH$_2$ (**T^{7}AU^{Py}**)

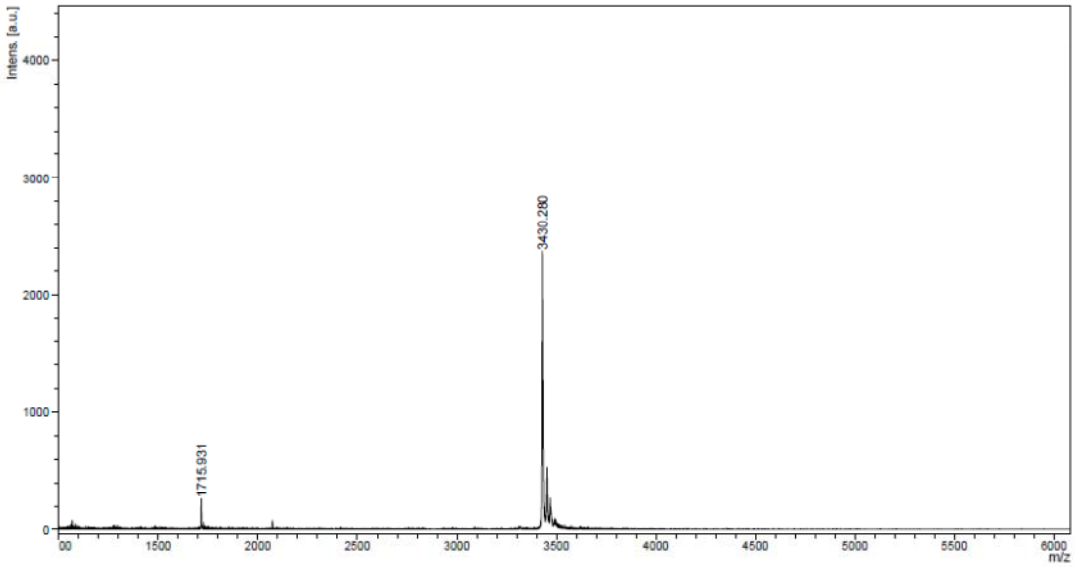

Figure A29. MALDI-TOF mass spectrum of Ac-ATAAU^{Py}AAAA-LysNH$_2$ (**T^{8}AU^{Py}**) (calcd for $[M+H]^+$: m/z=3428.74)

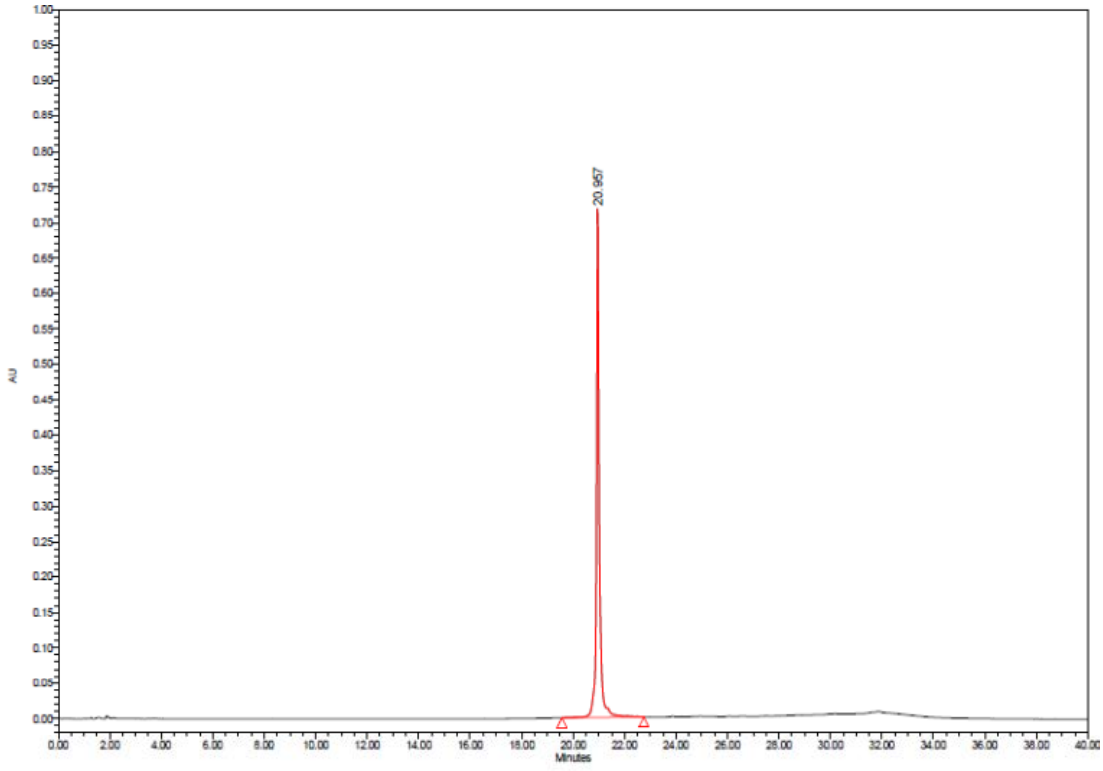

Figure A30. HPLC chromatogram of Ac-ATAAU^{Py}AAAA-LysNH$_2$ (**T^{8}AU^{Py}**)

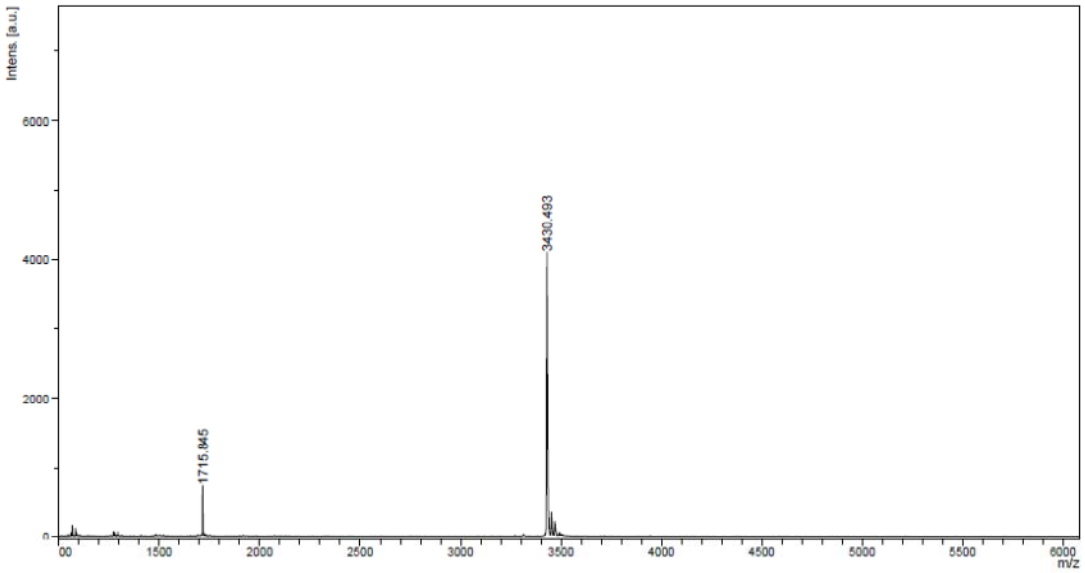

Figure A31. MALDI-TOF mass spectrum of Ac-TAAAU^{Py}AAAA-LysNH$_2$ (**T^{9}AU^{Py}**) (calcd for $[M+H]^+$: m/z=3428.74)

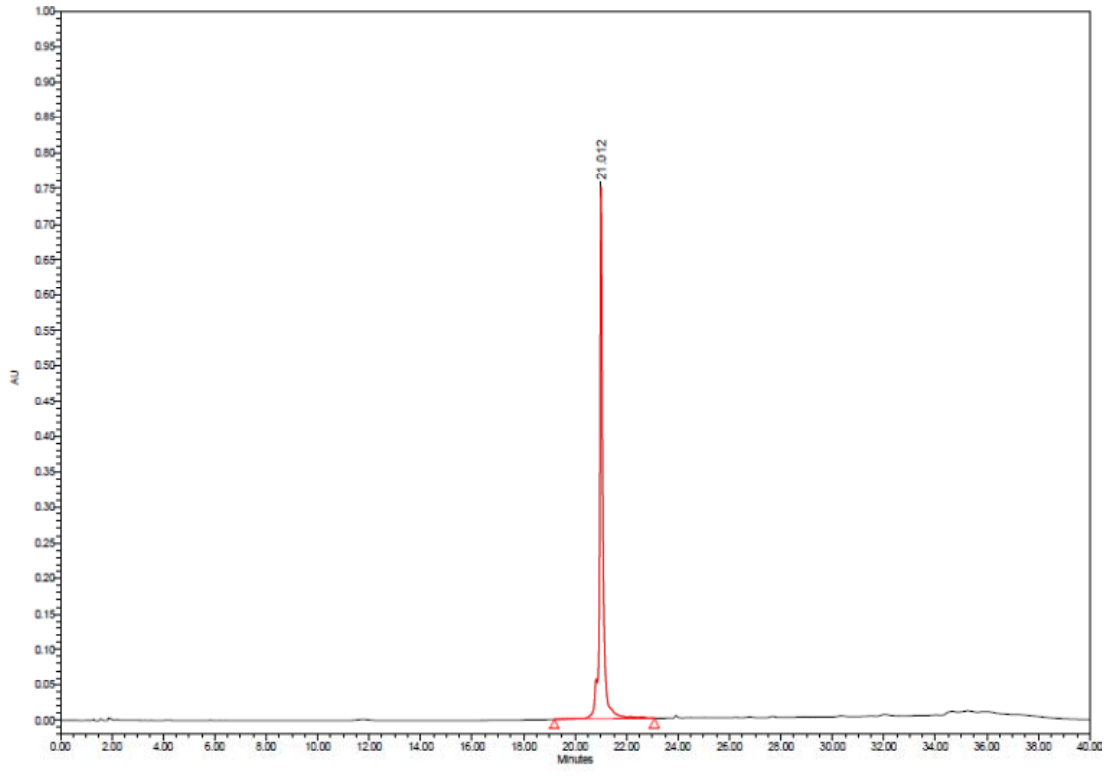

Figure A32. HPLC chromatogram of Ac-TAAAU^{Py}AAAA-LysNH$_2$ (**T^{9}AU^{Py}**)

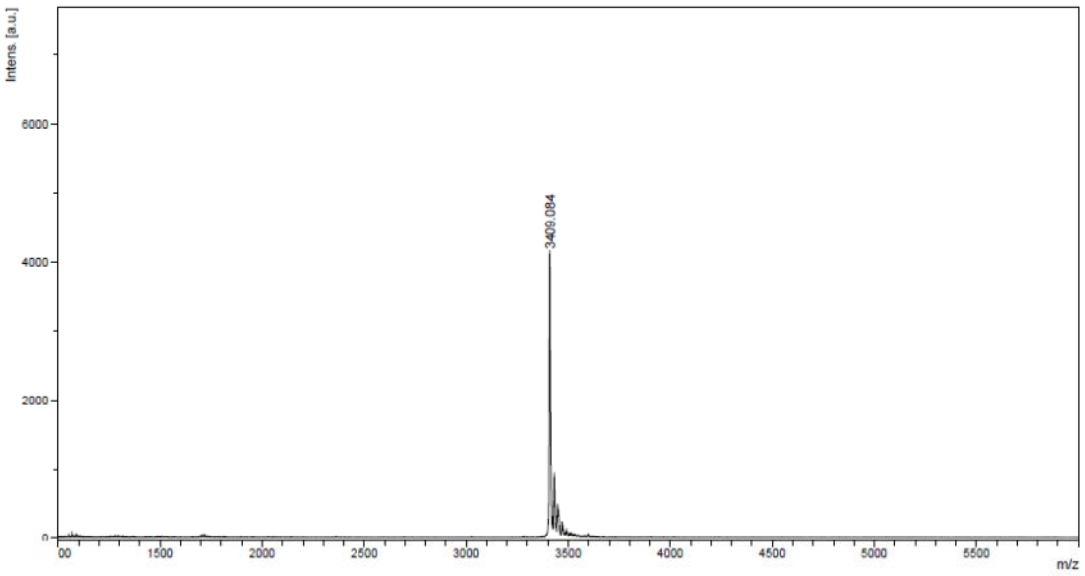

Figure A33. MALDI-TOF mass spectrum of Py-TTTTTTTTT-LysNH$_2$ (**PyT9**) (calcd for $[M+H]^+$: m/z=3407.73)

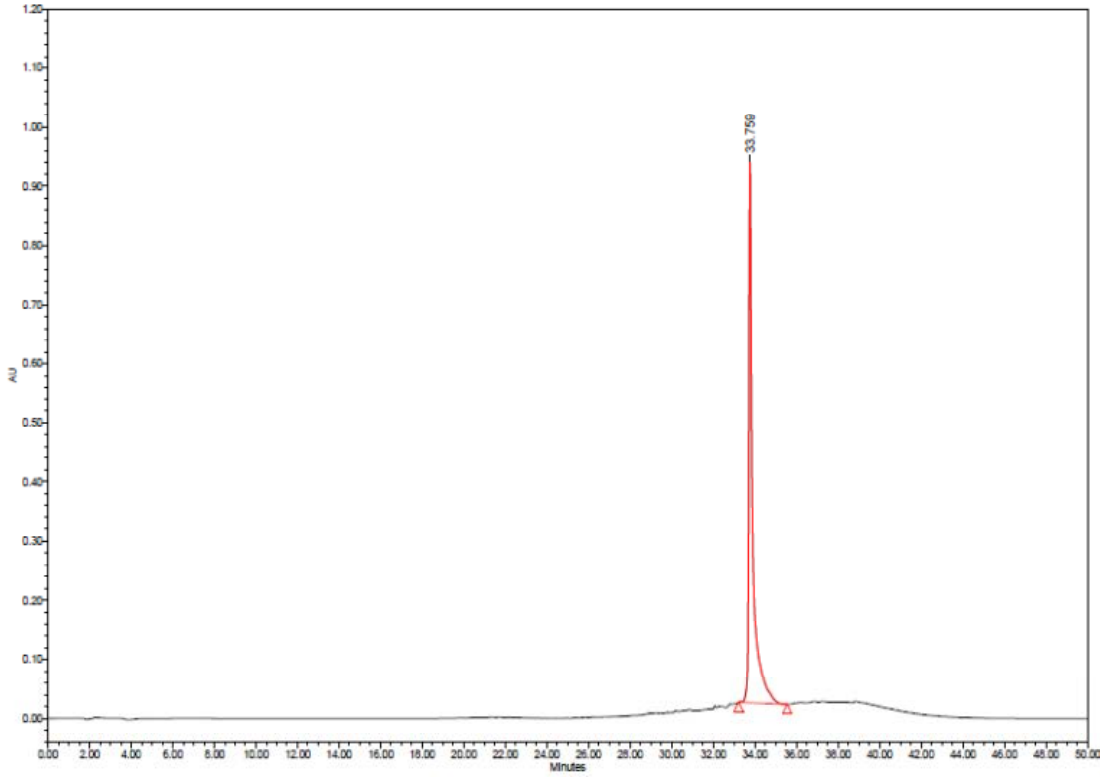

Figure A34. HPLC chromatogram of Py-TTTTTTTTT-LysNH$_2$ (**PyT9**)

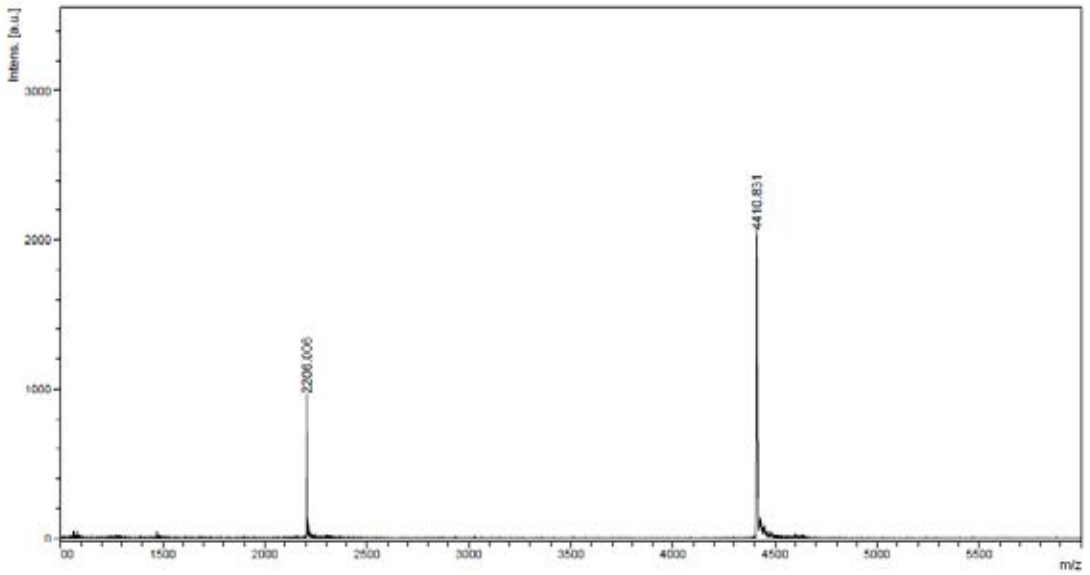

Figure A35. MALDI-TOF mass spectrum of Py-AGTTATCCCTGC-LysNH$_2$ (**PyM12**) (calcd for $[M+H]^+$: m/z=4412.80)

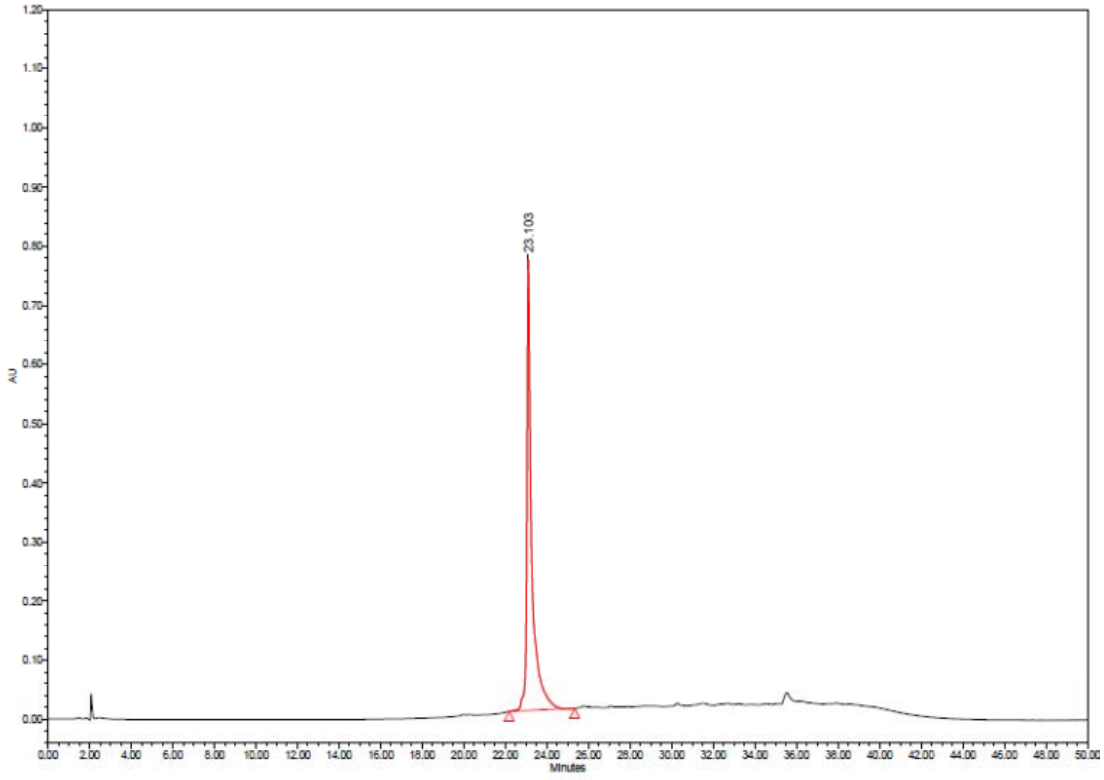

Figure A36. HPLC chromatogram of Py-AGTTATCCCTGC-LysNH$_2$ (**PyM12**)

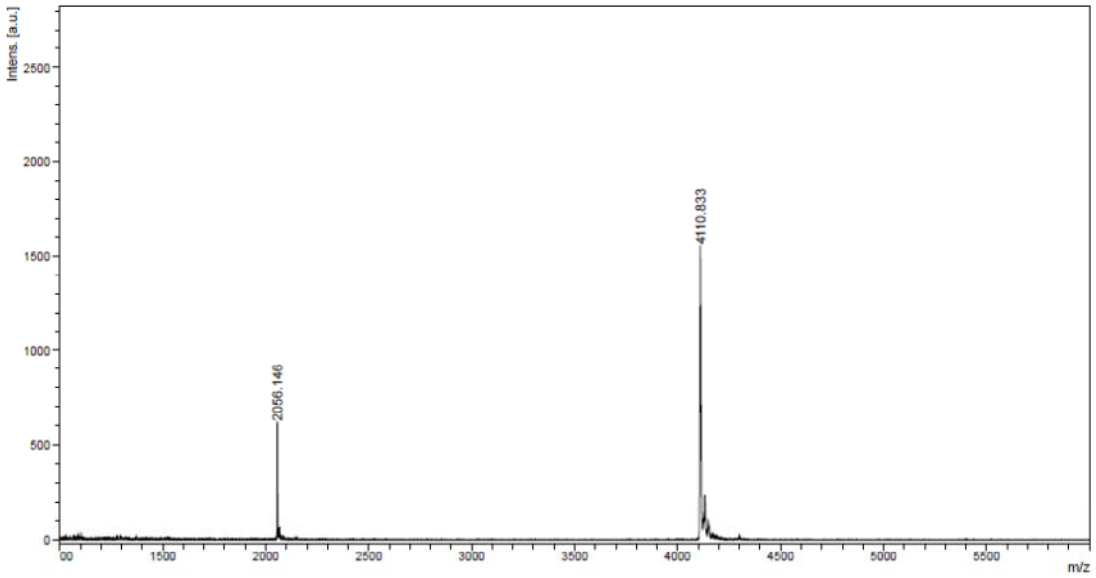

Figure A37. MALDI-TOF mass spectrum of Py-CTAAATTCAGA-LysNH_2 (**PyM11**) (calcd for $[M+H]^+$: m/z=4112.49)

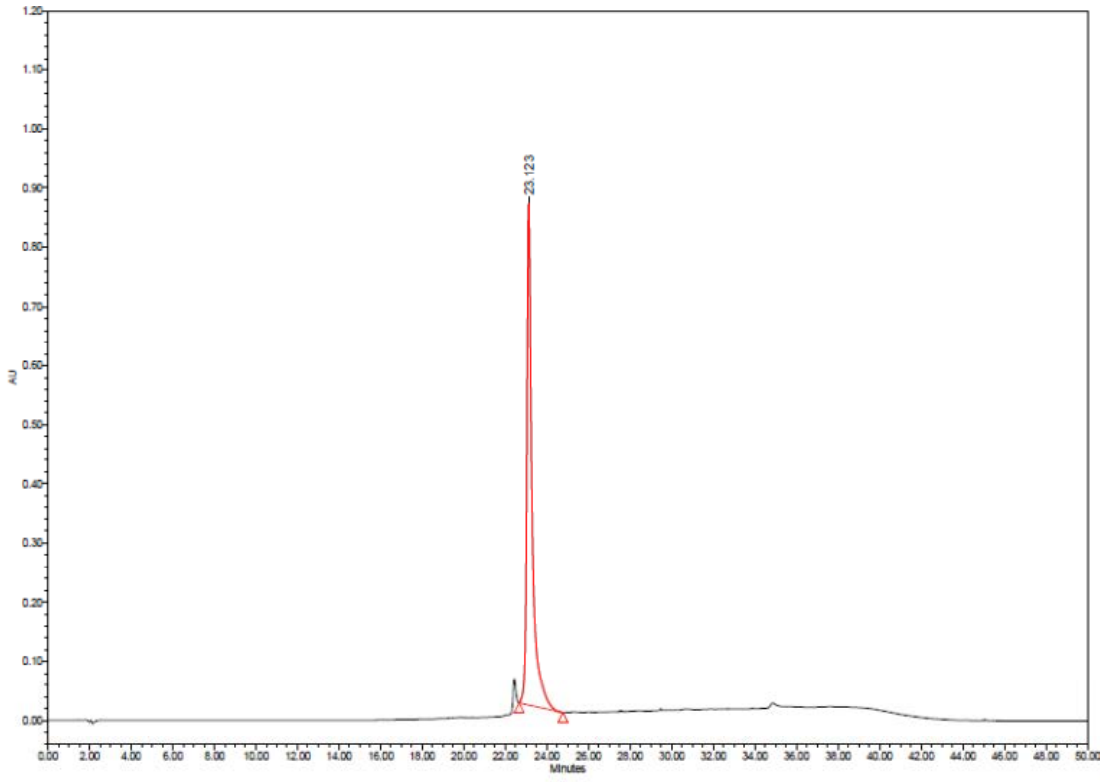

Figure A38. HPLC chromatogram of Py-CTAAATTCAGA-LysNH_2 (**PyM11**)

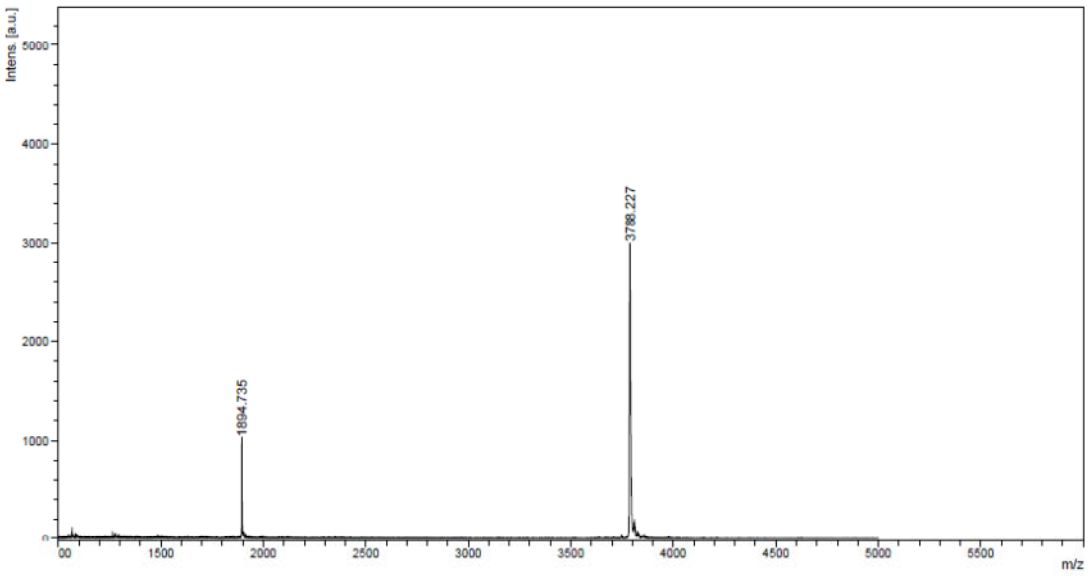

Figure A39. MALDI-TOF mass spectrum of Py-GTAGATCACT-LysNH$_2$ (**PyM10**) (calcd for $[M+H]^+$: m/z=3787.13)

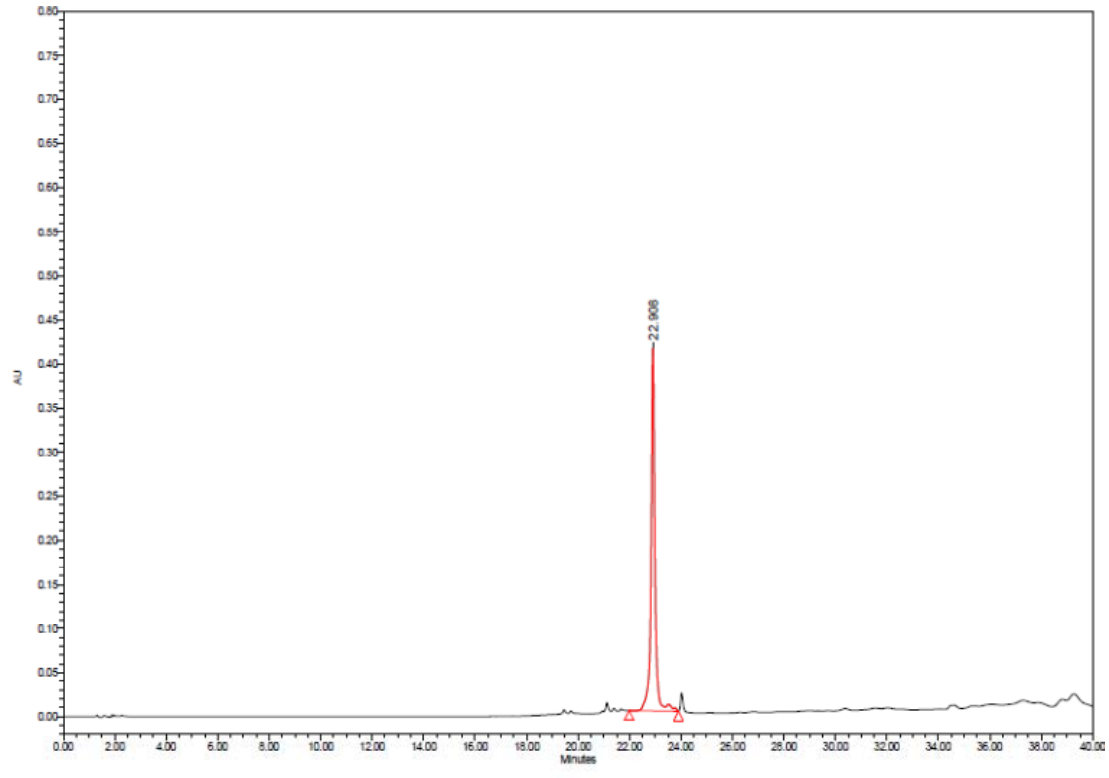

Figure A40. HPLC chromatogram of Py-GTAGATCACT-LysNH$_2$ (**PyM10**)

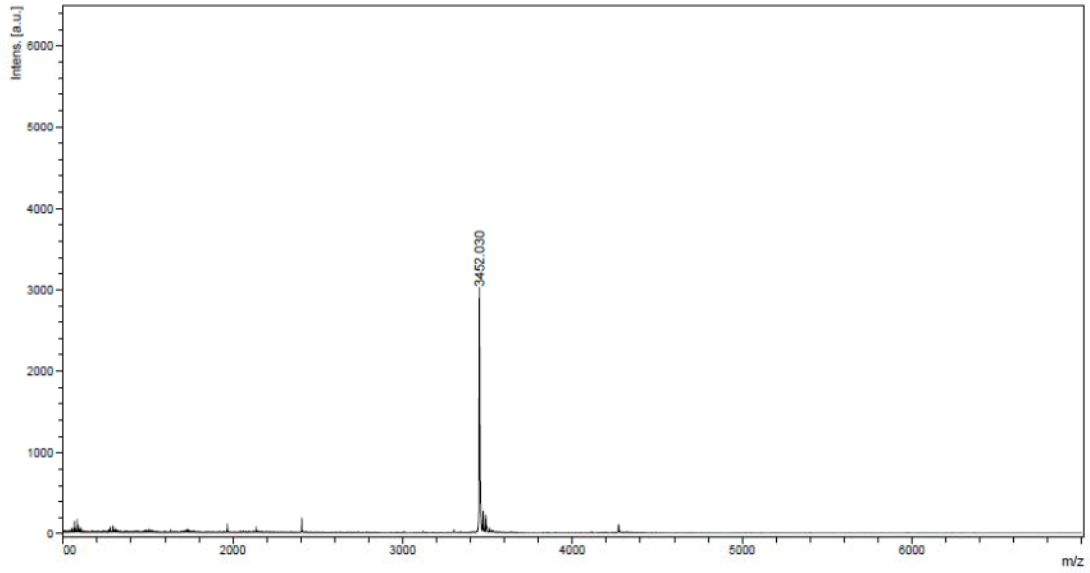

Figure A41. MALDI-TOF mass spectrum of Ac-TTTT$^{(Py)}$TTTTT-LysNH$_2$ (**T9^{Py}**) (calcd for $[M+H]^+$: m/z=3450.75)

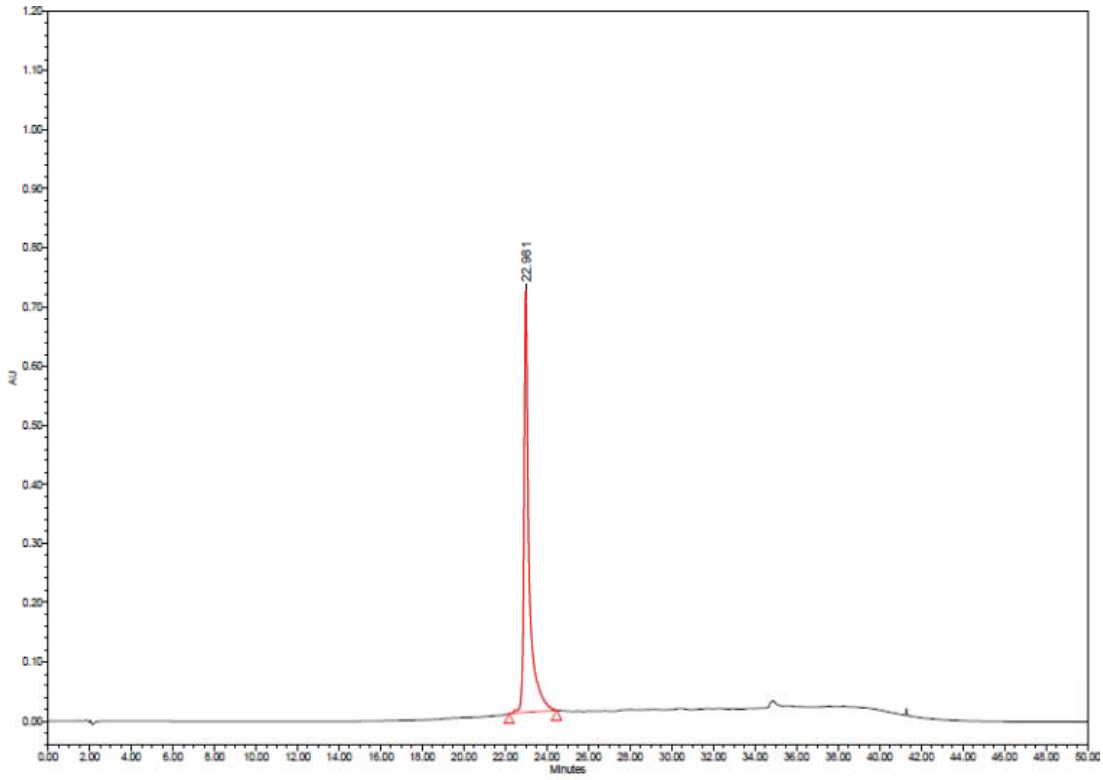

Figure A42. HPLC chromatogram of Ac-Lys-TTTT$^{(Py)}$TTTTT-LysNH$_2$ (**T9^{Py}**)

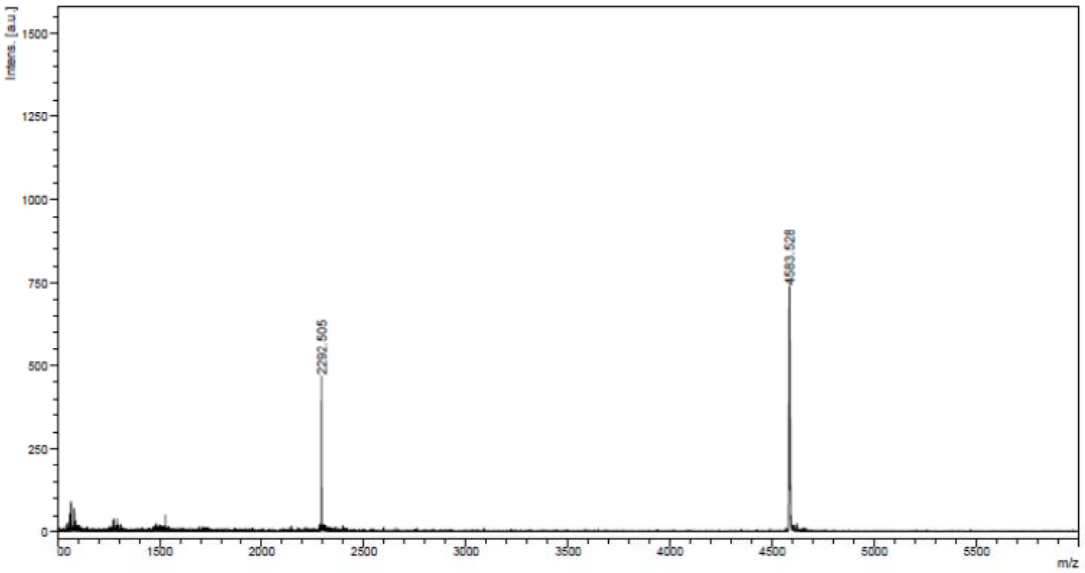

Figure A43. MALDI-TOF mass spectrum of Ac-Lys-AGTTA$^{(Py)}$TCCCTGC-LysNH$_2$ (**M12^{Py}T**) (calcd for $[M+H]^+$: m/z=4583.99)

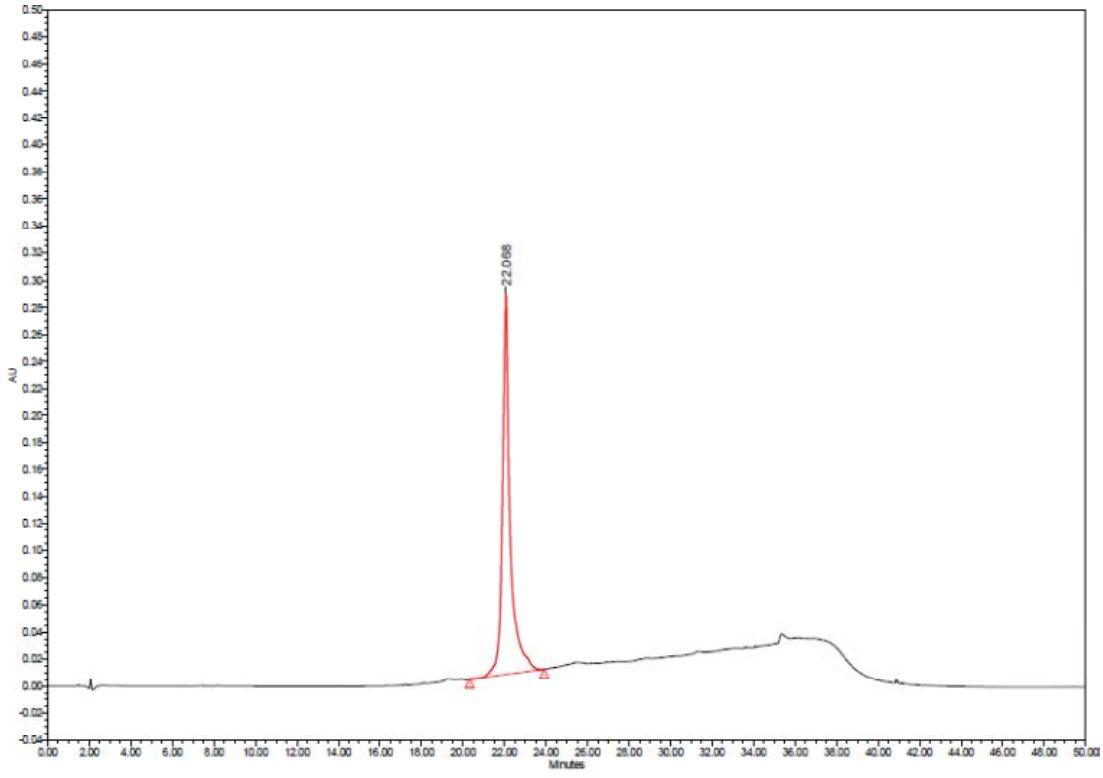

Figure A44. HPLC chromatogram of Ac-Lys-AGTTA$^{(Py)}$TCCCTGC-LysNH$_2$ (**M12^{Py}T**)

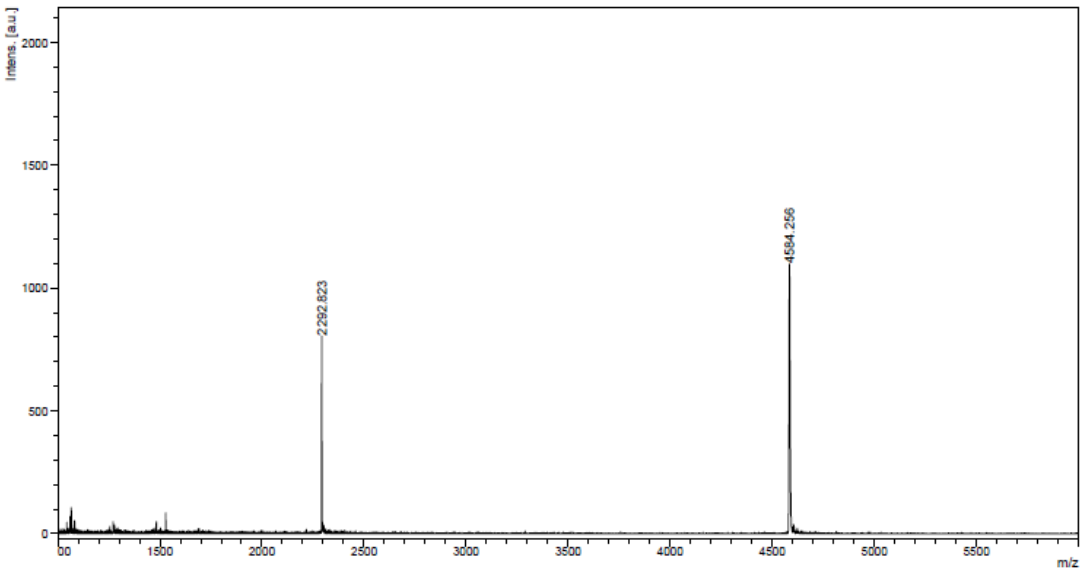

Figure A45. MALDI-TOF mass spectrum of Ac-Lys-AGTTAT$^{(Py)}$CCCTGC-LysNH$_2$ (**M12^{Py}C**) (calcd for $[M+H]^+$: m/z=4583.99)

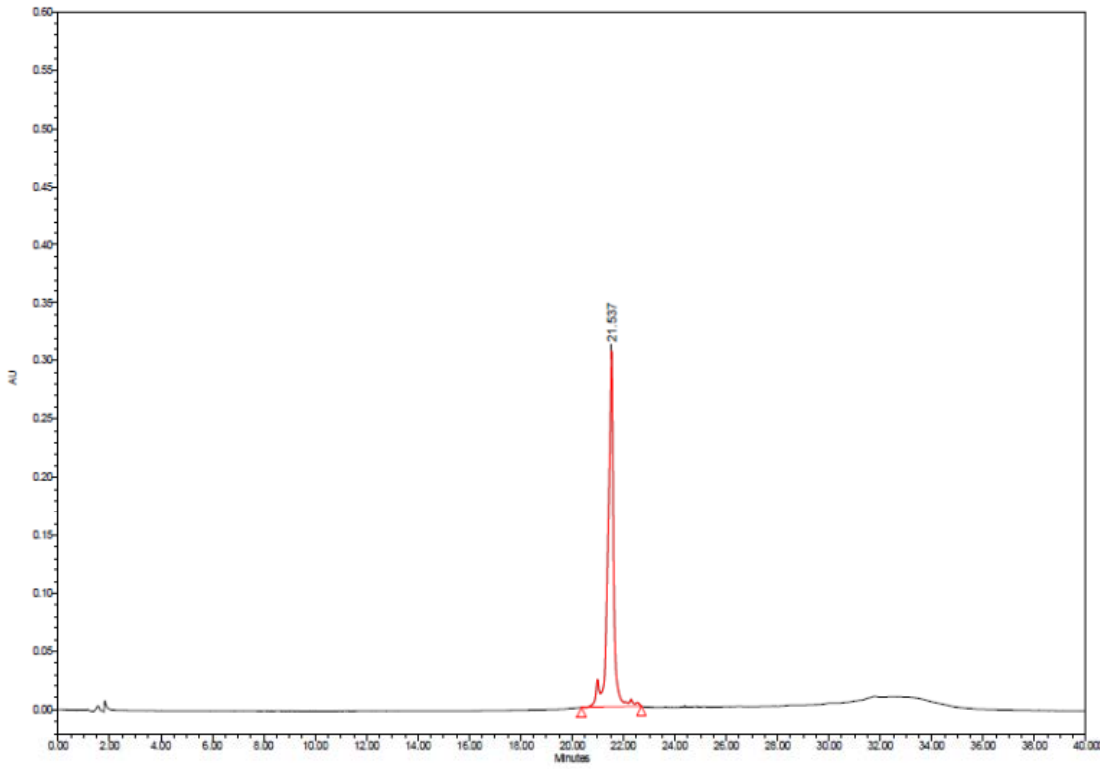

Figure A46. HPLC chromatogram of Ac-Lys-AGTTAT$^{(Py)}$CCCTGC-LysNH$_2$ (**M12^{Py}C**)

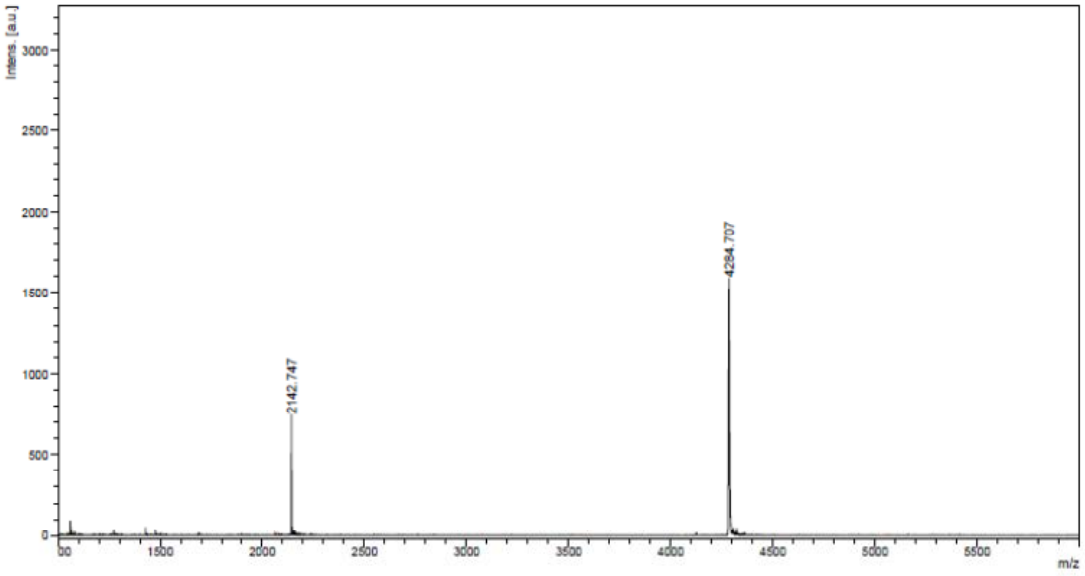

Figure A47. MALDI-TOF mass spectrum of Ac-Lys-CTAA$^{(Py)}$ATTCAGA-LysNH$_2$ (**M11^{Py}A**) (calcd for $[M+H]^+$: m/z=4283.69)

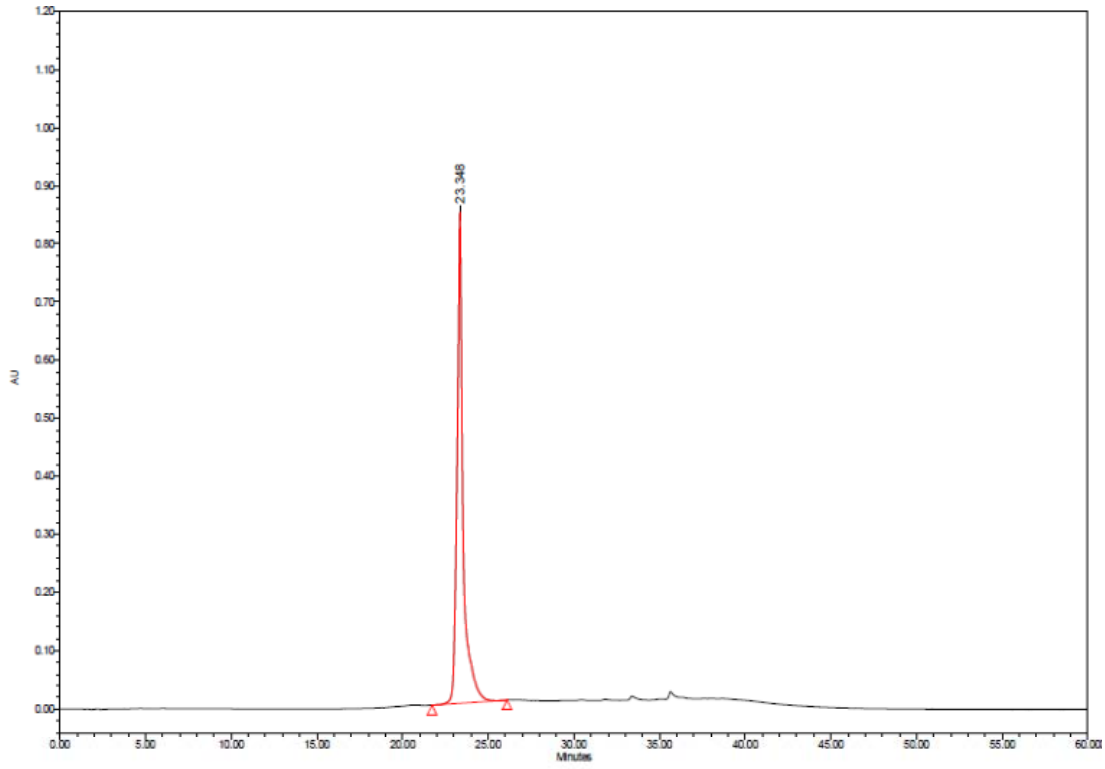

Figure A48. HPLC chromatogram of Ac-Lys-CTAA$^{(Py)}$ATTCAGA-LysNH$_2$ (**M11^{Py}A**)

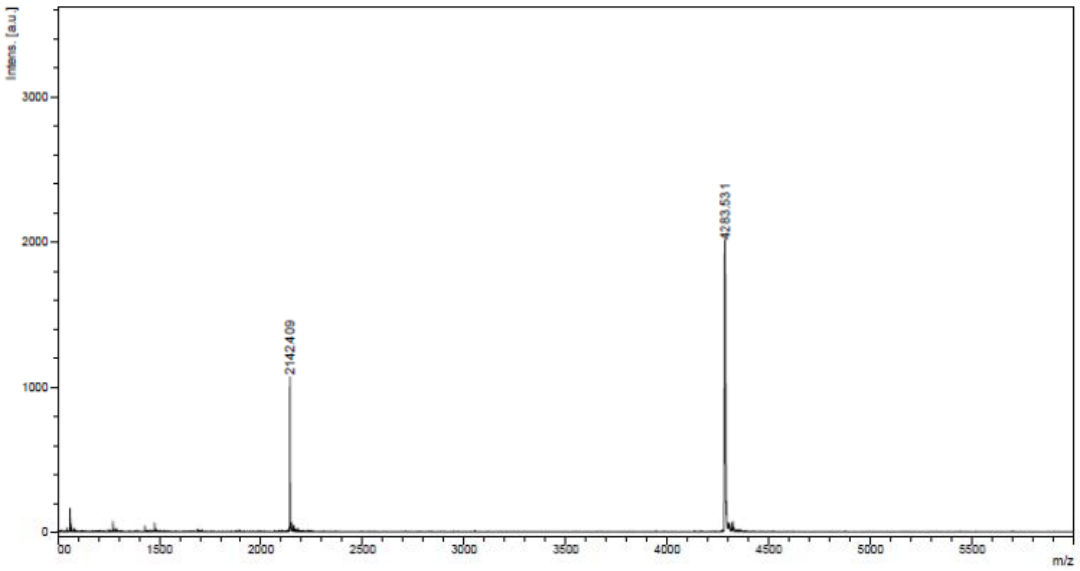

Figure A49. MALDI-TOF mass spectrum of Ac-Lys-CTAAAT$^{(Py)}$TCAGA-LysNH$_2$ (**M11^{Py}T**) (calcd for $[M+H]^+$: m/z=4283.69)

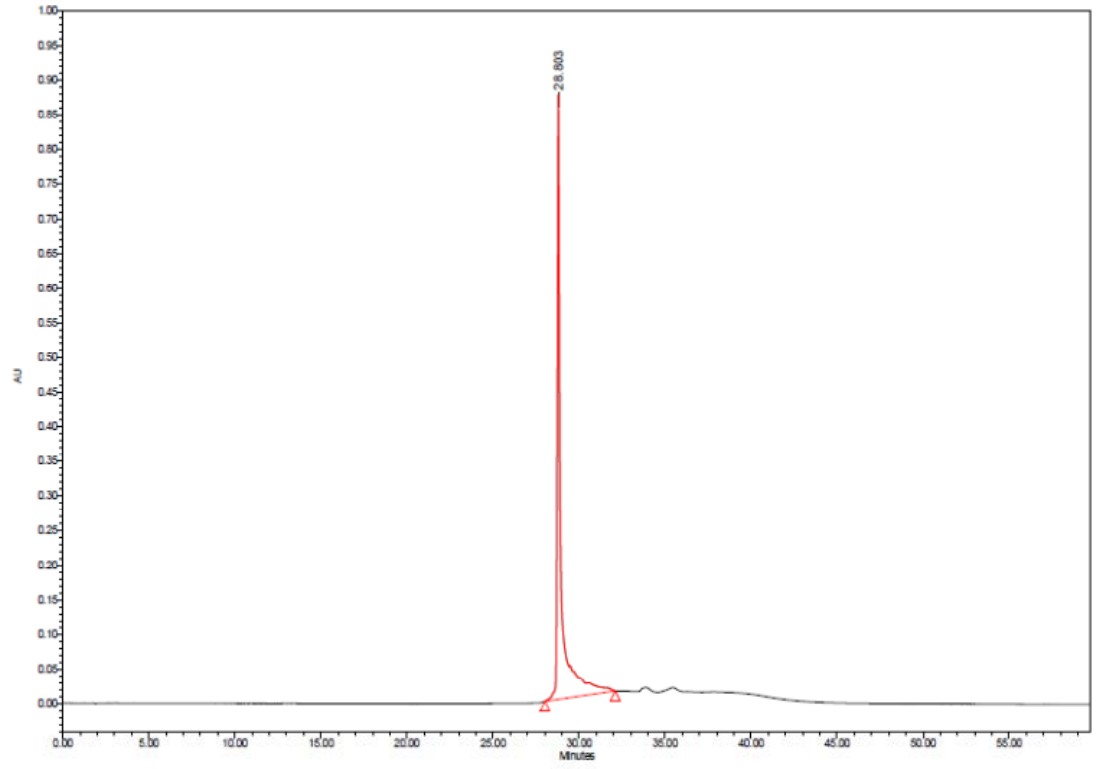

Figure A50. HPLC chromatogram of Ac-Lys-CTAAAT$^{(Py)}$TCAGA-LysNH$_2$ (**M11^{Py}T**)

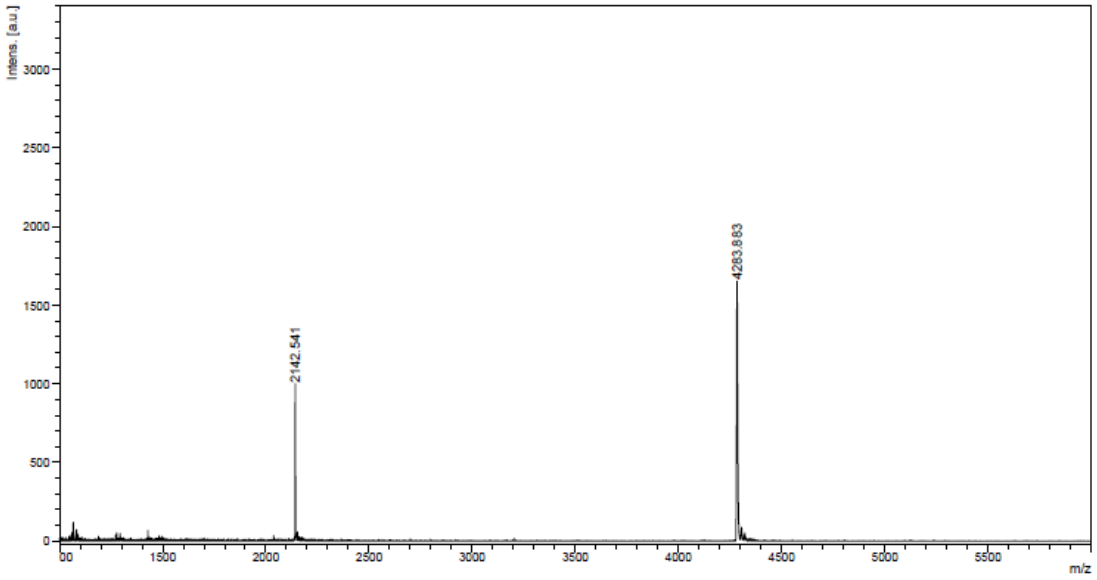

Figure A51. MALDI-TOF mass spectrum of Ac-Lys-CTAAATT$^{(Py)}$CAGA-LysNH$_2$ (**M11^{Py}C**) (calcd for $[M+H]^+$: m/z=4283.69)

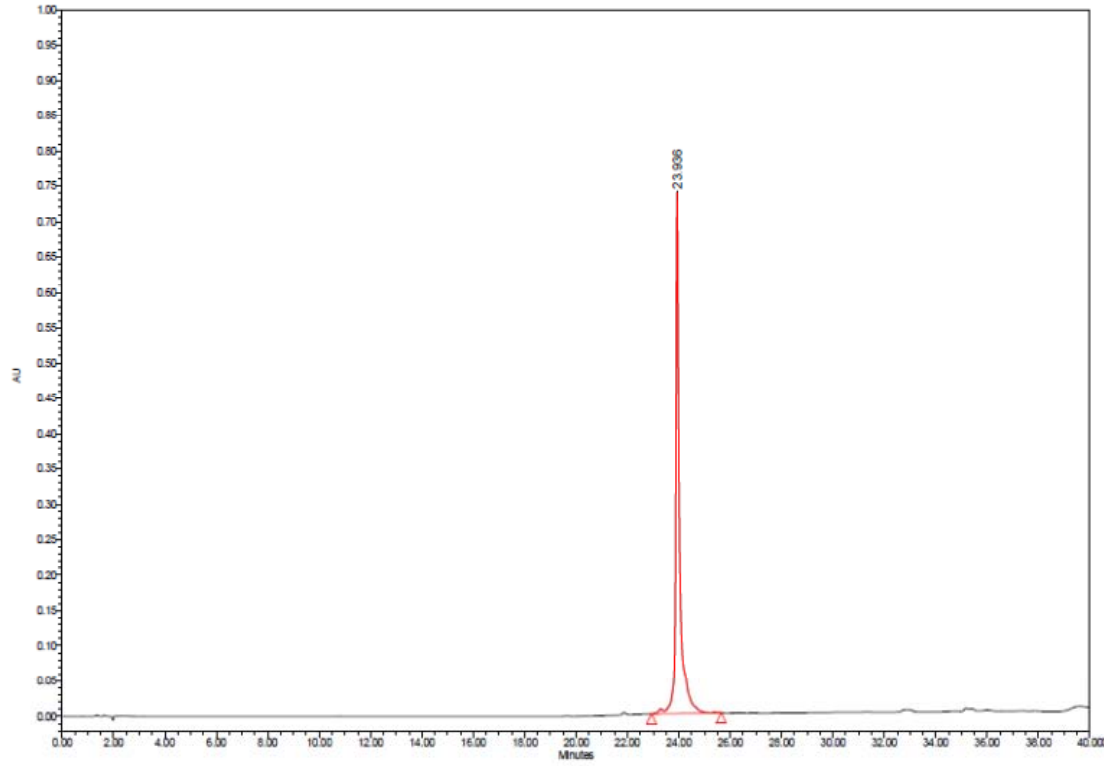

Figure A52. HPLC chromatogram of Ac-Lys-CTAAATT$^{(Py)}$CAGA-LysNH$_2$ (**M11^{Py}C**)

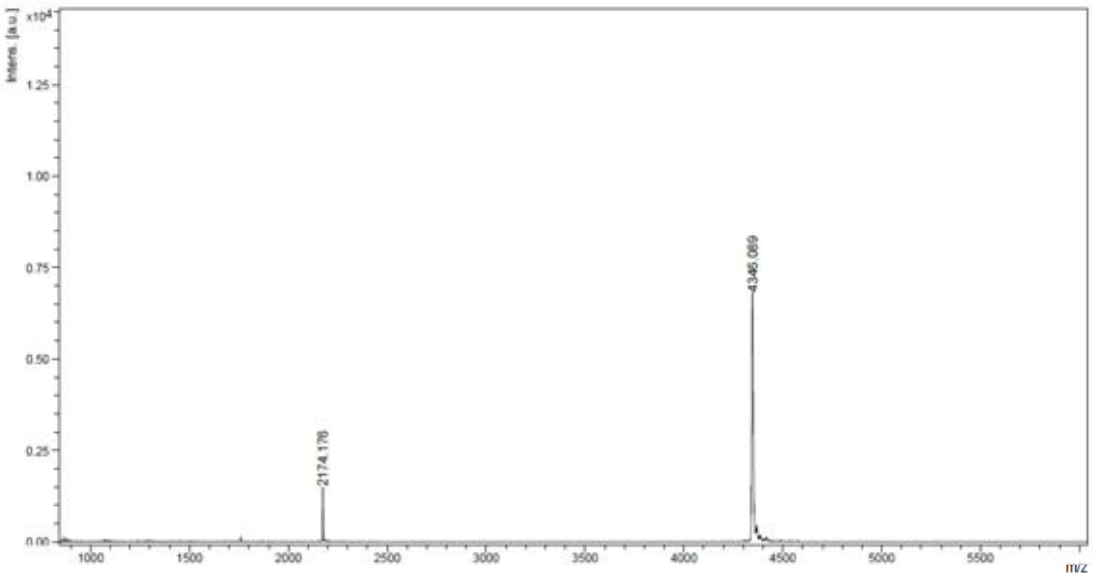

Figure A53. MALDI-TOF mass spectrum of Flu-O-CTAAATTCAGA-LysNH_2 (**Flu1**) (calcd for $[M+H]^+$: m/z=4345.63)

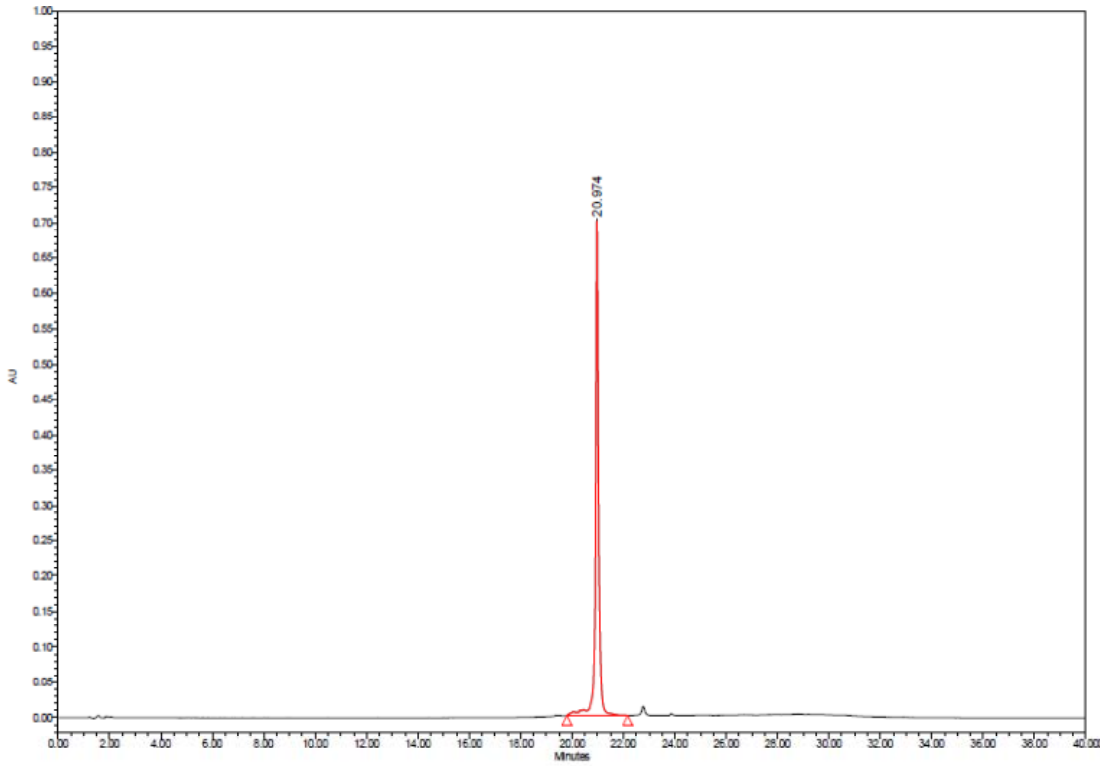

Figure A54. HPLC chromatogram Flu-O-CTAAATTCAGA-LysNH_2 (**Flu1**)

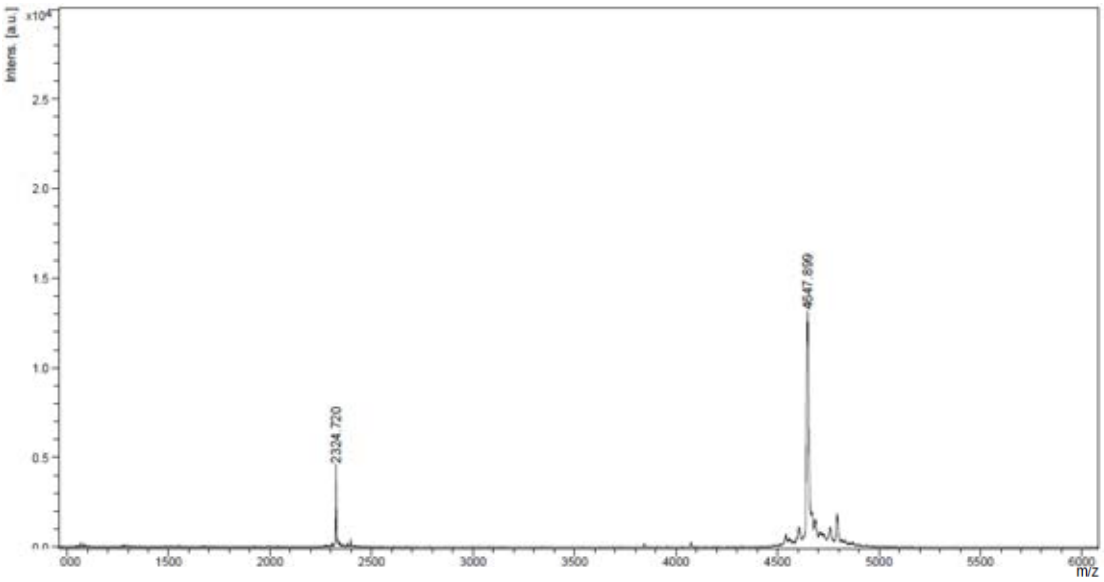

Figure A55. MALDI-TOF mass spectrum of Flu-O-AGTTATCCCTGA-LysNH_2 (**Flu2**) (calcd for $[M+H]^+$: m/z=4645.93)

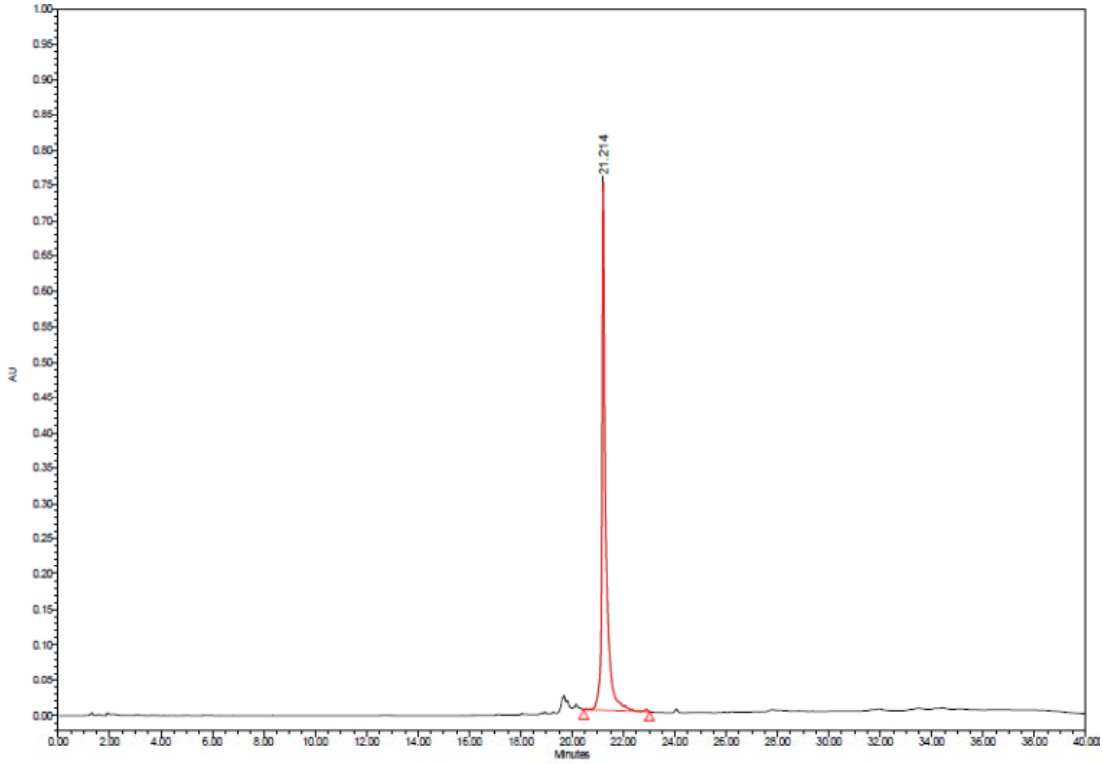

Figure A56. HPLC chromatogram of Flu-O-AGTTATCCCTGA-LysNH_2 (**Flu2**)

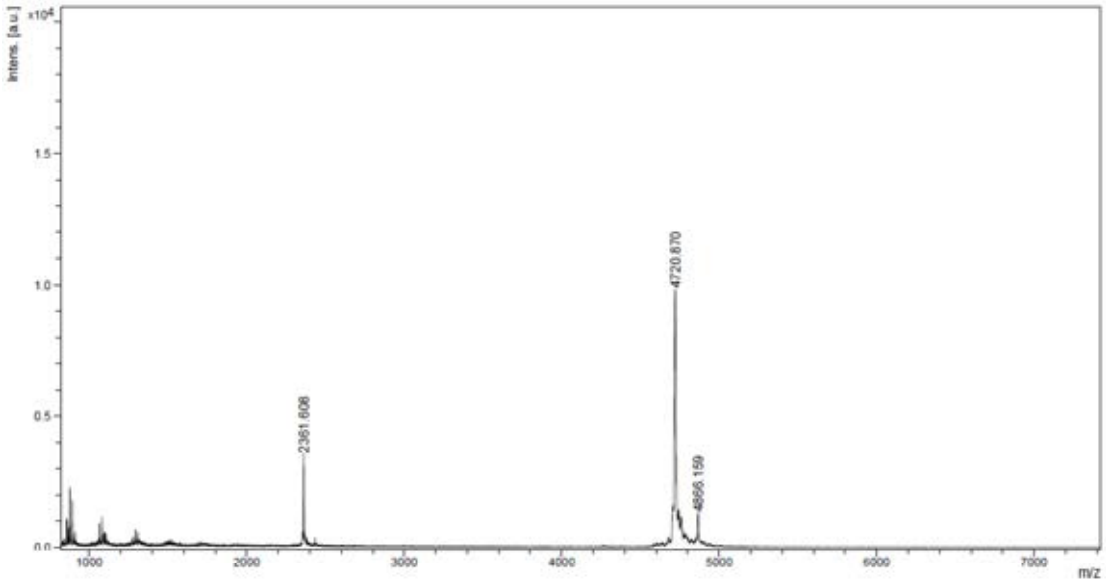

Figure A57. MALDI-TOF mass spectrum of TMR-O-TTATCACTATGA-LysNH_2 (**TMR1**) (calcd for $[M+H]^+$: m/z=4724.11)

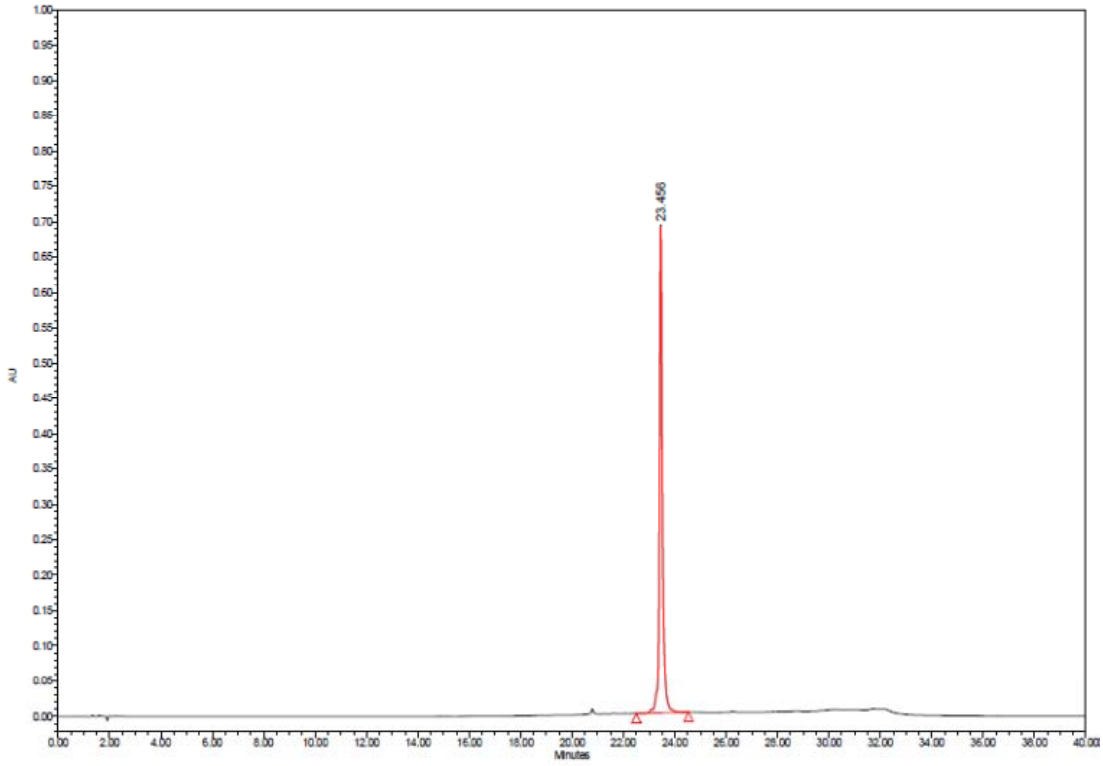

Figure A58. HPLC chromatogram of TMR-O-TTATCACTATGA-LysNH_2 (**TMR1**)

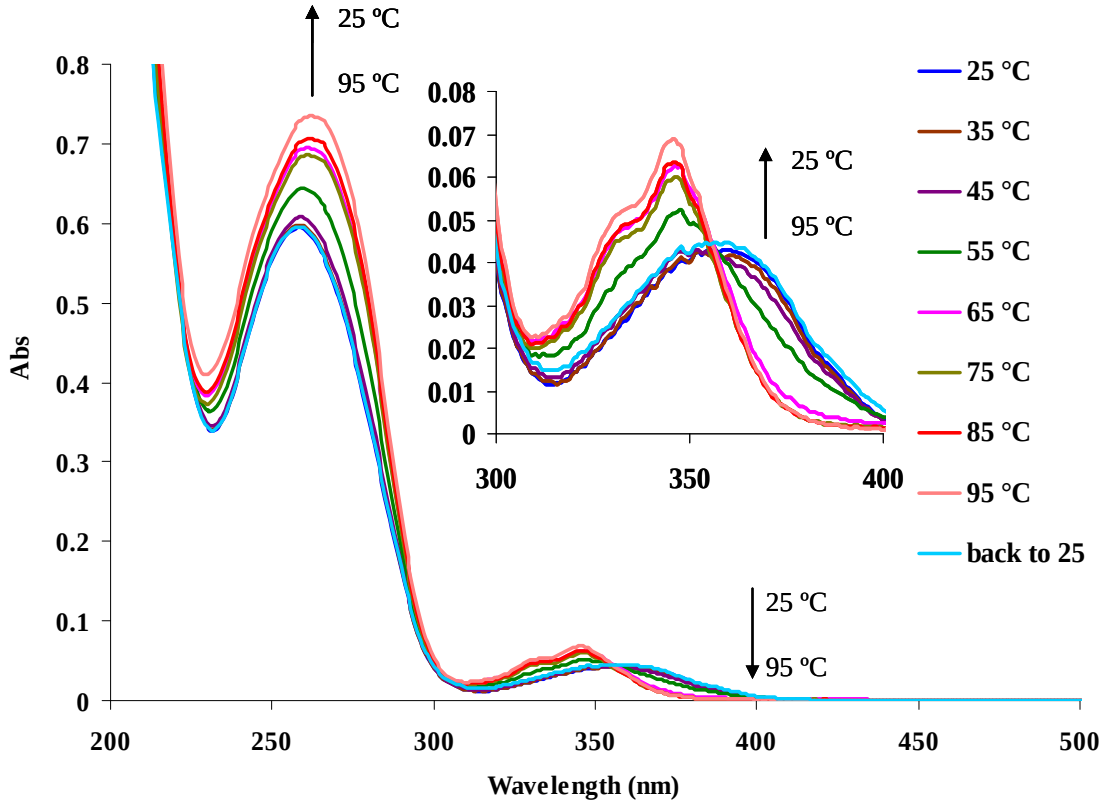

Figure A59 UV/Vis spectra of **MixU^{Py}+dmTMix** in 10 mm sodium phosphate buffer pH 7.0, [PNA] = 2.5 μM and [DNA] = 3.0 μM, from 25 to 95 ºC and back to 25 ºC, temperature step=10 ºC.

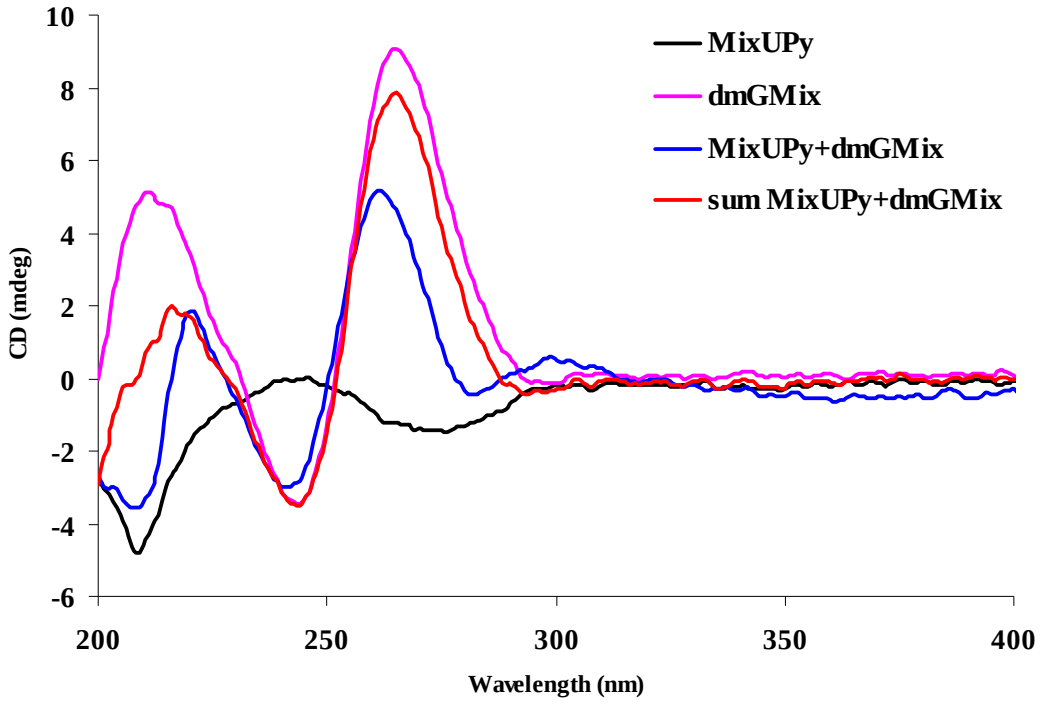

Figure A60 CD spectra of **MixU^{Py}** with **dmGMix** in 10 mm sodium phosphate buffer pH 7.0, [PNA] = 2.5 μM and [DNA] = 3.0 μM.

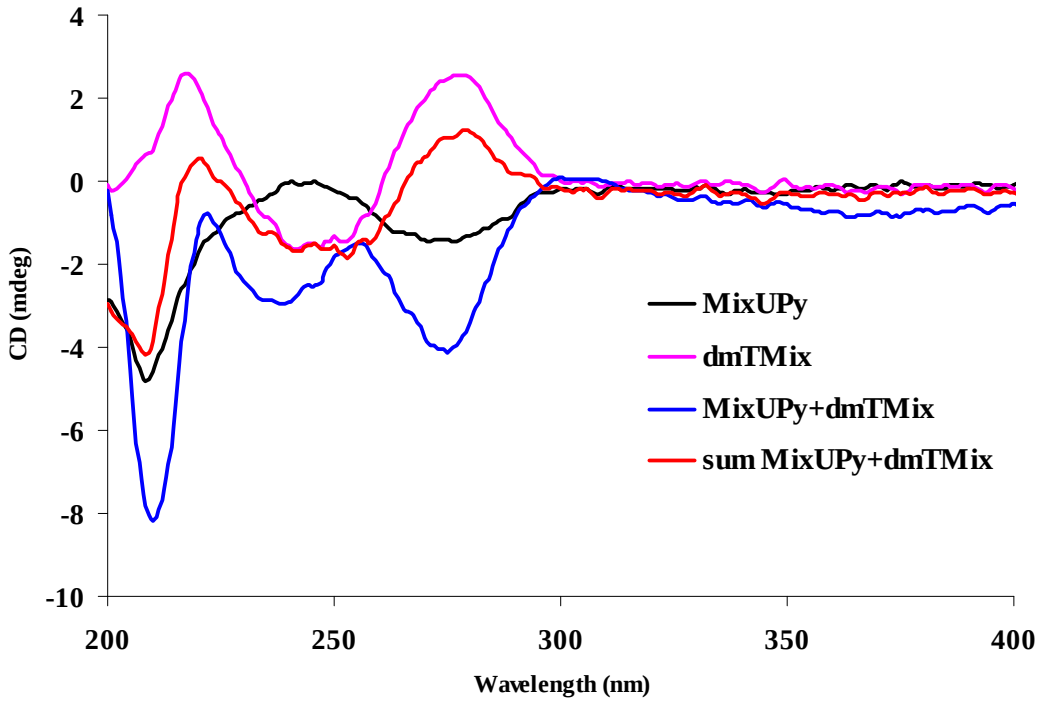

Figure A61 CD spectra of **MixU^{Py}** with **dmTMix** in 10 mm sodium phosphate buffer pH 7.0, [PNA] = 2.5 μM and [DNA] = 3.0 μM.

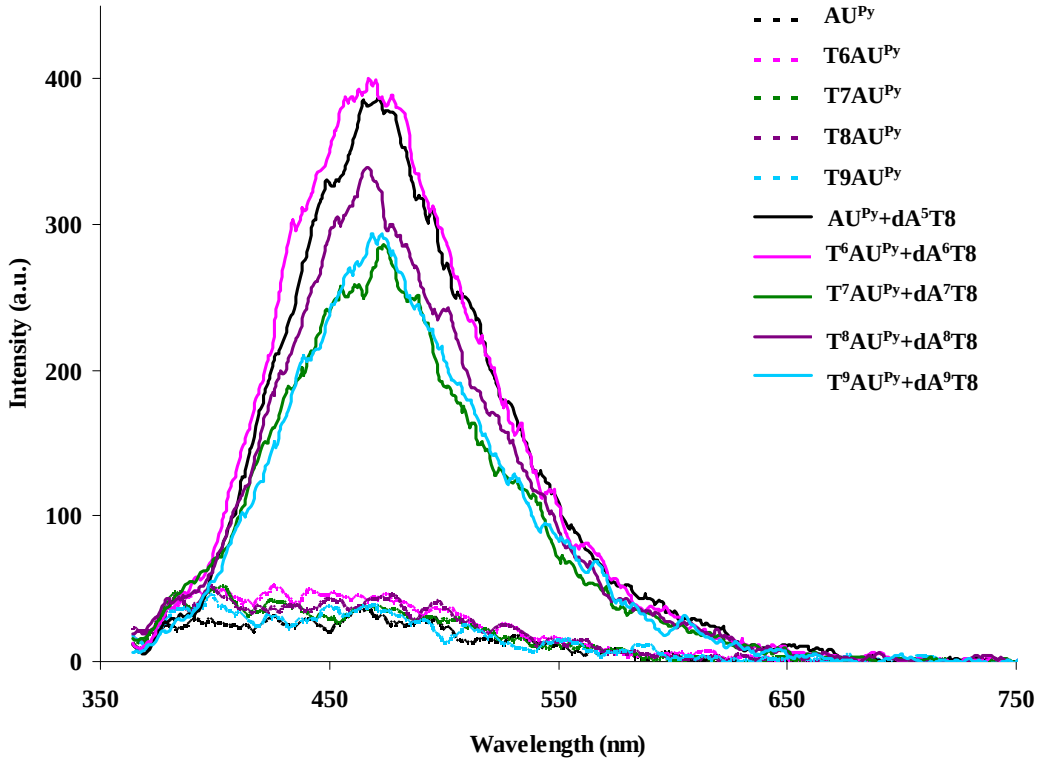

Figure A62 Fluorescence spectra of single strand **AU^{Py}–T^{9}AU^{Py}** and theirs hybrids with complementary DNA in 10 mM sodium phosphate buffer pH 7.0, [PNA] = 2.5 μM and [DNA] = 3.0 μM, excitation wavelength = 350 nm.

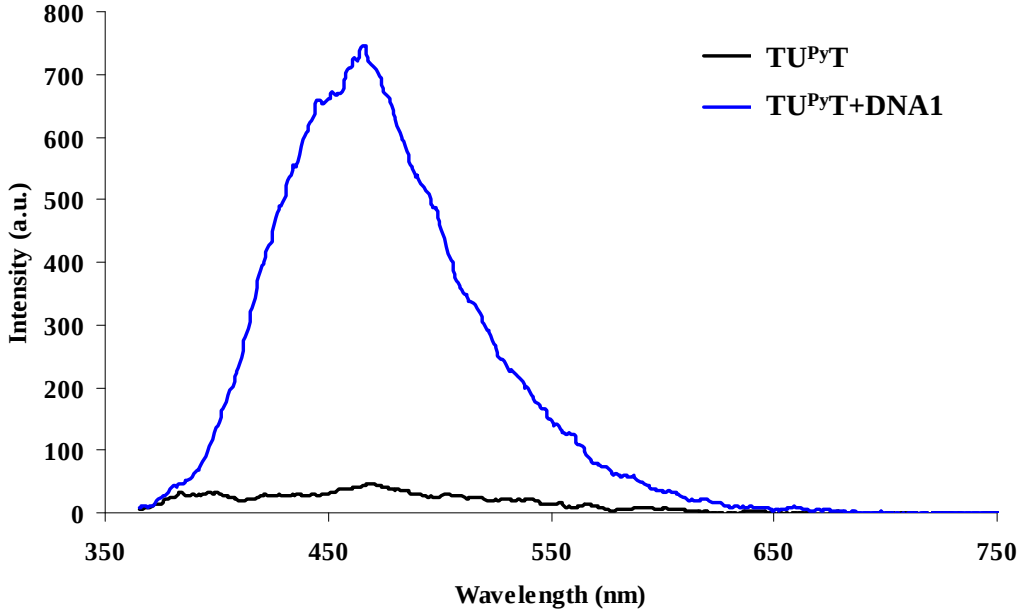

Figure A63 Fluorescence spectra of single strand **TU^{Py}T** and its hybrid with **DNA1** in 10 mM sodium phosphate buffer pH 7.0, 100 mM NaCl, [PNA] = 2.5 μM and [DNA] = 3.0 μM, excitation wavelength = 350 nm

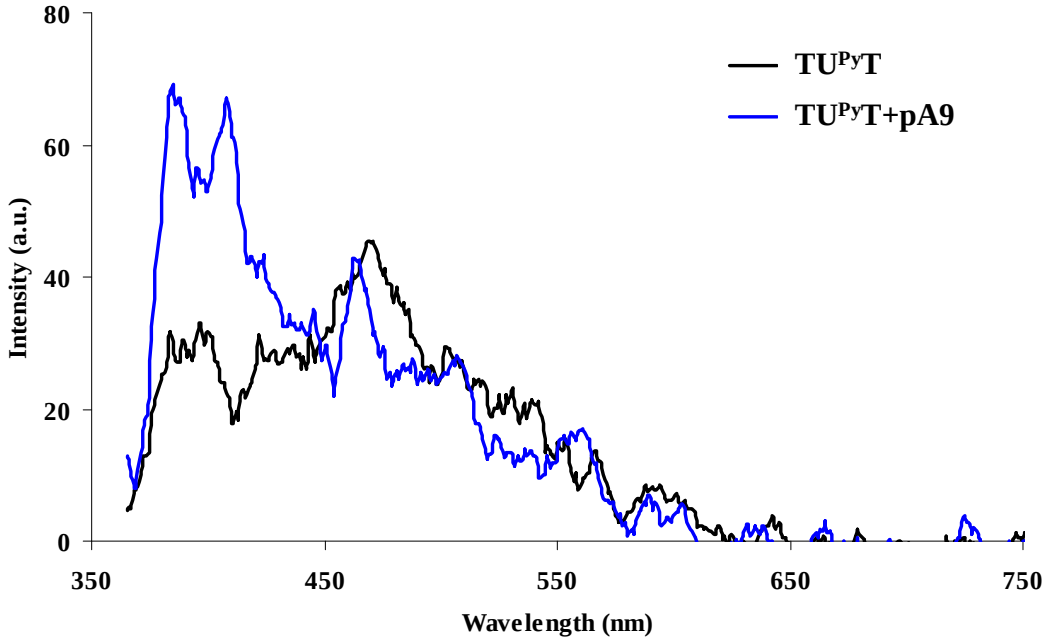

Figure A64 Fluorescence spectra of single strand **TU^{Py}T** and its hybrid with **DpA9** in 10 mM sodium phosphate buffer pH 7.0, 100 mM NaCl, [PNA] = 2.5 μM and [DNA] = 3.0 μM, excitation wavelength = 350 nm

TU^{Py}T **DNA1+DNA2** **DNA1+DNA2+ TU^{Py}T**

Figure A65 Photographs of **TU^{Py}T**, **DNA1+DNA2** and **DNA1+DNA2+ TU^{Py}T** in 10 mM sodium phosphate buffer pH 7.0, [PNA] = 2.5 μM and [DNA] = 3.0 μM under black light (365 nm).

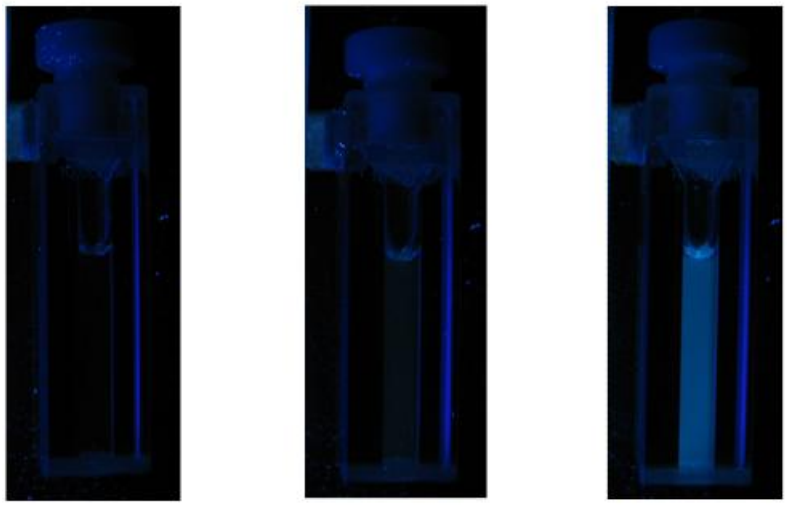

DNA3+DNA4 **DNA3+DNA4+ TU^{Py}T** **DNA3+DNA4 +TU^{Py}T+pA9**

Figure A66 Photographs of **TU^{Py}T**, **DNA1**+**DNA2** and **DNA1**+**DNA2**+ **TU^{Py}T** in 10 mM sodium phosphate buffer pH 7.0, [PNA] = 2.5 μM and [DNA] = 3.0 μM under black light (365 nm).

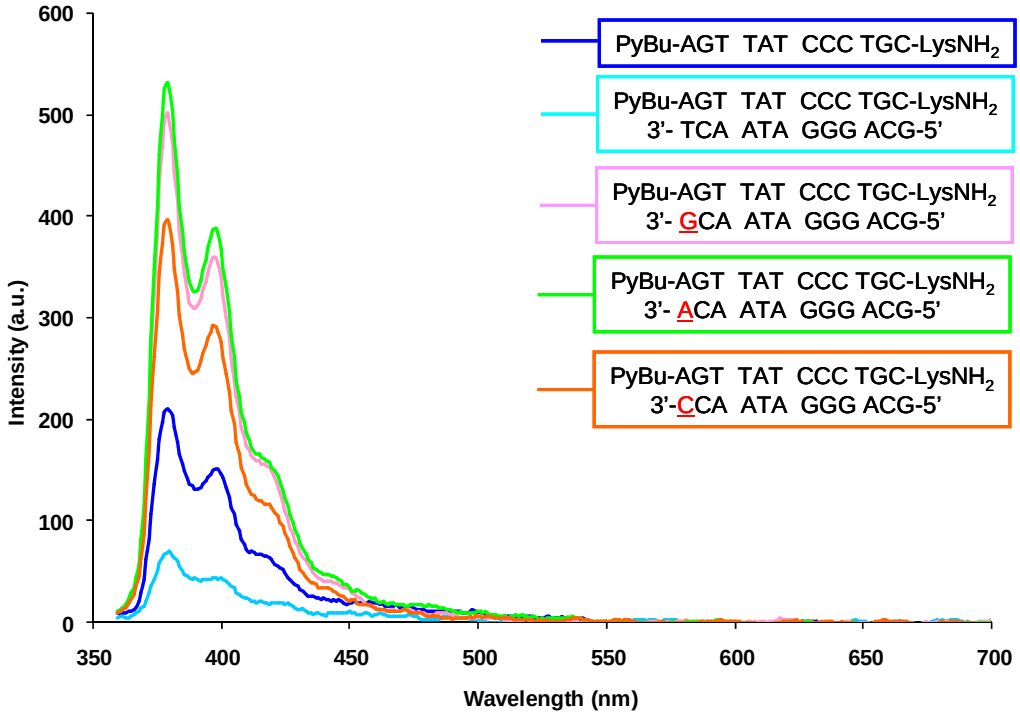

Figure A67 Fluorescence spectra of single strand **PyM12** and its hybrids with complementary DNA in 10 mM sodium phosphate buffer pH 7.0, [PNA] = 2.5 μM and [DNA] = 3.0 μM, excitation wavelength = 345 nm.

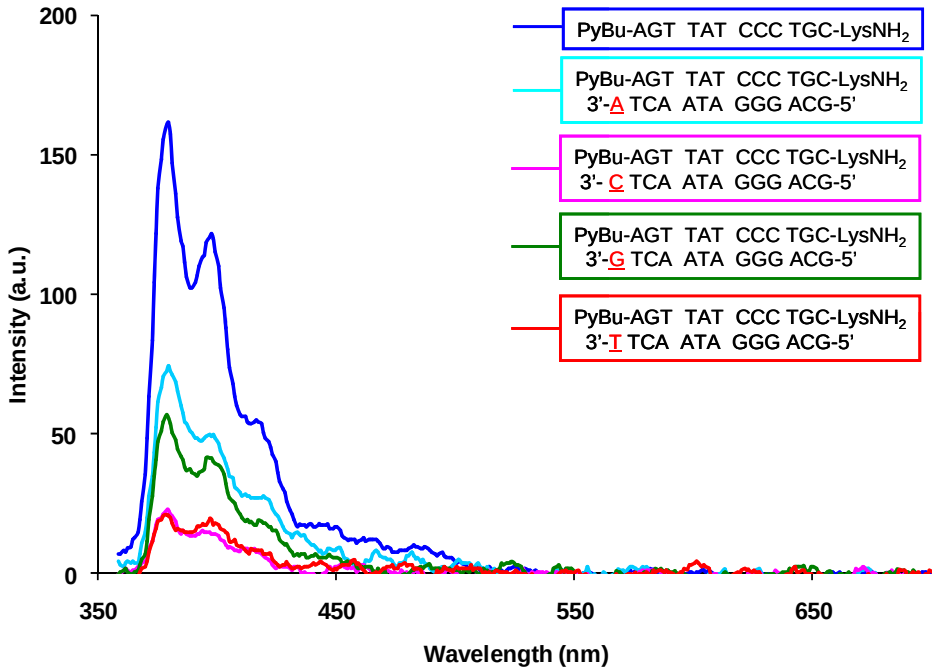

Figure A68 Fluorescence spectra of single strand **PyM12** and its hybrids with complementary DNA in 10 mM sodium phosphate buffer pH 7.0, [PNA] = 2.5 μM and [DNA] = 3.0 μM, excitation wavelength = 345 nm.

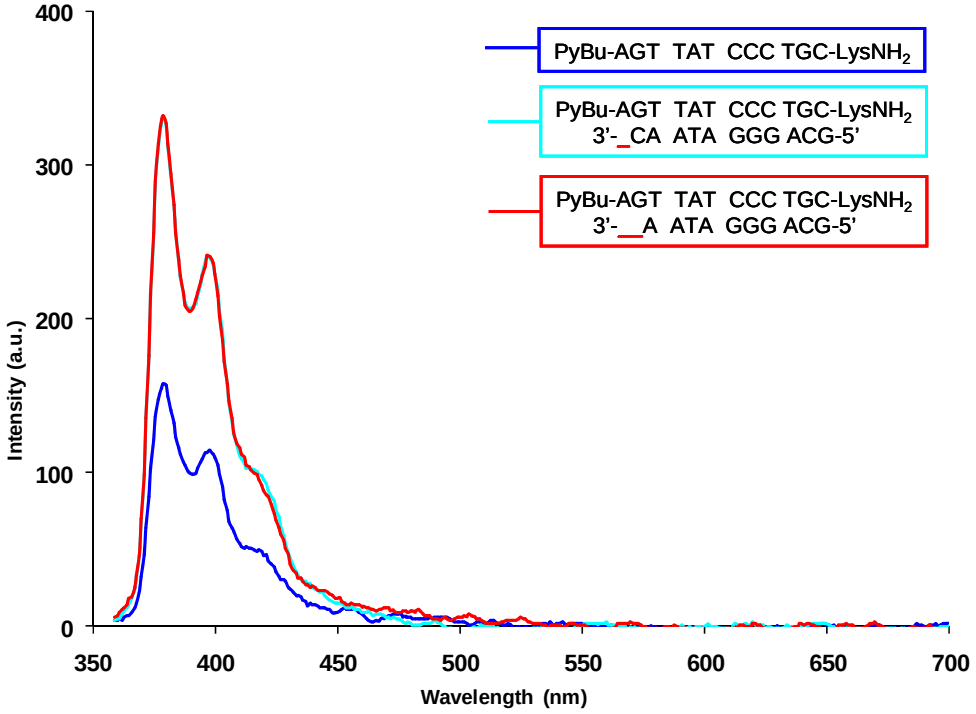

Figure A69 Fluorescence spectra of single strand **PyM12** and its hybrids with complementary DNA in 10 mM sodium phosphate buffer pH 7.0, [PNA] = 2.5 μM and [DNA] = 3.0 μM, excitation wavelength = 345 nm.

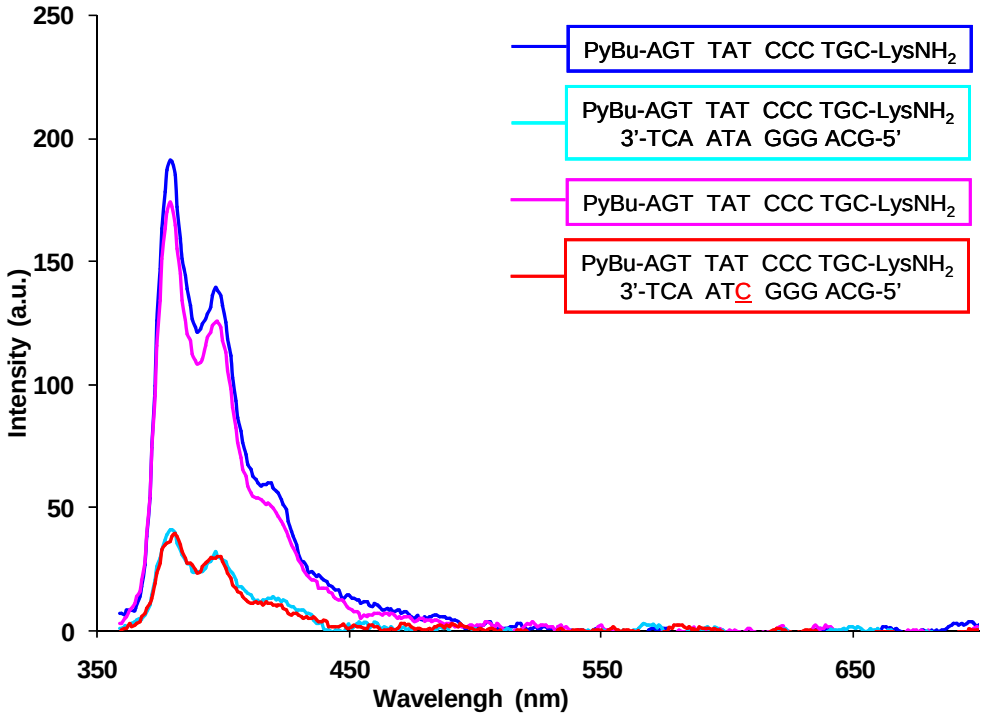

Figure A70 Fluorescence spectra of single strand **PyM12** and its hybrids with complementary DNA in 10 mM sodium phosphate buffer pH 7.0, [PNA] = 2.5 μM and [DNA] = 3.0 μM, excitation wavelength = 345 nm.

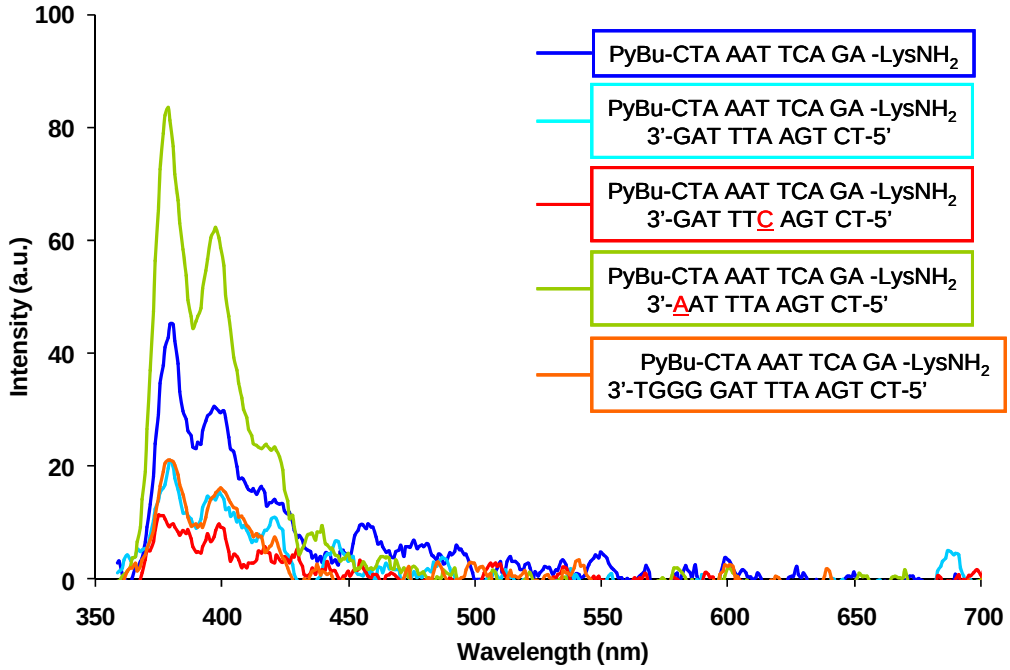

Figure A71 Fluorescence spectra of single strand **PyM11** and its hybrids with complementary DNA in 10 mM sodium phosphate buffer pH 7.0, [PNA] = 2.5 μM and [DNA] = 3.0 μM, excitation wavelength = 345 nm.

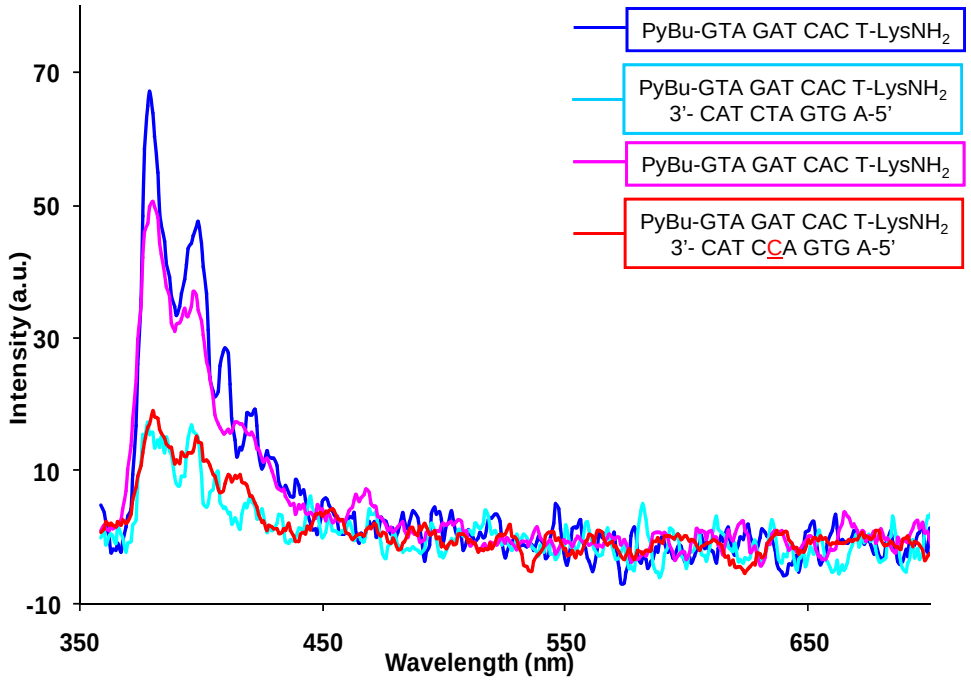

Figure A72 Fluorescence spectra of single strand **PyM10** and its hybrids with complementary DNA in 10 mM sodium phosphate buffer pH 7.0, [PNA] = 2.5 μM and [DNA] = 3.0 μM, excitation wavelength = 345 nm.

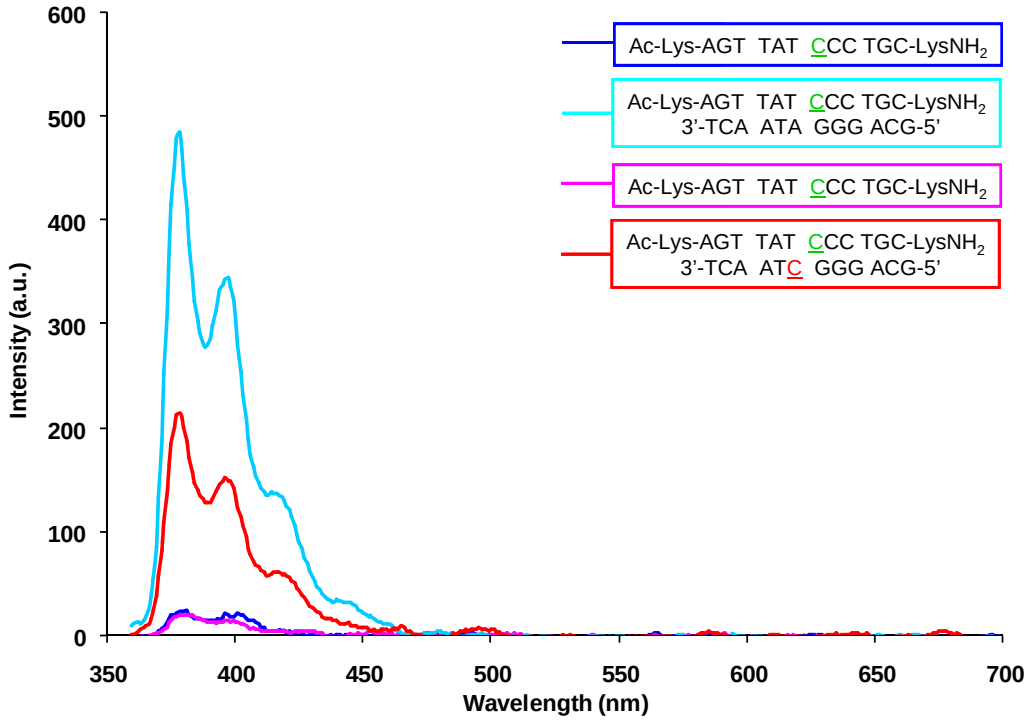

Figure A73 Fluorescence spectra of single strand **M12^{Py}C** and its hybrids with complementary DNA in 10 mM sodium phosphate buffer pH 7.0, [PNA] = 2.5 μM and [DNA] = 3.0 μM, excitation wavelength = 345 nm.

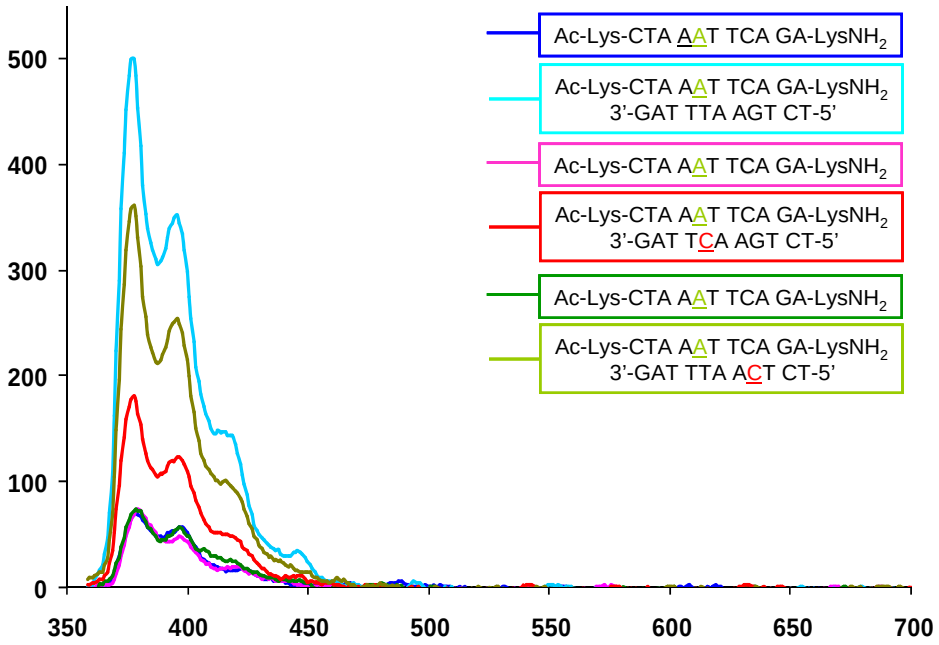

Figure A74 Fluorescence spectra of single strand **M11^{Py}A** and its hybrids with complementary DNA in 10 mM sodium phosphate buffer pH 7.0, [PNA] = 2.5 μM and [DNA] = 3.0 μM, excitation wavelength = 345 nm.

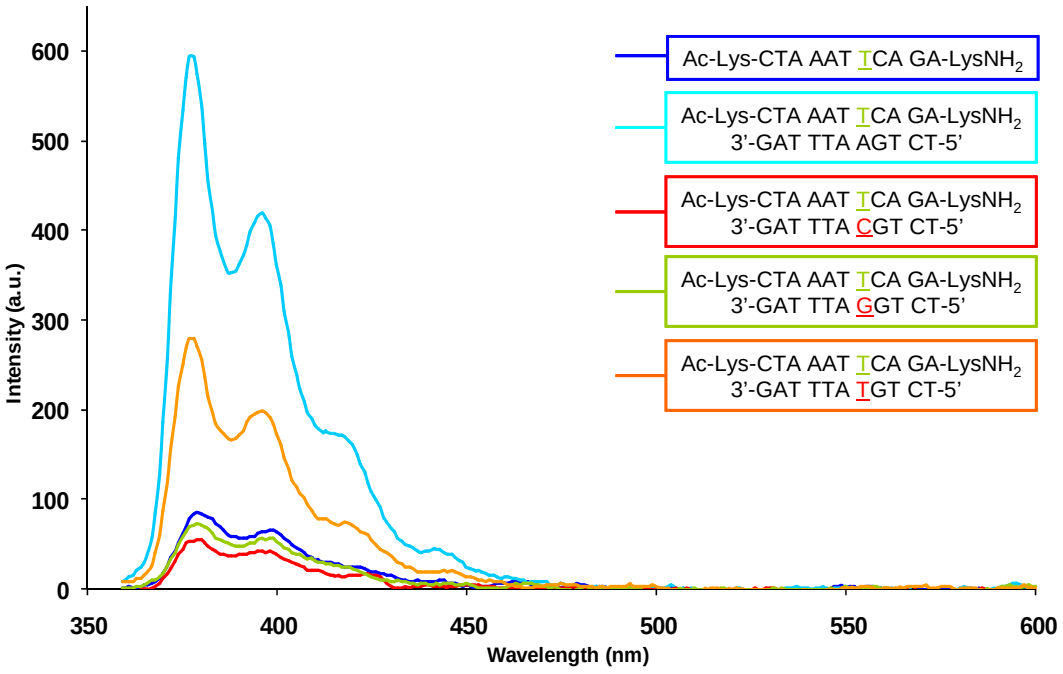

Figure A75 Fluorescence spectra of single strand **M11^{Py}T** and its hybrids with complementary DNA in 10 mM sodium phosphate buffer pH 7.0, [PNA] = 2.5 μM and [DNA] = 3.0 μM, excitation wavelength = 345 nm.

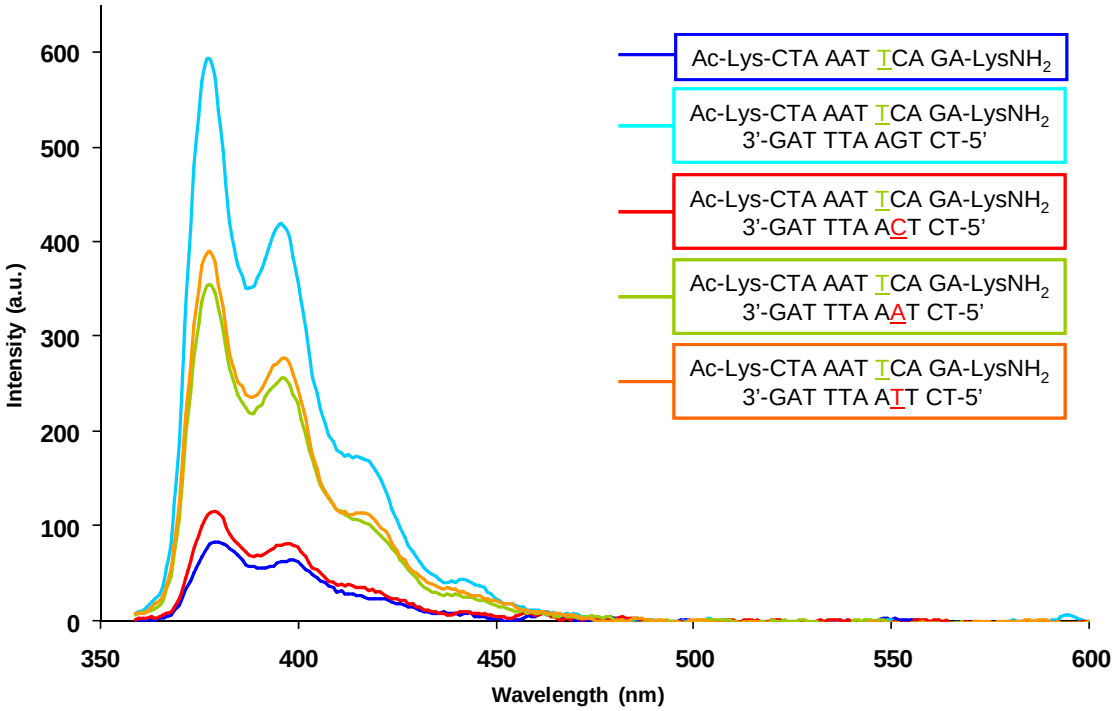

Figure A76 Fluorescence spectra of single strand **M11^{Py}T** and its hybrids with complementary DNA in 10 mM sodium phosphate buffer pH 7.0, [PNA] = 2.5 μM and [DNA] = 3.0 μM, excitation wavelength = 345 nm.

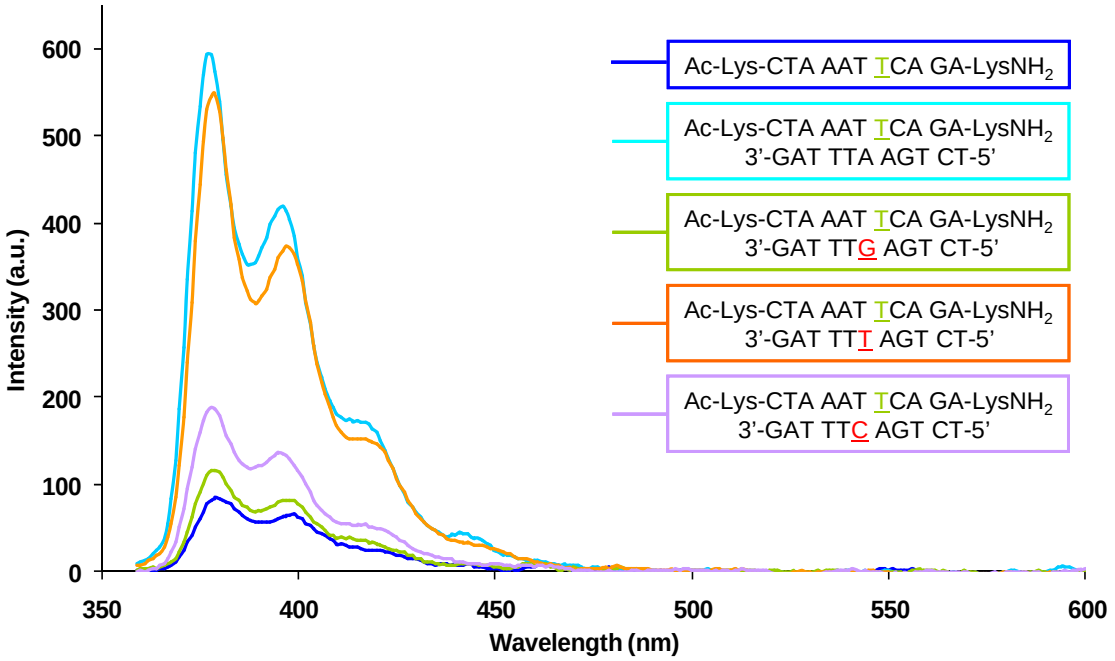

Figure A77 Fluorescence spectra of single strand **M11^{Py}T** and its hybrids with complementary DNA in 10 mM sodium phosphate buffer pH 7.0, [PNA] = 2.5 μM and [DNA] = 3.0 μM, excitation wavelength = 345 nm.

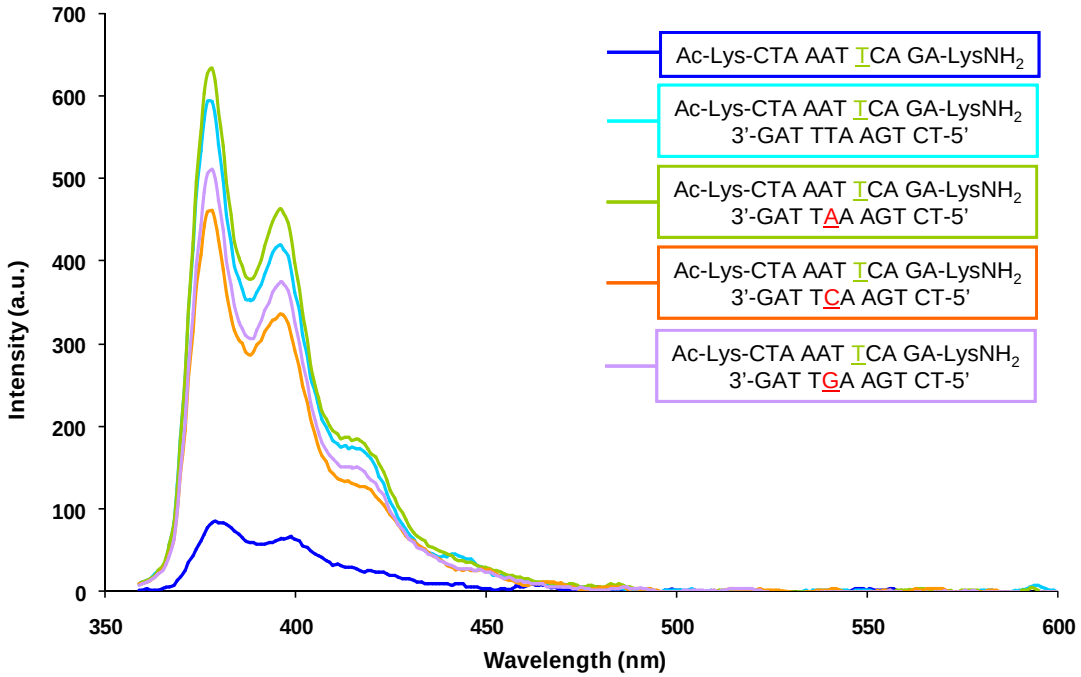

Figure A78 Fluorescence spectra of single strand **M11^{Py}T** and its hybrids with complementary DNA in 10 mM sodium phosphate buffer pH 7.0, [PNA] = 2.5 μM and [DNA] = 3.0 μM, excitation wavelength = 345 nm.

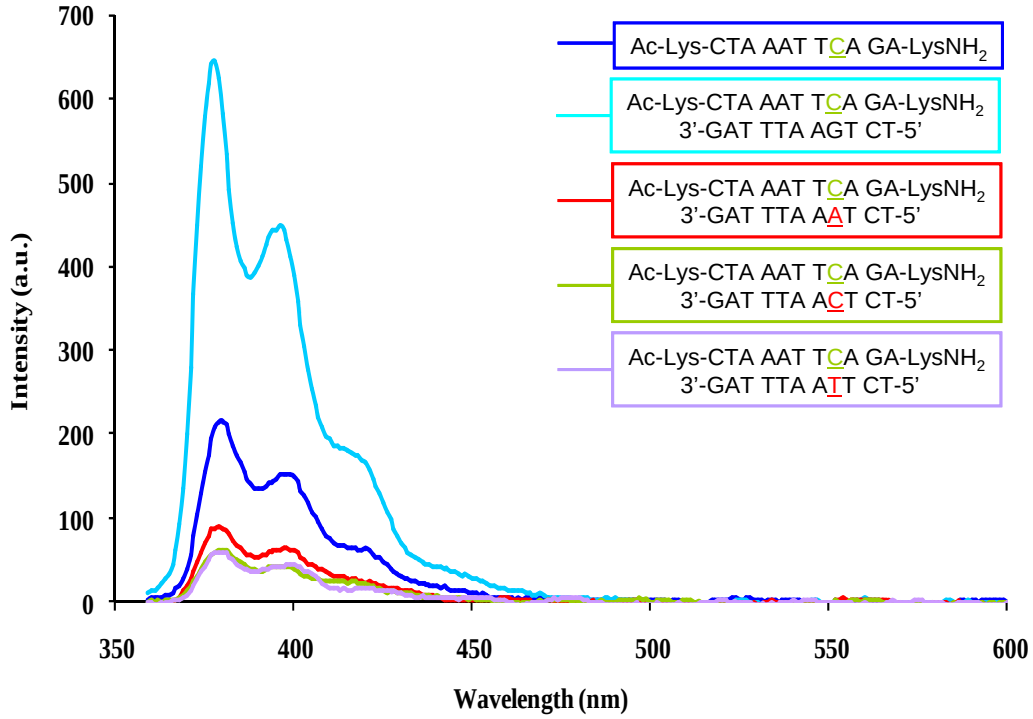

Figure A79 Fluorescence spectra of single strand **M11^{Py}C** and its hybrids with complementary DNA in 10 mM sodium phosphate buffer pH 7.0, [PNA] = 2.5 μM and [DNA] = 3.0 μM, excitation wavelength = 345 nm.

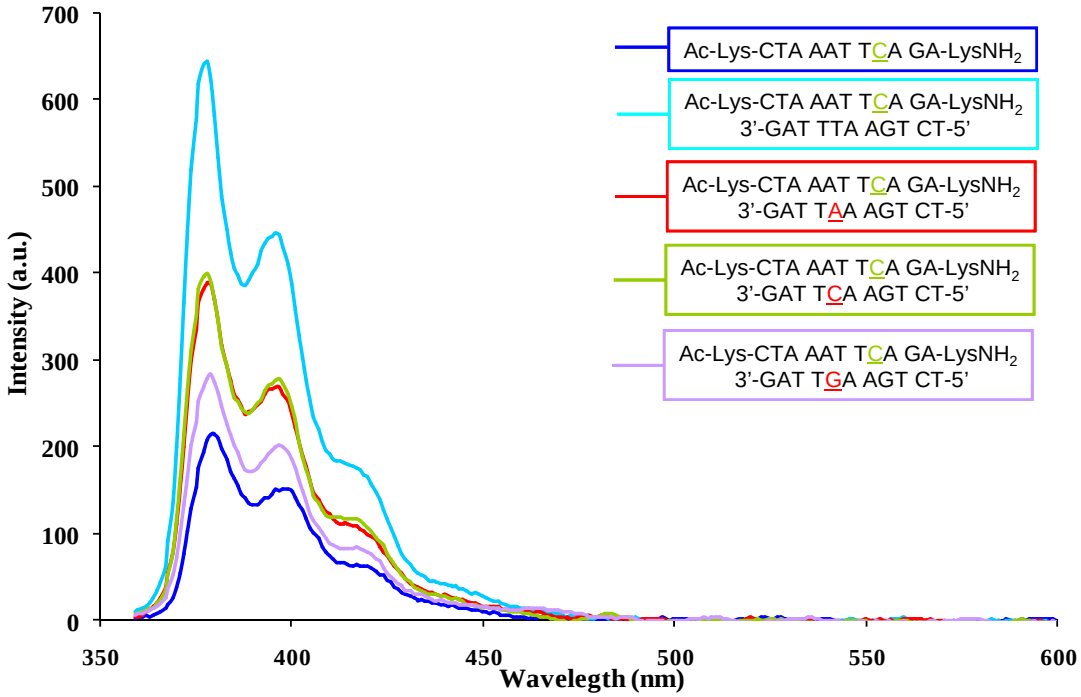

Figure A80 Fluorescence spectra of single strand **M11^{Py}C** and its hybrids with complementary DNA in 10 mM sodium phosphate buffer pH 7.0, [PNA] = 2.5 μM and [DNA] = 3.0 μM, excitation wavelength = 345 nm.

VITAE

Miss Chalothorn Boonlua was born on November 29th, 1982 in Bangkok province, Thailand. She received the Bachelor Degree of Science, majoring in Chemistry from Silpakorn University in 2005 and graduated with the Master Degree of Science, majoring in Chemistry from Faculty of Science, Silpakorn University in 2007. She began Ph.D. studying in Program in Chemistry, Faculty of Science, Chulalongkorn University in the academic year of 2007 and graduated in the academic year of 2012.

Publications

Boonlua, C., Vilaivan, C., Wagenknecht, H-A., Vilaivan, T. 5-(Pyren-1-yl)uracil as a Base-Discriminating Fluorescent Nucleobase in Pyrrolidinyl Peptide Nucleic Acids. *Chem. Asian J.* **2011**, 6, 3251–3259.